Teratogenic activity of selected drugs. Morphogenesis of the notochord and of the fore-limbs investigated at the light and electron microscope level

X

Structure and development of certain subcellular organelles and cytoplasmic symbionts in Paramecium aurelia

by A. Jurand

Submitted to the University of Edinburgh as a thesis in the fulfilment of the requirements for the degree of Doctor of Science

April 1969

Contents

The candidate

Date of birth	30th March, 1914		
Nationality	British		
Degrees	B.Sc.(Drug Chemistry)	Cracow (Poland)	1937
	Ph.D.	Cracow (Poland)	1947
	B.Sc.(Biology)	Cracow (Poland)	1952
	Docent degree	Cracow (Poland)	1954
Position	Lecturer in the Institute of Animal Genetics, University of Edinburgh		
Fellowships	1957 - Scholar of the British Council in the Institute of Animal Genetics, University of Edinburgh 1958 - 1963 Fellow of the British Empire Cancer Campaign, Institute of Animal Genetics: University of Edinburgh 1965 - 1966 Research Fellow in the Oak Ridge National Laboratory, Biology Division, Oak Ridge, Tennessee - U.S.A.		

Participation in International Congresses

1) 3rd International Embryological Conference, Cambridge, 1957
2) 1st International Conference on Congenital Malformations, London, 1960
3) 5th International Embryological Conference, London, 1961
4) 6th International Embryological Conference, Helsinki, 1963
5) 7th International Embryological Conference, London, 1965
6) 8th International Embryological Conference, Interlaken, 1967

Membership of Learned Societies

Society for Experimental Biology
Society for Developmental Biology
British Section of the Society of Protozoologists

Introduction

The publications presented here are arranged in two groups: the first consists of works in the field of morphogenesis and experimental teratology, the second of works on the cytology, reproduction and ultrastructure of various organelles and cytoplasmic symbionts, mainly in Paramecium aurelia.

Group I

Several of the papers comprising this group deal with early and later effects of teratogens on chick and mouse embryos. In papers on the cytotoxic and early embryotoxic effects of triethanomelamine (TEM) and some nitrogen mustard derivatives (papers No. 1, 2 and 3) it was shown that these chemical compounds have a common property: they affect the morphogenesis of organs of mesodermal origin. Their anti-mesodermal activity was detected even after short treatment, and early in embryonic development, in the form of necrotic changes in the somitic cells and occasionally in the cells of the limb-bud mesoblast. As later effects of treatment with these compounds, there was observed a syndrome of malformations which included kinking of the axial organs, liver hernia, uni- or bilateral microphthalmia and micromelia. The anti-mesodermal activity of N-p-amino-phenyl-nitrogen mustard and its acetyl and fluoro-acetyl derivatives

(papers No. 4 and 5) although noticeable, is less severe than their specific activity against the medullary plate and neural tube cells.

The teratogenic properties of thalidomide were investigated at early stages of the wing-buds in chick embryos (paper No. 8). The first effect is dilatation of the wing-bud axial artery; this is followed by scattered necrosis of the mesoblast tissue. At the ultrastructural level, after thalidomide treatment the endothelial cells of the axial arteries contain vacuolated and swollen mitochondria and an increased number of lysosomes and cytolysomes. Golgi apparatus, lysosomes and cytolysomes show considerable acid phosphatase activity.

Hydrocortisone acetate was investigated for embryotoxicity on mouse embryos (paper No. 9). When injected into pregnant mice on the 10th, 11th and 12th day of pregnancy, hydrocortisone causes, in the limb buds of 14-day-old embryos, dilatation of the venous marginal sinuses (14.5% of embryos), extensive distal mesoblast necrosis (7.9% of embryos), distal haemorrhages (10.7% of embryos) and necrotic centres in the limb skeleton blastemas. Deformations of the foot-plates found in about 5% of embryos are ascribed to healing of previous necrotic lesions and haemorrhages. Other malformations include micromelia (9.4 %), necrosis of the maxillary processes (1.8 %) and cleft palate in 18-day-old embryos (52.7 % of embryos).

The development of notochord in the chick was investigated using light and electron microscopy techniques (paper No. 5).

There are three main stages in the development of this organ: 1) formation of the compact rod-like structure, 2)vacuolization of the cells by formation of cell vacuoles filled with a gelatinous substance and 3) involution of the notochord associated with the development of the vertebral column. Initially the mitotic activity shows uneven distribution, being confined to the caudal portion of the organ. Later, the mitotic figures are distributed at random. During the stage of vacuolization the rough endoplasmic reticulum develops extensively and is probably engaged in the synthesis of the contents of the vacuoles.

The work on ultrastructural aspects of fore-limb development was concerned with the first two periods of morphogenesis, i.e., with the period initiating activity of the somatopleural mesenchyme and the period of interaction between the mesoblast and the epiblast (paper No. 7). In the earliest stages, the outer nuclear membrane in the mesoblast cells shows formation of the rough endoplasmic reticulum, which is regarded as a characteristic symptom of an increased cytodifferentiation process. In addition, there was found an indication that the mesoblast cells are forming a secretion which may be the apical ectodermal ridge maintenance factor postulated by other investigators. During the period of interaction between the epiblast and the mesoblast the apical ectodermal ridge is a highly complicated tissue with numerous subcellular systems. The cytoplasm of these cells at the time of maximal development of this transient structure is much richer

in RNA than other epithelial cells covering the limb bud. This fact indicates high synthetic activity within these cells, which is in agreement with the notion that the apical ectodermal ridge is the organizer in limb development.

The work on limb development also contains informations on the relationship between acid phosphatase activity and cell death in the apical ectodermal ridge, on the ciliary structures in the ectodermal cells, and on the basement membrane underneath the epiblast.

Group II

In the paper dealing with the food vacuoles in Paramecium aurelia (paper No 2) it is suggested that during the digestion period the food vacuole membrane is forming small vacuoles by means of pinocytosis. These vacuoles are later released into the cytoplasm as secondary food vacuoles. The food vacuole membrane is a very active structure in the digestive process and should be regarded not only as an interface between the food vacuole and the cytoplasm.

The other organelle investigated was the macronucleus of Paramecium aurelia; both its ultrastructure and its development were studied (papers No. 12 and 13). The nature of the two main components of this organelle was examined, and it was suggested that the large bodies were likely to be the "sub-nuclei" postulated from genetic work. In more recent paper (not included) it was concluded, however, that the large bodies are nucleoli and the small bodies most probably macronuclear chromosomes.

In the paper dealing with the development of macronuclear anlagen (paper No. 13) it is shown the DNA originally derived from the micronucleus in very young anlagen is extremely diffuse; there is no detectable RNA. Shortly afterwards there appear single, large, electron dense RNA-

containing bodies which later disintegrate, forming the so called "large bodies" of the mature macronucleus. At this stage DNA is detectable cytochemically in a diffuse state throughout the entire anlage. The last structures to be formed are numerous "small bodies" which are initially much smaller than those in the mature macronucleus.

In the paper on the cytology of a suctorian, Podophrya paramecicorum, attention is paid to the general ultrastructure of the organism, to its micro- and macronucleus, and to the structure and function of the tentacles and the missile-shaped bodies associated with them (paper No. 14).

The remaining papers in this group are concerned with investigations on cytoplasmic symbionts such as mu, lambda and kappa particles found in various stocks of Paramecium aurelia (papers No. 10, 15, 17 and 18). The general conclusion reached in these investigations is that these different symbionts are characterized by different morphological and ultrastructural properties, but all of them are prokaryotic organisms, most probably obligatory symbiotic bacteria.

Apart from the papers in this group, in collaboration with Dr. G.G. Selman, we have recently completed a monograph "The Anatomy of Paramecium aurelia" which is at present in its last stages of the publication procedure (by Macmillan & Co., London). This book consists of an account on the ultrastructure, development and physiology of all the cell organelles and contains 15 text-figures and 53 plates with 40 light and 200 electron micrographs.

List of enclosed publications

Group I

1. Jurand, A. Action of triethanomelamine (TEM) on early stages of chick embryos. J. Embryol. exp. Morph. 6, 357 - 362 (1958).

2. Jurand, A. Action of triethanomelamine (TEM) on early and later stages of mouse embryos. J.Embryol.exp. Morph. 7, 526 - 539 (1959).

3. Jurand, A. Comparative investigations of the action of two nitrogen mustard derivatives on the early stages of development of chick embryos. J.Embryol. exp. Morph. 8, 60 - 67 (1960).

4. Jurand, A. Further investigations of the cytotoxic and morphogenetic effects of some nitrogen mustard derivatives. J. Embryol. exp. Morph. 9, 492 - 506 (1961).

5. Jurand, A. The development of the notochord in chick embryos. J. Embryol. exp. Morph. 10, 602 - 621 (1962).

6. Jurand, A. Anti-mesodermal activity of a nitrogen mustard derivative. J. Embryol. exp. Morph. 11, 689 - 696. (1963).

7. Jurand, A. Ultrastructural aspects of early development of the fore-limb buds in the chick and the mouse. Proc. Roy. Soc. B. 162, 387 - 405 (1965).

8. Jurand, A. Early changes in limb buds of chick embryos after thalidomide treatment. J. Embryol. exp. Morph.16, 289 - 300, (1966).

9. Jurand, A. The effect of hydrocortisone acetate on the development of mouse embryos. J. Embryol. exp. Morph. 20, 355 - 366 (1968).

Group II

10. Beale, G.H. and Jurand, A. Structure of the mate-killer (mu) particles in Paramecium aurelia, stock 540. J. gen. Microbiol. 23, 243 - 252,(1960).

11. Jurand, A. An electron microscope study of food vacuoles in Paramecium aurelia. J. Protozool. 8, 125 - 130, (1961).

12. Jurand, A., Beale, G.H. and Young, M.R. Studies on the macronucleus of Paramecium aurelia. I. (with a note on the ultra-violet micrography). J. Protozool. 9, 122 - 131, (1962).

13. Jurand, A., Beale, G.H. and Young, M.R. Studies on the macronucleus of Paramecium aurelia. II. Development of macronuclear anlagen. J. Protozool. 11, 491 - 497, (1964).

14. Jurand, A. and Bomford, R. The fine structure of the parasitic suctorian Podophrya parameciorum. J. Microscopie, 4, 509 - 522, (1965).

15. Beale, G.H. and Jurand, A. Three different types of mate-killer (mu) particle in Paramecium aurelia (syngen 1). J. Cell. Sci. 1, 31 - 34, (1966).

16. Jurand, A., Simões, L.C.G. and Pavan, C. Changes in the ultrastructure of salivary gland cytoplasm in Sciara ocellaris (Comstock, 1882) due to microsporidian infection. J. Insect Physiol. 13, 795 - 803, (1966).

17. Jurand, A. and L.B. Preer. Ultrastructure of flagellated symbionts in Paramecium aurelia. J. gen. Microbiol. 54, 359 - 364, (1968).

18. Preer, J.R. and Jurand, A. The relation between virus-like particles and R bodies of Paramecium aurelia. Genet. Res., Camb. 12, 331 - 340, (1968).

Declaration regarding the share in joint papers

The joined investigations were in each case initiated and planned in discussions with the co-authors, and the papers are the outcome of close collaboration with them. It would be virtually impossible to disentangle the observations and data contributed by each of the co-authors, but in general the cytological and electron microscope part of the work was carried out by me.

During the last three years, I have supervised the work of a Ph.D. candidate, Mr. S.C. Goel, who has studied the differentiation of cartilage in limb buds of chick and mouse embryos, using electron-microscopical and autoradiographic techniques. It is expected that this work, which developes naturally from my studies recorded in papers No. 6, 7, 8 and 9, will eventually be published in a series of 2 - 3 papers over the name Mr. Goel.

First group of publications

Action of triethanomelamine (TEM) on early stages of chick embryos

by A. Jurand

Action of Triethanomelamine (TEM) on Early Stages of Chick Embryos

by A. JURAND[1]

From the Institute of Animal Genetics, Edinburgh

WITH TWO PLATES

OF many closely related compounds investigated recently from the point of view of cytotoxity and tumour-inhibiting properties 2,4,6-tri-(ethyleneimino)-1,3,5-triazine (called also triethanomelamine or TEM) proved to be the most effective substance against the Walker rat carcinoma. First descriptions of this fact were published in 1950 (Buckley *et al.* and Burchenal *et al.*). Also in 1950 appeared the publication of the first results of the clinical application of TEM at the First International Cancer Congress (Mueller & Miller). Later on Karnovsky *et al.* (1951) and Petersen *et al.* (1951) recommended procedures for parenteral and oral administration of this substance in clinical treatment. Very recently TEM has been introduced in a commercial form for oral and parenteral administration in cases of leukaemia, Hodgkin's disease, polycythaemia vera, and other neoplastic conditions.

The cytotoxic activity of TEM is very similar to that of the nitrogen mustards (Philips & Thiersch, 1950), chromosome breakage with simultaneous chromosomal rearrangements, chromosome bridges and other malformations being observed by Fahmy & Fahmy (1953, 1954, 1955), Lüers (1953), and Herskowitz (1955). In somewhat higher doses TEM appears to act as an antimitotic agent (Hendry *et al.*, 1951).

The present work was undertaken to investigate the influence of TEM on early stages of the embryonic development of chick embryos and on the formation of the first anlagen of some organs.

MATERIAL AND METHODS

In the first part of this work a solution of TEM in 0·9 per cent. NaCl was injected into the albumen of fertilized chicken eggs, which had been incubated at 37·5° C. for 22 hours until the stage of the primitive streak was reached. The puncture in the shell was closed with wax and the eggs left for approximately 20 hours to allow the injected solution to diffuse throughout the albumen. The eggs were afterwards reincubated for another 24 hours, the embryos taken out, rinsed in saline solution, and fixed. The whole period of the incubation *in ovo*

[1] *Author's address*: Institute of Animal Genetics, West Mains Road, Edinburgh 9, U.K.

[J. Embryol. exp. Morph. Vol. 6, Part 2, pp. 357–362, June 1958]

was consequently about 46 hours with a break of about 24 hours for injection and diffusion.

In the second part of this work we used chick embryos cultivated *in vitro* according to the method described by New (1955). The fertilized eggs were incubated for 22–23 hours, then the embryos transferred to watch-glasses; those which were in the stage of the primitive streak were selected and treated with TEM or left as controls. TEM was applied in solution in the liquid egg albumen put round the plastic ring used for this method. The embryos were then incubated *in vitro* for different periods of time, usually about 24 hours, but always till the controls reached the stage of 12–16 somites.

In the experiments in the first part of this work, after preliminary tests, three concentrations of TEM were used: 10^{-5}, 2×10^{-5}, and 5×10^{-5}. Embryos cultivated *in vitro* were treated with lower doses: 2×10^{-6}, 3×10^{-6}, and 5×10^{-6}. Higher concentrations were used *in ovo* because of the additional dilution of TEM by the albumen.

For the comparison of the developmental stages the works of Patten (1950) and Hamburger & Hamilton (1951) were used.

The embryos were examined histologically and cytologically. For histological purposes the embryos were fixed in alcoholic Bouin solution, embedded in wax, and after sectioning stained with haematoxylin and eosin. For cytological purposes the embryos were fixed in Carnoy's fluid and stained with methyl green pyronin. The whole mounts were stained with Mayer's haematoxylin.

The TEM used was supplied by Imperial Chemical (Pharmaceuticals) Ltd., Manchester.

RESULTS

In both groups of experiments, i.e. whether TEM was applied *in ovo* or *in vitro*, the results were very similar and the intensity of changes depended roughly on the concentration used. However, there was a considerable variation in response between embryos treated with the same concentrations, this variation being much greater between embryos treated *in ovo* than between embryos cultivated *in vitro*.

Macroscopical changes

The lowest concentrations, 10^{-5} and 2×10^{-6} *in ovo* and *in vitro* respectively, caused a distinct retardation of the growth and development of embryos. Whereas the control embryos injected with saline, or treated with the corresponding mixture of the liquid albumen and saline solution, were normally in the stage of 12–16 somites by the end of the experiment, the experimental embryos had only 6–9 somites. Many of the experimental embryos appeared to have peculiar hollows inside the somites, more particularly in the posterior ones, though in some embryos many somites were damaged. The embryos in this group also showed some changes in the head, which was considerably widened,

probably due to increased accumulation of the head mesenchyme cells, whereas the development of the brain appeared to be slightly retarded (Plate 1, compare figs. 1 and 2).

The intermediate concentrations, 2×10^{-5} and 3×10^{-6} respectively, caused more distinct changes in development. The retardation was stronger, often with almost complete atrophy or considerable under-development of the somites. The neural tube, whether closed or not, was almost normal in appearance and shape. In the head there was usually much less mesenchyme than in embryos given the lower concentrations (Plate 1, fig. 3).

The strongest concentrations (5×10^{-5} or 5×10^{-6}) caused also strong retardation of development. The somites were often completely atrophied. In some embryos vesicles were found on both sides of the axis (Plate 1, fig. 4). They were usually located a short distance away from the axis, not right against it as is typical for the vesicles seen in embryos treated with purine analogues (Waddington, Feldman, & Perry, 1955).

Microscopic changes

According to histological observations it appears that the influence of TEM on these embryos is directed mainly to the mesodermal organs, primarily against somites. In fig. 5 (Plate 1) is shown a transverse section of the 8th pair of somites of a control embryo. In fig. 6 is a similar section of the 5th pair of an experimental embryo treated with TEM at a concentration of 10^{-5} injected *in ovo*. Comparison shows that the development in this case was nearly the same, but the somites of the experimental embryo are empty with an absence of the core of the somites, which normally consists of irregularly arranged cells.

After treatment of embryos *in vitro* with TEM of 3×10^{-6} concentration or *in ovo* with a concentration of 2×10^{-5} the somites of some embryos were further damaged. In some cases there was an extreme retardation of development with very marked effects on the somites, which appeared to be completely hollow (Plate 1, figs. 7 and 8). In other cases the cells of the somites have been more or less separated, and the whole organ to some extent disintegrated, the somitic cells becoming more like mesenchymal cells. In such embryos changes could be found in other tissues and organs, for instance in the neural tube and notochord, though these seem to be more resistant to TEM than the somites (Plate 2, fig. 9).

Many of the embryos in the second and third group, i.e. those treated with TEM *in ovo* using concentrations of 2×10^{-5} or 5×10^{-5} and *in vitro* using concentrations of 3×10^{-6} or 5×10^{-6}, appeared to have very large vacuoles or bubbles lying along both sides of the central organs of the embryo. In the transverse sections of such embryos a distinct disintegration of the somites and a marked widening of the coelom could be seen. These widenings were visible in the whole mounts as vesicles, which appeared to be present not only between

both somato- and splanchnopleure, but also between splanchnopleure and the entoderm layer (Plate 2, fig. 10). The vesicles were thus of quite a different kind to those resulting from purine analogues, which are due to the disintegration of the mesoderm being formed from the primitive streak (Waddington *et al.*, 1955).

The changes in the amount of the head mesenchyme caused by the lowest doses of TEM usually appeared distinctly, but did not occur in all the embryos examined. A moderate accumulation of mesenchyme cells is seen in fig. 11 (Plate 2) in comparison with the control head of fig. 12.

After treatment with any of the concentrations of TEM, both *in ovo* and *in vitro*, pronounced changes in nuclei and nucleoli of cells of the somites, neural tube, and notochord could be seen. By staining with methyl green pyronin after fixation with Carnoy's fluid the nuclei of experimental embryos appeared to be nearly three times larger than those of the controls, the nucleoli showing still greater hypertrophy, and the cells were as a whole hyperplastically changed (Plate 2, figs. 13 and 14).

DISCUSSION

2,4,6-Tri-(ethyleneimino)-1,3,5-triazine is an extremely toxic compound, as can be seen from the concentrations used in the experiments in this and other works. In medicine it is being increasingly used against leukaemia, Hodgkin's disease, polycythemia vera, i.e. against neoplastic conditions of particular organs of mesodermal origin. It has a very toxic effect on the bone marrow, where it affects the haemopoetic activity selectively (Gellhorn, Klingerman, & Jaffe, 1952). In stronger doses it produces rapid and widespread damage in lymphoid tissues (Hendry *et al.*, 1951). The bone marrow and lymphatic glands are typical organs of mesodermal origin and this seems congruent with the rather selective activity of TEM in relation to the somites shown in this work. However, in amphibian embryos it is not the mesoderm but the neural tissue which is most sensitive to the drug (Waddington, 1958). Presumably this sensitivity depends on the precise chemical constitution of the cells; but since the mode of action of TEM on biological materials is not fully understood, it is not clear precisely what the relevant factors are.

Enlargement of the nuclei and nucleoli are frequent effects of the action of cytotoxic agents; after treatment with TEM these changes have been observed mostly in the tissues of the somites and the neural tube. They are presumably a consequence of the inhibition of mitosis. Similar enlargements of nucleoli and the production of giant cells were observed in a quite different material, planaria, in the process of regeneration after treatment with TEM (Pedersen, 1957), and also in amphibian embryos by Töndury (1955).

SUMMARY

1. Triethanomelamine (TEM), applied to chick embryos in the stage of the primitive streak both *in ovo* and *in vitro*, produces retardation of development which is the greater the higher the dose used.

2. The embryonic organs most sensitive to TEM appeared to be the somites, which become empty through the disappearance of the central core.

3. In higher doses the somites undergo more or less complete disintegration, the somitic cells being separated and resembling mesenchyme cells.

4. TEM causes a considerable enlargement and widening of the coelom and of the space between splanchnopleure and the entoderm layer.

5. After treatment by lower doses there appears a slight accumulation of the head mesenchyme cells.

6. TEM causes a considerable enlargement of the cells, nuclei and nucleoli of the somitic, neural tube, and notochord cells.

ACKNOWLEDGEMENTS

This work was done during the tenure of a British Council studentship, for which grateful acknowledgement is made. I should like to thank Professor C. H. Waddington for suggesting this problem and for helpful advice.

REFERENCES

BUCKLEY, S. M., STOCK, C. C., CROSSLEY, M. L., & RHOADS, C. P. (1950). Inhibition of Crocker Mouse Sarcoma 180 by certain ethyleneimine derivatives and related compounds. *Cancer Res.* **10**, 207.

BURCHENAL, J. H., JOHNSTON, S. F., STOCK, C. C., CROSSLEY, M. L., & RHOADS, C. P. (1950). The effect of 2,4,6-triethyleneimino-s-triazine and related compounds on transplanted mouse leukaemia. *Cancer Res.* **10**, 208.

FAHMY, O. G., & FAHMY, M. J. (1953). The effect of dose on mutagenicity and chromosome breakage induced by 2,4,6-tri(ethyleneimino)-1,3,5-triazine. *Drosophila Inform. Serv.* **27**, 89.

—— —— (1954). Cytogenic analysis of the action of carcinogens and tumour inhibitors in *Drosophila melanogaster*. II. The mechanism of induction of dominant lethals by 2,4,6-tri-(ethyleneimino)-1,3,5-triazine. *J. Genet.* **52**, 603–15.

—— —— (1955). Cytogenic analysis of the action of carcinogens and tumour inhibitors in *Drosophila melanogaster*. III. Chromosome structural changes induced by 2,4,6,-tri(ethyleneimino)-1,3,5-triazine. *J. Genet.* **53**, 181–99.

GELLHORN, A., KLINGERMAN, M. M., & JAFFE, I. (1952). Triethylene melamine in clinical cancer chemotherapy. *Amer. J. Med.* **13**, 428–31.

HAMBURGER, O., & HAMILTON, H. L. (1951). A series of normal stages in the development of the chick embryo. *J. Morph.* **88**, 55–92.

HENDRY, J. A., HOMER, R. F., ROSE, F. L., & WALPOLE, A. L. (1951). Cytotoxic agents. III. Derivatives of ethyleneimine. *Brit. J. Pharmacol.* **6**, 357–410.

HERSKOWITZ, I. H. (1955). The incidence of chromosomal rearrangements and recessive lethal mutations following treatment of mature *Drosophila* sperm with 2,4,6-tri(ethyleneimino)-1,3,5-triazine. *Genetics*, **40**, 574.

KARNOVSKY, D. A., BURCHENAL, J. H., ARMISTEAD, G. C. JR., SOUTHAM, C. M., BERNSTEIN, J. L., CRAVER, L. F., & RHOADS, C. P. (1951). Triethylene melamine in the treatment of neoplastic disease. *Arch. intern. Med.* **87**, 477–516.

LÜERS, H. (1953). Untersuchung über die Mutagenität des Triäthylenmelamin (TEM) on *Drosophila melanogaster*. *Arch. Geschwulstforsch.* **6,** 77–83.

MUELLER, G. C., & MILLER, J. A. (1950). *Acta Un. int. Cancr.* **7,** 134.

NEW, D. A. T. (1955). A new technique for the cultivation of the chick embryo *in vitro*. *J. Embryol. exp. Morph.* **3,** 326–31.

PATTEN, B. M. (1950). *Early Embryology of the Chick*. London: H. K. Lewis.

PEDERSEN, K. J. (1957). Morphogenetic activities during planarian regeneration as influenced by triethylenemelamine. A paper read at the S.E.B. Conference, Cambridge, 1957.

PETERSEN, E., & BOLAND, F. (1951). Trisethyleneimino-s-triazine in human malignant disease. A preliminary trial. *Brit. J. Cancer*, **5,** 28–37.

PHILIPS, F. S., & THIERSCH, J. B. (1950). The nitrogen mustard-like actions of 2,4,6-*tris*(ethylenimino)-s-triazine and other *bis*(ethylenamines). *J. Pharmacol.* **100,** 398–407.

TÖNDURY, G. (1955). Einfluß chemischer Stoffe auf die embryonale Zelle. *Bull. schweiz. Akad. med. Wiss.* **11,** 332–45.

WADDINGTON, C. H. (1958). A note on the effects of some cytotoxic substances on amphibian embryos. *J. Embryol. exp. Morph.* **6,** 363–4.

—— FELDMAN, M., & PERRY, M. (1955). Some specific developmental effects of purine antagonists. *Exp. Cell Res.*, Suppl. **3,** 366–80.

EXPLANATION OF PLATES

PLATE 1

FIG. 1. Macroscopical view of a control chick embryo of 13 somite stage. ×20.

FIG. 2. Macroscopical view of a chick embryo treated *in ovo* with 0·5 ml. solution of TEM (concentration 10^{-5}). ×20.

FIG. 3. Macroscopical view of a chick embryo treated *in ovo* with 0·5 ml. solution of TEM (concentration 2×10^{-5}). ×20.

FIG. 4. Pronounced changes after injection into the egg of 0·5 ml. solution of TEM (concentration 5×10^{-5}). ×20.

FIG. 5. Transverse section of a control chick embryo through the 8th pair of somites. ×280.

FIG. 6. Transverse section through the 5th pair of somites of a chick embryo treated *in ovo* with 0·5 c.c. solution of TEM (concentration 10^{-5}). ×280.

FIG. 7. Transverse section through somites of a chick embryo treated *in ovo* with 0·5 c.c. solution of TEM (concentration 2×10^{-5}). ×280.

FIG. 8. Transverse section through somites of a chick embryo treated *in vitro* with solution of TEM (concentration 3×10^{-6}). ×280.

PLATE 2

FIG. 9. Transverse section of somites of a chick embryo treated *in vitro* with solution of TEM (concentration 3×10^{-6}). ×280.

FIG. 10. Transverse section of a chick embryo after treatment with solution of TEM *in ovo* (concentration 5×10^{-5}). On the left of the neural tube there are vesicles between somatopleure and splanchnopleure and between splanchnopleure and endoderm. ×110.

FIG. 11. Transverse section of the head of a chick embryo treated with TEM *in ovo* (concentration 10^{-5}). ×100.

FIG. 12. Transverse section of the head of a control chick embryo at 13 somite stage. ×100.

FIG. 13. The cells of the neural tube of a control chick embryo at 13 somite stage. ×700.

FIG. 14. The cells of the neural tube of a chick embryo after treatment with TEM *in vitro* (concentration 3×10^{-6}). ×700.

(Manuscript received 25 : x : 57)

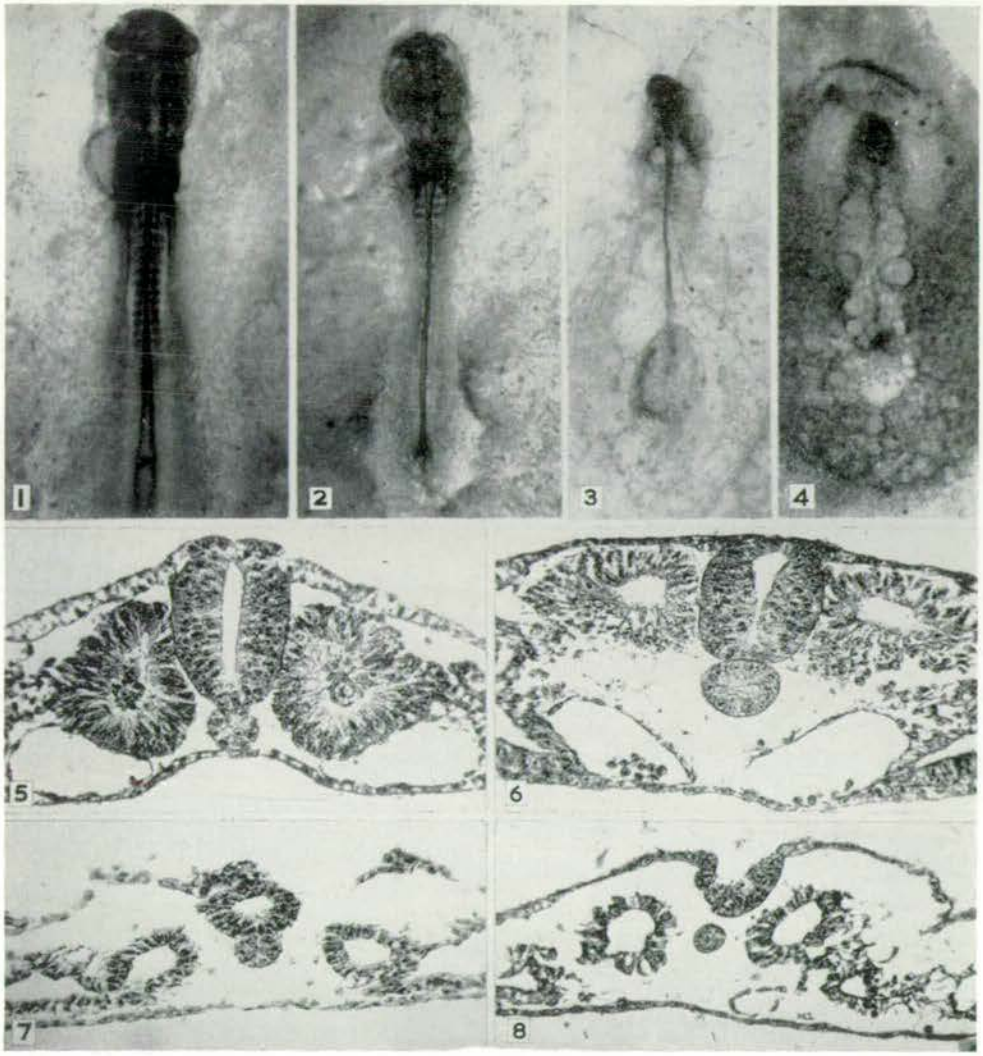

A. JURAND

Plate 1

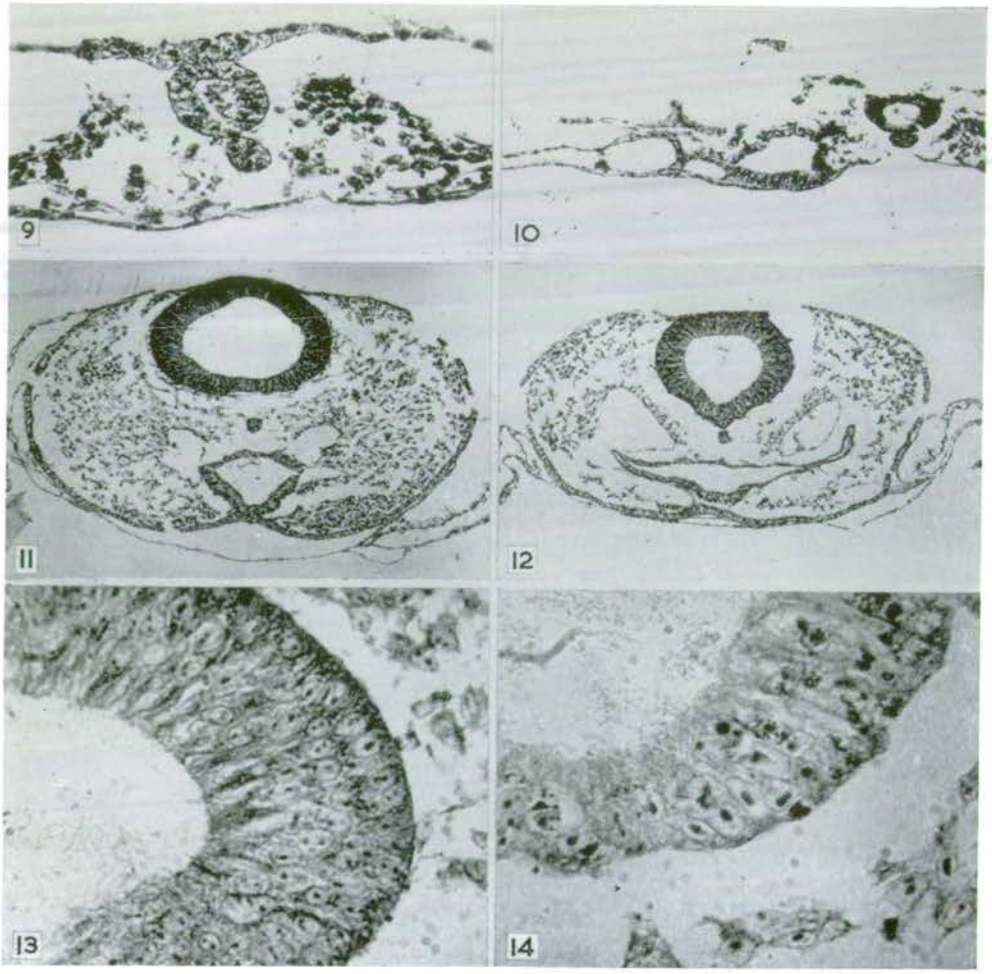

A. JURAND

Plate 2

Action of triethanomelamine (TEM) on early and later stages of mouse embryos

by A. Jurand

Action of Triethanomelamine (TEM) on Early and Later Stages of Mouse Embryos

by A. JURAND[1]

From the Institute of Animal Genetics, Edinburgh

WITH FOUR PLATES

SEVERAL years ago triethanomelamine (2,4,6-tri(ethyleneimino)-1,3,5-triazine, or TEM) was introduced into clinical chemotherapy for its tumour-inhibiting property. It was found, in addition, that TEM is a strong mutagenic factor.

In a previous paper (Jurand, 1958) it was shown that TEM severely retards the development of the chick in the early embryonic stages. This effect is directly proportional to the dose of TEM used. It was suggested that the sensitivity of individual embryonic tissues varies in the early stages of development, somites being the most sensitive embryonic organs. There was observed also, especially with larger doses of TEM, a considerable widening of the embryonic coelom and decomposition of the mid-trunk somites into mesenchyme-like loose tissue. There was, moreover, a considerable increase in cell size, and both the nuclei and the nucleoli in the nervous tissue were enlarged.

In the experiments to be described the influence of TEM on mammalian (mouse) embryonic development, and in particular its lethal effect on developing embryos and the changes it causes in embryonic tissues and organs, is investigated.

MATERIAL AND METHODS

The inbred strain JU and the outbred strain JC of the laboratory mouse were used. Strain JU, homozygous for *aa* and *cc*, was recently described by Falconer (1958). Strain JC has been observed at this Institute for a few years and is characterized by different non-homozygous colour genes present in its ancestry (*si*, *m*, *a*, *b*, *d*, *In*, *bt*, c^{ch}, c^{e}, and *c*). It also shows the non-homozygous gene *Ca* and one skeletal gene, short-ear (*se*). Both of these strains are believed to be free from any mutant genes causing abnormalities which could interfere with the present experiments.

Females, 2–5 months old, were kept with males overnight, and on the next morning were examined for the presence of copulation plugs in the vagina. The day on which the plugs were found was considered to be the first day of preg-

[1] *Author's address:* Institute of Animal Genetics, West Mains Road, Edinburgh 9, U.K.

[J. Embryol. exp. Morph. Vol. 7, Part 4, pp. 526–39, December 1959]

nancy. For convenience, stages of treatment and age are referred to as 5th, 6th, 9th, &c., but strictly speaking these stages should be regarded as $4\frac{1}{2}$, $5\frac{1}{2}$, $8\frac{1}{2}$ days, where $\frac{1}{2}$ days mean 10–14 hours.

The TEM used for these experiments was dissolved in distilled water. Injections were done subcutaneously after slight ether anaesthesia. The doses administered varied between 1·2 mg. and 2·7 mg. per kg. body-weight, being always divided into three equal parts which were injected on three consecutive days, either on the 5th, 6th, and 7th days (experimental series 1) or on the 7th, 8th, and 9th days of pregnancy (experimental series 2). All doses of TEM were calculated in relation to body-weight, the animals being weighed before each injection. Injections were always carried out at the same time of day. Some of the doses used, especially the largest and the smallest, were administered only in the preliminary experiments for the determination of the most effective dosage. The TEM used was supplied by Imperial Chemicals (Pharmaceuticals) Ltd., Manchester.

In both series of experiments mentioned above the females of the experimental and control groups were usually killed either on the 10th or the 15th day. Some animals, however, were killed between the 15th and 18th day of pregnancy.

A separate group of 72 animals was injected on the 7th, 8th, and 9th day of pregnancy with 1·5 mg. and 1·65 mg. per kg. respectively and kept to term.

Animals were killed by decapitation. Embryos were dissected 3 hours after preliminary fixation in the uterus. Carnoy's fluid and Bouin's solution were used as fixatives. Dissected embryos were embedded in wax for histological examination, serially sectioned, and finally stained with haematoxylin-eosin or methyl green-pyronin. Some 10-day embryos were prepared as whole mounts after staining with Mayer's Haemalum. Fifteen-day embryos were examined histologically and also by observation of their external appearance using $\times 8$ magnification. Some 15-day embryos were also stained with toluidin blue solution and cleared in benzyl benzoate for examination of the skeleton. The external characteristics examined included general body-shape, the straightness of the vertebral column and spinal cord, size and shape of eyes, shape of head, appearance of limbs, shape and number of digits, and appearance of the tail.

To enable the decrease in the developmental rate to be recorded, an approximate scale for the 10-day embryos was used:

1. Control 10-day embryos had 16–21 somites and had completed the turning process (Plate 1, fig. 1). All embryos of the experimental groups whose somite numbers fell within this range were regarded as unaffected as regards developmental rate.

2. Experimental 10-day embryos at the 7–15 somite stage, in the process of turning or immediately after completion (1st degree of retardation—Plate 1, fig. 2).

3. Experimental 10-day embryos at the 3–6 somite stage (2nd degree of retardation—Plate 1, fig. 3).

4. Experimental 10-day embryos at the 1–2 somite stage (3rd degree of retardation—Plate 1, fig. 4).

5. Experimental 10-day embryos with no signs of metamerism of the paraxial mesoderm, at the primitive streak stage, with or without head-fold (4th degree of retardation—Plate 1, fig. 5).

6. Experimental 10-day embryos found in a state of resorption (5th degree of retardation).

The 10-day embryos, both control and experimental, were sectioned longitudinally, as far as possible, and also transversely. The 15-day embryos were sectioned transversely, sagittally and tangentially to the back, depending on what organ system was to be examined.

TABLE 1

*Series 1**

Total dose of TEM (mg./kg. body-wt.)	*Number of females killed on 10th day*	*Number of embryos*		*Number of females killed on 15th day*	*Number of embryos*	
		examined	*dead*		*examined*	*dead*
1·2	8	75	..	5	42	5
1·35	14	102	2	8	77	6
1·5	24	112	1	8	35	30
1·65	32	211	4	6	28	39
1·8	12	90	23	7	18	57
1·95	11	65	25	7	6	52
2·1	8	48	32	8	4	67
2·25	6	33	28	4	..	31
2·4	6	28	20	3	..	28
2·7	7	30	38	..	..	..
Control	18	162	4	15	136	6
		Series 2†				
1·2	7	61	3	13	118	4
1·35	15	107	11	19	161	21
1·5	22	174	36	31	149	153
1·65	12	109	14	47	49	446
1·8	7	58	27	12	2	106
1·95	8	57	36	6	..	59
2·1	6	33	23	4	..	34
2·25	6	36	30	..	..	..
2·4	6	33	25	..	..	..
2·7	4	18	24	..	..	..
Control	20	184	..	20	195	6

* Females injected on the 5th, 6th, and 7th day of pregnancy.
† Females injected on the 7th, 8th, and 9th day of pregnancy.

Females belonging to the control groups were likewise anaesthetized on the injection days, without actually being injected.

For comparison of the developmental stages data of Keibel (1937), Snell (1941), and Grüneberg (1943) were used in addition to those obtained from my

own control embryos. The paper of Butcher (1929) was very useful for comparing the histology of the somites.

As there was no difference between the control embryos of JU and JC strains, and as the changes following treatment with TEM were the same in both strains, the results from the two strains are reported together.

Quantitative particulars of the animal material are summarized in Table 1.

RESULTS

Series 1

Total doses of 1·2–2·7 mg. per kg. of body-weight were injected on the 5th, 6th, and 7th day of pregnancy (see Table 1, series 1). Each total dose was divided into three equal portions.

10-day embryos. The two smallest doses, i.e. 1·2 mg. and 1·35 mg. per kg. generally did not affect the development of experimental embryos. The 1·35 mg. dose, however, produced in several cases a slight retardation of development. The difference between these and the control embryos did not exceed, on the average, 3–4 somites. Histological examination of the embryonic organs did not show any abnormalities except an occasional and moderate widening of the myocoele in single somites, especially in the 2nd to the 7th somite (Plate 1, figs. 6, 7).

With higher doses (1·5 and 1·65 mg. per kg.) the retardation of development was much more pronounced. The widening of the myocoele was much larger than in embryos of the previous group (Plate 1, fig. 8). The retardation was of the first and second, and in a few cases of the third, degree. In some of the somites an irregularity in shape was observed. They were polygonal in shape with an abnormal outline (Plate 1, fig. 9). Histological examination showed that in embryos treated with 1·65 mg. per kg. disintegration of some somites occurred, especially those in the thorax (Plate 1, fig. 10).

After injection of 1·8 mg. and 1·95 mg. per kg. most of the embryos did not reach stages of development later than that of the primitive streak, i.e. there occurred the 4th degree of retardation. There was also a higher percentage of dead embryos. Primitive streak-stage embryos showed a relatively good development of the head-fold, whereas the paraxial mesoderm did not show any signs of metamerism (Plate 1, fig. 11).

The larger the dose, the greater was the degree of retardation. In general, however, in all these experiments there was considerable variation in the retarding effect of TEM. After the injection of 1·8 and 1·95 mg. per kg. about 20 per cent. and 28 per cent., respectively, of the embryos were being resorbed (5th degree of retardation).

The largest doses (2·1–2·7 mg. per kg.) resulted in a considerably higher percentage of dead embryos, but even after the strongest dose some primitive streak embryos (4th degree of retardation) were still living.

From a comparison of cells in various tissues of 10-day control and experimental embryos it was noticed that, after the injection of 1·35–1·8 mg. per kg., the cells in somites of experimental embryos were slightly larger and with larger nuclei containing 2–3 nucleoli. In somites of the control embryos the majority of the cells contained one nucleolus, and some contained two (Plate 2, figs. 12, 13).

Numerical results of these experiments are shown in Table 2.

TABLE 2

Dose of TEM (mg./kg. body-wt.	*Number of embryos*	*Degrees of retardation*	*Histological characteristics*	*Figs.*
1·2	75	..	..	..
1·35	102	..	Slight widening of myocoele	7
1·5	112	1, 2, and 3	Pronounced widening of myocoele	8
1·65	211	1, 2, and 3	Widening of myocoele, disintegration of somites	10
1·8	90	4 and 5 (20%)	No metamerism of paraxial mesoderm. Head-folds well developed	11
1·95	65	4 and 5 (28%)	Primitive streak stage	5
2·1	35	4 and 5 (40%)	,,	..
2·25	22	4 and 5 (46%)	,,	..
2·4	14	4 and 5 (42%)	,,	..
2·7	16	4 and 5 (56%)	,,	..

15-day embryos. The percentage of live embryos on the 15th day of pregnancy, after the same treatment as in the previous group, was comparatively lower. One can assume that some of the retarded embryos still alive on the 10th day had meanwhile died. After the injection of higher doses (1·95–2·4 mg. per kg.) the surviving embryos showed some retardation in development, but there was never more than 24 hours difference between the experimental embryos and the controls. In the whole of this series no particular organic abnormalities were observed except for the rather rare occurrence (5 cases) of a fish-like tail tip (Plate 2, fig. 14). Histological examination of the axial organs did not show any anatomical abnormalities.

After the strongest doses, i.e. after 2·25 mg. and 2·4 mg. per kg., there were no live embryos on the 15th day. The highest dose (2·7 mg.) was therefore abandoned.

Series 2

In this series of experiments TEM was administered on three consecutive days later in pregnancy, i.e. on the 7th, 8th, and 9th day, the total dose being similarly divided into three equal portions injected subcutaneously under slight ether anaesthesia (Table 1, series 2).

10-day embryos. These showed degrees of retardation similar to those of series 1. However, the following differences were observed. The variation in the rate of development after particular dosages, especially that following the injection of 1·5–1·8 mg. per kg., was considerably lower. It was also noticed that, besides the changes in somites previously described, the mid-trunk region of the

5–8 somite stage embryo (at about the 2nd degree of retardation) showed a disproportionally slow development in comparison with the head and caudal regions. Such embryos were markedly shorter than most control embryos at the corresponding stage of development (Plate 2, fig. 15).

Histological examination of the retarded embryos showed that malformation and widening of the somite cavity (myocoele) were frequent. In those embryos which showed shortening of the body the somites in the mid-trunk were in a state of almost complete disintegration, and the somite space was filled with irregularly arranged mesenchyme-like tissue.

TABLE 3

Dose of TEM (mg./kg. body-wt.	*Number of embryos*	*Degrees of retardation*	*Histological characteristics*	*Figs.*
1·2	41	..	..	..
1·35	107	..	Slight widening of myocoele	..
1·5	174	2 and 3	Widening of myocoele, disintegration of somites	15, 16
1·65	109	2, 3, and 4	Underdevelopment of the mid-trunk region, oedematous heads	18
1·8	58	4 and 5 (32%)	Primitive streak stage	..
1·95	57	4 and 5 (35%)	,,	..
2·1	41	4 and 5 (42%)	,,	..
2·25	36	4 and 5 (46%)	,,	..
2·4	43	4 and 5 (43%)	,,	..
2·7	18	4 and 5 (57%)	,,	..

General or partial retardation of development was observed according to the dose administered, but extra-embryonic structures seemed not to be influenced so much by treatment with TEM. This was especially true of the allantois and yolk sac, which having been developed much more independently, are presumably less sensitive to the toxic effect of the drug. Many embryos showing the 3rd and 4th degrees of retardation had extra-embryonic structures similar, both in size and structure, to those in control embryos. The allantois in embryos retarded at the primitive streak stage or in the 1–2 somite stage was very long, straight or crooked, extending some distance to the large and spacious yolk sac (Plate 2, figs. 15, 16).

In a few cases, after injecting 1·65 mg. and 1·8 mg. per kg., embryos with pronouncedly oedematous heads and dilatation of brain ventricles were found (Plate 2, figs. 17, 18).

Numerical data for this group of experiments are summarized in Table 3.

15-day embryos. Administration of TEM on the 7th, 8th, and 9th day of pregnancy gave a more precise picture of its action on 15-day embryos. At this time of development it was found that there is a dose of TEM that kills about 50 per cent. of mouse embryos, which are found in a state of resorption in the uterus. This dose is 1·5 mg. TEM per kg., divided into three equal parts administered on the 7th, 8th, and 9th day of pregnancy. This dose may be called 'the

embryonic LD_{50}' of TEM. A dose 10 per cent. lower (1·35 mg. per kg.) results in about 90 per cent. survival of embryos, whereas a dose 10 per cent. higher (1·65 mg. per kg.) kills up to 90 per cent. of embryos.

The embryos surviving after administration of 'the embryonic LD_{50}' were always very much retarded in their development, but not by more than 24–36 hours. However, none of the embryos in this group were noticed to have developmental abnormalities.

The next higher dose, i.e. 1·65 mg. per kg., could be regarded as a 'teratological dose' if administered on the same three days. After this dose the majority of the surviving embryos showed changes of various kinds which could be either quantitative alterations in development or even teratological abnormalities.

TABLE 4

Kind of abnormality	*Number of embryos found**	*Percentage*	*General retardation of development in hours*
Kinking or convolution of axial organs (vertebral column and spinal cord)	14	28·5	36–48
Underdevelopment of the eye ball:			
1. unilateral	12	12	24–48
2. bilateral	8	16	36–48
3. coloboma	7	14	36
Brain hernia	4	8	36
Liver hernia	16	32·6	24–48
Underdevelopment of skull and vertebral column resulting in monsters	3	6	48
Shortening of limbs	5	10	36–48
Cauda bifida	13	26	24–36
General underdevelopment only	11	22	24–96

* Some of embryos in this group showed several of above abnormalities and therefore they are recorded more than once in the table.

The general retardation of the developmental rate, if there were no abnormalities observed, was much more severe than in the corresponding experimental groups of series 1. Surviving embryos showed in this case a slowing down of their development amounting to at least 48 hours, and in a few embryos up to 96 hours, compared with 15-day control embryos. Some of them, when examined both macroscopically and histologically, had the same size and appearance as corresponding normally developed 11- to 14-day control embryos. Among them there were, however, many with several developmental abnormalities. Table 4 above summarizes these abnormalities and their frequency.

Kinking and convolution of axial organs. This effect occurred fairly frequently (28·5 per cent.) after administration of the 'teratological dose' (1·65 mg. per kg.). The kinking of the neural tube and of the vertebral column was either one-sided, or in some cases bilateral, resulting in Z-shaped kinking (Plate 2,

figs. 19–22). Due to this deformation the body was visibly shortened. Histological examination showed that the kinkage of the axial organs is due to defective metamerism of vertebral column primordia and to irregularities of the spinal ganglia which tend to become fused (Plate 2, figs. 21, 22).

In some cases no real kinking of the vertebral column was observed, but the axial organs showed a slight waviness not found in any of the control embryos.

Underdevelopment of the eyeball. The control embryos of the JC strain, if not albinotic, have a dark pigmented iris shaped as a regular pigment ring (Plate 3, fig. 23). At the embryonic age of 15 days the eyelids are not fused and therefore the eyes are accessible for external examination.

In embryos affected by TEM in teratological dosage, the eyeball was frequently much smaller than normal, being proportionally reduced in all its components. The open eyelids left a smaller opening than usual and the reduced eyeball seemed to be deeper in the socket. The pigment ring in such eyes was irregular in shape or it appeared as a misshapen pigment spot with irregular outline (Plate 3, fig. 24).

Histologically the underdeveloped eyeball consisted of a very small lens surrounded by a relatively large amount of head mesenchyme. Behind this layer the vestigial optic vesicle had a slight invagination at the lens side, which consisted only of a thick layer of the pigment tissue of the retina. Very often the shape of the eye-cup showed that the eye was retarded at a very early stage. The differentiation of all parts of the retina, but not of the pigment layer, seemed to be almost completely retarded, so that the retina was almost non-existent. Strangely enough, the optic nerve in such malformed eyes was often found to be normally developed, being merely smaller than usual in diameter. It was covered with pigment tissue, especially at its distal end, like the control nerves (Plate 3, figs. 25, 26). In these cases penetration of mesenchyme cells and blood-vessels into the choroidal fissure was not observed, whereas it always takes place at that stage in normally developing eyes.

The degree of underdevelopment of the eyeball varied from only a slight diminution to its almost complete absence. The lens, though always present, was very much reduced in size and surrounded by a comparatively large amount of head mesenchyme without being pushed into the secondary optic vesicle.

In some cases, however, the eye appeared to be of normal size but its retinal layers showed a symmetrical concavity at the site of the *papilla nervi optici*. In these cases, although the outside of the eyes looked normal, in histological section it appeared to be almost divided into two parts due to the concavity in the retina. There was, however, one lens only (Plate 3, fig. 27).

Brain hernia. Besides the two cases described under 'Monsters' there was observed one embryo with greatly protruding brain tissue causing an eruption on the left side of the front of the head. The brain tissue was outside the brain cavity due to malformation of the skull cartilage in the left frontal region of the skull (Plate 3, fig. 28).

Liver hernia. Besides the normally occurring umbilical hernia in mouse embryos between the 12th and 16th days, the experimental embryos, after the 'teratological' dose of TEM, fairly often (32·6 per cent.) showed a pronounced liver hernia. One or more lobes of the liver protruded outside the adominal cavity, being as a rule covered with a thin, epidermal membrane (Plate 4, figs. 29–31). Often, however, this membrane seemed to be torn off so that the protruding lobes of the liver were completely unprotected. In some cases it should be noted that the opening in the abdominal wall was much smaller than the diameter of the protruding liver lobe.

In experimental embryos kept till term, and also in embryos dissected by Caesarian section on the 21st day of pregnancy, this condition apparently did not improve. It was presumably the cause of death during birth, because many dead embryos were born with liver hernia which left a round opening 2–3 mm. in diameter in the region of the navel.

Monsters. Among all the experimental embryos two 15-day embryos and one new-born mouse were classified as monsters. One 15-day embryo showed pseudencephaly in which the greatly protruding brain was not covered with any skull cartilage. The appearance of this embryo could be compared with mouse embryos described as 'extracranielle Dysencephalie' by Kaven (1938) or as 'pseudencephaly' by Russell (1950*a*). This embryo also showed a unilateral right microphthalmia, a left coloboma, a pronounced one-lobe liver hernia, and 48 hours general underdevelopment (Plate 4, fig. 32).

The second case showed similar pseudencephaly without any cartilaginous skull cover and a complete absence of some primordia of the vertebral column. This condition is known in teratology as pseudencephaly with total rachischisis. In appearance this monster was dominated by a cap of widely protruding brain on its head and a broad, flat, and unclosed plate of the spinal cord with a slightly marked central groove on its back. On the level of the upper thorax the spinal cord plate was deeply kinked towards the inside of the body. Simultaneously this embryo showed a few other malformations like bilateral microphthalmia, shortening of all limbs, a pronounced liver hernia, and about 48 hours general underdevelopment (Plate 4, fig. 33).

Shortening of limbs. This abnormality seems to affect the forelimbs mainly. It was unilateral in three cases, bilateral in two. If unilateral, it is usually correlated with unilateral microphthalmia on the same side of the body, and with kinking of the axial organs directed towards the same side. Shorter limbs did not, however, show any skeletal abnormalities when examined in embryos stained *in toto* with toluidin blue and cleared after dehydration in benzyl benzoate.

Cauda bifida. As a single malformation this was seldom observed, but it was often present with a general underdevelopment of the body. This malformation affected the very tip of the tail, which in some cases appeared to be divided into two parallel outgrowths $\frac{1}{4}$–$\frac{1}{2}$ mm. long (Plate 4, fig. 3). In others it was only a

marked flattening of the tail tip resulting in the formation of a fish-like tail tip (Plate 2, fig. 14) similar to those observed in series 1.

General underdevelopment. All the abnormalities described above were accompanied by general underdevelopment as compared with 15-day control embryos. There were also embryos which did not show any morphological abnormalities, but were nevertheless generally underdeveloped. This occurred after all doses of TEM, from 1·35 mg. per kg. upwards. After lower doses, however, and when injections were administered on the 5th, 6th, and 7th day of pregnancy, the retardation did not exceed 36 hours. After the higher doses in series 2, the general retardation of development was much more pronounced and reached as much as 96 hours in extreme cases, although the retarded embryos appeared in all respects to be morphologically normal compared with 11- to 14-day control embryos.

It is worth mentioning that in spite of the pronounced underdevelopment observed in 15-day embryos there was no delay in birth.

DISCUSSION

The toxicity of TEM for mouse embryos, resulting in pre-natal mortality, is a marked characteristic of the drug, especially if it is injected into pregnant females 3–5 days after implantation, i.e. during the formation period of the early embryonic organs. If the injections are done earlier (1–3 days after implantation), when the embryos are not beyond the late primitive streak stage, the toxicity of the drug is less. In surviving 15-day embryos there were almost no malformations, although pre-natal mortality was still high. It can be assumed that early treatment with TEM allows recovery or regeneration of the injured tissues. Similarly, irradiation during pre-implantation stages caused a high percentage of pre-natal mortality, but only a negligible incidence of abnormalities in embryos surviving to term (Russell, 1950*b*).

In amphibian embryos treated with TEM Waddington (1958) observed pronounced selective changes in the neural tube cells, which exhibited dense cytoplasmic aggregates of RNA. In chick embryos the neural tube cells increase in size, as do the nuclei and nucleoli (Jurand, 1958). In the mouse, however, there were no distinct differences in the appearance of the cells in nervous tissue; differences were restricted to somite cells only.

In treated 10-day embryos in series 1 and 2 a progressive development of the head-fold was observed, whereas at that time the paraxial mesoderm did not show any signs of metamerism. Since both head-fold and somites normally make their appearance simultaneously at the $7\frac{1}{2}$-day stage (Snell, 1941) the observed feature can be regarded as an asynchronism in the development of these embryonic organs due to injury to mesodermal activity by TEM.

There is a rather sharply defined toxic dose of TEM (1·5 mg. per kg.) which could be called 'the embryonic LD_{50}', i.e. that dose which kills about 50 per cent.

of embryos when injected subcutaneously. Increasing the dose to 0·55 mg. per kg. per day (total dose, 1·65 mg. per kg.) results in the killing of about 90 per cent. of embryos and causes in the remainder several developmental malformations. These malformations, as well as developmental changes in the metamerism of the paraxial mesoderm, seem to be due to the relatively selective toxicity of TEM for organs originating from the mesoderm. This is confirmed by the kinking of the axial organs in 15-day embryos, this being presumably the consequence of the changes described in the somites in the early stages, which occurred in embryos in series 1 and 2. The previously suggested sensitivity of mesoderm structures to TEM (Jurand, 1958) seems to be confirmed.

Another confirmation of the relative selectivity of TEM is the liver hernia, and probably the brain hernia, which occur in mouse embryos after treatment with the 'teratological dose'. These malformations are presumably due to injury of the mesodermal derivatives taking part in the formation of the abdominal wall and skull cartilage, respectively. At the same time liver and brain, originating from other germ layers, develop at the normal rate, causing an asynchronism which results in excess pressure inside the abdominal cavity and the skull.

More difficult to explain is the mechanism of the abnormal development of the eyeball after TEM treatment. This has been known as a mutation in a strain of mouse and described as anophthalmia (Chase & Chase, 1941). Hertwig (1942) described microphthalmia, a similar condition, due to X-irradiation, but could not decide if it should be regarded as a mutation induced by X-rays. Russell (1950*b*) obtained in mouse embryos microphthalmia and coloboma as the result of irradiation of pregnant females.

The incidence of abnormality of the eyeball is fairly frequent after administration of the 'teratological' dose of TEM. The differentiation of the eye, as generally accepted, involves the induction of the lens and cornea by the developing optic cup, and in any case the optic cup plays the role of the factor responsible for lens development. More recently, however, we find claims that head mesenchyme, or its association with other components of the developing eye, plays an important role in the development of this organ. Holtfreter (1939) has proved that medullary eye-plate deprived of head mesenchyme *in vitro* does not develop beyond a very early stage. His experiments have shown that the eye has a very limited developmental potentiality if regarded as an autonomous unit. Similarly, it has been suggested by Liedke (1951) that in *Amblystoma punctatum* the induction of the lens by the eye-cup takes place only if head mesenchyme is able to make the lens ectoderm respond to the optic cup stimulus. Also Koch & Gowen (1939) have pointed out the failure of mesodermal (pseudoendothelial) tissue in an ophthalmic abnormality which they have described in the mouse.

These suggestions dealing with the role of head mesenchyme may support the following interpretation of the cause of the underdevelopment of the eye described in the present paper. As has been stated, in many cases of eyeball abnormality caused by TEM treatment there is a rudimentary lens surrounded

by a comparatively thick layer of head mesenchyme and a vestigial eye-cup with a differentiated pigment layer only. Both lens and eye-cup are fairly close to one another, but apparently their mutual inductive influence is not adequate to ensure full development. It is possible that the more sensitive mesenchyme cells are excluded from the formative process of the eyeball, and that this causes its underdevelopment.

In general, the eyeball underdevelopment induced by TEM treatment can be regarded as a phenocopy, especially of the mutant described by Chase & Chase (1941). The histology of specimens obtained in the present work resembles very closely those described in their paper, particularly those in Plate 2, figs. 20–22.

Malformations induced by TEM, such as cranial defects, anencephaly, and abnormalities of the facial structures were observed by Thiersch (1957) in rat embryos. A short abstract by Nishimura (1957) was also recently published on the influence of TEM on mouse embryos. He found malformations in limbs and jaw, shortening of the tail, inhibition of eyelid development and the splitting of the lips. In a later paper, Kageyama & Nishimura (1959) have shown some malformations of the neural tube and one case of pseudencephaly similar to those described in this paper. The findings of these authors were obtained in embryos kept to term.

SUMMARY

The influence of TEM on mouse embryos has been studied in 10-day and 15-day embryos. Pregnant females were treated on the 5th, 6th, and 7th day and on the 7th, 8th, and 9th day of gestation, respectively.

Ten-day embryos showed, after both variants of TEM administration, a retardation of development which, generally speaking, became more pronounced as the dose increased. A very frequent effect of TEM was the enlargement of the myocoele and, in more severe cases, their disintegration.

If on the 7th, 8th, and 9th days a total dose of 1·5 mg. per kg. was injected in three equal parts, it killed about 50 per cent. of the implanted embryos and was therefore regarded as 'the embryonic LD_{50}'.

A total dose amounting to 1·65 mg. per kg. injected on the same three consecutive days killed about 90 per cent. of the implanted embryos, and the majority of those surviving showed the following developmental malformations: (*a*) kinking and convolution of the axial organs, (*b*) underdevelopment of the eyeball, (*c*) brain hernia, (*d*) liver hernia, (*e*) underdevelopment of skull and backbone resulting in monsters, (*f*) shortening of the limbs, and (*g*) cauda bifida.

ACKNOWLEDGEMENTS

Thanks are due to the British Empire Cancer Campaign for a research grant which has made possible the execution of this work.

I would like to thank Professor C. H. Waddington for suggesting this problem, for helpful advice and discussion, and for reading the manuscript. I also

wish to thank Dr. D. S. Falconer, Deputy Director of the Agricultural Research Council Unit of Animal Genetics, for the facilities in the mouse house. I am grateful to Miss A. P. Gray and Mr. W. W. Taylor for editorial assistance and to Miss Anne R. Wightman for the photographs.

REFERENCES

BUTCHER, E. O. (1929). The development of the somites in the white rat (*Mus norvegicus albinus*) and the fate of the myotomes, neural tube, and gut in the tail. *Amer. J. Anat.* **44,** 381–439.

CHASE, H. B., & CHASE, E. B. (1941). Studies on an anophthalmic strain of mice. I. Embryology of the eye region. *J. Morph.* **68,** 279–95.

FALCONER, D. S. (1958). New inbred strain. *Mouse News Letter*, **18,** 5.

GRÜNEBERG, H. (1943). The development of some external features in mouse embryos. *J. Hered.* **34,** 88–92.

HERTWIG, P. (1942). Neue Mutationen und Koppelungsgruppen bei der Hausmaus. *Z. indukt. Abstamm.- u. VererbLehre*, **80,** 220–46.

HOLTFRETER, J. (1939). Gewebeaffinität, ein Mittel der embryonalen Formbildung. *Arch. exp. Zellforsch.* **23,** 169–209.

JURAND, A. (1958). Action of triethanomelamine (TEM) on early stages in chick embryos. *J. Embryol. exp. Morph.* **6,** 357–62.

KAGEYAMA, M., & NISHIMURA, H. (1959). Developmental anomalies in mouse embryos induced by triethanomelamine (TEM). (In press.)

KAVEN, A. (1938). Das Auftreten von Gehirnmißbildungen nach Röntgenbestrahlung von Mäuseembryonen. *Z. KonstLehre*, **22,** 247–57.

KEIBEL, F. (1937). *Normentafeln zur Entwicklungsgeschichte der Wirbeltiere.* Jena: G. Fischer.

KOCH, F. L. P., & GOWEN, J. W. (1939). Spontaneous ophthalmic mutation in laboratory mouse. *Arch. Pathol.* **28,** 171–6.

LIEDKE, K. B. (1951). Lens competence in *Amblystoma punctatum. J. exp. Zool.* **117,** 573–89.

NISHIMURA, H. (1957). Teratogenic effect of some new antimetabolite and antimitotic substances upon mouse embryos. *Jap. J. exp. Morph.* **11,** 79–80.

RUSSELL, L. B. (1950*a*). X-ray induced developmental abnormalities in the mouse and their use in the analysis of embryological patterns. I. External and gross visceral changes. *J. exp. Zool.* **114,** 545–601.

—— (1950*b*). The effect of radiation on the preimplantation stages of the mouse embryo. *Anat. Rec.* **108,** 521.

SNELL, G. D. (1941). The early embryology of the mouse. In *Biology of the Laboratory Mouse*, ed. G. D. Snell. Philadelphia.

THIERSCH, J. B. (1957). Effect of 2,4,6-triamino-s-triazine (TR), 2,4,6-tris-(ethyleneimino)-s-triazine (TEM) and N, N′, N″-triethylenephosphoramide (TEPA) on rat litter *in utero. Proc. Soc. exp. Biol. N.Y.* **94,** 36–40.

WADDINGTON, C. H. (1958). A note on the effects of some cytotoxic substances on amphibian embryos. *J. Embryol. exp. Morph.* **6,** 365–6.

EXPLANATION OF PLATES

PLATE 1

FIG. 1. 10-day control embryo at 20-somite stage. ×30.

FIG. 2. 10-day embryo at 11-somite stage after treatment with 1·5 mg. TEM per kg. body-weight (1st degree of retardation). ×30.

FIG. 3. 10-day embryo at 5-somite stage after treatment with 1·65 mg. TEM per kg. (2nd degree of retardation). ×30.

FIG. 4. 10-day embryo at 2-somite stage after treatment with 1·65 mg. per kg. (3rd degree of retardation).

FIG. 5. 10-day embryo at primitive streak stage after treatment with 1·95 mg. per kg. (4th degree of retardation). ×30.

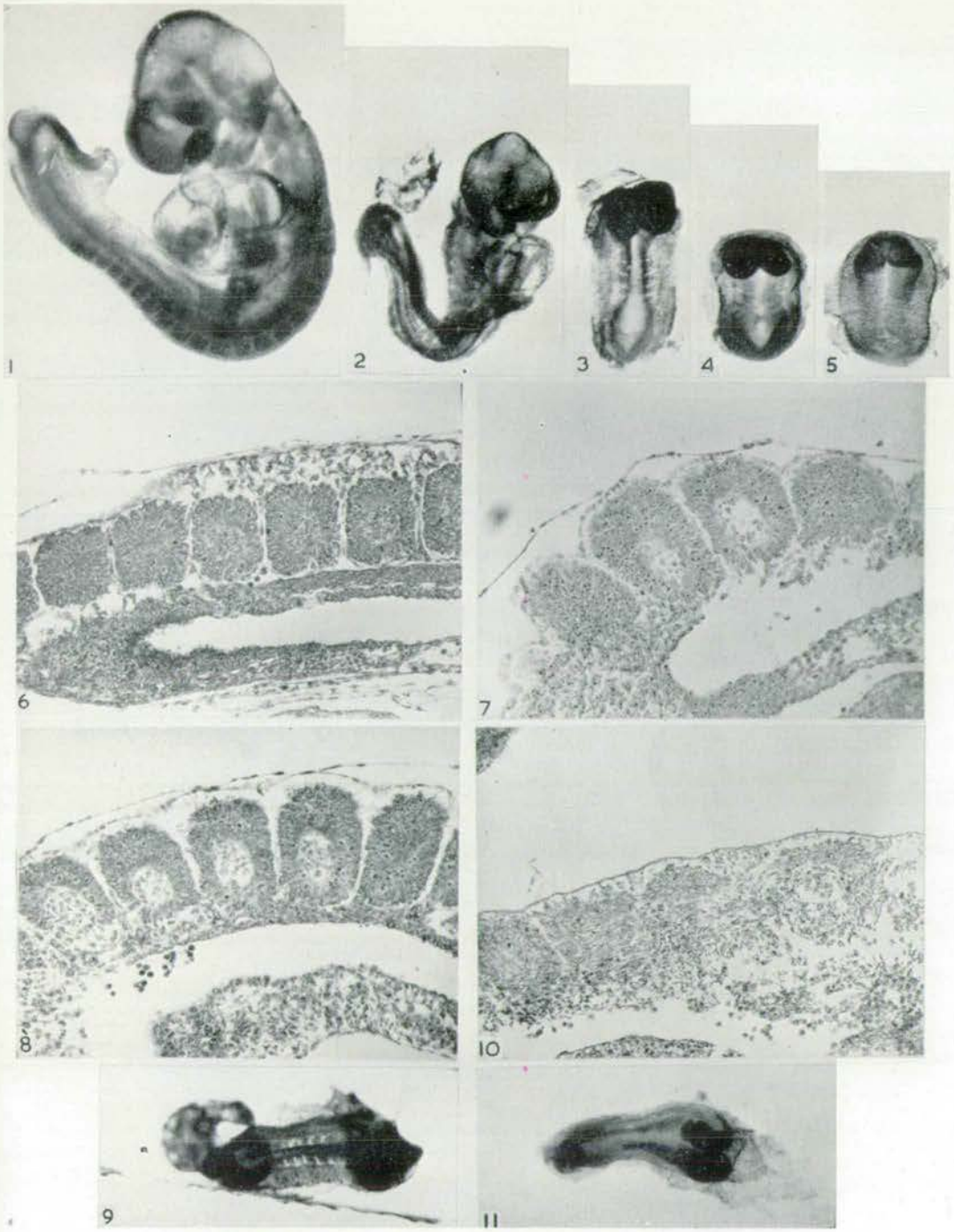

A. JURAND

Plate 1

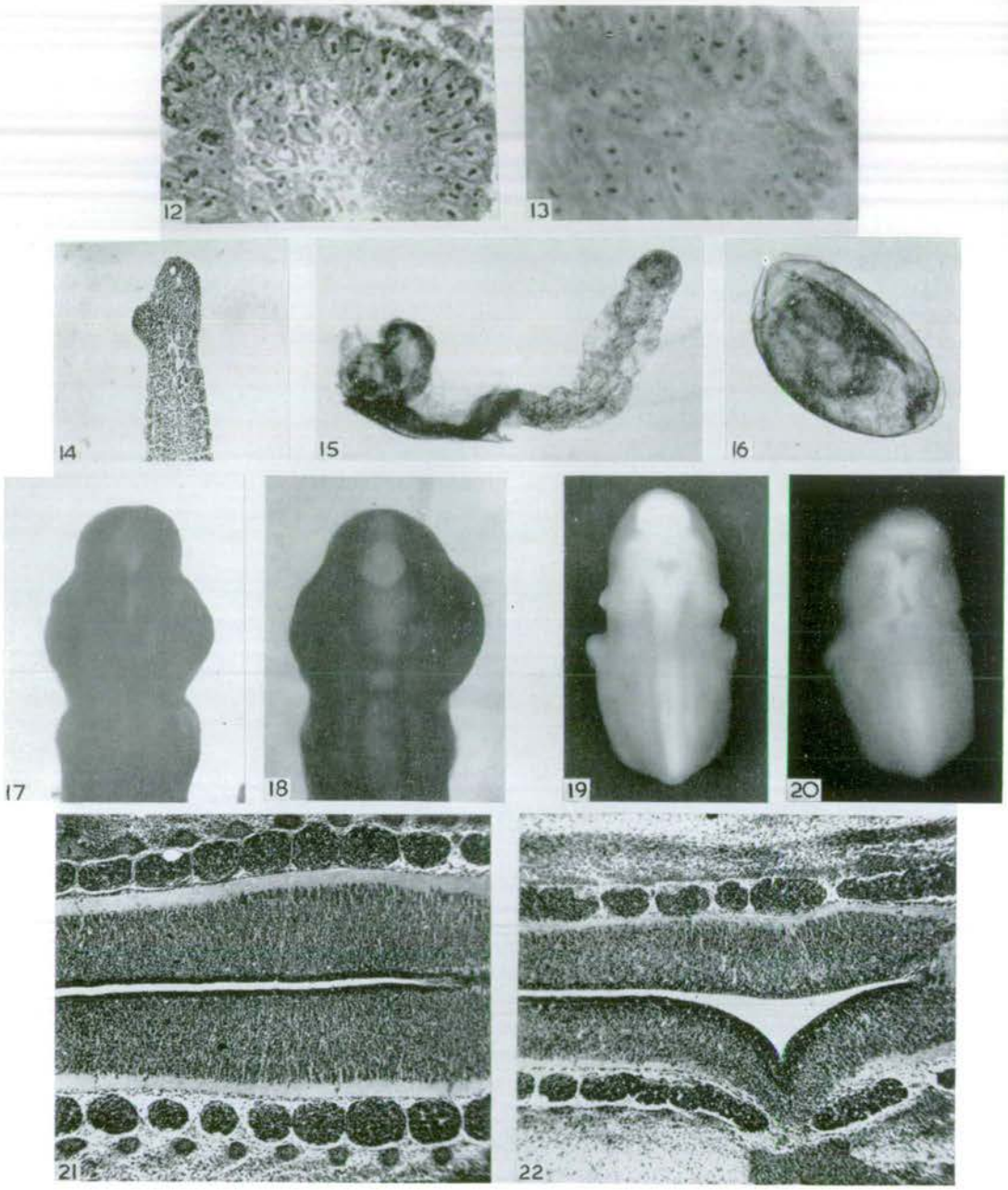

A. JURAND

Plate 2

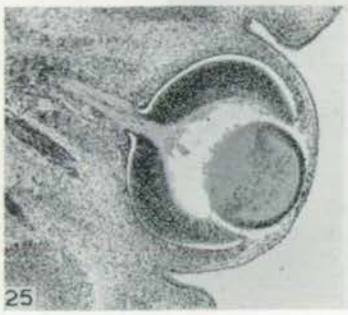

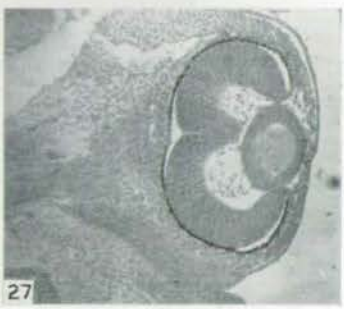

A. JURAND

Plate 3

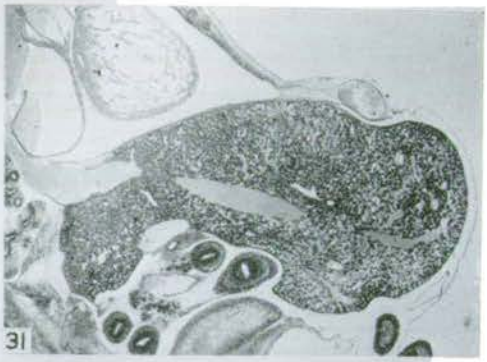

A. JURAND

Plate 4

FIG. 6. Somites of thorax region in 10-day control embryo. ×110.

FIG. 7. Somites of thorax region with moderate widening of myocoele after treatment with 1·35 mg. TEM per kg. ×110.

FIG. 8. Somites of thorax region with very pronounced widening of myocoele after treatment with 1·65 mg. per kg. ×110.

FIG. 9. 10-day embryo showing 2nd degree of retardation with somites of abnormal shape. ×30.

FIG. 10. Progressive disintegration of somites after 1·65 mg. TEM per kg. ×110.

FIG. 11. Primitive streak-stage embryo after treatment with 1·8 mg. per kg. Note well-developed head-fold and no metamerism in paraxial mesoderm. ×30.

PLATE 2

FIG. 12. Cytological picture of a control somite in 10-day embryo. ×380.

FIG. 13. Cytological picture of an experimental somite after treatment with 1·65 mg. per kg. ×380.

FIG. 14. Fish-like tail tip of a 15-day experimental embryo after 1·95 mg. per kg. ×40.

FIG. 15. Experimental 10-day embryo showing 2nd degree of retardation with a shortening of the mid-trunk region but very well-developed head-fold, heart region, and abnormally long allantois. ×30.

FIG. 16. 10-day embryo showing 3rd degree of retardation with a large and spacious yolk sac. ×30.

FIG. 17. Head of a 10-day control embryo. ×30.

FIG. 18. Head of 10-day experimental embryo after 1·65 mg. per kg. Note the dilatation of the brain ventricles (hydrocephalus). ×30.

FIG. 19. Back view of 15-day control embryo. ×4.

FIG. 20. Back view of 15-day experimental embryo with Z-shaped kinking of the axial organs after treatment with teratological dose of TEM. ×4.

FIG. 21. Tangential section of the back through the axial organs of a 15-day control embryo. ×38.

FIG. 22. Tangential section of the back through the kinkage of the axial organs of a 15-day control embryo after treatment with the teratological dose of TEM. ×38.

PLATE 3

FIG. 23. Lateral view of a 15-day control embryo. ×6.

FIG. 24. Lateral view of a 15-day embryo with underdeveloped eyeball after treatment with teratological dose of TEM. ×6.

FIG. 25. Cross-section through the eye of a control 15-day embryo. ×50.

FIG. 26. Cross-section through underdeveloped eye of an experimental 15-day embryo after treatment with the teratological dose of TEM. ×50.

FIG. 27. Cross-section through a malformed eye with concaved retina after treatment with the teratological dose. ×50.

FIG. 28. Experimental 15-day embryo with brain hernia after treatment with the teratological dose of TEM. ×4.

PLATE 4

FIG. 29. Experimental 15-day embryo with liver hernia after treatment with the teratological dose of TEM. ×4.

FIG. 30. Sagittal section through abdominal cavity of a 15-day control embryo. ×20.

FIG. 31. Sagittal section through abdominal cavity and liver hernia of 15-day experimental embryo, after treatment with the teratological dose. ×20.

FIG. 32. 15-day monstrous embryo with anencephaly. ×4.

FIG. 33. 15-day monstrous embryo with anencephaly and rachischiasis. ×4.

FIG. 34. Longitudinal section through the *cauda bifida* in 15-day experimental embryo. ×40.

(Manuscript received 19:iii:59)

Comparative investigations of the action of two nitrogen mustard derivatives on the early stages of development of chick embryos

by A. Jurand

Comparative Investigations of the Action of Two Nitrogen Mustard Derivatives on the Early Stages of Development of Chick Embryos

by A. JURAND[1]

From the Institute of Animal Genetics, Edinburgh

WITH TWO PLATES

CYTOTOXIC compounds act by combining with the biochemical constituents of cells. Because of the complexity of living matter, the cytotoxic activity is highly complicated in nature and is therefore far from being thoroughly understood. In order to analyse the cytotoxicity of any chemical compound, many biological variables concerned in determining the mode of action of the compound and its selectivity for any particular range of cells have to be taken into account (Danielli, 1952, 1954).

Cells of the early embryonic stages are a suitable material for cytotoxic investigations. Although not completely differentiated, they soon arrange themselves into a few embryonic tissues originating directly from the three fundamental germ layers. These tissues consist of cells which may be regarded as the precursors of all the cells of the adult organ. It is interesting to inquire whether they show in these early stages a specific selectivity to cytotoxic compounds which is similar to the selectivity of tumour cells, and which may later be derived indirectly from different germ layers.

One of many biological variables which should be taken into account in cytotoxic investigations is the presence or absence of particular enzymes causing the cells to be more sensitive or more resistant to the cytotoxic drugs concerned. So far, very little information is available on the enzymatic constitution of the germ layers (Steinbach & Moog, 1955). The experiments reported here aimed at comparing the cytotoxic activity of two related derivatives of nitrogen mustard, one of which is an acetyl derivative of the other. Their formulas are as follows:

$H_2N\text{-}C_6H_4\text{-}N(CH_2\text{-}CH_2\text{-}Cl)_2$	$H_3C\text{-}CO\text{-}NH\text{-}C_6H4\text{-}N(CH_2\text{-}CH_2\text{-}Cl)_2$
N-(*p*-amino-phenyl)-2,2′-dichloro-diethylamine ('parent compound')	N-(*p*-acetyl-amino-phenyl)-2,2′-dichloro-diethylamine ('acetyl derivative')

It has been shown that the acetyl derivative is relatively less toxic for rats, and

[1] *Author's address*: Institute of Animal Genetics, West Mains Road, Edinburgh 9, U.K.

[J. Embryol. exp. Morph. Vol. 8, Part 1, pp. 60–67, March 1960]

that it is readily decomposed into its parent compound in tissues where hydrolytic peptidase is available (Danielli, 1954). This takes place particularly in cells of the Walker rat carcinoma, and the acetylation allows a much greater degree of selectivity in the cancerostatic properties. It seemed interesting to find out whether similar decomposition takes place in embryonic tissues and, if so, where and to what extent.

MATERIAL AND METHODS

Chick embryos at the definitive-streak stage (stage 4 according to Hamburger & Hamilton, 1951) explanted from eggs and cultured *in vitro* (New, 1955) were used. The chemical compounds were both obtained from Boots Drugs Co. Ltd., and were applied in a solution of liquid egg albumen containing 10 per cent. of sterile saline (0·9 per cent.). The concentrations of the two compounds are shown in the following table.

TABLE 1

No.	*Concentration*	*Number of embryos treated*	
		Parent compound	*Acetyl derivative*
1	4×10^{-6}	6	5
2	8×10^{-6}	5	4
3	$1{\cdot}6 \times 10^{-5}$	6	6
4	$3{\cdot}2 \times 10^{-5}$	6	7
5	$6{\cdot}4 \times 10^{-5}$	27	21
6	10^{-4}	23	26
7	$1{\cdot}28 \times 10^{-4}$	8	6
8	$1{\cdot}5 \times 10^{-4}$	32	35
9	2×10^{-4}	10	16
10	5×10^{-4}	8	12
11	10^{-3}	4	4

In all the experiments the solutions were administered in amounts of 0·5 c.c. put round the plastic ring used. In the control experiments liquid egg albumen containing 10 per cent. of physiological saline was used. Reincubation of both control and experimental embryos lasted about 24 hours, until the control embryos had developed 15–19 somites, i.e. to stages 12–13 according to Hamburger & Hamilton (Plate 1, fig. 1).

Carnoy's liquid was used as a fixative. For macroscopical examination fixed embryos were stained with Carmalum or Mayer's haematoxylin and prepared as whole mounts. For histological and cytological purposes embedding was performed by standard methods. Transverse or longitudinal sections 6 μ thick were stained with methyl green-pyronine or in Feulgen reagent.

RESULTS

At concentrations lower than $6{\cdot}4 \times 10^{-5}$ (nos. 1–4 in Table 1) neither the parent compound nor the acetyl derivative affected the external appearance or

the microscopical structure of the treated embryos. Higher concentrations (nos. 5–9) of either compound proved to be cytotoxically effective. There was no significant difference between the compounds in degree of cytotoxicity. At the last two concentrations (nos. 10 and 11) both compounds appeared to be highly toxic, causing detachment, shrinkage, and necrosis of the blastoderms.

Macroscopical observations

After the lowest effective doses (nos. 5 and 6) the experimental embryos were found to be at stages 10 or 11, whereas the controls were at stages 12 or 13. Retardation of development became more evident as the concentration increased, being greater in some regions of the embryo than in others. The most severely affected organs appeared to be the paraxial mesoderm, the somites, and the neural tube.

Macroscopical observations indicated that the axial mesodermal structures were the most sensitive parts of the embryo. When solution no. 6 was used, both the parent compound and the acetyl derivative produced embryos with severely affected somites. A mild degree of change was characterized by complete emptiness of the somites, due to the absence of the somite core, and a considerable widening of the myocoele, which made the somites appear to consist of ring-shaped accumulations of mesodermal tissue. Along with this abnormality there was observed a marked shortening of the longitudinal axis of the body as compared to the control embryos. This was due more to the changes in the somite region than to those in the head part (Plate 1, figs. 2, 3).

Further changes, observed after treatment with concentrations nos. 7 and 8 of both compounds, were severe disturbances in the shape and arrangement of the somites, which were much fewer in number and far less dense in structure than those in the control embryos (Plate 1, figs. 4, 5). After higher concentrations, and especially after concentration no. 9, there were found embryos with almost completely disintegrated somites, or with only a few vestigial groups of mesodermal cells in the somite region bearing little resemblance to somites in their arrangement (Plate 1, fig. 6).

In all effective concentrations both compounds frequently caused the paraxial mesoderm to move away from the axial line in the region of the sinus rhomboidalis caudal to the somite region, leaving free areas on both sides. In some embryos there were characteristic symmetrical patterns of defective structure in the paraxial mesoderm (Plate 1, figs. 6, 7, 8, 9).

The neural tube was affected by both substances in the same manner. After concentrations nos. 7, 8, and 9 the brain roof usually remained unclosed (asyntaxia dorsalis), while the rest of the neural tube was unclosed in some parts or, in extreme cases, throughout its entire length (Plate 1, figs. 7, 9).

There were some differences in appearance between heads of embryos treated with the parent compound and those treated with the acetyl derivative. After doses nos. 5 and 6 of the parent compound the heads, although nearly normally

developed, appeared to be much narrower than those of embryos treated with the corresponding solutions of the acetyl derivative, which did not differ very much from the heads of control embryos. Although deprived of some somites and with partially unclosed neural tubes, the heads of these embryos treated with the acetyl derivative appeared almost normal and had mesenchyme cavities filled with the normal quantity of head mesenchyme (Plate 1, figs. 4, 7).

Microscopical observations

After treatment with both compounds, in cytotoxically effective concentrations chosen from the range used in preliminary experiments, the neural tube (i.e. brain and spinal cord), the somites, and, to some extent, the mesenchyme showed pronounced changes in their cytological structure.

The neural tube, after treatment with both compounds in the effective concentrations, showed degenerating cells of various types depending on the concentration used. In embryos treated with concentrations nos. 5–7, both compounds caused an increase in the number of neural tube cells containing nuclei 2–3 times larger than normal, with similarly enlarged nucleoli (Plate 1, figs. 10, 11). Nuclear enlargement, whether slight or very pronounced, appeared to be the first sign of the cytotoxic activity of these compounds. The enlarged nuclei showed poor stainability with methyl green, as can be seen in Plate 1, fig. 11, in which the enlarged nuclei appear to be almost colourless. Experiments using the Feulgen reaction proved, however, that the DNA content of these nuclei did not differ from that of control cells, except that it was more dilute due to the nuclear enlargement.

In embryos treated with the more concentrated solutions (nos. 8 and 9) there were, besides the changes in the size of the cell components, many neural tube cells showing necrotic changes such as karyorrhexis, pycnosis, and nuclear disintegration. Nevertheless, in the immediate neighbourhood of the degenerating cells there were found cells in different phases of cell-division. In the cytoplasm of the degenerating cells there were often found large and fine pyronine-positive granules stained like the nucleoli (Plate 2, figs. 12, 13).

Simultaneously with the changes on the cellular level the neural tube tissue showed increased retardation of its organogenetic development, particularly as regards its closure, as the degenerative changes in the cells became more pronounced.

Microscopical investigations of the somite region in embryos treated with both compounds showed that, in general, these structures are extremely sensitive to increases in the concentrations of the cytotoxic agents. Comparing figs. 14, 15, 16, and 17 of Plate 2 (demonstrating the histological structure of corresponding somites in longitudinal section) one can see the associated stages of degeneration in these important embryonic organs following treatment with different concentrations of the compounds. The more severely affected somites fail to show any differentiation into sclerotome, dermatome, and myotome. In such cases they

represent merely unorganized cell aggregations showing almost no metamerism and are sometimes fused into irregular lumps of mesodermal tissue.

In the experimental embryos examined the somite cells showed changes similar to those in the neural tube cells, although they did not undergo the extreme degenerative processes observed commonly in the latter. The enlargement of the somite cells and of their internal constituents was usually associated with a more or less marked disintegrating effect in their organogenetic appearance.

Other mesodermal structures (heart and extraembryonic mesoderm) did not show any other cytological changes than those described in the somites. Heart anlage, along with the general retardation of development, was usually also retarded. The blood islands showed a normal structure and contained similar numbers of dividing cells to those found in the control embryos.

The head mesenchyme also underwent degenerative changes, which were more noticeable after treatment with the parent compound than after the acetyl derivative. The differences are shown in Plate 2, figs. 18, 19, 20. After treatment with the parent compound the head mesenchyme tissue became less dense and its cells appeared slightly larger, with enlarged nuclei and nucleoli. Their cytoplasm was often vacuolized and their external shape was in most cases spherical, without the usual amoeboid character. These morphological changes suggest loss of the ability of the cells to form pseudopodia and, therefore, defective motility (Plate 2, figs. 21, 22). In extreme cases, after administration of the parent substance in the highest effective concentration (no. 9), the head mesenchyme was almost completely absent and the head mesenchyme cavities were shrunken.

Treatment with the acetyl derivative in similar concentrations did not have any distinct influence on the number or cytological appearance of the head mesenchyme cells. Even after treatment with the highest concentrations they remained similar to the control embryos.

The endodermal cells of the fore-gut and archenteron roof appeared not to be easily influenced by either compound. A comparison of the severely affected neural tube cells with the endodermal cells of the same embryo demonstrated the greater resistance of the latter.

Similarly, the notochord cells were more resistant to the cytotoxic activity of both compounds than were the neural tube and mesodermal cells.

DISCUSSION

According to data given by Danielli (1954, 1959) the LD_{50} (rats) of the parent compound is 6–8 mg. per kg., whereas that of the acetyl derivative is 48–50 mg. per kg. This means that in rats the former compound is roughly 7 times more toxic than the latter.

In the experiments reported here it was found, however, that there was no difference between the two compounds in the effective and toxic doses. This fact seems to suggest that the cytotoxic mechanism of these compounds in embryonic tissues is in some way different from that in the adult rat. If it is true that the acetyl derivative acts cytotoxically after being enzymatically activated, due to hydrolysis by some kind of peptidase, and that it does not act as a whole molecule, it can be assumed that in chick embryos it is decomposed in all the cells except those of the head mesenchyme.

In all the affected tissues degenerative changes were observed. After the lower concentrations the affected cells underwent either slight or severe cytoplasmic, nuclear, and nucleolar enlargement, sometimes reaching as much as 3 times their normal size. At higher doses they showed, in addition, karyorrhexis, pycnosis, and nuclear fragmentation. Similar degenerative effects have been recorded after nitrogen mustard in chicks (Karnofsky, 1950), after triethanomelamine in amphibian embryos (Waddington, 1958) and in chick and mouse embryos (Jurand, 1958, 1959), and after many different antimetabolites and antagonists (Waddington, Feldman, & Perry, 1955; Schultz, 1959).

Changes in somite differentiation have been observed in chick embryos after treatment with amino-acid analogues (Rothfels, 1954; Herrmann, Königsberg-Rothfels, & Curry, 1955) after purine antagonists (Waddington, Feldman, & Perry, 1955), and triethanomelamine (Jurand, 1958, 1959). There is a suggestion that all these changes, induced in such different ways, are due to some not fully understood disturbances in protein synthesis which give rise to the abnormal appearance and the loss of differentiation capacity of the affected tissue.

After treatment with either of these compounds cells at various mitotic stages are always found in the immediate neighbourhood of cells in the process of degeneration. This suggests that neither the parent compound nor its acetyl derivative can be regarded as having antimitotic properties.

The difference between the marked sensitivity of the neural tube, mesodermal structures, and head mesenchyme cells on the one hand, and the resistance of the entoderm and notochord on the other, is striking. There is no clear explanation of this difference. It is known that nitrogen mustard and its derivatives, as well as other related compounds, sometimes have an effect in the case of neoplastic diseases of blood-forming organs that are of mesodermal origin; but in the embryos neural tissue appears to be as sensitive as the axial mesoderm, and there is no evidence for any strong effect on the blood-islands.

The only difference found between the two compounds in the experiments reported here was that the parent compound affects the head mesenchyme cells whereas the acetyl derivative appears to have less effect on this tissue. A possible explanation is that it is due to the low content of hydrolytic protease in the head mesenchyme cells, but, so far, no proof of this has been obtained by cytochemical or histochemical investigations.

SUMMARY

1. N-(*p*-amino-phenyl)-2,2′-dichloro-diethylamine and its acetyl derivative have the same degree of toxicity for early stages of chick embryo development.

2. In concentrations of $6{\cdot}4 \times 10^{-5}$ to 2×10^{-4} they cause degeneration of the neural tube and somite cells. The first sign of degeneration is the enlargement of the affected cells. More severe damage (karyorrhexis, pycnosis, and nuclear disintegration) leads to pronounced disturbances in the differentiation of the affected organs.

3. The parent substance causes degeneration of the head mesenchyme, whereas its acetyl derivative is much less effective in this tissue.

4. Both compounds have comparatively little effect on the endodermal structures, the notochord, the heart, or the lateral mesoderm.

ACKNOWLEDGEMENTS

The author wishes to express his gratitude to the British Empire Cancer Campaign for the grant which enabled the prosecution of this work. Grateful thanks are due to Professor C. H. Waddington under whose direction this work was done and who was so kind as to read and discuss the manuscript. Last, but not least, the author thanks Miss A. P. Gray for the editorial advice and Miss A. R. Whightman for printing the photographs.

REFERENCES

DANIELLI, J. F. (1952). Cytochemical and cytological studies of drug action. *Nature, Lond.* **170,** 863–5.

—— (1954). The designing of selective drugs. In *Leukaemia Research* (Ciba Foundation Symposium). London: Churchill. 263–74.

—— (1959). Personal communication.

HAMBURGER, V., & HAMILTON, H. L. (1951). A series of normal stages in the development of the chick embryo. *J. Morph.* **88,** 49–92.

HERRMANN, H., KÖNIGSBERG-ROTHFELS, U., & CURRY, M. F. (1955). A comparison of the effects of antagonists of leucine and methionine on the chick embryo. *J. exp. Zool.* **128,** 359–78.

JURAND, A. (1958). Action of triethanomelamine (TEM) on early stages of chick embryo. *J. Embryol. exp. Morph.* **6,** 357–62.

—— (1959). Action of triethanomelamine (TEM) on early and later stages of mouse embryo. *J. Embryol. exp. Morph.* **7,** 526–39.

KARNOFSKY, D. A. (1950). Nitrogen mustards in the treatment of neoplastic disease. *Advanc. internal Med.* **4,** 1–75.

NEW, D. A. T. (1955). A new technique for the activation of the chick embryo *in vitro*. *J. Embryol. exp. Morph.* **3,** 326–31.

ROTHFELS, U. (1954). The effect of some amino-acid analogues on the development of the chick embryo *in vitro*. *J. exp. Zool.* **125,** 17–35.

SCHULTZ, P. W. (1959). A note on Ω-brom-allyl-glycine-induced pycnosis in explanted chick embryos. *Exp. Cell Res.* **17,** 353–6.

STEINBACH, E. B., & MOOG, F. (1955). Cellular metabolism. In *Analysis of Development*, ed. Willier, Weiss, & Hamburger. Philadelphia and London: Saunders Co.

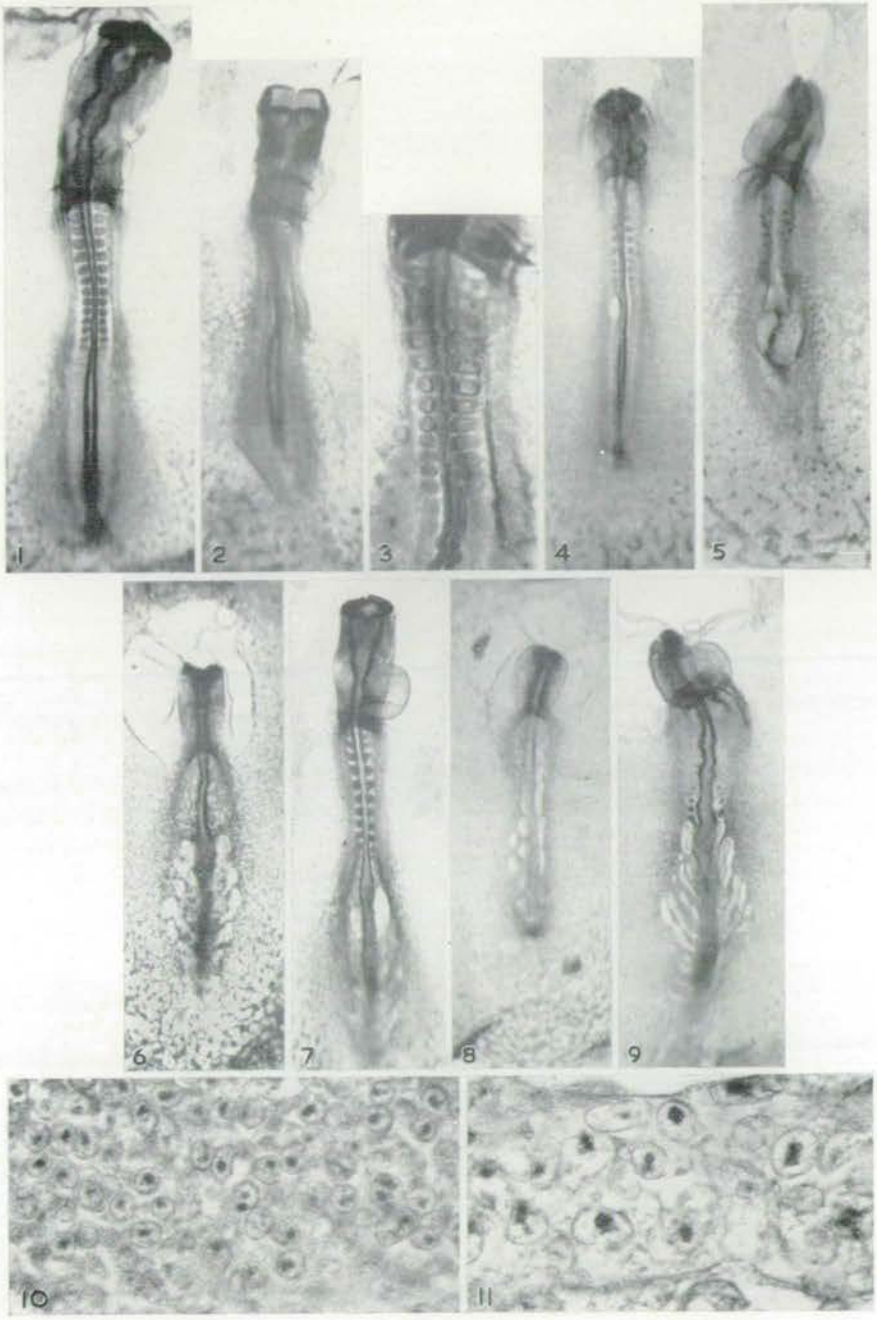

A. JURAND

Plate 1

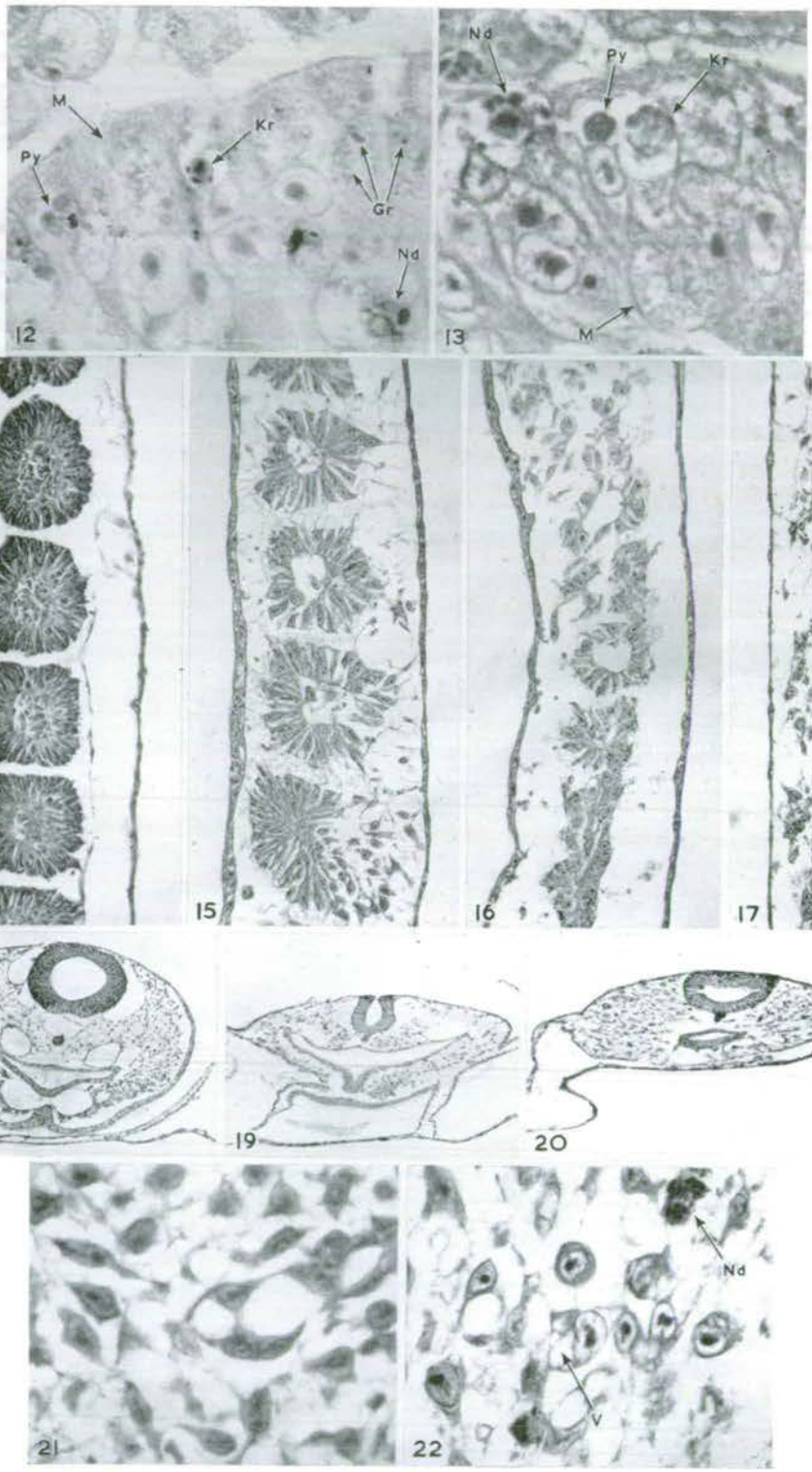

A. JURAND

Plate 2

WADDINGTON, C. H. (1958). A note on the effect of some cytotoxic substances on amphibian embryos. *J. Embryol. exp. Morph.* **6**, 365–6.

—— FELDMAN, M., & PERRY, M. M. (1955). Some specific developmental effects of purine antagonists. *Exp. Cell Res.* Suppl. 3, 366–80.

EXPLANATION OF PLATES

PLATE 1

FIG. 1. Macroscopical view of a control embryo of 15-somite stages. ×20.

FIG. 2. An embryo treated with the parent compound (concentration $6{\cdot}4 \times 10^{-5}$). Note a marked shortening of the body-length. ×20.

FIG. 3. The somite region of the same embryo as Fig. 2. Note ring-shaped somites. ×50.

FIG. 4. An embryo treated with the acetyl derivative ($1{\cdot}28 \times 10^{-4}$). Note the decreased number and the less dense structure of somites. ×20.

FIG. 5. An embryo treated with the parent compound ($1{\cdot}28 \times 10^{-4}$). Note irregular arrangement of somites. ×20.

FIG. 6. An embryo treated with the acetyl derivative (2×10^{-4}). Note nearly complete lack of somites. ×20.

FIG. 7. An embryo treated with the parent compound ($6{\cdot}4 \times 10^{-5}$) showing comparatively normal development, but narrow head and unclosed neural tube in its caudal end. ×20.

FIG. 8. An embryo treated with acetyl derivative ($1{\cdot}5 \times 10^{-4}$). Note nearly complete lack of somites, destructive changes in the paraxial mesoderm, unclosed neural tube, but almost normally developed head. ×20.

FIG. 9. An embryo treated with the parent compound ($1{\cdot}5 \times 10^{-4}$). Note unclosed neural tube, vestigial somites, and the symmetrical pattern of the destructive changes in the caudal mesoderm. ×20.

FIG. 10. Neural tube cells of a control chick embryo at 15-somite stage. ×500.

FIG. 11. Neural tube cells of an embryo treated with the parent compound (10^{-4}). ×500.

PLATE 2

FIG. 12. Neural tube cells of an embryo treated with the parent compound ($1{\cdot}5 \times 10^{-4}$). *Py*, pycnosis; *Kr*, karyorrhexis; *Nd*, nuclear disintegration; *Gr*, pyronin positive granules in the cytoplasm; *M*, dividing cell. ×830.

FIG. 13. Neural tube cells of an embryo treated with the acetyl derivative ($1{\cdot}5 \times 10^{-4}$). *Py*, pycnosis; *Kr*, karyorrhexis; *Nd*, nuclear disintegration; *M*, dividing cell. ×830.

FIG. 14. Longitudinal section through somites of a control embryo. ×150.

FIG. 15. Longitudinal section through the somites of an embryo treated with the parent compound ($6{\cdot}4 \times 10^{-5}$). ×150.

FIG. 16. Longitudinal section through somites of an embryo treated with the acetyl derivative ($1{\cdot}28 \times 10^{-4}$). ×150.

FIG. 17. Longitudinal section through the somite region of an embryo treated with acetyl derivative (2×10^{-4}). Note the vestigial structure of the somites. ×150.

FIG. 18. Transversal section through the head of a control embryo. ×80.

FIG. 19. Transversal section through the head of an embryo treated with the parent compound ($1{\cdot}5 \times 10^{-4}$). Note the unclosed neural tube and loose mesenchyme tissue. ×80.

FIG. 20. Transverse section through the head of an embryo treated with the acetyl derivative ($1{\cdot}5 \times 10^{-4}$). Note nearly normal condition. ×80.

FIG. 21. Head mesenchyme cells of a control embryo. ×600.

FIG. 22. Head mesenchyme cells of an embryo treated with the parent compound. *V*, vacuolization of the cytoplasm; *Nd*, nuclear disintegration. Note the spherical shape of the cells. ×600.

(Manuscript received 21:ix:59)

(4)

Further investigations on the cytotoxic and morphogenetic effects of some nitrogen mustard derivatives

by A. Jurand

Further Investigations on the Cytotoxic and Morphogenetic Effects of Some Nitrogen Mustard Derivatives

by A. JURAND[1]

From the Institute of Animal Genetics, Edinburgh

WITH FIVE PLATES

PREVIOUS experiments with TEM (triethanomelamine) on chick and mouse embryos (Jurand, 1958, 1959) have shown that some embryonic regions are more sensitive than others to its cytotoxic activity. TEM appeared to be specifically active against mesodermal structures, particularly against the somitic mesoderm, being relatively less active against other tissues. In amphibian embryos, however, the neural tube cells were the most sensitive (Waddington, 1958).

N-(*p*-amino-phenyl)-nitrogen mustard (the parent compound) and its acetyl derivative, which have been investigated on chick embryos (Jurand, 1960), have been shown to be specifically toxic to the mesodermal and neural cells. The affected regions were injured primarily at the cellular level, due to the cytotoxic properties of these compounds. The changes at the cellular level were followed by abnormal development of the somites and neural tube.

The present investigations represent further comparative studies on the activity of closely related nitrogen mustard derivatives in chick and mouse embryos, and aim at confirming localized susceptibility to these compounds. In addition to the parent compound and its acetyl derivative, a fluoro-acetyl derivative ('fluorine derivative') was used, viz.

$$FCH_2—CO—NH—C_6H_4—N(CH_2—CH_2—Cl)_2.$$

This compound is considered to be more readily decomposed by hydrolytic enzymes to the parent compound in Walker rat carcinoma cells than is the acetyl derivative and it therefore was expected to be more selective as a carcinostatic factor (Danielli, 1960).

MATERIAL AND METHODS

Experiments on chick embryos were performed with the fluorine derivative only, as the other two compounds had already been examined using this material and the results have been reported (Jurand, 1960).

[1] *Author's address*: Institute of Animal Genetics, West Mains Road, Edinburgh 9, U.K.

[J. Embryol. exp. Morph. Vol. 9, Part 3, pp. 492–506, September 1961]

The preliminary external examination of the embryos after they were excised from the uterus included an assessment of the degree of retardation of development and identification of the external characteristics, such as general body-shape, the line of the vertebral column and spinal cord, the size and shape of the eyes, the presence of liver hernia, the appearance of the limbs or limb-buds, &c. The central nervous system, eyes, mesodermal structures, and, where this seemed necessary, certain other structures were subjected to histological and cytological examination.

The stages of development of the mouse embryos were compared with data available in the literature (Grüneberg, 1943; Snell, 1941) and with the control material.

Table 1 gives the numerical data of the animal material used in all experiments.

TABLE 1

	Number of pregnant females	*Number of embryos*
Parent compound . . .	108	627
Acetyl derivative . . .	160	896
Fluorine derivative . . .	234	1,416
Control	66	528
TOTAL	568	3,467

RESULTS

The effect of the fluorine derivative on chick embryos

The effective dosage of this compound was determined after some preliminary experiments and appeared to be of a range similar to that of the parent compound and its acetyl derivative. Concentrations lower than 2×10^{-4} proved to have very little or no visible influence on development, whereas those higher than 8×10^{-4} were lethal for all experimental embryos. Hence there was a comparatively narrow range of concentrations which could be used for these experiments.

The lowest effective concentration, 2×10^{-4}, did not markedly retard the general development of the embryos. The number of somites averaged not less than the number of somites in the control embryos, but in 19 out of 24 cases the neural tube showed selective reactivity, remaining unclosed either in parts or along its entire length. In the first case the affected parts of the neural tube were the rhombencephalon, the region on the level of the 5th to the 9th somite and the caudal part of the neural plate. The latter remained unclosed so that the sinus rhomboidalis persisted longer than in the control embryos. In embryos of this group the anterior neuropore also failed to close.

In the case of total non-closure of the neural plate or neural groove, which

Chick embryos at stage 4 (Hamburger & Hamilton, 1951) were explanted from eggs and cultured *in vitro* according to the method described by New (1955). As the compound is hardly soluble, it was suspended in an appropriate volume of 0·9 per cent. saline solution. One part of this suspension was added to nine parts of liquid albumen, so that the final concentrations of the suspensions were: 10^{-4}, 2×10^{-4}, 4×10^{-4}, and 8×10^{-4} (w/v). The suspensions were administered in amounts of 0·5 ml. round the culture rings used for cultivation of the explanted embryos. Re-incubation took place for 22–24 hours, i.e. until the control embryos had reached 12 or 13 according to Hamburger & Hamilton (1951). In these experiments 109 experimental and 56 control chick embryos were used.

The material was prepared for histological examination by standard methods described previously (Jurand, 1958, 1960). Some of the experimental and control embryos were examined in the electron microscope in order to see the details of the necrotic changes in the neural tube. These embryos were fixed with 1 per cent. buffered osmic tetroxide solution (Palade, 1952), embedded in methacrylate, sectioned with an ultramicrotome, and viewed in a Siemens Elmiscop I.

In order to compare the results obtained from the experiments on chick embryos treated with the fluorine derivative and those reported previously, the specificities of the compounds were examined also on 10-, 13-, and 15-day-old mouse embryos mainly of the JC and to a lesser extent of the JU strain.

Two- to five-months-old females with vaginal plugs were injected subcutaneously under slight anaesthesia with the newly prepared solution or suspension of the drugs. (The parent compound is fairly soluble, but the other two had to be applied in the form of suspensions.) The doses were calculated in mg. per kg. of the actual body-weight as the differences between molecular weights of the compounds concerned are small, and were divided into three equal parts which were injected on three consecutive days, either the 6th, 7th, and 8th days or the 7th, 8th, and 9th days of pregnancy, the day on which the plug was found being regarded as the 1st day. The experimental animals were weighed before each injection and were injected at the same time each day.

The animals were killed by cervical dislocation on the 10th, 13th, or 15th day of pregnancy. After preliminary fixation with Carnoy's fluid (6:3:1) in the intact uterus for about 3 hours, the embryos were dissected and fixed again for another 12 hours in the same fixative. For histological purposes the embryos were dehydrated with absolute alcohol for 6 hours, then cleared in methyl benzoate and embedded in wax. The orientation of the embryos for sectioning was done according to the group of organs to be examined. Sections 6–7 μ thick were stained with methyl green-pyronin. Some embryos were prepared as whole mounts after staining with Mayer's haematoxylin.

For purposes of comparison control mouse embryos of ages from 8 to 15 days' post conception were used. Pregnant control females were anaesthetized on the injection days without being injected.

they are present in small numbers only, as most have undergone conversion into cytoplasmic constituents (Plate 2, fig. 7).

After treatment with the fluorine derivative there occurred many different necrotic changes which could be distinguished more easily by means of the electron microscope. From histological examination of the experimental embryos it is seen that the first symptom of cytotoxic activity is the enlargement of the cells; in extreme cases they may be referred to as giant cells. These cells may be up to 3 times larger than normal cells. The electron density of all their parts remains similar to that of the control cells. In the cytoplasm, however, signs of necrotic changes can be found, in particular pronounced vacuolization, side by side with large granules which appear to be thick-walled vacuoles, presumably identical with the pyronine-positive granules known from light microscope examination of these embryos. The mitochondria also appear to be enlarged (Plate 2, fig. 8).

Simultaneously with the enlargement of the nuclei, the nucleoli usually also become enlarged in relation to the nuclei, as is shown in Plate 2, fig. 8. In some cases, however, there occurred cells with enlarged nucleoli which showed no distinct change in the size of the nuclei (Plate 2, fig. 8).

Other necrotic changes that follow treatment with higher doses appear mostly in nuclei. The first sign is the dissolution of the nucleolus and the simultaneous gradual vacuolization of the structure of the nucleus which ceases to show its normal fine granular appearance. Underneath the nuclear membrane there appear dense masses which are known to be deeply stainable with nuclear stains. This stage of necrosis with more or less advanced changes in the cytoplasm, is assumed to be karyorrhexis (Plate 2, fig. 10).

In the cytoplasm of these cells further necrotic changes are observed which lead to advanced vacuolar destruction of the cells, resulting eventually in complete disintegration of both nuclei and cytoplasm. Such disintegrated tissue fragments, if examined in the electron microscope, are difficult to recognize as having cellular structure at all. They consist merely of very dense solid masses of homogeneous structureless material which presumably represent remains of nuclei, and complex yolk granules in various, probably abnormal, stages of delayed digestion (Plate 3, fig. 11).

True pycnosis of the nuclei is one of the stages in necrosis. It appears morphologically in various patterns as a less common response to the cytotoxic activity. In such cases the nuclei consist always of denser material, often surrounded by a more homogeneous envelope underneath the nuclear membrane. In general, the nuclei are smaller in these cells, but their cytoplasm is comparatively well preserved (Plate 3, fig. 12).

The effects of the parent compound, acetyl and fluorine derivatives on mouse embryos

Natural prenatal mortality in stages later than the 10th day of gestation

occurred sometimes after treatment with a concentration of 2×10^{-4} and always after 4×10^{-4}, general development was usually retarded. In cross-sections the neural plate appeared to be open and in most cases completely flat, forming a medullary plate instead of a neural tube. It was flat especially in the head region where it failed to show any depression in the median line (Plate 1, figs. 1, 2). In other cases the medullary plate, unclosed along its entire length, formed rather a V-shaped groove, also in the head region (Plate 1, fig. 3).

When intermediate concentrations were used there was no particular abnormalities in other tissues, except that, because of general under-development, the number of somites was, on average, less than that in control embryos, so that the experimental embryos were found to be only at stage 10 or 11 according to Hamburger & Hamilton (1951). The specificity of the fluorine derivative in these concentrations for the developing neural tube seemed to be more pronounced than in the case of the acetyl derivative.

At the cellular level, in the unclosed medullary plates, frequent abnormalities, confined exclusively to the neural cells, were observed. There were found many giant cells (i.e. hypertrophied cells each with a single nucleus) and cells with pycnotic and necrotically disintegrated nuclei (Plate 1, fig. 4). All these changes occurred alongside normal looking cells (which were in the majority) and those undergoing mitotic division. In some cases, however, mitosis was abnormal, e.g. tripolar metaphase (Plate 1, fig. 5).

After application of still higher concentrations, e.g. 6×10^{-4} and 8×10^{-4}, the neural tissue appeared to be completely destroyed. It consisted entirely of necrotic and deformed cells with very dense, shrunken nuclei staining dark greenish-blue with methyl green. The neural plate was in these cases practically non-existent; its necrotic cells formed only an open, more or less shallow groove (Plate 1, fig. 6). Other tissues of these embryos were also affected, although much less than the neural tube cells. The next most severely affected tissue appeared to be the somitic mesoderm.

Necrotic changes as seen by the electron microscope

The neural tube cells of control embryos at stages 12–13 of development appear in electron micrographs to consist of comparatively large nuclei surrounded by a thin layer of cytoplasm. The electron density of the internal content of the nuclei is slightly different from that of the cytoplasm. In some cases it is less, in others higher, presumably depending on what stage the cell is in its life-cycle. The nucleolus, with a diameter averaging one-fifth to one-quarter of that of nucleus, is much denser than is the nucleus, and contains many small vacuoles. There are also cells with more than one nucleolus and, in some cases, cells with small fragments of nucleolar material alongside the main nucleolus. The nuclear membrane has a double-layered structure. In the cytoplasm there are abundant, often elongated mitochondria with the usual lamellar structure, and yolk granules of all types, as described by Bellairs (1958), although at this stage

occurs very rarely in the strains of mice used in these experiments. In 34 control females only about 1 per cent. of dead embryos were found on the 15th day of pregnancy. Like TEM, the compounds used in the present experiments cause a high incidence of prenatal mortality if used in doses above a certain threshold. They differ considerably, however, in the level of their threshold dose, and, as in previous experiments on TEM, the embryonic LD_{50} was therefore determined for each of the compounds. The embryonic LD_{50} is the total dose which, if administered subcutaneously in three equal parts on the 7th, 8th, and 9th days of pregnancy, kills by the 15th day of pregnancy about 50 per cent. of implanted embryos. Similarly, the lethal doses (LD_{50}) for adult mice were determined.

Table 2 gives the embryonic LD_{50} as compared with the LD_{50} of the compounds under investigation.

TABLE 2

	LD_{50}	*Embryonic LD_{50}*
Parent compound .	15 mg. per kg.	12 mg. per kg.
Acetyl derivative .	65 ,,	36 ,,
Fluorine derivative .	80 ,,	45 ,,

The parent compound (108 pregnant females). Compared with the other two derivatives, the parent compound shows, in mice, a comparatively small difference between the embryonic LD_{50} and the dose resulting in the prenatal mortality of all embryos, and therefore the doses used in these experiments were restricted to 9, 10·5, 12, and 13·5 mg. per kg. All doses higher than the last named resulted in complete mortality of embryos, or caused the death of the pregnant females 24 hours or more after the last injection. In all cases death was preceded by acute diarrhoea, due to extensive inflammation of the intestinal tract.

After effective doses, injected in three equal parts either on the 6th, 7th, and 8th day or on the 7th, 8th, and 9th day of pregnancy, no selective effects in particular embryonic regions were recorded. The only effect was retardation of development, amounting, on the average, to about 1 day in 10-day-old embryos and up to 3 days in 13-day-old embryos, according to the dose used.

In 36 females injected with the embryonic LD_{50} or with 13·5 mg. per kg. on the 7th, 8th, and 9th day of gestation the 145 surviving embryos showed general retardation of development by 2–3 days. Among these embryos were some with unilateral microphthalmia (12 per cent.) and liver hernia (8 per cent.). Both these abnormalities were macroscopically and histologically of the same kind as those described previously after treatment with TEM (Jurand, 1959).

Microscopical examination of the retarded 10- and 13-day-old foetuses did not reveal any specificity of the parent compound. In less-retarded individuals no tissues appeared to deviate from their normal histological performance, whereas in those more retarded all the tissues were injured to the same extent, showing severe necrotic changes.

Acetyl and fluorine derivatives (394 pregnant females). The ranges of the

effective doses per kg., divided into three equal parts and injected on three consecutive days, were 24–45 mg. for the acetyl derivative and 30–54 mg. for the fluorine derivative. The results will be reported together as there were no qualitative differences between the effects of these two compounds on mice.

In 10-day-old embryos, after injection with low effective doses on the 6th, 7th, and 8th days of gestation, both compounds slowed down the rate of development by 1–2 days in rough proportion to the dose used. The most sensitive region appeared to be the medullary plate which remained open in the majority of embryos of this age group (Plate 4, fig. 13). The rest of the body did not show any abnormalities. After higher doses, however, besides the necrotic changes in the open medullary plate, the mesodermal structures showed scattered necrotic changes (Plate 4, fig. 14).

In 13-day-old embryos the susceptibility of the neural tube tissue was still more pronounced, particularly after injections on the 6th, 7th, and 8th days of gestation. The total doses used in these experiments were 36 or 45 mg. per kg. of the acetyl derivative and 45 or 54 mg. per kg. of the fluorine derivative; in other words, the doses were equal to, or 20–25 per cent. higher than, the respective embryonic LD_{50} of these compounds.

In the surviving embryos, apart from general underdevelopment by up to 3 days, necrotic changes which were confined, after lower doses, almost exclusively to the neural tube tissue, were observed after the use of both compounds. In the majority of surviving embryos of this group the neural tube was found to be closed. This was presumably due to the fact that all the more severely injured embryos with unclosed neural tubes had died before the 13th day of gestation, i.e. before the day of fixation. The extent of necrosis of the neural tube tissue showed a considerable individual variation. In some cases the necrosis was confined to the deeper part of the organ, affecting up to half of it, but in extreme cases the entire cross-section showed necrotic damage (Plate 4, figs. 15, 16, 17, 18).

In cases of confinement of necrosis to the deeper part of the neural tube, although the upper part contained also some randomly scattered necrotically changed cells, such as giant, karyorrhectic, and pycnotic cells, it consisted, in general, of healthy-looking cells, some of which were even in the process of mitotic division. The deeper part of the neural tube of these embryos consisted entirely of necrotic, apparently dead tissue, with deformed nuclei that stained deeply with methyl green. As can be seen in figs. 16, 17, and 18 of Plate 4, there was always present within the lumen of this part of the neural tube a kind of cellular debris which stained mainly red with pyronin. In addition, the damaged part showed in many cases complicated convolutions, whereas the healthy upper part did not deviate in its structure from the axial line (Plate 4, fig. 19).

In this group there were few embryos with necrosis of the deeper part of the neural tube, which was closed as far as the trunk region and open towards its caudal end (Plate 4, fig. 20).

All these anomalies occurred after the use of both acetyl and fluorine derivatives but with higher frequency with the latter. All but the last were identical with those observed after treatment with TEM (Jurand, 1959). Table 3 shows the frequency of the above malformations together with those after the parent compound expressed in percentages:

TABLE 3

*Type of malformation**	*Parent compound*	*Acetyl derivative*	*Fluorine derivative*
Kinking and convolution of the axial organs	—	16	19
Unilateral and bilateral microphthalmia	12	19	22
Liver hernia	8	17	24
Shortening of limbs	—	15	33
Number of embryos investigated	145	242	267

* In many cases embryos in these groups showed more than one of above malformations and therefore were recorded more than once.

DISCUSSION

The present investigations have shown that the two derivatives of aminophenyl nitrogen mustard, unlike the parent compound, first cause abnormalities in the process of neural tube closure if applied in the lowest effective dose at early stages of embryonic development. The appearance of this anomaly is parallel with or is followed by the first, still mild, necrotic changes in the cells of the neural plate, where giant cells and cells in the process of karyorrhexis or pycnosis are randomly scattered between normal cells.

After higher doses the neural plate tissue undergoes more profound necrosis with distinct localization, whereas the remaining structures of the embryo appear to be still normal or show only some minor necrotic changes. In extreme cases, when the dose used is still higher, all embryonic tissues undergo necrosis, resulting in early prenatal mortality and resorption of mouse embryos. Histologically these embryos, if fixed while still alive, resemble embryos treated with the parent compound.

A detailed comparison of all the experimental material of both chick and mouse embryos suggests that the embryonic germ-layers and the embryonic tissues derived from them can be arranged in the following approximate order of decreasing susceptibility to the compounds under investigation: medullary plate or neural tube > mesoderm and mesenchyme > entoderm > ectoderm.

Surviving 15-day-old mouse embryos, if examined histologically, are found to be largely those in which the neural tube injuries have been healed and which show only abnormalities caused by injury to the mesodermal structures similar to that following treatment with TEM (Jurand, 1959). This fact suggests that neural tube injury is much more critical for the future development of the embryo than is injury of the mesodermal structures.

Localized cell necrosis confined to particular embryonic regions has been

In cases in which the entire neural tube consisted of thoroughly necrotic cells, which occurred particularly after higher doses, extensive changes in some mesodermal structures, e.g. in the somitic mesoderm and mesenchyme cells, were also found. In such embryos the cells in the deepest part of the neural tube had already disappeared, so that in this region the continuity of the neural tube was broken (Plate 4, fig. 18).

A comparison of the effects of the above derivatives on the neural tube after different doses and in different embryos leads to the conclusion that there exists a gradient in the sensitivity of the neural tube to these compounds. The maximum sensitivity is in the deepest part, and it decreases in the opposite direction. This seems to be the reason why the continuity of the neural tube is broken in cases of severe necrosis, as the deepest part, being affected first, undergoes complete necrosis and resorption earlier.

In some cases regeneration of the neural tube presumably took place, so that no, or less severe, necrotic changes were actually present, but the organ showed some structural defects (Plate 4, fig. 21).

In other embryos, after the same doses, the brain and the medullary parts of the neural tube had a typically hydrocephalic appearance. In these cases the widened neural tube, when histologically examined, was seen to have extremely thin walls, in some regions only a single cell thick, showing at the same time scattered necrotic cells (Plate 4, fig. 22).

In a number of embryos of this group, particularly in those with more advanced necrosis of the neural tube, a very distinct difference could be seen between the susceptibilities of the two main components of the developing eye to the cytotoxic activity of the two derivatives. The optic cup was changed necrotically simultaneously with necrotic changes in the deepest part of the neural tube, whereas the lens primordium, which was by this time induced and invaginated, appeared to consist of healthy-looking cells, similar to those in corresponding control embryos (Plate 5, figs. 23, 24).

In the experimental embryos the mesoblast of the limb-buds also showed necrotic changes. In Plate 5, figs. 25 and 26, there are shown dorso-ventral sections through the limb-bud of an experimental embryo and corresponding control. The internal mesoderm of the experimental limb-bud shows extensive necrotic changes, whereas the epidermis and the 2- to 3-celled layer of the adjacent mesoderm are well preserved and do not differ from the corresponding layers of the control limb-bud.

In 15-day-old embryos, which survived the treatment with the embryonic LD_{50}, and in those receiving slightly higher doses (up to 10 per cent. more) injected either on the 6th, 7th, and 8th days or on the 7th, 8th, and 9th days of the gestation, there were found the following morphogenetic malformations: (1) kinking and convolution of the axial organs, (2) unilateral and bilateral underdevelopment of the eye ball resulting in microphthalmia, (3) liver hernia, and (4) shortening of the limbs.

reported by many authors working with cytotoxic substances, and with amino-acid and purine analogues. Recently Schultz (1959), for example, reported that the somitic mesoderm of early chick embryos, as well as other tissues, shows extensive pycnotic changes after treatment with Ω-brom-allyl-glycine (BAG) due to its leucine requirement.

The restriction of injury to the neural plate, which remains open and flat both in the chick and in the mouse embryos described in this report, recalls the results of Brachet (1958, 1959) and of Brachet & Delange-Cornil (1959), which were obtained after β-mercaptoethanol treatment of amphibian eggs. This compound was found to inhibit the movements of the presumptive medullary plate cells at the gastrula-neurula stage, which results in a flat medullary plate instead of neural tube without any visible influence on other systems. These authors attribute their findings to the reducing property of β-mercaptoethanol, which maintains the —SH groups in the neural plate cells in the reduced form, thus causing a disturbance in metabolism. It seems reasonable to assume that nitrogen mustard derivatives, after being decomposed by hydrolysing enzymes to their parent compound in tissues containing such enzymes in higher concentration, interfere with the biochemical balance, although they probably do so at a different point in the metabolic process. It is widely accepted that the alkylating agents disturb the mechanism of DNA synthesis (Bodenstein, 1954) and as a result they disturb the synthesis of specific proteins (Danielli, 1954) indispensable for the morphogenetic development of the sensitive organ.

It is true that the spontaneous failure of neural tube closure called platyneury occurs sometimes in normal chick embryos but this phenomenon is always associated with anomalies in somite formation (Grünwald, 1935). In the present investigations no such anomalies in the somites of experimental embryos with neural plate non-closure were found after fluorine derivative, and the frequency of the injury was so high, even when the lowest effective concentration was used, that this effect cannot be compared with spontaneous platyneury. Moreover, there were no control embryos similar to the experimental ones. Last, but not least, spontaneous platyneury in mouse embryos is not known and yet the acetyl and fluorine derivatives, if used in proper dosage, prevent the closure of the neural tube.

In addition to causing injury to the medullary plate, both the acetyl derivative, as reported previously (Jurand, 1960), and the fluorine compound (particularly in higher dosage) have an adverse effect on the mesoderm. In the present investigations the fluorine derivative caused necrosis of the mesoblast in the limb-buds, leaving unharmed the outer layer, which is 2–3 cells thick, and the limb-bud epidermis, as well as the apical ectodermal ridge. This fact suggests that the epidermis and the underlying thin mesoblast layer are less susceptible than the deeper mesodermal cells. What causes the difference between the outermost and the internal cells of the mesoblast is not known. Possibly there are some biochemical similarities between the external layer of the mesoblast and the

epidermal cells due to their close proximity anatomically, but it may also be that the outermost layer of the mesoblast has some relation to the so-called 'refractile' layer of the mesoblast, which seems to play an epidermis-like role in limb differentiation. This problem has recently been the subject of discussion (Bell, Saunders, & Zwilling, 1959; Grüneberg, 1960).

As far as the process of necrobiosis is concerned, it is well known that it is basically a natural process occurring in practically all living tissues, both in those in the course of differentiation and growth and those of adult organisms. The different stages of necrosis resulting from the cytotoxic activity of the compounds under investigation seem to be of the same nature as those described by many authors in normal tissues, like those in the regressing tissues of tadpoles' tails, or developing tissues (Leuchtenberger, 1950; Glücksmann, 1951; and others). It seems probable that cell death, regardless of its cause, follows the same pathway and results in the same cytological abnormalities of the nucleus, the cytoplasm, or both.

When the present data are looked at from a more general point of view some confirmation can be found of certain principles of teratogeny put forward by Wilson (1960). His second principle states that in some cases different agents produce characteristic patterns of defects due to similar action upon specific phases of metabolism in embryonic tissues. In other words, it seems that these characteristic patterns may result from the similar susceptibility of certain embryonic tissues to different agents, e.g. TEM, acetyl and fluorine derivatives, in respect of their activity against mesodermal structures. This might be the reason that in 15-day-old mouse embryos the teratological effects following the use of compounds under investigation are similar to those after triethanomelamine.

In conclusion, it should be emphasized that the influence of the acetyl and fluorine derivatives may be regarded as specific with regard to their morphogenetic effect on the neural plate non-closure; but the necrotic changes in the attacked organs are in general the same as after other radiomimetic agents. Some of the affected cells break down soon after treatment and others, arrested at the interphase, continue to grow and to reach giant proportions.

SUMMARY

The cytotoxic and morphogenetic activity of N-(*p*-amino-phenyl)-2, 2′-dichlorodiethylamine and its acetyle and fluoro-acetyl derivatives was studied on chick and mouse embryos.

In chick embryos the fluorine derivative showed a specific affinity for the medullary plate, causing inhibition of neural tube closure at lower concentrations and complete destruction of the medullary plate at higher concentrations.

Electron microscope observations of the affected neural cells showed some examples of necrotic changes after treatment with the fluorine derivative in chick embryos.

The parent compound and its acetyl and fluorine derivatives slow down the developmental rate of the mouse embryos. Here also, the tissue most sensitive to acetyl and fluorine derivatives appeared to be the neural tube, particularly it deepest part. The extent to which it is affected depends on the dose of the cytotoxic agent, so that a gradient in the sensitivity of the neural tube seems likely.

After higher doses the cytotoxic influence extends to other embryonic tissues which can be arranged as follows according to decreasing sensitivity: medullary plate or neural tube > mesoderm and mesenchyme > entoderm > ectoderm.

Older (i.e. 15-day-old) mouse embryos show malformations due to injury to the mesodermal structures, presumably because those with neural tube injuries either fail to survive or regenerate them. In the last case the injury to the mesodermal structures result in anomalies like convolution and kinking of axial organs, liver hernia, microphthalmia, &c.

RÉSUMÉ

Nouvelles recherches sur les effets cytotoxiques et morphogénétiques de quelques dérivés de l'ypérite nitrée

On a étudié, sur des embryons de poulet et de souris, l'activité cytotoxique et morphogénétique de la N-(*p*-amino-phényl)-2,2′-dichlorodiéthylamine et de ses dérivés acétylé et fluoro-acétylé.

Sur l'embryon de poulet, le dérivé fluoré a montré une affinité spécifique pour la plaque médullaire, inhibant la fermeture du tube nerveux aux concentrations les plus faibles, et détruisant complètement la plaque médullaire aux concentrations élevées.

Observées au microscope électronique, les cellules neurales atteintes montraient quelques exemples de modifications nécrotiques après un traitement par le dérivé fluoré, chez l'embryon de poulet.

Le composé initial et ses dérivés fluoré et acétylé ralentissent le rythme de développement des embryons de souris. Ici encore, le tube nerveux apparaît comme étant le tissu le plus sensible aux dérivés fluoré et acétylé et, en particulier, dans sa région la plus profonde. L'extension des lésions dépend de la dose du facteur cytotoxique, de sorte que l'existence d'un gradient de sensibilité du tube nerveux paraît vraisemblable.

Aux doses élevées, l'influence cytotoxique s'étend aux autres tissus embryonnaires, qui peuvent être rangés comme suit selon leur sensibilité décroissante: plaque médullaire ou tube nerveux > mésoderme et mésenchyme > endoderme > ectoderme.

Les embryons de souris plus âgés (15^{e} jour) présentent des malformations dues aux lésions des structures mésodermiques, sans doute parce que ceux dont le tube nerveux a subi des lésions ou bien ne survivent pas, ou bien les réparent. Dans ce dernier cas, les lésions des structures mésodermiques provoquent des

anomalies telles que: enroulement et plissement des organes axiaux, hernie hépatique, microphtalmie, &c.

ACKNOWLEDGEMENTS

The author would like to express his gratitude to the British Empire Cancer Campaign for the research grant which made execution of this work possible.

Grateful thanks are due to Professor C. H. Waddington for helpful discussions and advice, as well for reading the manuscript.

I am indebted to Professor J. F. Danielli for supplying the compounds used in the investigations. I also wish to thank Dr. D. S. Falconer, Deputy Director of the Agricultural Research Council Unit of Animal Genetics, Edinburgh, for the facilities in the mouse house, Miss A. P. Gray for editorial help, and Miss Patricia Collins for technical assistance.

REFERENCES

BELL, E., SAUNDERS, J. W., JR., & ZWILLING, E. (1959). Limb development in the absence of ectodermal ridge. *Nature, Lond.* **184,** 1736–7.

BELLAIRS, R. (1958). The conversion of yolk into cytoplasm in the chick blastoderm as shown by electron microscopy. *J. Embryol. exp. Morph.* **6,** 149–61.

BODENSTEIN, D. (1954). Effects of radiomimetic substances on embryonic development, with special reference to nitrogen mustard. *J. cell. comp. Physiol.* **43,** 179–205.

BRACHET, J. (1958). Effect of β-mercaptoethanol on morphogenesis in amphibian eggs. *Nature, Lond.* **181,** 1736–7.

—— (1959). The role of sulfhydryl groups in morphogensis. *J. exp. Zool.* **142,** 115–39.

—— & DELANGE-CORNIL, M. (1959). Recherches sur le rôle des groupes sulfhydriles dans la morphogénèse. *Develop. Biol.* **1,** 79–100.

DANIELLI, J. F. (1954). The designing of selective drugs. In *Leukemia Research* (Ciba Foundation Symposium). London: Churchill. 263–74.

—— (1960). Personal communication.

GLÜCKSMANN, A. (1951). Cell death in normal vertebrate ontogeny. *Biol. Rev.* **26,** 59–86.

GRÜNEBERG, H. (1943). The development of some external features in mouse embryos. *J. Hered.* **34,** 88–92.

—— (1960). Genetical studies on the skeleton of the mouse. XXV. The development of syndactylism. *Genet. Res.* **1,** 196–213.

GRÜNWALD, P. (1935). Teratologische Untersuchungen über die mutmasslichen Beziehungen der abnormen und normalen Medullaranlage zur Entwicklung der Urwirbel beim Huhne. *Roux Arch. EntwMech. Organ.* **133,** 664–93.

HAMBURGER, V., & HAMILTON, H. L. (1951). A series of normal stages in the development of the chick embryo. *J. Morph.* **88,** 49–92.

JURAND, A. (1958). Action of triethanomelamine (TEM) on early stages of chick embryos. *J. Embryol. exp. Morph.* **6,** 357–62.

—— (1959). Action of triethanomelamine (TEM) on early and later stages of mouse embryos. *J. Embryol. exp. Morph.* **7,** 526–39.

—— (1960). Comparative investigations of the action of two nitrogen mustard derivatives on the early stages of development of chick embryos. *J. Embryol. exp. Morph.* **8,** 60–67.

LEUCHTENBERGER, C. (1950). A cytochemical study of pycnotic nuclear degeneration. *Chromosoma,* **3,** 449–73.

NEW, D. A. T. (1955). A new technique for the cultivation of the chick embryo *in vitro*. *J. Embryol. exp. Morph.* **3,** 326–31.

PALADE, G. E. (1952). A study of fixation for electron microscopy. *J. exp. Med.* **95,** 285–98.

SNELL, G. D. (1941). The early embryology of the mouse. In *Biology of the Laboratory Mouse,* ed. G. D. Snell, Philadelphia.

SCHULTZ, P. W. (1959). A note on Ω-bromo-allyl glycine-induced pycnosis in explanted chick embryos. *Exp. Cell Res.* **71,** 353–6.

WADDINGTON, C. H. (1958). A note on the effect of some cytotoxic substances on amphibian embryos. *J. Embryol. exp. Morph.* **6,** 365–6.

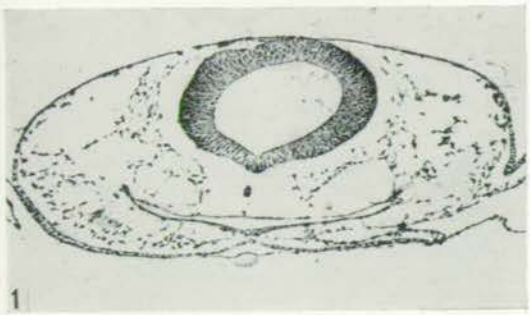

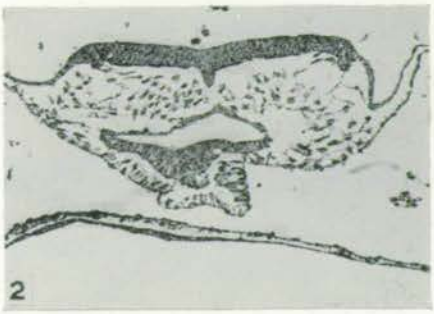

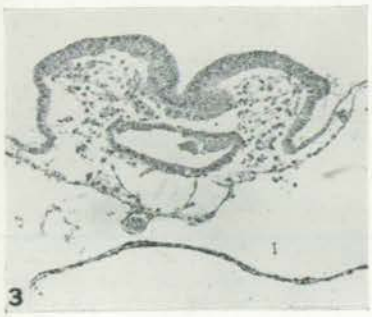

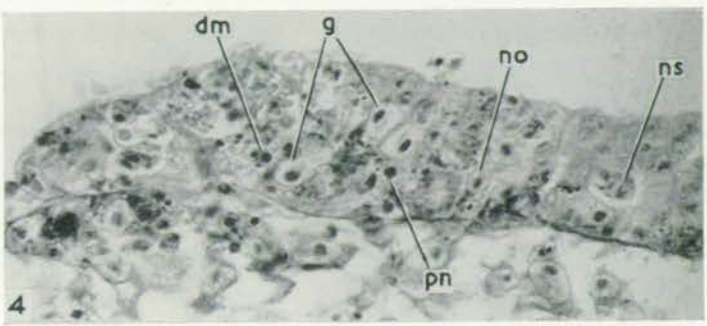

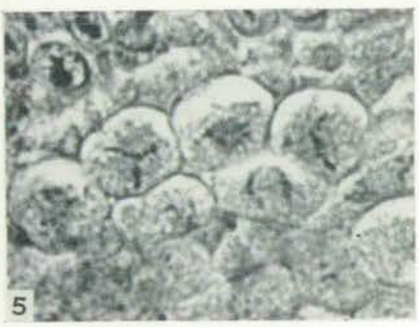

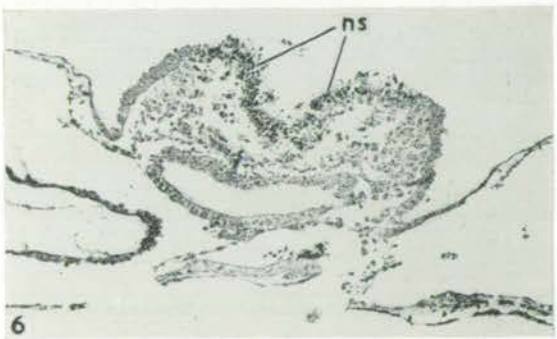

A. JURAND

Plate 1

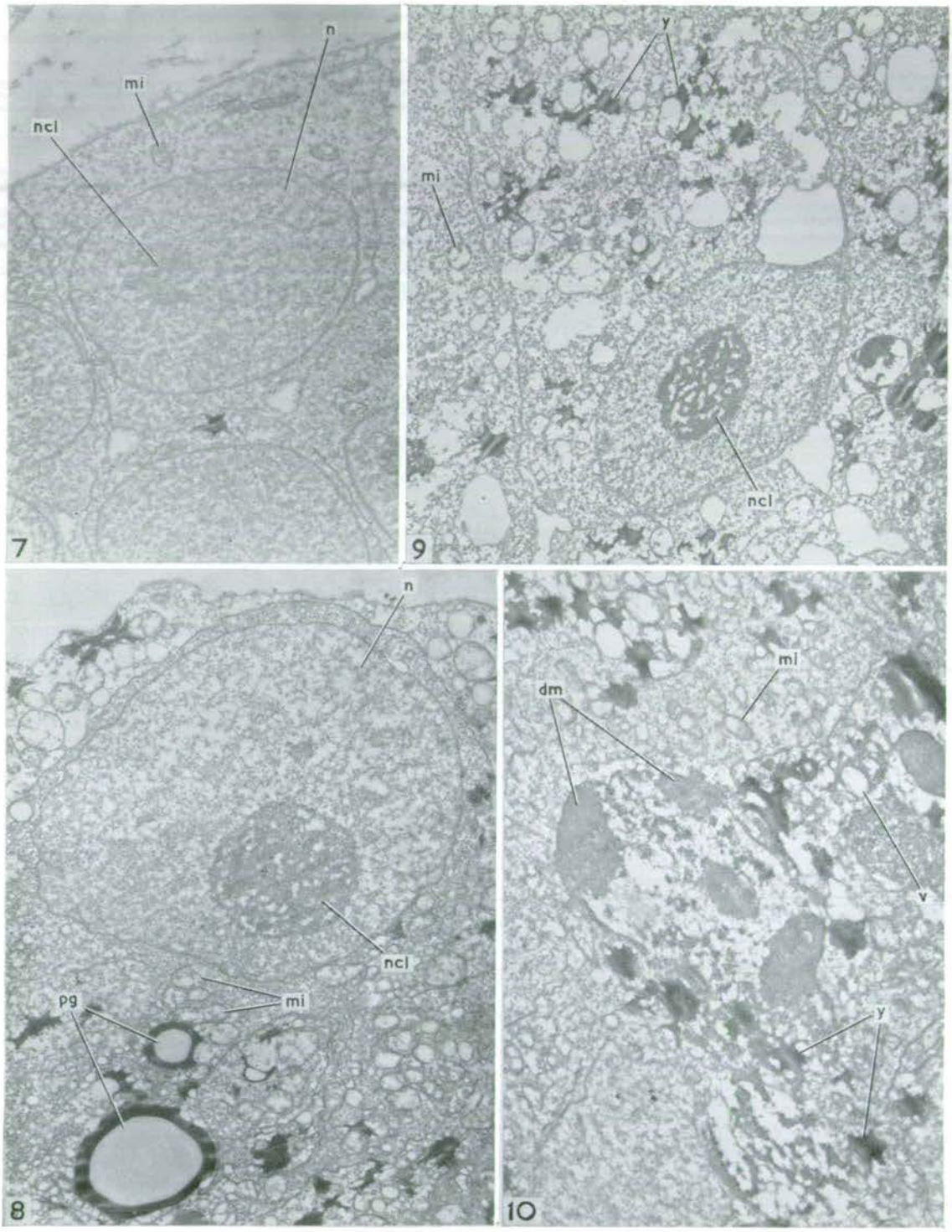

A. JURAND

Plate 2

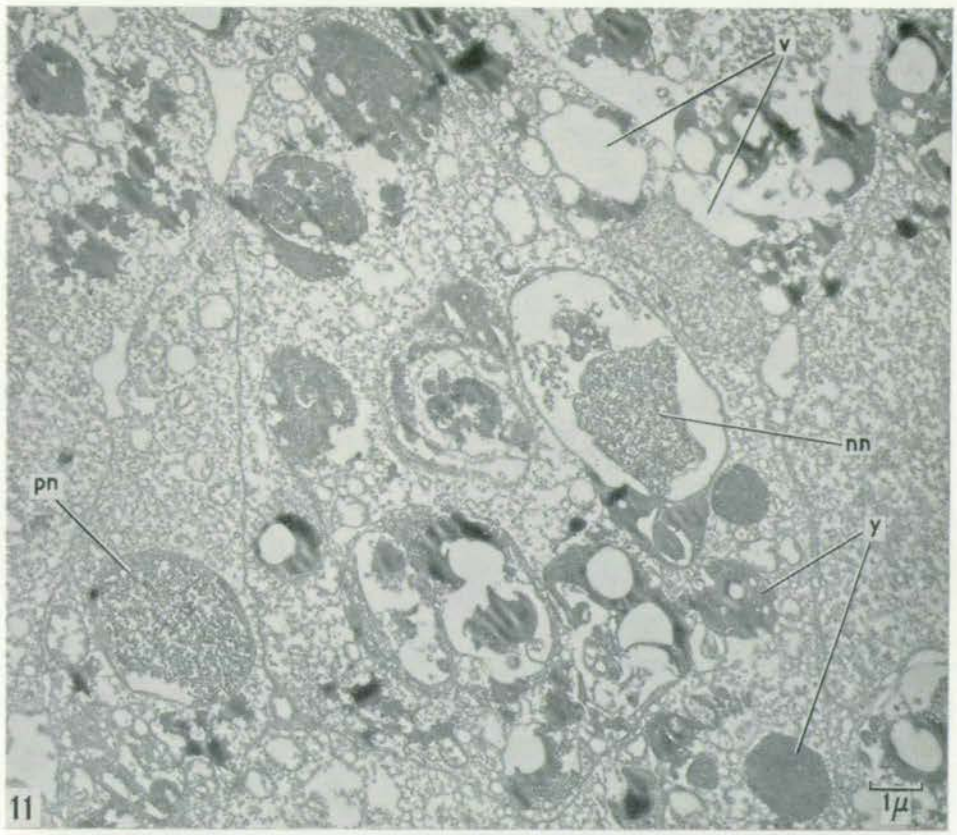

A. JURAND

Plate 3

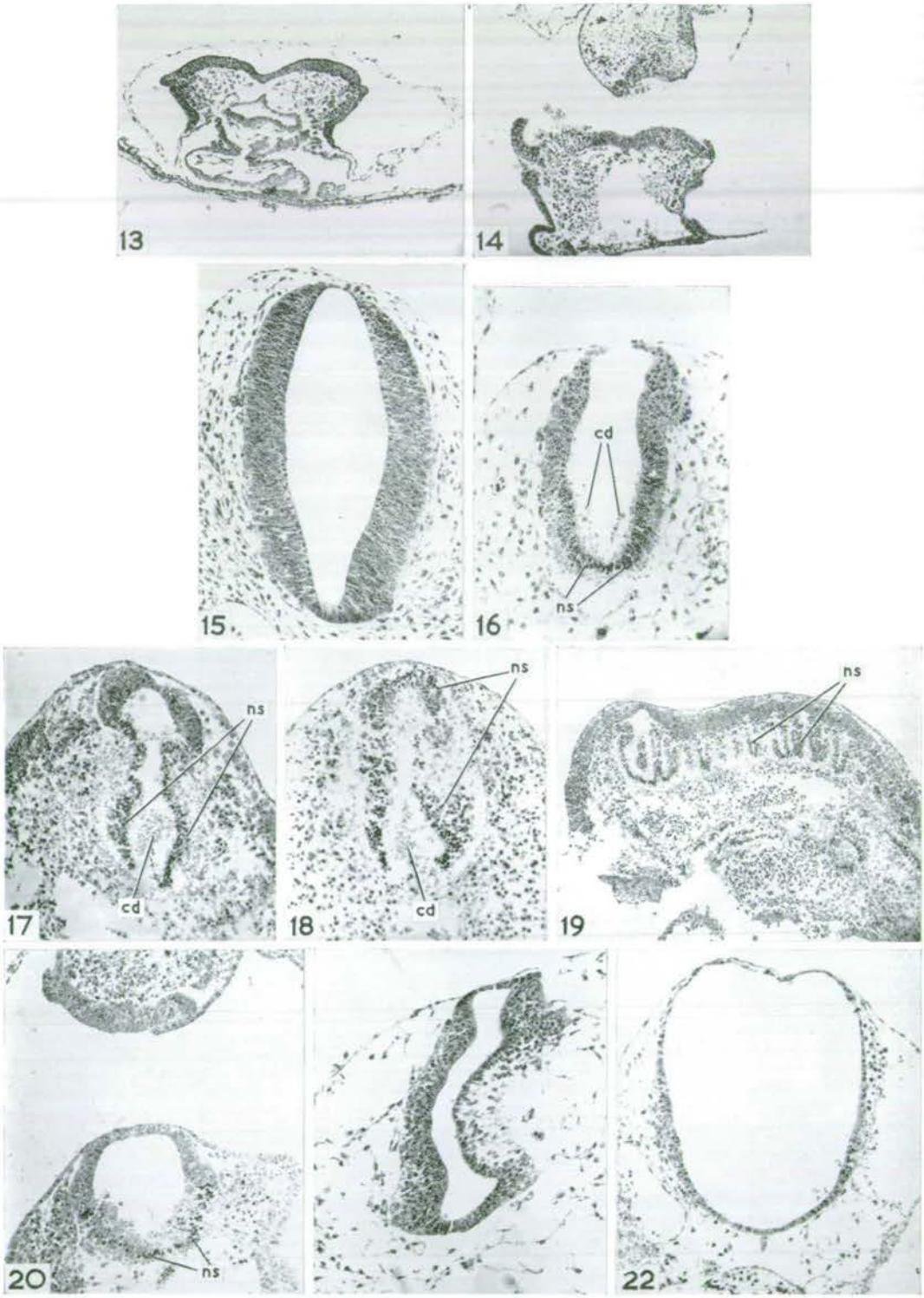

A. JURAND

Plate 4

EXPLANATION OF PLATES

Abbreviations: *cd*, cellular debris; *dm*, dense masses of necrotic chromatin; *ec*, eye cup; *g*, giant cells; *lp*, lens primordium; *mi*, mitochondria; *nc*, nucleus; *ncl*, nucleolus; *nn*, nuclear necrosis; *no*, normal cell; *ns*, necrosis; *pg*, pyronin positive granules; *pn*, pycnotic nucleus; *v*, vacuolization of cytoplasm; *y*, yolk granules.

PLATE 1

FIG. 1. Transverse section through the head of a control chick embryo (stage 12). ×80.

FIG. 2. Transverse section through the head of a chick embryo treated with fluorine derivative in concentration 2×10^{-4}. Note the flat neural plate. ×80.

FIG. 3. Transverse section through the head of a chick embryo treated with fluorine derivative (4×10^{-4}). Note a few necrotic cells at the bottom of the groove. ×80.

FIG. 4. Portion of an open neural plate of a chick embryo treated with fluorine derivative (4×10^{-4}). ×420.

FIG. 5. Tripolar metaphase in the neural plate of a chick after treatment with fluorine derivative. ×700.

FIG. 6. Transverse section through the head of a chick embryo treated with fluorine derivative (8×10^{-4}). Note complete necrosis of neural cells. ×80.

PLATE 2

FIG. 7. Electron micrograph of a control neural tube cell (chick). *mi*, mitochondria; *nc*, nucleus; *ncl*, nucleolus. ×8750.

FIG. 8. Electron micrograph of a giant cell in the chick neural plate after treatment with fluorine derivative (4×10^{-4}). ×8750.

FIG. 9. A chick neural tube cell with an enlarged nucleolus (*ncl*)–fluorine derivative (4×10^{-4}). ×8750.

FIG. 10. A chick neural tube cell in the stage of karyorrhexis after treatment with fluorine derivative (6×10^{-4}). Note the dense masses of necrotic chromatin (*dm*) at the periphery of the nucleus. ×8750.

PLATE 3

FIG. 11. Severely damaged neural tube tissue after treatment with fluorine derivative (8×10^{-4}). Note an advanced stage of nuclear necrosis (*nn*) in comparison with slightly less injured pycnotic nucleus (*pn*) in the lower left side of the photograph and yolk granules (*y*) in different stages of preservation. ×6600.

FIG. 12. Neural tube cells in chick after treatment with fluorine derivative (6×10^{-4}). In the middle there is a cell with a dense pycnotic nucleus (*pn*), beside a normal cell (*no*) with well-preserved nucleoli (*ncl*). ×10000.

PLATE 4

FIG. 13. Transverse section through the head of a 10-day-old mouse embryo after treatment with fluorine derivative (total dose 36 mg. per kg.). ×60.

FIG. 14. Transverse section through the head of a 10-day-old mouse embryo after treatment with acetyl derivative (total dose 45 mg. per kg.) ×60.

FIG. 15. Transverse section through the neural tube of a control 13-day-old mouse embryo. ×115.

FIG. 16. Transverse section through the neural tube of a 13-day-old mouse embryo treated with fluorine derivative (total dose 36 mg. per kg.). Note the necrotic changes (*ns*) at the bottom of the neural tube and the cellular debris (*cd*). ×115.

FIG. 17. Transverse section through the neural tube of a 13-day-old mouse embryo treated with fluorine derivative (total dose 42 mg. per kg.). Necrotic changes (*ns*) occupy more than half of the neural tube. ×115.

FIG. 18. Similar section after treatment with acetyl derivative (total dose 45 mg. per kg.). Note extensive necrosis (*ns*) in all tissues. ×115.

FIG. 19. Longitudinal section through a 13-day-old embryo treated with fluorine derivative (total dose 45 mg. per kg.). Note the comparatively well-preserved upper part of the neural tube and necrosis (*ns*) of the lower part, with convolutions. ×60.

FIG. 20. Transverse section through a 13-day-old mouse embryo after treatment with acetyl derivative (total dose 42 mg. per kg.). Note partial necrosis (*ns*) of the deeper part of the neural tube in the

trunk region and the open neural plate in the tail region. Retardation in the development amounted in this case to about 3 days. ×100.

FIG. 21. Transverse section through the neural tube which regenerated after injury by fluorine derivative (total dose 36 mg. per kg.). ×115.

FIG. 22. Transverse section through the hydrocephalic neural tube after treatment with fluorine derivative (total dose 42 mg. per kg.).

PLATE 5

FIG. 23. Section through the developing eye of a control 11-day-old mouse embryo. ×330.

FIG. 24. Section through the developing eye of a 13-day-old mouse embryo treated with fluorine derivative (total dose 42 mg. per kg.). Note well-preserved lens primordium (*lp*) and many necrotic changes (*ns*) in the eye-cup. ×330.

FIG. 25. Dorso-ventral section through the limb-bud of an 11-day-old control mouse embryo. ×125.

FIG. 26. Dorso-ventral section through the limb-bud of a mouse embryo treated with fluorine derivative (total dose 48 mg. per kg.). Note the well-preserved epidermis and the adjacent layer of the mesoderm in comparison with necrosis (*ns*) of the internal part of the mesoblast. ×125.

(*Manuscript received 30:i:61*)

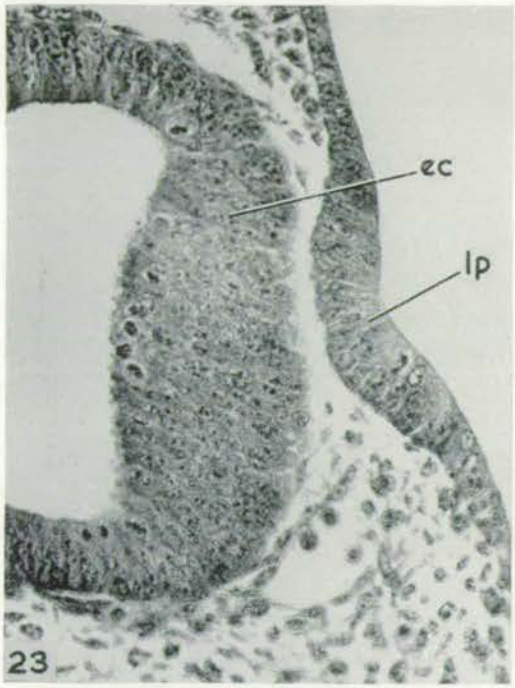

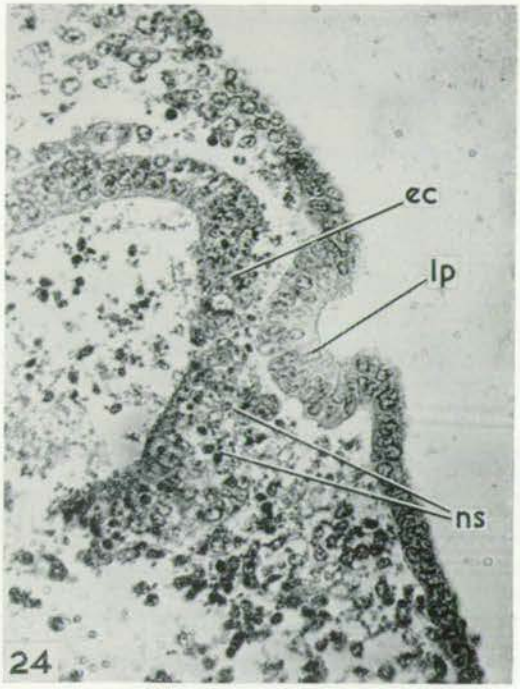

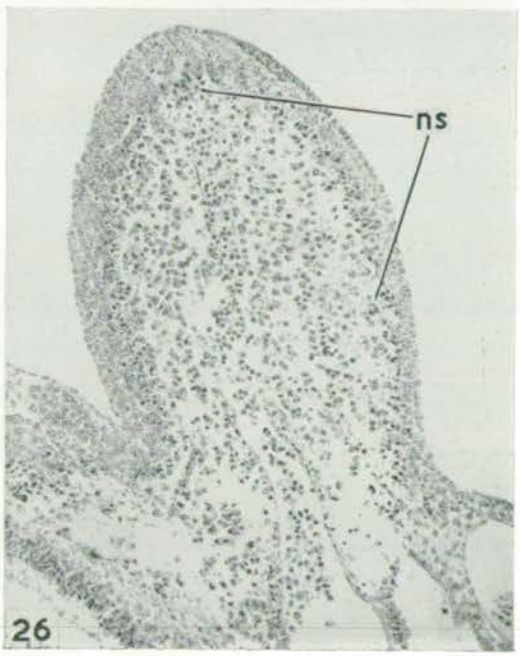

A. JURAND

Plate 5

The development of the notochord in chick embryos

by A. Jurand

The Development of the Notochord in Chick Embryos

by A. JURAND[1]

From the Institute of Animal Genetics, Edinburgh

WITH EIGHT PLATES

THE literature on the notochord, a structure characteristic of all vertebrates, is very extensive, due to the phylogenetic importance of this organ, its role in early embryonic development, and its central position in the developing vertebral column. As early as 1834 the notochord tissue was described by Müller as being similar in appearance to the parenchyma of plants. Surprisingly, however, in the chick embryo, which is so widely used by embryologists, its development has not very often been the subject of descriptive or experimental investigations. From the early days most work on this fundamental organ was done on fish and amphibians, probably because the notochord in lower vertebrates is more suitable for investigations, as it persists longer, carrying out its function as an embryonic and larval skeleton.

Papers have been published in the past describing the fate of the notochord in birds, but mostly in connexion with wider problems, such as the development of the vertebral column (Bruni, 1912; Harman, 1922; Piiper, 1928; Kuhlenbeck, 1930; Williams, 1942; and others) or dealing with some details connected with the notochord, as, for instance, its sheath (Klaatsch, 1895; Held, 1921; Baitsell, 1925; Duncan, 1957 *a*, *b*; and others).

The life-span of the notochord in birds and mammals is comparatively short. Its transient role, which is to provide rigidity of the longitudinal axis of the embryo, and its inductive potencies in cartilage formation become obsolete as soon as the definite skeleton begins to be formed. In chick embryos the whole period of development and existence of the notochord is limited to about 10 days (i.e. from the 2nd until the 11th day of embryonic life). During this period the formation of the prechordal material, its moulding into a rod-like organ, and, later, profound intracellular changes take place. The rate of the morphogenetic process, as well as the process of internal cytodifferentiation, is undoubtedly much faster in the notochord than in embryonic structures which develop more slowly but persist longer.

For the reasons given, investigations on the morphogenesis and cytodifferentiation of the chick notochord appear to be particularly interesting. In the

[1] Author's address: The Institute of Animal Genetics, West Mains Road, Edinburgh 9, U.K.

[J. Embryol. exp. Morph. Vol. 10, Part 4, pp. 602–21, December 1962]

normal developmental table of the chick prepared by Hamburger & Hamilton (1951), which still remains the best guide for all embryological work on the development of chick embryos, the changes in the notochord are not actually taken into account, as this work was based exclusively on external characteristics. Some general information on the development of the chick notochord can be found in monographs or textbooks such as those of Waddington (1952, 1956), Hamilton (1952), and Romanoff (1960). More detailed data based on light microscopy have been published by Kuhlenbeck (1930) and Williams (1942).

It seemed desirable to investigate more closely the process of normal development of the chick notochord by means of light- and electron-microscope techniques in order to try to co-ordinate all that is known so far.

MATERIAL AND METHODS

Chick embryos at all developmental stages from the 5th to the 31st were obtained from Brown Leghorn eggs incubated at 38·5° C. (The stages are numbered throughout the paper according to Hamburger & Hamilton (1951).) For histological reasons, after being dissected from the eggs while the entire yolk was immersed in Pannet–Compton's saline solution, the embryos were fixed for 1 hour in Carnoy's fluid (with chloroform), rinsed thoroughly with absolute alcohol, and, after clearing in methyl benzoate, were embedded in wax (m.p. 54° C.). Serial transverse or sagittal sections were stained with methyl green–pyronine.

For electron-microscope examination the embryos were fixed *in toto* for 15–45 minutes, depending on age, after being dissected in Pannet–Compton's solution. As a fixative, a modified 1 or 2 per cent. osmium tetroxide solution buffered with sodium barbitone and sodium acetate was used (Palade, 1952; Caulfield, 1957). As the original Palade buffer proved unsatisfactory, a number of modifications were tried. As a result of these technical approaches it was established that the best preservation of tissues in general, and of the notochord in particular, can be achieved by using a 2 per cent. osmium tetroxide solution made up according to the following formula:

Sodium barbitone B.D.H.	0·117 g.
Sodium acetate cryst.	0·078 g.
Sucrose	0·18 g.
Osmium tetroxide	0·2 g.
0·1 N hydrochloric acid	2 ml.
Distilled water up to	10 ml.

The pH of the above buffer solution without osmium tetroxide is 8·15. Its osmotic pressure is similar to that of the original Palade's buffer. The use of a higher pH than that recommended by Palade and other authors greatly improves the results, and so do the replacement of sodium chloride by sucrose

(Caulfield, 1957) and the increased percentage of osmium tetroxide (Pease, 1960).

In preliminary investigations, a methyl-butyl methacrylate mixture proved to be unsatisfactory as an embedding medium, presumably due to its tendency to polymerization damage. All final embeddings were carried out with Araldite epoxy resin made up according to the original formula recommended by Glauert & Glauert (1958).

After being fixed at about 4° C. the embryos were dehydrated with 35, 70, and 95 per cent. alcohol (5–10 minutes in each), and then with three changes of absolute alcohol. Embedding was carried out either with prepolymerized methacrylate mixture after two changes of liquid methacrylate or with the final Araldite mixture after replacing the absolute alcohol by two changes of 1:2-epoxy-propane.

In the majority of cases ultra-thin sections were cut transversely to the longitudinal axis at the following levels: (1) In head-process and head-fold embryos, approximately in the middle of the length of the chorda-mesoblast concentration. (2) In embryos with 1–12 somites, at the level of the first somite or just anterior to it. (3) In older embryos in the cervical region of the notochord.

The methacrylate sections were viewed without using electron 'stains', whereas the Araldite sections were contrasted either by floating, after being mounted on grids with collodion–carbon films, on potassium permanganate (1 per cent.) with uranyl acetate (2·5 per cent.) solution (modification of Lawn's method, 1960) for 20 minutes, or mounted straight on uncovered grids (e.g. Athene, No. 483) and subsequently stained by immersing in saturated lead acetate solution in ether–absolute alcohol (1:1) for 20–30 minutes. The latter method proved to be the more satisfactory. Some Araldite sections were treated by floating them on 10 per cent. phosphotungstic acid solution for 15 minutes and then washed for 5 minutes (Watson, 1958).

The material used in the present investigations consisted of 185 chick embryos at various stages.

RESULTS

Light-microscope observations

The aim of this part of the investigations was to have a preliminary and more general look at the developmental process taking place in the notochord, as, for example, the changes in the arrangement of the cells in the course of morphogenesis of the organ. In particular, an attempt was made to re-examine the changes in the relationship of the chorda-mesoblast and, subsequently, of the notochord to the surrounding derivatives of the germ-layers, to determine the time of formation of the rod-like notochord, and to trace the vacuolization process and the subsequent appearance of the first involutive changes in the cells.

The histological material was also used in observations on the distribution of dividing cells by counting them at early stages (5–9) to get more information about the mechanism of elongation and growth of the notochord.

The chorda-mesoblast condensation first appears at stage 5, at a point anterior to Hensen's node, as an extension of the primitive streak along the axis, in the form of an elongated, dorso-ventrally flattened strip of loosely arranged cells (Plate 1, fig. 1). It is distinctly separated from the medullary plate throughout its entire length by a definite boundary, but at the same time it remains very closely attached to it. The contact surface between the chorda-mesoblast and the medullary plate, which appears to be very intimate, is, however, not even; at regular intervals of about 30–50 μ along the longitudinal axis of that surface distinct indentations can be found in the medullary plate, into which notochordal cells protrude. These indentations, which continue up to stage 7, can be seen particularly well in sagittal sections. It seems that during these stages the whole chorda-mesoblast tissue is being anchored by means of these indentations to the bottom of the medullary plate (Plate 2, fig. 11).

Laterally, the central, comparatively loose mass of the presumptive notochord tissue is confluent with the paraxial mesoblast whose cells are, however, much looser than the axially situated prechordal cells.

On the ventral side the chorda-mesoblast condensation at this stage, as well as in a few later stages, appears to be intimately fused with the unicellular layer of the endoderm. At the median line, therefore, the endodermal cells are difficult to distinguish from the prospective notochord cells as described by Hamilton (1952) and also by Fraser (1954) in somewhat older embryos in the pharyngeal region. The unification of both tissues at the head-process stage was described by Ussow (1906) as 'entochorda'. Laterally the endoderm is free and consists of a single layer widely separated from the paraxial mesoblast elements (Plate 1, fig. 2).

At later stages (6–9) the relationship of the chorda-mesoblast to the surrounding tissues changes, primarily due to its more and more marked separation from the paraxial mesoderm (Plate 1, figs. 2, 3, 4). Simultaneously, the cell-to-cell contact between the presumptive notochord cells increases, probably being, in consequence, the main cause of the transformation of the chorda-mesoblast into the true, typically rod-shaped notochord. At this stage the morphogenetic changes leading to the moulding of the definite shape proceed, due to proliferation of the cells in front of the node (Spratt, 1947), from caudal to anterior. At the end of this period the notochord detaches itself from the endoderm, although it still remains closely associated with the neural plate (Plate 1, fig. 5).

During these stages dividing cells are found more frequently in the hind part of the notochord than in the cephalic region, up to 60 per cent. of them being confined to a definite region about 100 to 200 μ anterior to the notochord bulb. In the rest of the organ they are scarce and distributed at random. The confinement of dividing cells to this particular region during the early stages

of development explains the fact that the anterior end of the head-process moves forward only slightly, as nearly all growth in length occurs at the posterior end.

During the next stages (10–13) the increase in the size of the notochord keeps pace with the general growth of the embryo. First of all it elongates as much as is necessary. However, in spite of very frequent mitotic divisions during these stages, which now become more and more randomly distributed throughout the organ, the diameter of the notochord not only does not increase, but it even shows a slight decrease (Plate 1, fig. 6). This fact indicates that the morphogenetic changes in the notochord are due partly to an increase in the number of cells and partly to the migration of cells along the median axis. By the end of this period, i.e. at stage 13, the notochord begins to separate itself from the bottom of the neural tube. The separation occurs first at the cephalic region and then moves slowly backwards.

During stages 14–16 the notochord shows a considerable increase in its diameter, due partly to increased proliferation of cells and partly to the fact that at this period numerous intercellular spaces appear, which are located to a large extent in the centre of the organ (Plate 1, fig. 7). These intercellular spaces form small lumina of about 5–10 μ in diameter. They are most clearly visible in sagittal sections where they appear to be interconnected, thus representing a system of small, irregular, communicating spaces (Plate 2, fig. 12).

Simultaneously the notochord cells arrange themselves like a pile of coins, as also happens in amphibian embryos (Mookerjee, Deuchar, & Waddington, 1953). In chick embryos, however, this feature usually is less regular (Plate 2, fig. 13).

By stage 16 the separation of the notochord from the ventral side of the neural tube is complete in the cephalic and cervical regions, but towards the caudal end the association still persists. The separation presumably takes place because of the formation of the fibrous notochordal sheath which penetrates into the narrow space between the two organs, being followed at later stages by mesodermal cells.

At the end of this period, usually at stage 16, the process of vacuolization of the notochord cells starts. First, intracellular vacuoles appear in the cervical region, primarily in the core of the organ (Plate 1, fig. 8), but shortly afterwards the process spreads towards the periphery of the notochord as well as in both cephalic and caudal directions. From stage 16 onwards it becomes the main feature in the cytodifferentiation of the notochord. When the process is sufficiently advanced, the appearance of vacuoles causes the above-mentioned intercellular spaces to disappear, and the 'pile-of-coins' arrangement is disturbed (Plate 2, fig. 14).

During stage 17 or 18 the notochord tissue, in sections stained with methyl green–pyronine, begins to exhibit two kinds of cells: one with the cytoplasm more pyronine-positive, and the other with paler cytoplasm. At stages 20 and 21 up to 30 per cent. of cells have the more pyronine-positive cytoplasm. These

cells are mainly distributed near the periphery of the organ, although they are also present deeper within it (Plate 1, figs. 9, 10). Together with the less pyronine-positive cells, these form the so-called notochord epithelium. As will be seen later, these epithelial cells do not actually differ from the cells situated deeper in the notochord tissue. The presence of these two kinds of cells in other vertebrates has been reported by several workers: in Holocephala (Schauinsland, 1906), in Amniota (Bruni, 1912), and in duck embryos (Kuhlenbeck, 1930).

At stages later than 16 the mitotic activity of the notochordal cells appears to be still considerable (0·5 per cent.), without, however, having any particular distribution. The vacuolated cells divide at the same rate, irrespective of whether the cytoplasm is more or less pyronine-positive. In such cells the chromosome sets are usually pushed by the vacuole from the centre of the cell towards the periphery. However, this does not seem to disturb the mitotic process (Plate 2, fig. 15).

About stage 22 mitotic divisions become gradually less frequent, although they do not disappear completely even at the latest stages under investigation. From stage 25 there begin to appear more and more frequently cells with pycnotic or karyorrhectic nuclei scattered randomly throughout the organ, foreshadowing the onset of the process of involution.

Electron-microscope observations

Presumptive and early notochord cells

During the earliest stages under investigation (stages 5–9) the cells of the chorda-mesoblast exhibit all the characteristic morphological properties of early embryonic cells. At the head-process and head-fold stages they are loosely arranged, forming a dorso-ventrally flattened, axially elongated accumulation with numerous intercellular spaces. Being more or less spherical in shape they remain attached to each other at a few limited contact points. Many of the parts of cell membranes that take part in adhesion points show, in cross-sections in electron micrographs, characteristic thickenings called terminal bars or attachment bodies (Plate 3, figs. 16, 17).

The nuclei of such early cells are comparatively large, with one or several nucleolar aggregations and a double nuclear membrane. In the cytoplasm there are numerous yolk granules of all types, as described in the chick blastoderm by Bellairs (1958). In comparison with later stages, both mitochondria and endoplasmic reticulum elements are scarce. Golgi complex groups can frequently be found in such cells, as well as in the older ones, in the form of one or more separate structures per section, as parallel profiles of flat vesicles and round canaliculi (Plate 3, figs. 16, 19; Plate 6, fig. 30).

At somewhat later stages (10–15), after the notochord has become rounded and taken on its rod-like shape, its tissue loses the previous intercellular spaces, the cells become polyhedral in shape and adhering closer to each other. About stage 15 the contact between the peripheral cells becomes particularly intimate,

as at that stage the cells form complicated interdigitations between themselves (Plate 3, fig. 18).

In between, the terminal bars can be still found in cross-sections through some parts of the cell membranes, but they appear to be less frequent and much shorter than at earlier stages. By the end of stage 15 they have disappeared altogether.

In the cytoplasm the profiles of endoplasmic reticulum elements gradually become more frequent and by stage 15 they are already numerous. Characteristic of these stages are small profiles of endoplasmic reticulum, or at least profiles of an identical structure, which can frequently be found attached to the outer nuclear membrane, which suggests the possible manner of formation of that organelle in early stages of differentiating notochord cells. Its profiles, however, are still comparatively short and wide, being limited by a single rough-surfaced membrane (Plate 3, figs. 20, 21). At later stages, when the endoplasmic reticulum profiles appear to be much more flattened and elongated, forming lake-like dilatations, they can also occasionally be found continuous with the outer nuclear membrane (Plate 4, figs. 22, 23).

Further cytodifferentiation

At stage 16, when the vacuolization of the cytoplasm begins, small vacuoles in the course of formation are frequently found to be surrounded by one or more profiles of the endoplasmic reticulum (Plate 5, fig. 24). At the same time other fragments remain often in close proximity to single mitochondria. The connexions between them, particularly at later stages, are often provided by socket-like depressions formed by endoplasmic reticulum cysternae which embrace the mitochondria (fig. 25).

It is probable that the endoplasmic reticulum also takes part in the process of yolk utilization, as yolk granules, when in course of digestion, are also at least partly surrounded by profiles of endoplasmic reticulum.

The topographical relationship between the nuclear membranes, endoplasmic reticulum, mitochondria, and intracellular vacuoles in the course of formation is the most characteristic feature in the cytodifferentiation of notochord cells. Later, when the vacuolization process has progressed further, the contact between the mitochondria and the endoplasmic reticulum persists, apparently becoming even more intimate. As the process of vacuolization proceeds, the continuity between the outer nuclear membranes and the endoplasmic reticulum seems to be much less frequent, but in spite of this the endoplasmic reticulum system develops further in the cytoplasm, so that at stages later than 18 it extends throughout the whole cytoplasm, forming a complicated and highly convoluted complex of flat cisternae with abundant ribosomes attached to their surface (Plate 4, fig. 23).

At about stage 18 the endoplasmic reticulum cisternae start to form wide dilatations which remain continuous with the rest of the flat cisternae. In trans-

verse sections the profiles of these dilatations appear to be lake-like structures of considerable size (up to 3 μ in diameter) connected by several tributary-like profiles of flat cisternae at their circumference (Plate 4, fig. 2; Plate 5, fig. 26). In the appearance of their contents and in their rough-surfaced membranes the dilatations are similar to the flat cisternae of the endoplasmic reticulum.

Towards the end of the vacuolization process, which is completed by about stage 26, the dilatations become smaller, and eventually, at still later stages, disappear, so that the system of rough-surfaced endoplasmic reticulum persists only in the form of interconnected, uniformly narrow, flat cisternae, represented in sections by more or less compact, often parallelly arranged profiles (Plate 5, fig. 27). In favourable cases, when the endoplasmic reticulum of later stages has been tangentially sectioned, the ribosomes attached to their limiting membranes appear to be arranged in patterns of circular, linear, or rosette-like groups. Occasionally, branchings of the limiting membranes and fenestrae can also be found (Plate 6, figs. 28, 29).

As has already been mentioned, another feature of the cytodifferentiation of the notochordal cells is the fact that from about the 3rd day of embryonic development, i.e. from stage 17 or 18 onwards, after the vacuolization process has started, two kinds of cells can be distinguished in the notochord tissue. These differ in the stainability of their cytoplasm with pyronine. An electron-microscope examination showed that the difference between these two types of cells is even more conspicuous than can be revealed by light microscopy. The cells described as more pyronine-positive ('dark' cells) appear to have much more electron-dense cytoplasm closely packed with endoplasmic reticulum profiles, mitochondria, and Golgi complex, all spaces not containing these being packed uniformly with large numbers of microsome granules (Plate 6, figs. 28, 30).

The cytoplasm of the second kind of cells ('light' cells) appears to be comparatively much 'emptier' with, here and there, scattered profiles of endoplasmic reticulum elements and, usually attached to them, single mitochondria. Microsomal granules, which are very scarce in these cells, are confined almost exclusively to the close proximity of the limiting membranes of the endoplasmic reticulum structures (Plate 6, figs. 28, 30). The appearance of the cytoplasm of the second type of cells suggests that their low affinity to pyronine is due to the scarcity of microsomal granules.

Electron microscopy of these two types of cells has confirmed that the distribution of the dense cells appears at first to be random, but at later stages (21–25) these cells are found mainly in the external layers of the notochord (i.e. in the chorda epithelium), forming groups each consisting of several such cells. However, there are always lightly stained cells between the dense ones, and dense cells can also frequently be found situated more centrally in the organ. Both kinds of cells undergo the process of vacuolization to the same degree and at the same time.

By means of electron-microscope examination of stages later than stage 20 it could be shown that the older, well-established vacuoles very often possess definitive limiting membranes separating them from the cytoplasm of the cell inside which they are found. These membranes frequently form small invaginations directed towards the lumen of the vacuole. This suggests that the vacuolar membranes are not merely interfaces between the cytoplasm and the contents of the vacuole, but that they are active in replenishing the content of the vacuoles. There are, however, also vacuoles that do not show any definite limiting membrane, passing gradually at their peripheries into the general substance of the loose cytoplasmic constituents (Plate 4, fig. 22).

Electron-microscope observations have also confirmed that chromosome sets in dividing cells containing intracellular vacuoles are pushed away from their usual position towards the periphery of the cells by the thrust exerted by the vacuoles (Plate 7, fig. 31).

Finally, it has been shown that there is no period during the whole process of development of the notochord of the chick during which cell membranes do not exist, i.e. in which notochord tissue could be described as being syncytial in nature, as was frequently assumed in older papers. At all stages the notochord cells possess definite cell membranes which can easily be detected round the cells. In cross-sections the cell membranes of two adjacent cells are represented by a continuous double line.

When the vacuolization process has progressed so far that the intracellular vacuoles occupy about half of the cell volume, there are also found intercellular spaces between the cell membranes which contribute to the network pattern of the notochord tissue. They, too, are filled with an electron-transparent (also semi-liquid) substance, which undoubtedly contributes to the rigidity of the organ. During later stages these intercellular spaces widen considerably, filling gaps between adjacent cells and even forming vesicles of considerable size between the cell membranes (Plate 7, fig. 32).

Notochord sheath

Commencing from the stages in which the notochord becomes definitely shaped into an elongated, round, rod-like organ, i.e. from stage 11 onwards, there begins to be formed outside the organ an extracellular membrane named the perichordal sheath. This appears gradually, first as a thin deposition of loose, fibrous elements close to the external surface of the notochord (Plate 8, fig. 33). Very soon, however, at the close proximity to the notochord surface the microfibrils become so dense that they form a delicate membrane (Plate 8, fig. 34). On the other hand, the accumulation of microfibrils from the very beginning of its formation, and also at all later stages, is devoid of any limiting outer membrane. Moreover, the microfibrils are more thinly scattered farther away from the notochord in the ambient intercellular spaces between the perichordal mesenchyme cells.

At older stages (18–22) the density of the microfibrils increases considerably and the whole structure becomes thicker. The internal membrane of the sheath formed on the surface of the notochord now appears to be continuous and exactly parallel to the peripheral membranes (Plate 8, fig. 35).

From stage 22 onwards the notochord sheath begins to be composed of two layers which in cross-section form two concentric zones: an external, denser layer which is undoubtedly the older one deposited on the surface of the notochord from the outside, and an inner, much narrower layer, also fibrous, but less dense, probably produced by the notochordal cells and deposited from the inside (Plate 8, fig. 36). This suggestion is supported by three facts. Firstly, the inner layer appears much later than the outer. Secondly, in the period during which the inner layer is formed some kind of fibrous material similar to that of the sheath can be found inside the peripheral cell of the notochord, usually deposited close to the outer cell membranes (Plate 8, fig. 37). Thirdly, when the two layers described above have been formed, a fibrous boundary is found between them which is probably identical with the internal membrane formed by microfibrils on the surface of the notochord at earlier stages, but due to the formation of the internal layer from inside, this membrane forms now a boundary between the layers.

The fine structure of the notochord sheath microfibrils, particularly in later stages, in spite of slight affinity to phosphotungstic acid, do not exhibit the characteristic periodic structure of collagen fibres. They are about 200 Å thick and appear to be formed by 2–4 rows of fine granules 30–50 Å in diameter. The microfibrils form a network whose prevailing arrangement is parallel to the outline of the notochord, with numerous transverse branchings between the concentric fibres (Plate 8, fig. 38).

Just prior to the formation of the cartilage tissue in the vertebral column, i.e. at stage 21, there is formed externally to both layers of the fibrous sheath a third layer, consisting of mesodermal cells of sclerotomal origin. In the proximity of the fibrous sheath its cells are flattened and closely applied to the surface in parallel rows.

Pinocytic activity of the peripheral cell membranes

Throughout the period of vacuolization, i.e. from stage 15 onwards, there are present in the outer cell membranes, limiting the organ from outside, small invaginated vesicles, usually with narrow bottle-neck connexions. These vesicles are formed presumably by the pinocytic activity of the cell membranes. Similar vesicles (pinosomes) can also be seen deeper in the cytoplasm, suggesting that after being formed by the cell membrane they are taken inwards by the cytoplasm (Plate 8, figs. 34, 39).

It must be emphasized that this pinocytic activity coincides in time with the onset of the vacuolization process, when water requirements become critical. Pinocytosis, together with the diffusion of water through the cell membranes,

may be the process which enables this requirement to be satisfied, as the notochord itself always remains avascular.

DISCUSSION

Light and electron microscopy of the early stages (up to stage 8) show that in the chick the notochord tissue is formed by loosely arranged cells, the areas of contact between the contiguous cells being only limited. These contact points are often reinforced by so-called terminal bars outside which there are extensive intercellular spaces. Soon afterwards the cell-to-cell contact increases, intercellular gaps gradually disappear, and the terminal bars are replaced by adhesion of the entire cellular membranes of adjacent cells. These changes coincide in time with the morphogenetical progress in formation of the cylindrical rod-like notochord. Virtually the same changes in roughly corresponding stages have been observed in urodele notochords by Waddington & Perry (1962). It seems therefore that the subsequent increase of the cell-to-cell contact is generally the morphogenetic factor in the process of moulding the notochord into its definite cylindrical shape.

According to Spratt's marking experiments (1957) the elongation of the notochord in the early stages of development is accomplished mainly by the addition of cells originally situated posterior to the chorda bulb, and only to a lesser extent by mitotic activity. He emphasizes that the region of maximum elongation is just anterior to the notochord bulb, but concludes that it is mainly due to migration of cells from behind. In the present investigations, however, it was shown that in the region just anterior to the bulb there are confined about 60 per cent. of the total number of dividing cells, and presumably this indicates that elongation takes place here mainly due to mitotic division.

The light-microscope observations reported in the present paper did not aim at confirming what is known, but were intended to serve as a preliminary guide to more detailed investigations by means of the electron microscope. In general they are in agreement with those of Kuhlenbeck (1930), but in certain details there are differences to which attention should be drawn.

Kuhlenbeck, who worked mainly on duck eggs, describes in the notochords of 48- to 72-hour-old embryos round lumina with sharp edges which are situated centrally inside the organ. Similar lumina have been reported in the notochords of the grass snake and the owl (Ussow, 1906), as well as in human embryos (Johnson, 1917).

In the material used in the present work no such lumina were observed. However, at stages 14–16 there were found numerous intercellular spaces, mostly located centrally, which appear to form an interconnected system. They are, however, small and irregular in shape, and never form the round, wider lumina with sharp edges described in other species.

In duck notochords about 90 hours old Kuhlenbeck observed scattered cells with elongated nuclei and denser cytoplasm situated near the periphery of the

organ. These cells are presumably identical to the more pyronine-positive cells in the chick, although in the chick these cells can be found not only at the periphery but also deeper within the organ, forming groups consisting of up to 20 cells.

In older papers dealing with investigations on the development of notochord tissue carried out by means of light microscopy, it is often accepted that this tissue undergoes a cyclic process of transformation. According to this view, the notochord starts to develop as a population of single cells, then becomes syncytial, especially in its internal part, and finally ends up as a true tissue again. This belief was formulated for the first time by Williams (1908), and since then it has been repeated many times (Bruni, 1912; Kuhlenbeck, 1930; Dawes, 1930; and others). More recently, however, Kocher (1957) expressed himself less decisively about this when describing the normal development of the notochord in *Triton alpestris*.

By means of electron-microscope resolution, the cell-walls can now be followed, at least in chick embryos, throughout the whole period of the development and differentiation of the notochord. Even at the stages when vacuolization reaches its maximum and the tissue is being transformed into a network-patterned 'gelatinous body', the individual cytoplasmic bridges (trabeculae) appear to consist of at least two parts longitudinally separated by the cell membranes belonging to the two adjacent cells. These cell boundaries can be traced as they go round individual, enormously vacuolated cells. The same fact was also reported by Leeson & Leeson (1958) in the case of the rabbit notochord, so that it seems feasible to conclude on the basis of electron-microscope observations that notochord tissue is not syncytial in nature at any period of its development. On the contrary, it is always a tissue consisting of well-separated, individual cells.

Regarding the cytodifferentiation process which results in the formation of the gelatinous network structure, due to far-reaching vacuolization of cells, it can be assumed on the basis of the present findings that the main cell organelles taking part in it are the nuclear membranes, the endoplasmic reticulum, and the mitochondria. It seems to be established that about stage 15 the nuclear membrane forms at least part of the existing endoplasmic reticulum, and even at later stages connexions between these two can be found. This has been observed in the chick by Duncan (1957*b*) and also in the amphibian notochord, where Waddington & Perry (1962) distinguish two types of ergastoplasm which appear one after another in the course of the development of the organ, the latter being much better developed in the peripheral cells lying just under the notochord sheath. In the chick notochord, however, there was no evidence for postulating the existence of two separate types. In early stages of development these intracellular structures originate, at least partly, from the outer nuclear envelopes, whereas later it develops independently in the cytoplasm.

In the chick the endoplasmic reticulum seems to take a direct part in the formation of vacuoles, as its profiles are found to surround small vacuoles at the time of their first appearance. At the same time the endoplasmic reticulum remains in very close contact with the mitochondria, both during the process of vacuolization and later, after the maximal stage of vacuolization has been reached. It is interesting that a similar topographical relationship between the endoplasmic reticulum and the mitochondria has been found in a quite different but also highly active tissue, namely intensely regenerating rat liver (Bernhard & Rouiller, 1956). It seems reasonable to assume that the endoplasmic reticulum–mitochondria system is responsible for, or at least takes part in, the physiological processes of biologically intensively active cells, especially those in the course of differentiation. This opinion was expressed also by Palade (1956). The role of the endoplasmic reticulum in differentiating cells was extensively discussed also by Waddington & Perry (1962).

Another feature of the chick notochord cells during the first and most active period of differentiation is the formation of extensive dilatations of the otherwise flat cisternae of the endoplasmic reticulum. As far as the author is aware, such dilatations have not been described so far in any other normal tissue, although a similar feature was noticed in plasma cells (Thiery, 1960) and in human chordoma cells investigated by means of the electron microscope (Friedmann, 1961).

In the literature there are numerous descriptions of the formation of the perichordal sheath, but views on its origin differ considerably. Until now it has been regarded, in the chick, as consisting of two layers: an internal membraneous and fibrillar layer, and an external layer built up of flattened mesodermal cells (Romanoff, 1960).

The internal acellular sheath has been regarded as originating from the intercellular ground substance, which is widely present between the embryonic organs, or from the mesodermal cells or their cytoplasmic processes (Studnička, 1913; Held, 1921; Baitsell, 1925; Kuhlenbeck, 1930; Williams, 1942). More recently, strong support for the theory of external origin of the sheath has been provided by S. Mookerjee (1953). On the other hand, Klaatsch (1895), Schauinsland (1906), Dawes (1930), H. K. Mookerjee (1935), and Gadow (1933) have suggested that in the mouse and in anuran amphibians the fibrillar sheath is a product of the notochordal cells themselves. Duncan (1957*b*) assumes that microfibrils deposited on the surface of the chick notochord are pealed off by the external cell-walls of the notochord rather than produced inside the organ.

When tracing the morphogenesis of the fibrous sheath on electron micrographs at different stages in the chick one is inclined to assume that in the beginning the fibrous sheath is produced outside the notochord as a thin layer consisting of microfibrils arranged randomly but in greater density towards the surface of the organ. Identical single microfibrils can be found at the same time scattered in the surrounding intercellular spaces between the mesenchymal cells.

This situation can be attributed to the fact that the microfibrils being produced by the mesodermal cells are subsequently attracted by some unknown force towards the surface of the notochord. However, the other possibility cannot be excluded, as the microfibrils are denser at the surface of the notochord and less dense away from it.

Later, from stage 21 onwards, the electron-microscope investigations seem to throw more light on this complicated problem, showing that underneath the previous single fibrous sheath there appears another one, also fibrous but consisting of less densely packed microfibrils. Considering the fact that both layers are separated at these stages by an irregular fibrous boundary, it can be assumed that the later formed inner layer originates, after all, from the notochord cells. This view is supported by the fact that at the time of the appearance of the inner layer there are often found in the cytoplasm of the notochord epithelium cells dense masses of some kind of fibrous material which might be the source from which the microfibrils of the internal zone are formed.

A rather similar interpretation was suggested by Tretjakoff (1927) to explain the formation of the amphibian notochord sheath. According to Waddington & Perry (1962), however, the formation of the notochord sheath in Urodela seems to differ considerably from that described here in the chick. In the chick the sheath never comes to be fully developed into a well-defined membraneous hollow cylinder. Also, the arrangement of the microfibrils is never so regularly concentric in the chick. On the other hand, in both cases there is an indication of two different layers in the sheath, and the material for the inner layer is presumably produced by the peripheral cells of the notochord.

Finally, it should be mentioned that the chick notochord and probably the notochords of all vertebrates are organs that never become vascularized. This detail is seldom emphasized, although it is of great importance. In the classical work of Sabin (1917) on the primitive blood-vessels in chick embryos there is in fact no indication of the existence of blood-vessels which would, during development, penetrate towards the notochord tissue. The notochord is also not vascularized in rabbit embryos (Leeson & Leeson, 1958).

The fact that the peripheral cell membranes form pinocytic vesicles during the vacuolization process reported in this paper suggests that the considerable water requirements at this time are met by pinocytic activity, as normal diffusion is not sufficiently effective.

SUMMARY

1. Light-microscope observations on the developmental changes in the notochord of the chick embryo have shown that the chorda-mesoblast occupying the axial position at first remains in contact with the surrounding embryonic organs, i.e. with the medullary plate, paraxial mesoderm, and entoderm. In the course of several hours, however, it detaches itself, first from the paraxial mesoderm cells, and then, about 12 hours later, from the entoderm. Its association

with the ventral side of the neural groove persists much longer, but eventually a separation occurs, beginning from the cephalic region and proceeding towards the caudal end of the notochord.

2. A 'pile-of-coins' arrangement of the notochord cells can be observed in chick embryos, but it is never so obvious as in the amphibian notochord.

3. Vacuolization of the notochord tissue begins about stage 15 and reaches its maximum at about stage 25.

4. Mitotic activity persists throughout the whole period of development of the notochord until the stage of maximal vacuolization, and even beyond it, when the first signs of the involution of the organ appear. Only during the head-process and head-fold stages does mitotic activity show an uneven distribution, being then mainly confined to the caudal region, just anterior to the bulb of the notochord. At all later stages mitotic figures are distributed at random.

5. Electron microscopy of different stages has revealed that the notochord tissue never at any time becomes syncytial.

6. During the early period of the cytodifferentiation of the notochord cells (about stage 15) endoplasmic reticulum structures are often found attached to the outer nuclear membranes. Occasionally they may still remain connected with them at later stages. This fact suggests that the endoplasmic reticulum is probably formed, at least partly, by the nuclear membranes.

7. At the beginning of the vacuolization process endoplasmic reticulum surrounds the vacuoles, when they are still small, presumably contributing to the endosecretion of the gelatinous contents of the vacuoles. It seems likely that the endoplasmic reticulum takes part also in the process of yolk utilization. Endoplasmic reticulum profiles are also found closely attached to mitochondria during the vacuolization period, creating with them a system which seems to play a most important role in the cytodifferentiation of the notochord cells.

8. The presence of two kinds of cells, those with less dense cytoplasm and those in which the cytoplasm is densely packed with endoplasmic reticulum, mitochondria, microsomes, and Golgi structures, has also been investigated and the results discussed.

9. It has been found that the notochord sheath is formed originally from microfibrillar material produced, presumably, outside the notochord by mesenchyme cells. In the final stage of its formation, however, the sheath appears to consist of two fibrous layers, the inner of which seems to be produced by the notochord epithelium cells.

RÉSUMÉ

Développement de la notochorde chez l'embryon de Poulet

1. L'étude microscopique de l'évolution de la notochorde au cours du développement chez l'embryon de Poulet a montré que le chordomésoblaste situé axialement reste d'abord en contact avec les organes voisins, c'est à dire la

plaque médullaire, le mésoderme paraxial et l'endoderme. En quelques heures toutefois il s'en détache par la suite, en commençant par les cellules du mésoderme paraxial; douze heures plus tard environ il se sépare de l'endoderme. Ses relations avec la région ventrale de la gouttière neurale persistent plus tard, mais une séparation se produit enfin, qui débute dans la région céphalique et progresse en direction caudale jusqu'à l'extrémité de la notochorde.

2. La disposition en 'pièces empilées' des cellules chordales est visible chez l'embryon de Poulet, sans être aussi nette que chez l'Amphibien.

3. La vacuolisation du tissu chordal commence au stade 15 et atteint son maximum au stade 25 environ.

4. L'activité mitotique persiste tout au long du développement de la chorde jusqu'au stade de la vacuolisation maximum et même un peu au delà, jusqu'à l'apparition des premiers signes d'involution de l'organe. Ce n'est qu'aux stades du processus céphalique et des bourrelets céphaliques que l'activité mitotique est inégalement répartie. Elle se manifeste alors surtout dans la région caudale juste en avant du renflement de la notochorde. Plus tard les mitoses sont réparties au hasard.

5. La microscopie électronique a montré que jamais le tissu chordal ne devient syncytial.

6. Au début de la cytodifférenciation des cellules chordales on trouve souvent un réticulum endoplasmique attaché aux membranes nucléaires externes. Il arrive que ces relations persistent à des stades plus avancés. Ces faits inclinent à penser que le réticulum endoplasmique est produit, au moins en partie, par les membranes nucléaires.

7. Au début des phénomènes de vacuolisation le réticulum endoplasmique entoure les vacuoles, alors qu'elles sont encore petites, contribuant vraisemblablement à l'endosécrétion de leur contenu gélatineux. On peut penser que ce réticulum endoplasmique intervienne aussi dans les processus d'utilisation du vitellus. Par ailleurs, durant cette période de vacuolisation, certaines parties du réticulum endoplasmique sont étroitement associées aux mitochondries. Le système ainsi réalisé semble jouer un rôle fondamental dans la cytodifférenciation des cellules chordales.

8. L'existence de deux types de cellules a été envisagée et discutée, les unes au cytoplasme peu dense, les autres au cytoplasme fortement concentré, possédant un réticulum endoplasmique, des mitochondries, des microsomes et un appareil de Golgi.

9. La gaine de la chorde s'est révélée formée initialement de microfibrilles, probablement produites à l'extérieur de la notochorde par les cellules mésenchymateuses. Cependant, à la fin de sa formation, la gaine comporte deux couches fibreuses, la couche interne semblant produite par les cellules de l'épithélium chordal.

ACKNOWLEDGEMENTS

The work was executed during the tenure of a British Empire Cancer Campaign research grant for which gratitude is to be expressed. The author would like to thank Professor C. H. Waddington for his encouragement and helpful discussion, as well as for reading the manuscript, and to Miss A. P. Gray for infallible editorial advice. Thanks are also due to Mr. D. E. Bradley for the facilities in the Electron Microscopy Unit of the Department of Zoology, University of Edinburgh, and to Miss Patricia Collins for technical assistance.

REFERENCES

BAITSELL, G. A. (1925). On the origin of the connective-tissue ground substance in the chick embryo. *Quart. J. micr. Sci.* **69**, 571–89.

BELLAIRS, R. (1958). The conversion of yolk into cytoplasm in the chick blastoderm as shown by electron microscopy. *J. Embryol. exp. Morph.* **6**, 146–61.

BERNHARD, W., & ROUILLER, C. (1956). Close topographical relationship between mitochondria and egastoplasm of liver cells in a definite phase of cellular activity. *J. biophys. biochem. Cytol.* **2**, Suppl. 73–78.

BRUNI, A. (1912). Über die evolutiven und involutiven Vorgänge der Chorda dorsalis in der Wirbelsäule mit besonderer Berücksichtigung der Amnioten. *Anat. Hefte*, **45**, 309–469.

CAULFIELD, J. B. (1957). Effects of varying the vehicle for OsO_4 in tissue fixation. *J. biophys. biochem. Cytol.* **3**, 827–9.

DAWES, B. (1930). The development of the vertebral column in mammals, as illustrated by its development in *Mus musculus*. *Phil. Trans.* B, **218**, 115–70.

DUNCAN, D. (1957*a*). The notochord as the earliest source of fibrillogenesis. *Anat. Rec.* **127**, 411.

—— (1957*b*). Electron microscope study of the embryonic neural tube and notochord. *Texas Rep. Biol. Med.* **15**, 367–77.

FRASER, R. C. (1954). Studies on the hypoblast of the young chick embryo. *J. exp. Zool.* **126**, 349–99.

FRIEDMANN, I. (1961). Personal communication.

GADOW, H. (1933). *The Evolution of the Vertebral Column*. Cambridge University Press.

GLAUERT, A. M., & GLAUERT, R. H. (1958). Araldite as an embedding medium for electron microscopy. *J. biophys. biochem. Cytol.* **4**, 191–4.

HAMBURGER, V., & HAMILTON, H. L. (1951). A series of normal stages in the development of the chick embryo. *J. Morph.* **88**, 49–92.

HAMILTON, H. L. (1952). *Lillie's Development of the Chick. An Introduction to Embryology*. New York: Henry Holt & Co.

HARMAN, M. T. (1922). Concerning the origin of the notochord in the chick. *Anat. Rec.* **23**, 363–9.

HELD, H. (1921). Über die Entwicklung des Axenskeletts der Wirbeltiere. I. Die Bildung der Chordascheiden. *Abh. sächs. Ges. (Akad.) Wiss.* **38**, 1–28.

JOHNSON, F. P. (1917). A human embryo of twenty-four pairs of somites. *Contr. Embryol. Carneg. Instn.* **6** (No. 19), 125–68.

KLAATSCH, H. (1895). Beiträge zur vergleichenden Anatomie der Wirbelsäule. III. Zur Phylogenese der Chordascheiden und zur Geschichte der Umwandlung der Chordastruktur. *Morph. Jb.* **22**, 514–60.

KOCHER, W. (1957). Vacuolisierung der Chorda dorsalis und Wirkung extrachordalen Defekte auf die Differenzierung von Chorda- und Neuralstrukturen bei *Triton alpestris*. *Roux Arch. EntwMech. Organ.* **149**, 443–503.

KUHLENBECK, H. (1930). Beobachtungen über das Chordagewebe bei Vogelkeimlingen. *Anat. Anz.* **69**, 485–520.

LAWN, A. M. (1960). The use of potassium permanganate as an electron-dense stain for sections of tissue embedded in epoxy resin. *J. biophys. biochem. Cytol.* **7**, 197–8.

LEESON, T. S., & LEESON, C. R. (1958). Observations on the histochemistry and fine structure of the notochord in rabbit embryos. *J. Anat.* **92**, 278–85.

MOOKERJEE, H. K. (1935). The development of the vertebral column and its bearing on the study of organic evolution. *Proc. 23rd Indian Sci. Congr.*

MOOKERJEE, S. (1953). An experimental study of the development of the notochordal sheath. *J. Embryol. exp. Morph.* **1**, 411–16.
—— DEUCHAR, E. M., & WADDINGTON, C. H. (1953). The morphogenesis of the notochord in amphibia. *J. Embryol. exp. Morph.* **1**, 399–409.
MÜLLER, J. (1834). Vergleichende Anatomie der Myxinoiden, der Cyclostomen mit durchgebohrten Gaumen. Erster Teil. Osteologie und Myologie. *Abh. Akad. Wiss. Berlin*, 65–340.
PALADE, G. E. (1952). A study of fixation for electron microscopy. *J. exp. Med.* **95**, 285–98.
—— (1956). The endoplasmic reticulum. *J. biophys. biochem. Cytol.* **2**, Suppl. 85–98.
PEASE, D. C. (1960). *Histological Techniques for Electron Microscopy*. New York: Academic Press.
PIIPER, J. (1928). On the evolution of the vertebral column in birds illustrated by its development in *Larus* and *Struthio*. *Phil. Trans.* B, **216**, 285–351.
ROMANOFF, A. L. (1960). *The Avian Embryo. Structural and Functional Development*. New York: The Macmillan Co.
SABIN, F. R. (1917). Origin and development of the primitive vessels of the chick and the pig. *Contr. Embryol. Carneg. Instn.* **6**, No. 18, 61–124.
SCHAUINSLAND, H. (1906). Die Entwicklung der Wirbelsäule nebst Rippen und Brustbein. In *Hertwig's Handbuch der vergleichenden und experimentellen Entwicklungslehre der Wirbeltiere*, Bd. III/2, 339–572. Jena: Gustav Fischer.
SPRATT, N. T., Jr. (1947). Regression and shortening of the primitive streak in the explanted blastoderms. *J. Exp. Zool.* **104**, 69–100.
—— (1957). Analysis of the organizer center in the early chick embryo. II. Studies of the mechanics of notochord elongation and somite formation. *J. exp. Zool.* **134**, 577–612.
STUDNIČKA, F. K. (1913). Das extrazelluläre Protoplasma. *Anat. Anz.* **44**, 561–93.
THIERY, J. P. (1960). Microcinematographic contributions to the study of plasma cells. In *Ciba Foundation Symposium on Cellular Aspects of Immunity*. London: Churchill Ltd.
TRETJAKOFF, D. (1927). Die Chordascheiden der Urodelen. *Zeit. Zellforsch.* **5**, 174–207.
USSOW, S. A. (1906). Vergleichend-embryologische Studien des axialen Skelettes. *Anat. Anz.* **29**, 433–52, 501–10, 561–79.
WADDINGTON, C. H. (1952). *The Epigenetics of Birds*. Cambridge University Press.
—— (1956). *Principles of Embryology*. London: George Allen & Unwin Ltd.
—— & PERRY, M. M. (1962). The ultrastructure of the developing urodele notochord. *In press*.
WATSON, M. L. (1958). Staining of tissue sections for electron microscopy with heavy metals. *J. biophys. biochem. Cytol.* **4**, 475–8.
WILLIAMS, J. L. (1942). The development of cervical vertebrae in the chick under normal and experimental conditions. *Amer. J. Anat.* **71**, 153–79.
WILLIAMS, L. W. (1908). The later development of the notochord in mammals. *Amer. J. Anat.* **8**, 251–84.

EXPLANATION OF PLATES

Abbreviations for plates and legends: b, branchings of the endoplasmic reticulum membrane; *c*, circular arrangement of ribosomes; *ch*, chromosomes; *cm*, cell membranes; *dc*, 'dark' cell; *er*, endoplasmic reticulum profile; *fm*, fibrous material in the peripheral cells; *G*, Golgi complex; *is*, intercellular space; *l*, linear arrangement of ribosomes; *lc*, 'light' cell; *m*, mitochondrion; *ner*, endoplasmic reticulum fragment continuous with the nuclear membrane; *pi*, pinocytic activity; *r*, rosette-like arrangement of ribosomes; *sm*, membraneous accumulation of sheath fibres at the surface of peripheral notochord cells; *tb*, terminal bar, v_1, intracellular vacuole with limiting membrane; v_2, intracellular vacuole without limiting membrane; *y*, yolk in the state of digestion.

Abbreviations for legends only: L.A., lead acetate staining method for unsupported sections (Watson, 1958); P.–U., Potassium permanganate with uranyl acetate; P.T.A., 10 per cent. phosphotungstic acid.

The scale marks on plates 3–8 represent 1 micron.

PLATE 1

FIGS. 1–10. A series of transverse sections through the chorda-mesoblast accumulation in the middle of its length or through the notochords at the cervical level. Fig. 1, stage 5 (head-process); fig. 2, stage 6 (head-fold); fig. 3, stage 7 (1 somite); fig. 4, stage 8 (4 somites); fig. 5, stage 9 (7 somites); fig. 6, stage 12 (16 somites); fig. 7, stage 14 (22 somites); fig. 8, stage 18 (35 somites); fig. 9, stage 21 (44 somites); and fig 10, stage 23. Note in figs. 9 and 10 cells with more pyronine-positive cytoplasm (*dc*). ×430.

PLATE 2

FIG. 11. Longitudinal section through the head-process chorda mesoblast (on the right) and the bottom of the neural groove (on the left). Note the periodic indentations between the two organs. ×600.

FIG. 12. Longitudinal section through the notochord at stage 13 (18 somites). Note irregular spaces between the cells inside the organ. On the left—part of the neural tube; on the right—endoderm. ×600.

FIG. 13. Longitudinal section through the notochord at stage 14 (21 somites). Note the 'pile-of-coins' arrangement of cells. ×600.

FIG. 14. Longitudinal section through the notochord at stage 19 (40 somites). Note the vacuolization process. ×600.

FIG. 15. Highly vacuolated cell during the process of mitotic division. Stage 25. ×1,025.

PLATE 3

FIG. 16. Presumptive notochord cell (stage 9). Note scarce endoplasmic reticulum profiles (*er*), terminal bars (*tb*), and Golgi complex (*G*). Araldite, P.–U. ×9,000.

FIG. 17. Terminal bar (*tb*) between cells of chorda-mesoblast accumulation (stage 7). Methacrylate. ×18,000.

FIG. 18. Fragment of a notochord cell at stage 14 showing in the cytoplasm an interdigitation of another cell. Note scarcity of endoplasmic reticulum profiles. Araldite, L.A. ×7,500.

FIG. 19. Several adjacent notochord cells inside the organ (stage 16) showing comparatively scarce endoplasmic reticulum (*er*), a yolk granule in state of digestion (*y*), Golgi complexes (*G*), numerous mitochondria (*m*), and some remainders of terminal bars (*tb*). Araldite, P.–U. ×14,400.

FIG. 20. Peripheral notochord cells at stage 15 showing a small fragment of the endoplasmic reticulum being formed by the outer nuclear membrane (*ner*). In the adjacent cell on the right another profile of a free fragment of endoplasmic reticulum (*er*). Araldite, P.–U. ×12,600.

FIG. 21. Similar example of endoplasmic reticulum (*ner*) being formed by nuclear envelope. Note the similarity of the contents of this fragment and that of the free endoplasmic reticulum (*er*). Araldite, L.A. ×10,800.

PLATE 4

FIG. 22. Several fragments of adjacent notochord cells at stage 20 showing an endoplasmic reticulum profile continuous with outer nuclear membrane (*ner*) and numerous endoplasmic reticulum fragments forming lake-like dilatations (*er*). Note many mitochondria and two vacuoles: with and without the limiting membrane (v_1 and v_2). Methacrylate. ×13,500.

FIG. 23. Formation of endoplasmic reticulum by the outer nuclear membrane (*ner*), and free endoplasmic reticulum in the cytoplasm covered with numerous ribosomes (*er*). Stage 22. Araldite, L.A. ×33,300.

PLATE 5

FIG. 24. Fragment of a notochord cell at stage 15 showing the beginning of vacuolization with endoplasmic reticulum profiles (*er*) surrounding the appearing vacuole. Araldite, L.A. ×12,600.

FIG. 25. Fragment of a 'light' notochord cell at stage 20 showing the relation between mitochondria (*m*) and endoplasmic reticulum (*er*), the latter forming in some cases sockets surrounding mitochondria. Araldite, P.–U. ×29,400.

FIG. 26. Dilatation of the endoplasmic reticulum (*er*) at stage 18. Methacrylate. ×20,300.

FIG. 27. Appearance of the endoplasmic reticulum after the vacuolization has reached its maximum. Araldite, P.–U. ×9,800.

PLATE 6

FIG. 28. Comparison of a 'light' cell (*lc*) and a 'dark' cell (*dc*) at stage 25. In the 'light' cell there is visible a tangential section through the limiting membrane of the endoplasmic reticulum with circular (*c*), linear (*l*), and rosette-like (*r*) groups of ribosomes. Araldite, L.A. ×28,800.

FIG. 29. Tangential section through endoplasmic reticulum membrane showing branchings (*b*) at stage 25. Araldite, L.A. ×39,000.

FIG. 30. Fragment of a 'dark' cell (*dc*) at stage 25 with numerous Golgi complexes (*G*), endoplasmic reticulum fragments (*er*), and ribosomes. Between that cell and the adjacent 'light' one (*lc*) there are two intercellular spaces (*is*). Araldite, P.–U. ×32,000.

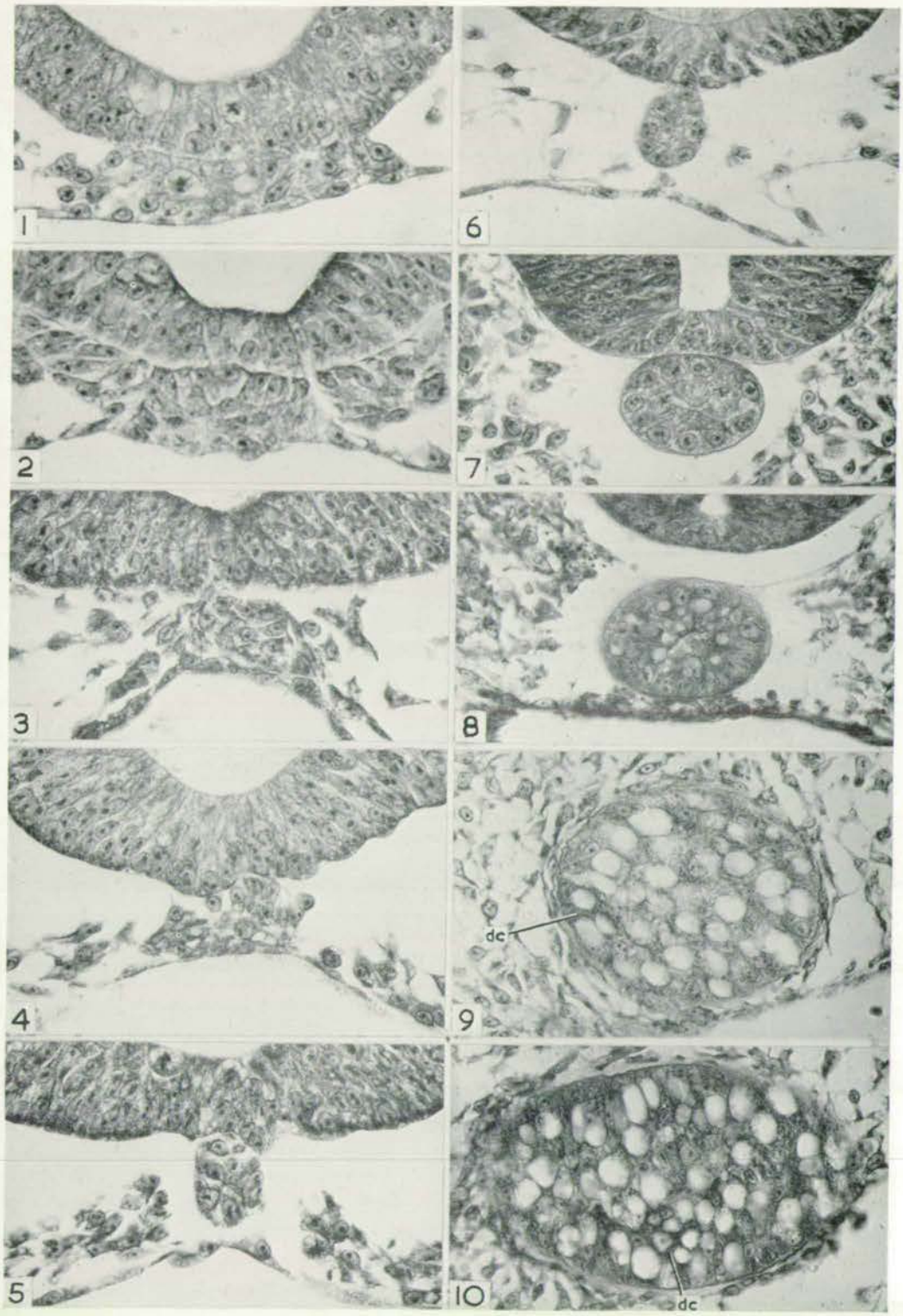

A. JURAND

Plate 1

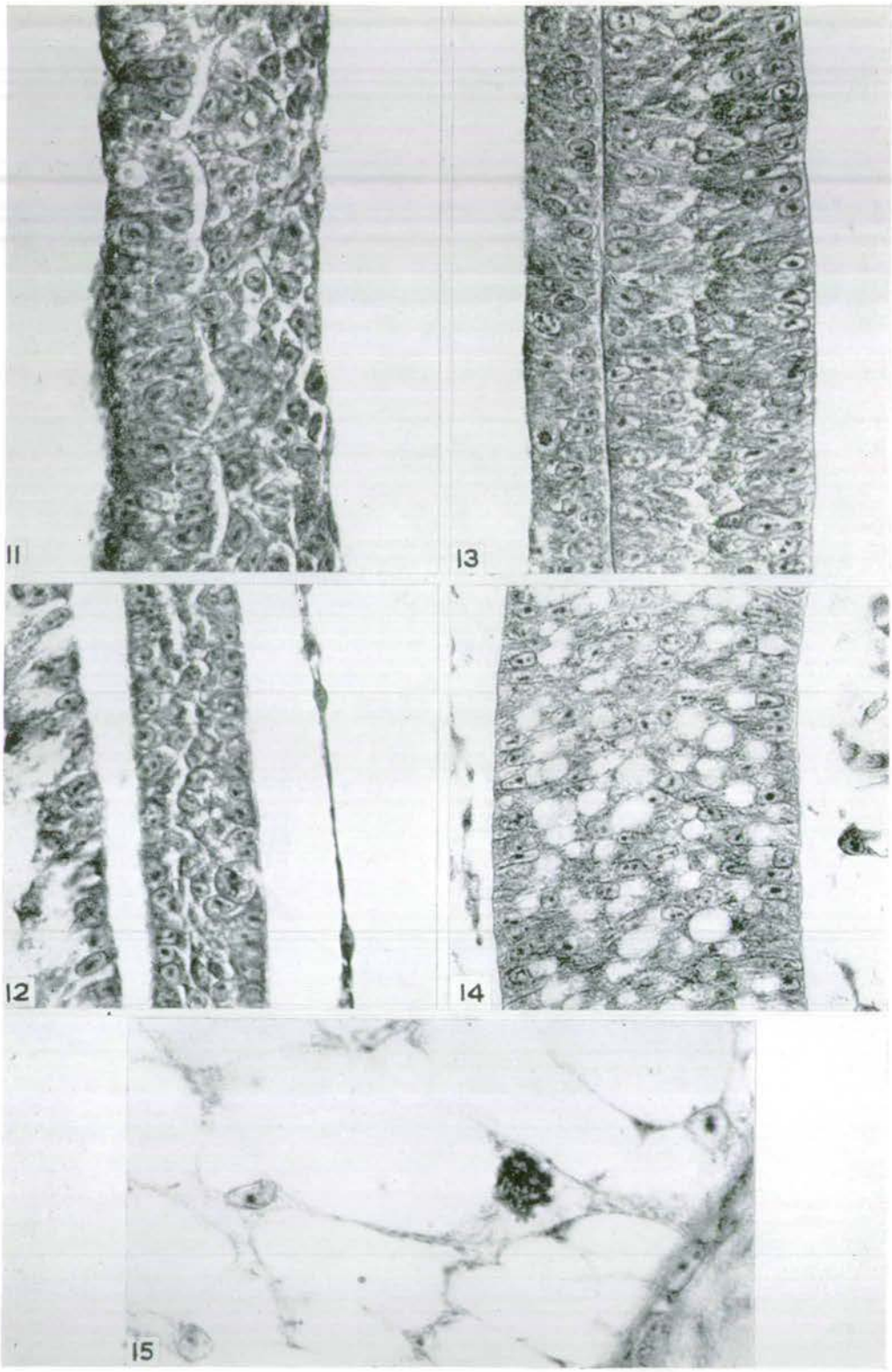

A. JURAND

Plate 2

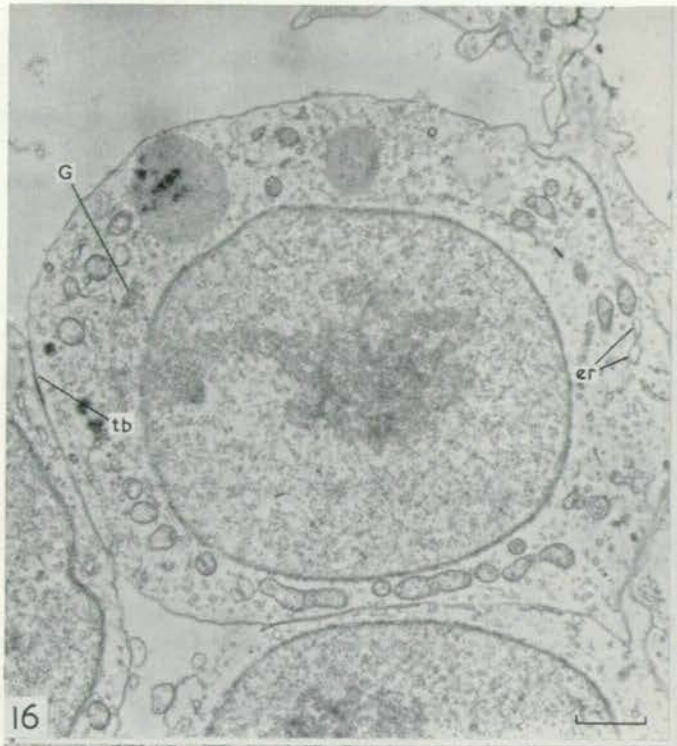

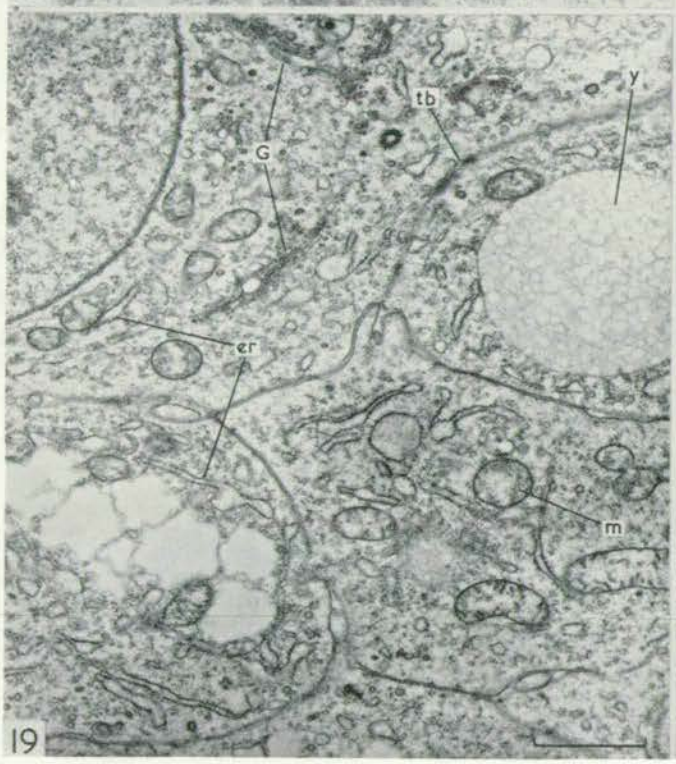

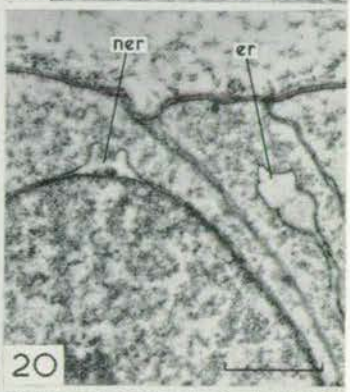

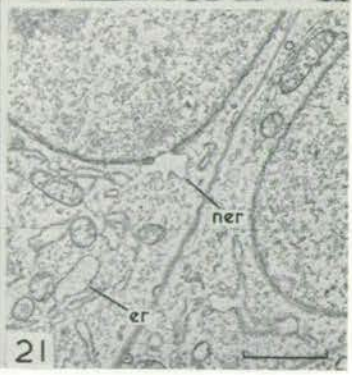

A. JURAND

Plate 3

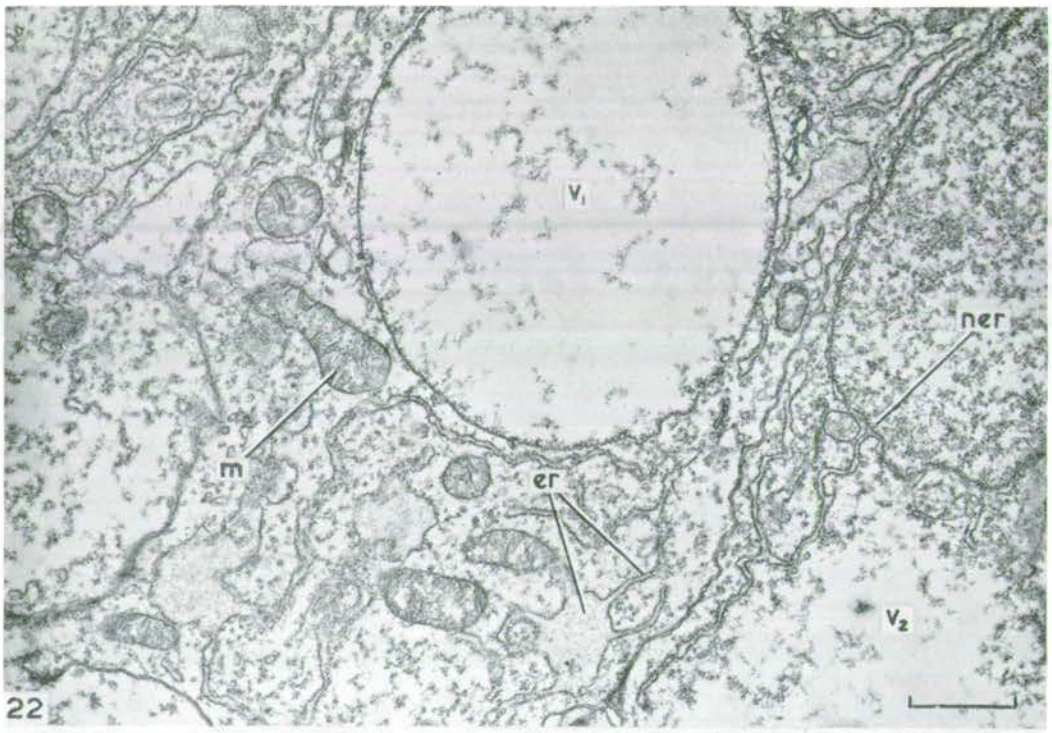

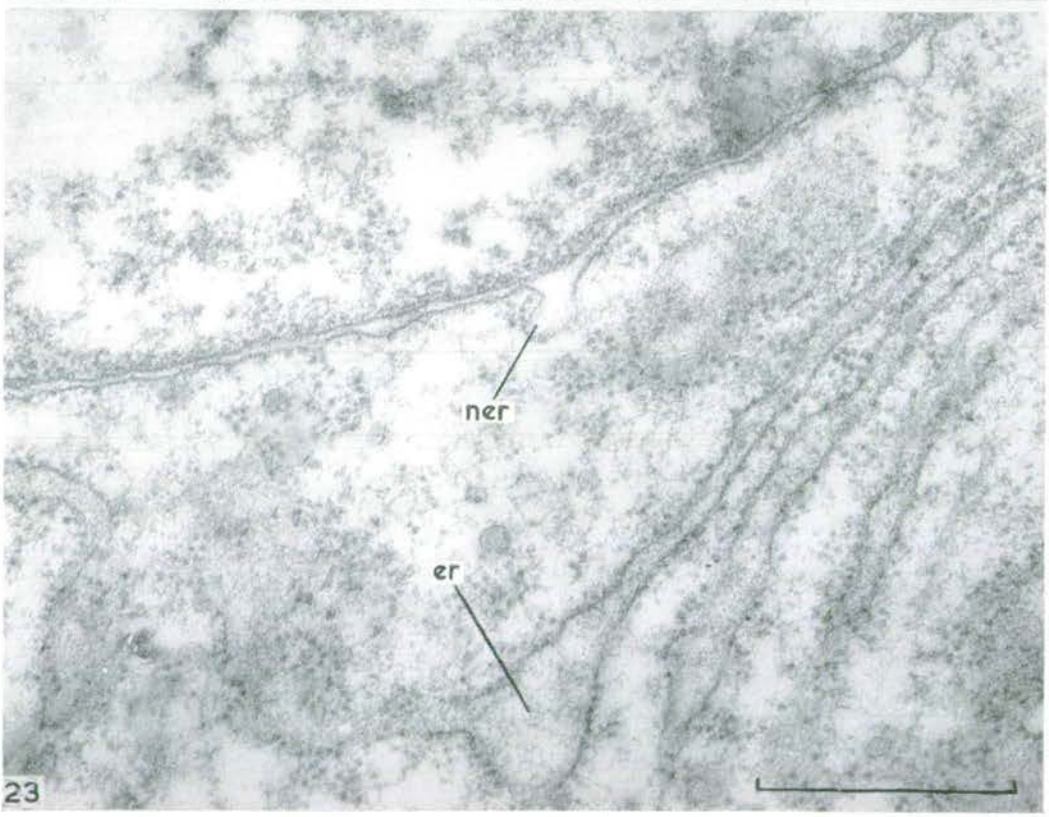

A. JURAND

Plate 4

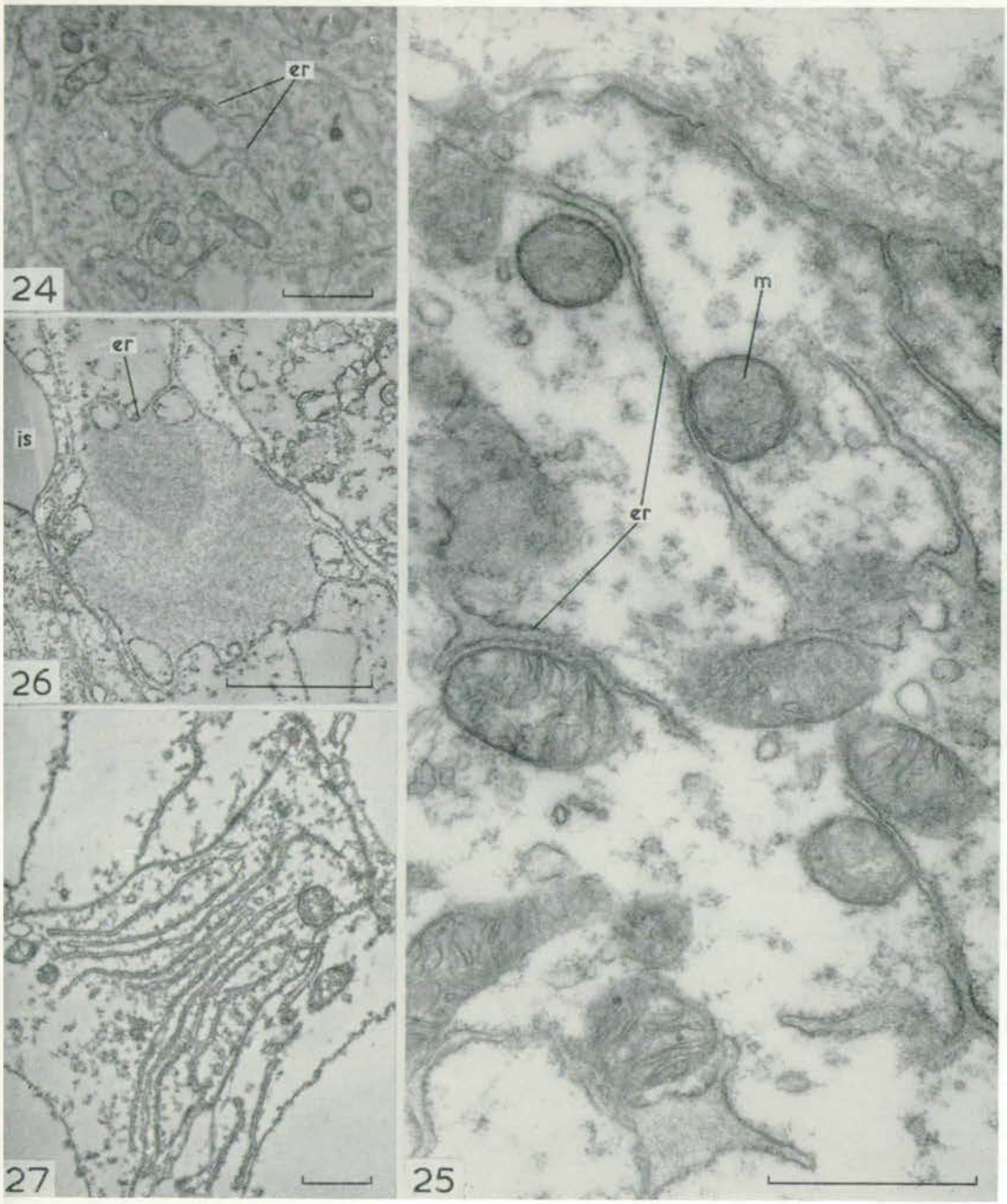

A. JURAND

Plate 5

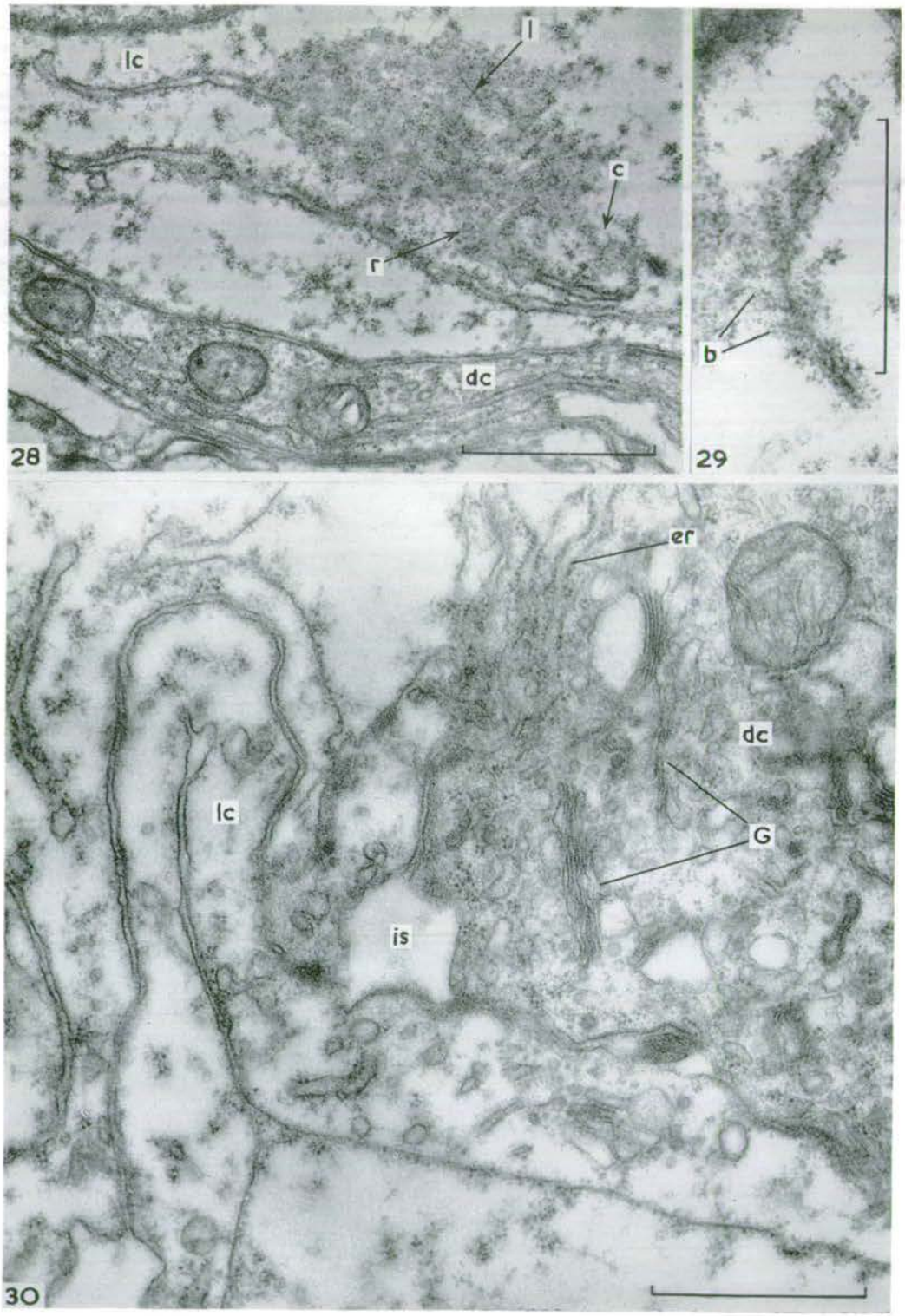

A. JURAND

Plate 6

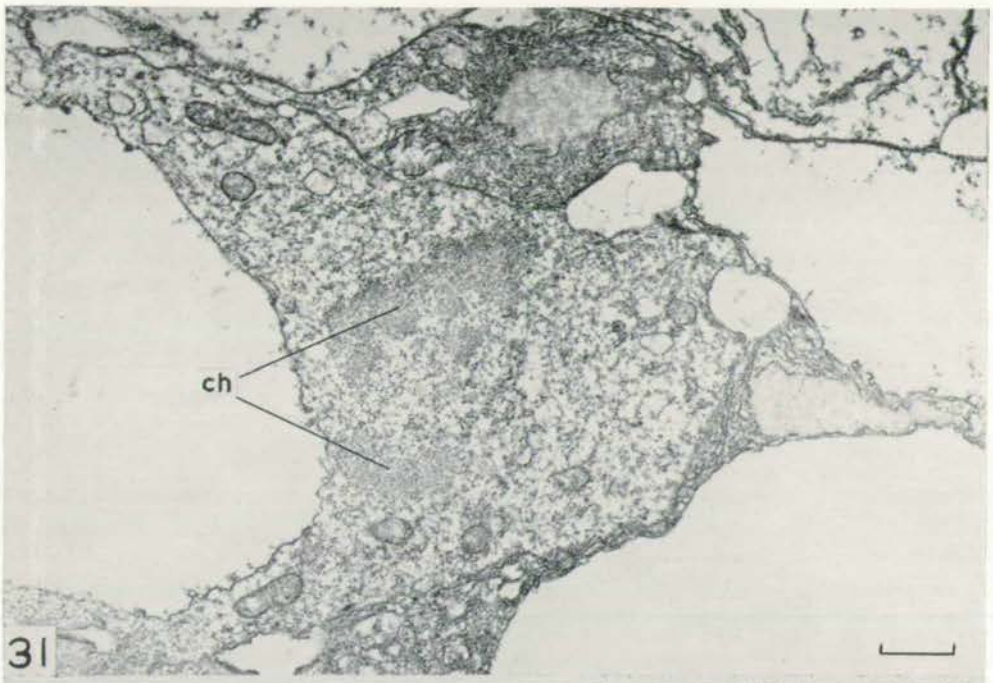

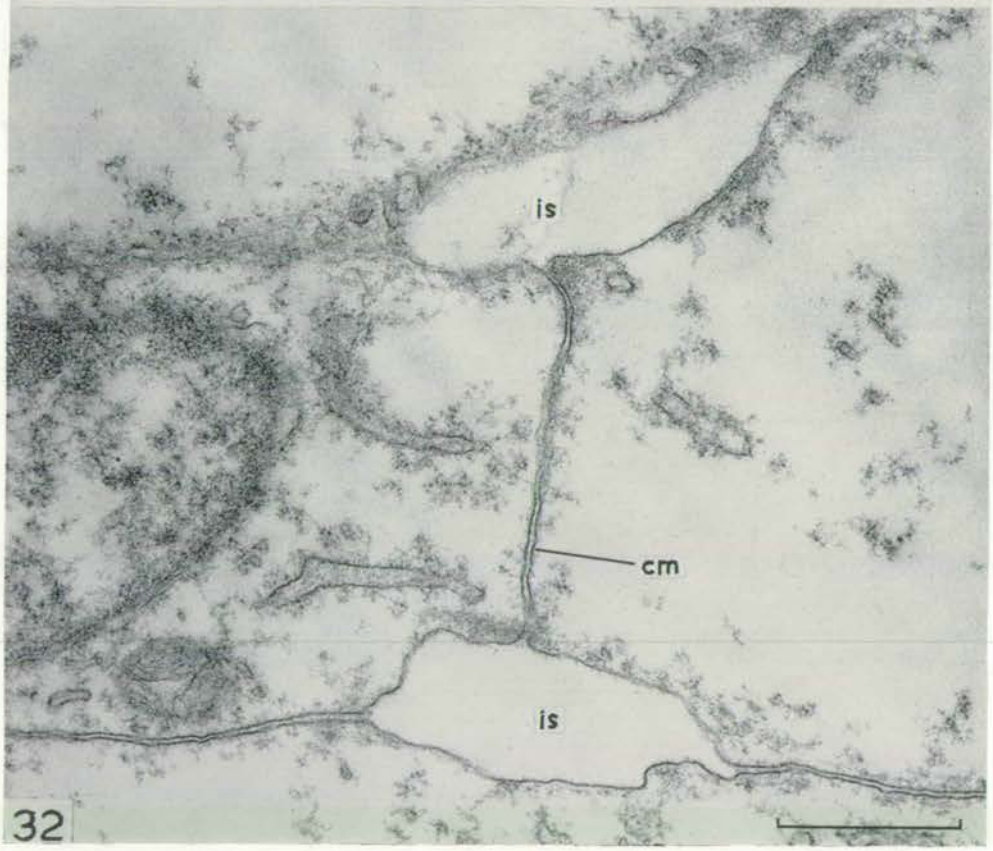

A. JURAND

Plate 7

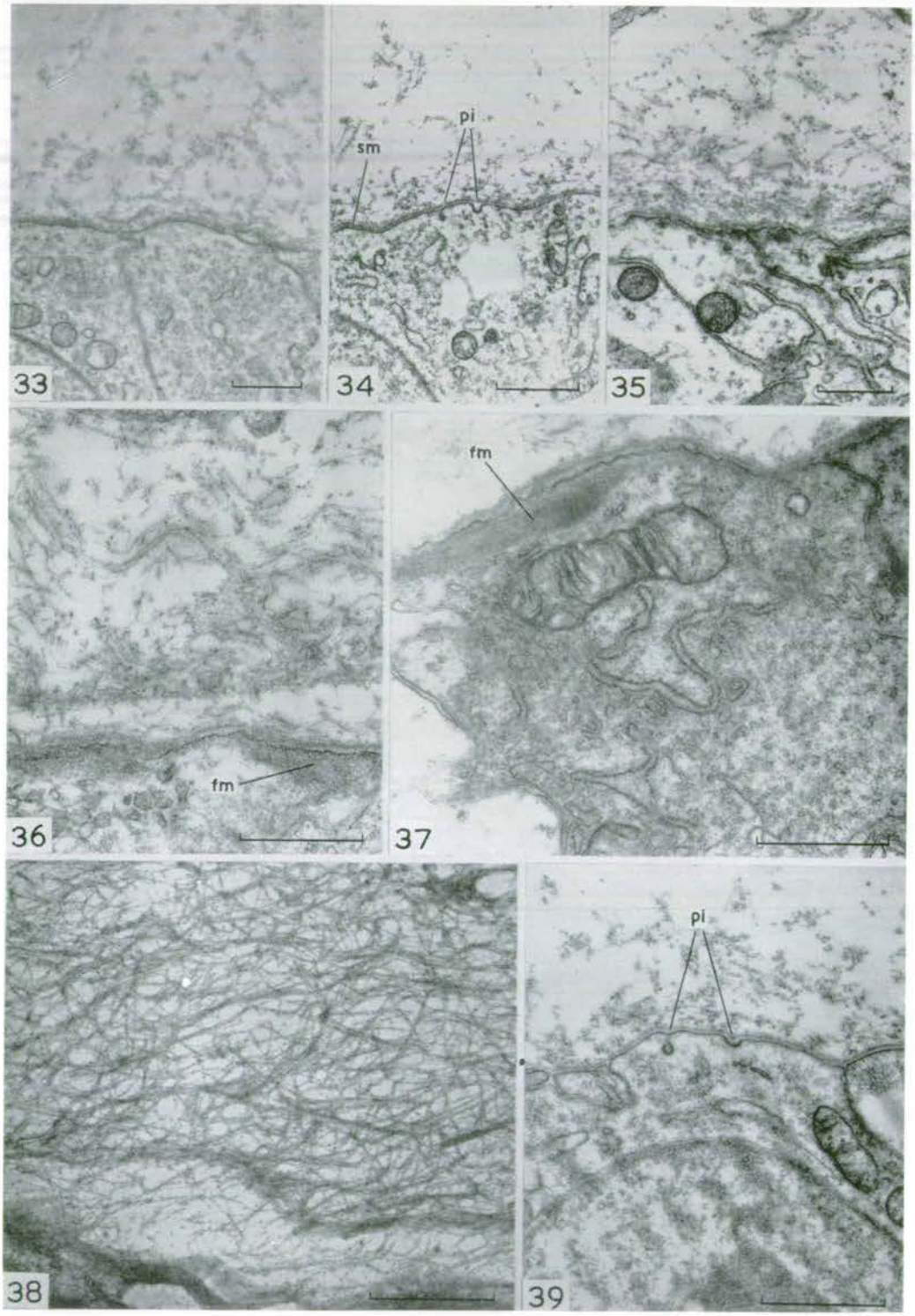

A. JURAND

Plate 8

PLATE 7

FIG. 31. Highly vacuolated cell during mitosis with sets of chromosomes (*ch*) pushed aside by the vacuole (v_1). Stage 21. Methacrylate. ×9,600.

FIG. 32. Fragments of adjacent 'light' cells at stage 24 to show the continuity of cell membranes and intercellular spaces between them (*is*). Araldite, P.–U. ×24,000.

PLATE 8

FIG. 33. Appearance of the perichordal sheath at stage 14. Fibrous material consisting of lumps scattered outside the notochord is only slightly denser at the surface of the organ. Araldite, L.A. ×10,000.

FIG. 34. Fibrous material forming a membrane (*sm*) covering the outer surface of the notochord at stage 17. Note pinocytic-like activity of the peripheral cell membrane (*pi*). Araldite, P.–U. ×12,000.

FIG. 35. Stage 20—notochord sheath still denser and thicker. Note no membrane outside the sheath. Araldite, P.–U. ×10,800.

FIG. 36. Notochord sheath at stage 25 consisting of two layers, upper one presumably the older, and the lower, newly formed, less dense and narrower with denser part at the very surface of the organ. Note some fibrous material (*fm*) in the cytoplasm below the peripheral cell membranes. Araldite, P.–U. ×18,000.

FIG. 37. Fragment of a peripheral 'dark' cell at stage 25 to show the presence of a fibrous material (*fm*) in the cytoplasm just below the cell membrane suggesting to be the source of material forming the internal zone of the notochord sheath. Araldite, L.A. ×19,200.

FIG. 38. Higher magnification of notochord sheath fibres at stage 25. Araldite, P.T.A. ×22,000.

FIG. 39. Stage 17—pinocytic activity of the peripheral cell membranes (*pi*). Araldite, P.–U. ×18,000.

(*Manuscript received 5:iv:62*)

Anti-mesodermal activity of a nitrogen mustard derivative

by A. Jurand

J. Embryol. exp. Morph., Vol. 11, Part 4, pp. 689–696, December 1963
Printed in Great Britain

Anti-mesodermal Activity of a Nitrogen Mustard Derivative

by A. JURAND[1]

From the Institute of Animal Genetics, Edinburgh

WITH TWO PLATES

AMONGST the numerous derivatives of nitrogen mustard that have been tested for their anti-tumour activity on Walker carcinoma by Danielli and his collaborators (1961), $(Cl—CH_2—CH_2)_2$: $N—C_6H_4—O—CO—NH—C_6H_4—COOH$, i.e., *p*-(*NN*-Di-2-chloroethyloamino)-phenyl-*N*-(*p*-carboxyphenyl)-carbamate (later referred to as I.C. 140), has been found to be particularly promising. To check its cytotoxic activity for embryos, and to find out, if possible, whether I.C. 140 has any specific selectivity for particular embryonic tissues, chick and mouse embryos were treated during the early stages of development.

MATERIAL AND METHODS

Chick embryos were explanted according to the method described by New (1955) at Stage 4 or 5 (Hamburger & Hamilton, 1955), i.e., after a pre-incubation period of 22 hr. As I.C. 140 is difficult to dissolve in water, it was first suspended in an appropriate volume of 0·9 per cent. saline solution. One part of this suspension was then diluted with nine parts of liquid albumen to give the final concentration of 50 or 100 μg. per ml. In these concentrations I.C. 140 appeared to dissolve almost completely. The embryos were treated with 0·5 ml. of either solution administered round the culture rings used for cultivation of the explanted embryos. Re-incubation of treated embryos took place for 22-24 hr., i.e., until the control embryos had reached Stage 12–13. For these experiments forty-two experimental and eighteen control chick embryos were used.

Mouse embryos were treated by injecting I.C. 140 subcutaneously into 2–5 month-old pregnant females of the outbred J.C. strain which had been selected for the genes *a*, *b* and *bt* and inbred by brother–sister matings for eight generations with the retention of sub-lines. Suspensions for the injections were

[1] *Author's address:* The Institute of Animal Genetics, West Mains Road, Edinburgh 9, Scotland, U.K.

TABLE 1

Compound	*Molecular weight*	*Range of effective concentrations for explanted chick embryos*		*Effective doses for mouse embryos in mg. per kg. body weight pregnant female*	
		In μg. per ml.	*In millimols* (mm.)	*Embryonic LD_{50}*	*Teratogenic range*
1	2	3	4	5	6
p-Amino-phenyl derivative of nitrogen mustard (parent compound)	233	64–200	0·27–0·85	12	9–13·5
p-Acetyl-amino-phenyl derivative of nitrogen mustard (acetyl derivative)	275	64–200	0·23–0·72	36	24–45
p-Fluoro-acetyl-amino-phenyl derivative of nitrogen mustard (fluorine derivative)	293	200–800	0·68–2·7	45	30–54
Triethanomelamine (TEM)	204	2–5	0·0097–0·024	1·5	1·35–1·65
I.C. 140	397	50–100	0·12–0·25	72	60

prepared fresh every day, shortly before use, in 0·9 per cent. saline solution. The injected doses were calculated in milligrams per kilogram body weight.

As in previous investigations (Jurand, 1959, 1961), the 'embryonic LD_{50}' was first determined. This is the total dose which, if administered subcutaneously in three equal parts on the 7th, 8th and 9th days of pregnancy, kills about 50 per cent. of the implanted mouse embryos by the 15th day of pregnancy. For I.C. 140 this dose was found to be 72 mg. per kg. body weight (see Table 1).

All experimental females received a total of 60 mg. per kg. body weight divided into three equal parts and injected on the same three consecutive days. The day on which the plug was found was regarded as the first day of pregnancy.

The females were killed by cervical dislocation on the 10th, 11th or the 15th day of pregnancy. After external examination of the embryos some of those with abnormalities and corresponding control embryos were prepared for histological examination. After preliminary fixation with Carnoy's fluid (with chloroform) in the uterus the embryos were dissected and refixed in the same fixative for another 12–24 hr. Afterwards the fixative was replaced by absolute alcohol (three changes) and the embryos, after being cleared in methyl benzoate, were embedded in 54°C. wax. The orientation of the embryos was adjusted according to the organs to be examined. Sections 6–7μ thick were stained with methyl green-pyronine. The chick embryos were prepared for histological examination in similar way.

The total number of pregnant mice used in the above experiments was 142 (925 embryos).

RESULTS

The effective concentrations of I.C. 140 for treatment of explanted chick embryos were chosen on the results of preliminary experiments. The most satisfactory results were obtained with concentrations of 50 and 100 μg. per ml.

When examined macroscopically, chick embryos treated with I.C. 140 showed considerable retardation in development, the number of somites being, on average, less than in the control embryos. After treatment with I.C. 140 at a concentration of 50 μg. per ml., the experimental embryos usually reached Stage 10 or 11 (10–13 somites), whereas the control embryos were at Stage 12 or 13 (16–19 somites).

The majority of the experimental embryos showed enlarged myocoeles in the somites (Plate 1, figs. 1, 2). In other embryos, which developed up to Stage 11, the somites suffered severe disorganization, and the embryos showed a complete lack of segmentation of the paraxial mesoderm (Plate 1, fig. 3). It should be mentioned that the embryos with these changes in the somite region were otherwise well developed and did not show any other major abnormalities.

After treatment at the higher concentration, i.e. 100 μg. per ml., the degree of underdevelopment was in all cases more pronounced, the embryos reaching only Stage 8 or 9. In these embryos the somitic mesoderm was invariably disorganized. It was never segmented, and the neural groove was in almost all cases open, or only partially closed.

Microscopical examination of chick embryos confirmed that the somites, when formed, showed enlarged myocoeles, while in more severely affected embryos the paraxial mesoderm remained scattered without being divided into individual somites (Plate 1, fig. 4). In more severely affected embryos, particularly in those treated with I.C. 140 at a concentration of 100 μg. per ml., head mesenchyme was scarce and many necrotic cells could be found in it (Plate 1, fig. 5).

In experiments with mouse embryos the effective dose used was 60 mg. per kg. divided into three equal parts injected subcutaneously on the 7th, 8th and 9th days of pregnancy. In 10-day-old and 11-day-old embryos the most severely affected tissue also appeared to be the mesoderm. This could be observed in the underdeveloped, and in the underdeveloped and necrotically changed somites (Plate 1, figs. 6, 7, 8). It was also very pronounced in sections through the front and hind limb buds of 11-day-old embryos (Plate 2, figs. 9, 10). In this group of embryos general retardation of development was only slightly marked.

In 15-day-old embryos, which were retarded by about 24 hr., the anomalies found on macroscopical examination were strikingly similar, or actually identical, to those known from previous experiments with triethanomelamine (TEM) and other nitrogen mustard derivatives. Kinking of the vertebral column and spinal cord was found in 32 per cent. of the embryos (Plate 2, figs. 11, 12), unilateral or bilateral underdevelopment of the eyeball in 38 per cent. (Plate 2, figs. 13, 14), liver hernia in 48 per cent., and shortening of the

---

PLATE 1

FIG. 1. Trunk region somites of a control chick embryo at Stage 13. × 50.

FIG. 2. Trunk region somites in chick embryo after treatment with I.C. 140 at concentration of 50 μg. per ml. Note enlarged myocoeles. × 50.

FIG. 3. Trunk region in chick embryo with a complete lack of segmentation of the paraxial mesoderm after treatment with I.C. 140 at concentration of 50 μg. per ml. × 50.

FIG. 4. Transverse section through the somite region in chick embryo after treatment with I.C. 140 at concentration of 50 μg. per ml. × 190.

FIG. 5. Necrotic changes in the head mesenchyme in chick embryo after treatment with I.C. 140 at concentration of 100 μg. per ml. × 190.

FIG. 6. Somites of thorax region in 10-day control mouse embryo. × 110.

FIG. 7. Somites of thorax region in 10-day mouse embryo after treatment with a total dose of 60 mg. per kg. body weight. × 110.

FIG. 8. Somitic mesoderm necrotically changed after the same treatment as in Fig. 7, but in a more severely affected embryo. × 110.

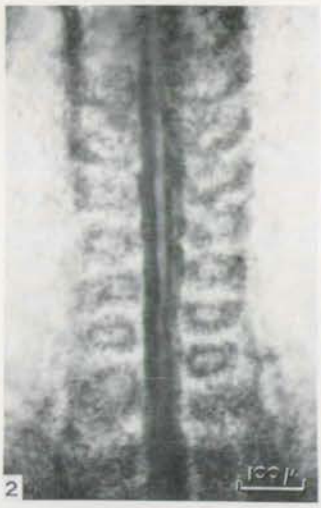

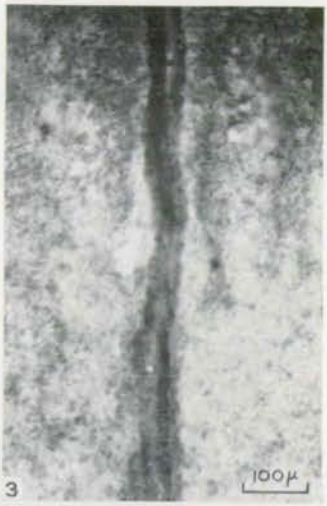

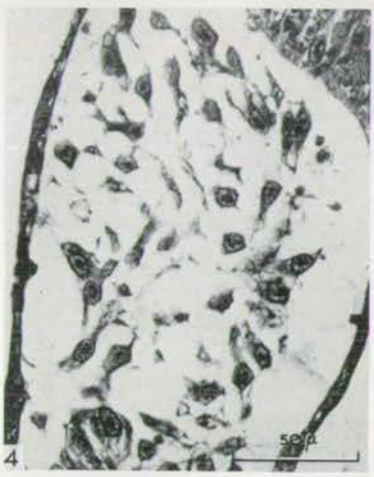

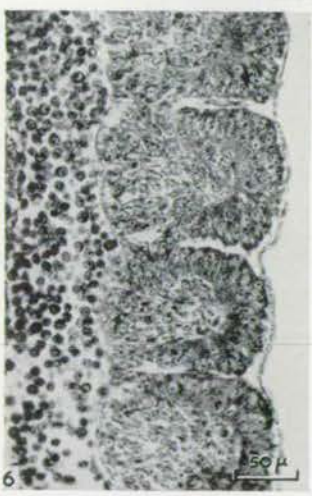

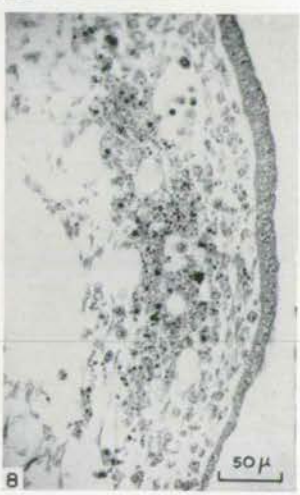

PLATE 1

A. JURAND

(*Facing page* 692)

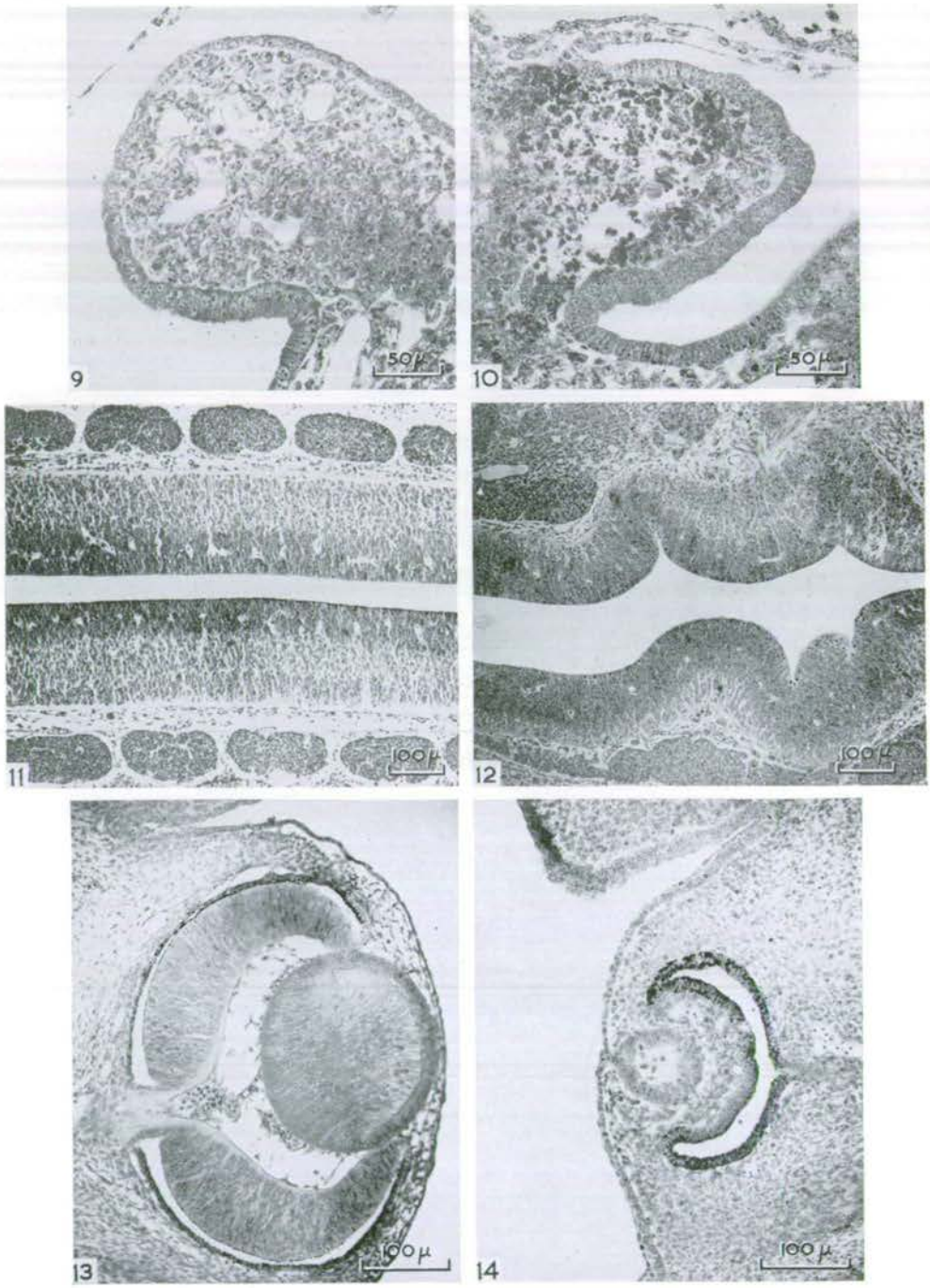

PLATE 2

A. JURAND

(*Facing page* 693)

fore limbs in 12 per cent. In many cases several of the above abnormalities were recorded in the same embryos.

Histological examination of all the affected organs confirmed that the mechanism of the changes was of the same type as that described previously as resulting from treatment with TEM and other nitrogen mustard derivatives.

DISCUSSION

In Table 1, numerical data are presented for the concentrations and effective doses used in the present and previous experiments. From a comparison of the effective concentrations of the first three compounds used in the chick experiments, expressed in molar terms (column 4), it may be concluded that the acetyl derivative, used in practically the same concentration as the parent compound, undergoes complete hydrolysis to form the parent compound. The fluorine derivative, on the other hand, appears to be less readily hydrolysed to the parent compound, and this is why it must be used in higher concentration before it shows cytotoxicity. The molarity of the effective concentration of I.C. 140 is, however, on average, considerably lower than that of other derivatives of nitrogen mustard. This may be explained by the fact that the cytotoxic activity of I.C. 140 is higher, due to the higher cytotoxicity of the active molecules formed by the hydrolysis, which are undoubtedly different from the molecules of the parent compound. In comparison with TEM, on the other hand, I.C. 140 appears much less cytotoxic for both chick and mouse embryos. This is understandable, because TEM acts with all its molecules as it does not undergo hydrolysis, and, being an alkylating agent, is apparently by its very nature much more cytotoxically active than the nitrogen mustard derivatives. Moreover, its molecules contain three active centres instead of two as in nitrogen mustard derivatives.

The teratogenic doses of the above mentioned compounds for mouse embryos (columns 5 and 6) are different from the effective concentrations of these compounds for explanted chick embryos. Particularly striking is the large amount

---

PLATE 2

FIG. 9. Section through a control front limb-bud of 11-day mouse embryo. × 154.

FIG. 10. Section through a front limb-bud of an experimental 11-day mouse embryo after treatment with a total dose of 60 mg. per kg. body weight. Note the extensive necrosis of the mesoderm of the limb-bud. × 154.

FIG. 11. Tangential section of the back through the axial organs of a 15-day control mouse embryo. × 62.

FIG. 12. Tangential section of the back through the kinks in the axial organs of a 15-day experimental mouse embryo after treatment with I.C. 140. × 62.

FIG. 13. Section through normal eye of a control 15-day mouse embryo. × 100.

FIG. 14. Section through an underdeveloped eye of 15-day mouse embryo after treatment with I.C. 140. × 100.

of I.C. 140 necessary for a teratogenic dose compared with its comparatively low effective concentration for chick embryos. To explain this it must be assumed that I.C. 140 is very rapidly hydrolysed in the presence of egg albumen and that the resulting molecules are more cytotoxic than those formed by the hydrolysis of the other two derivatives of nitrogen mustard, viz., the acetyl and fluorine derivatives. This difference is due to differences in the chemical structure of the compounds concerned.

Danielli and his collaborators (1961) have pointed out that when I.C. 140 was tested for its anti-tumour activity on Walker carcinoma, it decomposed rapidly in the alimentary canal with a consequent increase in general toxicity and a reduction in anti-tumour activity. When, however, the compound was administered by the intramuscular route its anti-tumour activity was much more pronounced. As far as the author is aware, Danielli *et al.* do not give any further explanation of their results, but probably the chemical changes following the two types of administration are different. In the first case the molecules formed are more generally toxic but less cancero-static, while in the second, due to hydrolysis which takes place locally in the tumour, the anti-tumour activity is more pronounced.

When the chemical formula of I.C. 140 is taken into consideration, it seems quite possible that there may be at least two different types of decomposition taking place in the body fluids; these will depend on the presence or absence of particular enzymes, and probably also on the pH of the body fluids in the alimentary canal, the tissues or the blood.

There appears to be a certain similarity between Danielli's results and those presented in this paper. It has been shown that a relatively lower concentration of I.C. 140 is needed to treat explanted embryos than might have been expected from the dose necessary in the case of subcutaneous administration to pregnant mice. This also can be explained by differences in the chemical conditions under which the decomposition of I.C. 140, by hydrolysis or otherwise, takes place.

The experiments reported here were designed to reveal any affinity of I.C. 140 for particular embryonic organs. There is no doubt that such an affinity exists, as it is the mesoderm which suffers first. The same is true of the other alkylating agents examined previously (Jurand, 1958, 1959, 1960), except the fluorine derivative (Jurand, 1961) which first affects the neural tissue. In the later stages of development, i.e., in mouse embryos 15 days old, after treatment with any of these compounds, all abnormalities such as kinking of the vertebral column, microphthalmia, liver hernia, anencephaly, brain hernia, and shortening of the limbs, can be attributed to induced injury of the mesodermal elements which are indispensable for the normal development of the structures involved. In general, the mesodermal elements seem to be more sensitive to cytotoxic agents than any other embryonic cells, and this is probably true not only for nitrogen mustard derivatives.

It is widely accepted that teratogens become effective at the beginning of, or

during, differentiation, and that susceptibility to them decreases as differentiation proceeds (Ebert, 1961). Mesodermal cells are widely involved in the structure of very many organs, and so the differentiation of mesodermal derivatives lasts much longer than that of any other germ layer. This might be at least a partial explanation of the fact that mesoderm is the embryonic tissue which is so often affected by teratogens.

Strangely enough, the mechanism of chemically induced teratogenesis is not very often discussed along these lines, mainly because insufficient comparative information is available about the cytological side of the cytotoxic activity of different compounds in the early stages of embryonic development. The fact that anti-mesodermal activity is by no means confined to nitrogen mustard derivatives was proved by the numerous abnormalities induced in human embryos by thalidomide which, although not an alkylating agent, also affected mainly mesodermal structures (McBride, 1961).

SUMMARY

1. In explanted early chick embryos p-(*NN*-Di-2-chloroethylamino)-phenyl-*N*-(*p*-carboxyphenyl)-carbamate (I.C. 140), used at concentrations of 50 or 100 μg. per ml., brings about disorganization and lack of segmentation of the somitic mesoderm, with simultaneous retardation by about 2 stages.

2. The 'embryonic LD_{50}' of I.C. 140 for mouse embryos is 72 mg. per kg. body weight.

3. In 10- and 11-day-old mouse embryos, 60 mg. per kg. body weight of I.C. 140, divided into three equal parts injected subcutaneously on the 7th, 8th and 9th days of pregnancy, affects primarily the somitic mesoderm and the limb-bud mesoderm.

4. In 15-day-old mouse embryos receiving the same treatment all the developmental anomalies characteristic of the other alkylating agents tested previously were found, e.g., kinking of the axial organs, unilateral or bilateral underdevelopment of the eyeball, liver hernia and shortening of the fore-limbs.

RÉSUMÉ

Activité anti-mésodermique d'un dérivé d'une ypérite nitrée

1. Utilisé à des concentrations de 50 ou 100 μg par ml sur de jeunes embryons de poulet, le p-(*NN*-Di-2-chloroéthylamino)-phényl-*N*-(*p*-carboxyphényl)-carbamate (I.C. 140) provoque la désorganisation et l'absence de segmentation du mésoderme somitique, et un retard simultané d'environ 2 stades.

2. La 'DL_{50} embryonnaire' de l'I.C. 140 pour les embryons de souris est de 72 mg. par kg. de poids corporel.

3. Chez des embryons de souris de 10 et 11 jours, 60 mg. d'I.C. 140 par kg. de

poids corporel, divisés en trois parties égales administrées en injections sous-cutanées les 7e, 8e et 9e jours de la gestation, affectent primitivement le mésoderme somitique et celui du bourgeon du membre.

4. Chez les embryons de souris de 15 jours subissant le même traitement, on a trouvé toutes les anomalies du développement caractéristiques des autres agents alkylants essayés auparavant, par exemple vrillage des organes axiaux, sous-développement unilatéral ou bilatéral du globe oculaire, hernie hépatique et raccourcissement des membres antérieurs.

ACKNOWLEDGEMENTS

The author wishes to express thanks to the British Empire Cancer Campaign for the research grant under which this work was carried out and to Professor C. H. Waddington for reading the manuscript.

Thanks are also due to Dr L. N. Owen of the Imperial College of Science and Technology, London, for supplying the samples of I.C. 140, to Dr D. S. Falconer for facilities in the mouse house, to Mr D. W. Pinkney for his highly skilled help in the photomicrography and to Miss Patricia Collins for technical assistance.

REFERENCES

DANIELLI, J. F. (1961). Effect of route of administration upon action. British Empire Cancer Campaign Annual Report, pp. 574–5.

EBERT, J. D. (1961). First International Conference on Congenital Malformations. Summary and Evaluation. *J. Chron. Dis.* **13,** 91–132.

HAMBURGER, V. & HAMILTON, H. L. (1951). A series of normal stages in the development of the chick embryo. *J. Morph.* **88,** 49–92.

JURAND, A. (1958). Action of triethanomelamine (TEM) on early stages of chick embryos. *J. Embryol. exp. Morph.* **6,** 357–62.

JURAND, A. (1959). Action of triethanomelamine (TEM) on early and later stages of mouse embryos. *J. Embryol. exp. Morph.* **7,** 526–39.

JURAND, A. (1960). Comparative investigations of two nitrogen mustard derivatives on the early stages of development of chick embryos. *J. Embryol. exp. Morph.* **8,** 60–7.

JURAND, A. (1961). Further investigations on the cytotoxic and morphogenetic effects of some nitrogen mustard derivatives. *J. Embryol. exp. Morph.* **9,** 492–506.

MCBRIDE, W. G. (1961). Thalidomide and congenital abnormalities. *Lancet*, **2,** 1358.

NEW, D. A. T. (1955). A new technique for the cultivation of the chick embryo *in vitro*. *J. Embryol. exp. Morph.* **3,** 326–31.

(Manuscript received 11th February 1963: revised 17th May 1963)

Ultrastructural aspects of early development of the fore-limb buds in the chick and the mouse

by A. Jurand

Reprinted without change of pagination from the
Proceedings of the Royal Society, B, *volume* 162, pp. 387-405, 1965

Ultrastructural aspects of early development of the fore-limb buds in the chick and the mouse

By A. Jurand
The Institute of Animal Genetics, Edinburgh

(*Communicated by C. H. Waddington, F.R.S.*—
Received 12 *August* 1964—*Revised* 11 *November* 1964)

(Plates 40 to 49)

Light microscope investigations of the early development of the fore-limb buds in chick and mouse were made to guide electron microscope studies with these tissues. At the time of maximal development of the ectodermal apical ridge there is a higher concentration of cytoplasmic *RNA* in the apical ridge cells than in the other cells of the limb bud.

Ultrastructural investigations showed that, in the mesoblast cells at the earliest stages, profiles of endoplasmic reticulum are often found attached to the outer nuclear membrane. Somewhat later, discontinuities of nuclear envelope occur by which the content of the nucleus may communicate with the endoplasmic reticulum. In the cytoplasm of the mesoblast cells at these stages there were many granules similar in form and size to secretory granules of gland cells. Ribosomes are in the polysomal condition. At stages later than 20 in chick and in 11-day-old mouse embryos, the mesoblast shows the character of a syncytial tissue.

Epiblast cells possess all the characters of an epithelium with well-developed junctional complexes. The desmosomes form a chain consisting of units equipped with individual dense plaques, but connected by continuous bundles of fibres running parallel to the chain. The free cell membrane of the epiblastic cells, particularly at early stages, forms numerous microvilli and single cilia. In later stages during the formation of the ectodermal apical ridge, cilia have been found between the cells. This fact indicates that when the apical ridge is formed ectodermal cells migrate towards the margin of the limb bud. At these stages microvilli are also found between the apical ridge cells where they contribute to the cell-to-cell adhesion.

Beginning at stage 22 in chick embryos and from the 12th day in mouse embryos there are in cells of the apical ridge numerous and extensive Golgi systems spread throughout the cytoplasm. Somewhat later there appear successively lysosomes, cytolysomes and extra-nuclear necrotic centres. All these organelles manifest acid phosphatase activity and are thought to initiate the involutive process in the apical ridge. Pycnosis and karyorrhexis appear as the last stage of cellular degeneration. Degenerating cells undergo phagocytosis by neighbouring epithelial cells.

A basement membrane is present at all stages of development of the chick and mouse limb buds. It is an acellular continuous structure lining the internal (basal) surface of the epiblast, but in chick embryos it shows discontinuities immediately under the apical ectodermal ridge at the time of its maximum development.

Introduction

The complex and indeed controversial problem of the mutual interaction between epiblast and mesoblast in developing limbs has long been a subject of extensive descriptive and experimental work. There are in the literature numerous review articles dealing with this problem (e.g. Steiner 1928; Mangold 1928; Balinsky 1931; Saunders 1948; Nicholas 1955). Probably the most comprehensive and up-to-date accounts, referring particularly to chick wing buds, have been published by Zwilling (1961*a*, *b*).

It is generally believed that the first morphogenetic activity at the beginning of the development of a limb bud is the proliferation and accumulation of mesodermal

cells deriving from the somatopleural mesoderm in predetermined paraxial regions which later become the fore- and hind-limb primordia. It is not known, however, what actually initiates the very early morphogenetic changes in the limb primordia at their appropriate sites; this can be ascribed to the genetically conditioned symmetrical field phenomena in embryos of all tetrapods which arise locally from interaction of many biophysical and biochemical factors. It is hardly possible that we shall ever know all of these factors involved in limb formation although we may hope to discover and correlate some of them (Waddington 1956).

The epithelium covering the presumptive limb area does not seem to differ, at least morphologically, from non-limb epithelium in adjacent areas. It is assumed that, soon after the proliferation of mesoblastic cells has begun, the latter induce the covering epithelium to thicken on the circumference of the still flat limb bud swelling, which in amniote and some anamniote vertebrates soon leads to the formation of the apical ectodermal ridge (calotte epidermique, la cape apicale, apicale Epidermisleiste, epitheliale Randleiste, cresta apicale). This structure was first described by Kölliker in 1879, but for many years the limb-bud epithelium as a whole was thought to play the role of limb-bud organizer (Filatow 1928; Steiner 1928; Balinsky 1931). This is apparently true only in the case of most amphibians where there is no real ectodermal ridge on early limb primordia.

More recently the inducing function of the epithelium was located by Saunders (1948) in the apical ectodermal ridge itself. This view was later proved experimentally, particularly by Zwilling (1949) who used the wing buds of a 'wingless' mutant in the chick. Later, Carter (1954) recognized the precursor of the ectodermal ridge as 'the limb-bud inductor'.

Zwilling (1956) has also demonstrated that in normal conditions a reciprocal genetically conditioned factor exists in the mesoblast which is responsible for the maintenance of the apical ectodermal ridge (the 'maintenance factor'). Thus, it is clear that the relationship between the ectoderm and mesoderm in limb buds is mutual in nature, as it is probably in other sites where these two germ layers come into contact.

The whole problem is obviously highly complex and it has not yet been elucidated in all details. The present work was undertaken to investigate the developing fore-limb buds of the chick and mouse mainly at the ultrastructural level in order to find out whether there are any features in the cells of the two components of the limb buds in which changes can be traced in successive stages of development. It was assumed that the morphogenetic processes would be reflected in some way at the ultrastructural level and it was hoped that the findings would throw light on the interpretation of previously published work.

Material and methods

Electron microscopy

Chick wing buds at all stages from 16 to 31 (Hamburger & Hamilton 1951) were obtained from Brown Leghorn eggs incubated at 38·5 °C. After opening the shell, as much as possible of the egg white was removed, and the yolk, together with the

embryo, was placed in a large Petri dish of Pannet–Compton's solution. After dissection the embryos were fixed for electron microscopy with 2% osmic acid solution buffered at pH 8·15 with veronal-acetate buffer containing sucrose (Jurand 1962).

Mouse embryos aged 9½, 10, 10½, 11, 12, 13 and 14 days were obtained from 2- to 5-month-old pregnant females of the outbred J.C. strain which had been selected for genes *a*, *b* and *bt*, and inbred by brother-sister litter-mate matings for ten generations with the retention of sublines. The day on which the plug was found was considered to be the first day of pregnancy. The embryos were dissected immediately after the females had been sacrificed by cervical dislocation. The fixative used was 1 or 2% osmic acid buffered with veronal acetate buffer at pH 7·2, according to Palade (1952), but with 3·5% sucrose instead of sodium chloride (Caulfield 1957).

For both kinds of embryos the temperature of the fixative was 0 °C at the moment of fixation. The fixative was subsequently allowed to warm up to room temperature. The overall time of fixation ranged from 30 to 45 min, depending on the age of the embryo.

During dehydration with graded alcohols (35, 70, 95 and three changes of 100%) the limb buds were cut off the embryos and transferred to a 1:1 mixture of 100% ethyl alcohol and the final mixture of Araldite epoxy resin (Glauert & Glauert 1958). The whole procedure of dehydration usually took approximately 1 h. After soaking for about 30 min in this mixture the limb buds were transferred to the final mixture of Araldite and stirred gently for 1 h at 45 to 50 °C using a slow-moving rotating shaker designed for the purpose. This technique effectively enhances the penetration of the viscous epoxy-resin. Stirring was usually repeated three times, each time changing the embedding medium, which was kept in a refrigerator. Meanwhile pre-dried gelatine capsules were filled up to approximately ⅚ of their volume with the final mixture of Araldite which was prepolymerized at 54 °C for about 4 h so that the limb buds could be embedded at the top of the capsules by filling up the rest of the available volume. At this stage the embedded limb buds were usually left for 24 to 48 h and then polymerization was induced for 15 to 18 h at 54 °C. This method of embedding prevents the material from sinking to the bottom during polymerization and permits easier orientation of the material which can be adjusted according to the intended plane of sectioning shortly before polymerization takes place.

Ultra-thin sections (about 600 Å) prepared with a Porter–Blum ultramicrotome were mounted on collodion-carbon-coated grids and stained by floating on a 1% potassium permanganate solution containing 2·5% uranyl acetate for 20 min. Excess stain was rinsed off by floating the grids face downwards on distilled water (1 to 2 min), then 0·25% citric acid solution (30 s), then distilled water again (a few minutes).

In addition, 11, 12 and 13-day-old mouse embryos were fixed with 5% glutaraldehyde solution buffered at pH 7·2 with sodium cacodylate buffer (Plumel 1948) and then post-fixed for 30 min with 1% osmic fixative, as described above. Dehydration and embedding were carried out in the same way as above, but the

sections were stained by floating on a 10% solution of uranyl-zinc acetate for 1 to 1½ h.

Separate experiments to localize acid phosphatase within the apical ectodermal ridge were carried out with stage 24 chick wing buds and with 11-, 12- and 13-day-old mouse fore-limb buds according to the Gomori procedure (1952) adapted to electron microscopy by Holt & Hicks (1962). As the first fixative, 5% glutaraldehyde buffered with sodium cacodylate at pH 7·2 (Plumel 1948) was used instead of formalin. The limb buds, after fixation for 4 h in glutaraldehyde at 0 to 4 °C and rinsing three times, 5 min each, with chilled 7·5% sucrose solution buffered with 0·1 M sodium cacodylate at pH 7·2, were not sectioned on a freezing microtome, but instead narrow distal portions were cut off with opthalmic scissors. This modification appeared sufficiently accurate for the selection of the ectodermal ridge and the adjacent lateral epiblast, together with the adjoining mesoblast. Material prepared in this manner could be used for the enzymic reaction in a medium containing 0·3% sodium β-glycerophosphate (β-glycerophosphate, Na. 5½ H_2O, C grade, California Corporation for Biochemical Research) as substrate and 0·12% lead nitrate buffered at pH 5 with 0·05 M acetate buffer. After 45 min of incubation at 37 °C the limb-bud fractions were dehydrated with graded alcohols and embedded in Araldite as described above. Sections were stained for 1 to 1½ h with 10% uranyl-zinc acetate solution and rinsed with distilled water.

All the ultra-thin sections were examined and photographed using a Philips EM 75, a Siemens Elmiscop I or an AEI EM 6 electron microscope.

Light microscopy

Chick and mouse embryos of the same stages as used for the electron microscope investigations were fixed with a 5% solution of trichloro-acetic acid containing 1·37% lanthanum acetate for 3 h. During the dehydration procedure with graded alcohols the fore-limb regions of the embryos were dissected and embedded in 54 °C paraffin wax. Serial sections of 6 μm were cut parallel to the axial plane of the limb bud and stained with methyl green-pyronin. The Hamburger & Hamilton (1951) stages of chick embryos were identified using their description of the external characters of the embryos as well as by the appearance of the notochord (Jurand 1962). Both chick and mouse saggital sections of the fore-limb buds were photographed at low magnification and arranged in sequential order to provide a reference guide for further work (figure 3, plate 41).

Light microscope observations

This part of the work was planned to provide a general background for electron microscope investigations of the intracellular changes taking place during early development of the fore-limb buds in chick and mouse embryos. Hamburger & Hamilton's normal table for chick embryos (1951) is based exclusively on external characteristics, and so is that for mouse embryos in the only available paper of Grüneberg (1943).

In the earliest stages (stages 16 and 17 in the chick and 9½ days in mouse embryos) the fore-limb buds are beginning to be formed as elongated thickenings

appearing on the ventro-lateral sides of the trunk at the level of the 15th to the 20th somite in the chick and of the 7th to the 12th somite in the mouse. They are covered by a uniformly thick epithelium consisting of roughly equidimensional cells. In the chick the epithelium is double layered with considerable intercellular spaces, whereas in the mouse it is single layered devoid of intercellular spaces. The mesodermal component forming the early limb bud proliferates radially from the parieto-pleural mesoderm and probably also from the adjacent somites (figures 4 and 11, plate 42). At these stages there is no visible difference in stainability between epiblast and mesoblast cells when methyl green–pyronine is used.

In slightly older embryos (stage 18 to 20 in the chick and 10 to 11 days in the mouse) the limb buds, which are still undivided appendages, show rapid growth with simultaneous thickening of the epiblast on the ventral side of the free edge of the limb bud. This is the first appearance of the apical ectodermal ridge (figures 5 and 12, plate 42). At these stages the epiblast acquires the peridermal layer of widely separated cells. The latter are probably those which move actively on the surface of the limb-bud epithelium towards its margin (figures 17 and 18, plate 43) and contribute to the formation of the ectodermal ridge together with the mitotic activity of the local cells (figure 13, plate 42). The stainability of the ectodermal and mesodermal cells is still equal. In figures 5 and 12, plate 42, it can be seen that nucleoli in the epiblastic cells are markedly smaller than those in the mesoblast cells.

At stages 21 to 25 in the chick embryos the apical ectodermal ridge reaches the maximal degree of development. It consists of several (3 to 4) layers of cells, of which the outer cells are flat, those next to them roughly equidimensional and the deepest ones radially elongated. In transverse sections the ridge now resembles a spread-out fan in shape. It is located like a nipple on the extreme edge of the cross-section of the limb bud (figures 7 to 9, plate 42). In the mouse the apical ridge is at its maximum in 12-day-old embryos, but it is here a much flatter structure consisting of 3 or 4 layers of cells, all of them being roughly equidimensional except for the outer layer of flat cells (figure 14, plate 42). In the mesoblast at these stages the first blastemal condensations appear.

Below the circumferential edge within the mesoderm there appears in both species, simultaneously with the apical ridge, the marginal blood vessel which afterwards remains a constant feature in the pre-skeletal stages of limb development (figures 12 to 15, plate 42).

At the time of maximal development of the apical ridge and somewhat later, the cytoplasm of the ectodermal ridge cells has a higher affinity for pyronine than have the cells of the lateral epithelium or the mesoblast (e.g. figures 7 and 9, plate 42). About stage 22 in the chick, and in 11-day-old mouse embryos, there start to appear in the ectodermal ridge necrotic changes which are confined mainly to the outer layers of the structure (figures 8 to 10, plate 42). This indicates that the beginning of the involution process of the ectodermal ridge starts somewhat earlier than the time of its maximal growth. From now on, necrotic cells can be found throughout the whole remaining period of existence of the ectodermal ridge. In mouse embryos, in which the ridge disappears comparatively earlier, necrotic

cells are found only up to the 13th day, so that on the 14th day there are no necrotic cells, the apical ridge having disappeared (figure 16, plate 42). In the chick the apical ridge is a much larger structure, hence its involution probably takes longer and lasts well into the period of formation of the skeletal blastemas, i.e. until stage 31 or perhaps somewhat later. Plate 41 and table 1 show the comparative stages of development of the fore-limb buds in the chick and the mouse.

TABLE 1. COMPARATIVE STAGES OF DEVELOPMENT OF FORE-LIMB BUDS IN CHICK AND MOUSE EMBRYOS

chick embryos			mouse embryos		
stage	ectoderm and apical ectodermal ridge (a.e.r.)	mesoderm	days	ectoderm and apical ectodermal ridge (a.e.r.)	mesoderm
16	double-layered cuboidal epithelium	first signs of accumulation	9½	single-layered cuboidal epithelium	first signs of accumulation
18	first appearance of the apical ectodermal ridge	proliferation	10	first appearance of the apical ectodermal ridge	proliferation
20	elongation of a.e.r. cells, mitosis, migration		10½	accumulation of a.e.r. cells, mitosis, migration	
22	further development of a.e.r. appearance of necrotic cells		11	further development of a.e.r. appearance of necrotic cells	
24	apical ectodermal ridge at its maximum	first skeletal blastema appears	12	apical ectodermal ridge at its maximum	first skeletal blastema appears
26	regressive changes in a.e.r.	further growth and development	13	regression of the a.e.r.	further growth and development
28	regressive changes in a.e.r. continue		14	disappearance of the a.e.r.	
30	continued		—	—	—
31	disappearance of the a.e.r.		—	—	—

ELECTRON MICROSCOPE OBSERVATIONS

The mesoblast

The youngest fore-limb buds of stage 16 and 17 chick embryos and those of 9½-day-old mouse embryos represent elongated condensations of mesoderm covered by a single- or double-layered epithelium. In both species the mesoblast at this stage is composed of cells with well-defined cell membranes (figure 19, plate 43). In the cytoplasm of these cells there is only a little rough-surfaced endoplasmic reticulum to be found in the form of scattered single profiles, small

numbers of round or oval mitochondria with scarce but conspicuous cristae, and a low density matrix (figure 20, plate 43). Free ribosomes are abundant, forming groups of 5 to 10 granules scattered throughout the cytoplasm. There are relatively more ribosomes in the mesoblast cells in the mouse than in the chick. Groups of Golgi membranes occur in these cells fairly frequently, but they are small in size, never amounting to more than one group per section per cell.

In both species there also occur in the cytoplasm of the mesoblast cells at these stages vesicles, about 0·5 μm in diameter, which seem empty or contain a small electron-dense granule concentrated near the centre of the vesicle (figure 21, plate 43).

In these cells the nucleus shows the usual double nuclear envelope with pores about 1000 Å in total diameter which are scattered at intervals of about 0·2 μm from each other. In higher power micrographs of tangential sections through the nuclear envelope it is possible to resolve in the rim of the pores 6 to 9 subannuli about 150 Å in diameter (figures 22 and 23, plate 43).

In many mesoblast cells at these early stages single profiles of endoplasmic reticulum can be found which are clearly continuous with the outer of the two nuclear membranes (figure 24, plate 43). In some cases such profiles have even been observed to be attached at two points to the outer nuclear envelope, forming a loop profile (figure 25, plate 44). In all these cases the profiles appear to be densely studded with ribosomes in the same manner as are profiles of the free endoplasmic reticulum in these cells.

The continuity of the endoplasmic reticulum with the outer nuclear membrane suggests that segments of endoplasmic reticulum are in the process of formation, and this is assumed to be a symptom of increased intracellular activity in embryonic cells during cyto-differentiation.

In addition to this continuity there were observed, particularly in slightly older mouse embryos (11 days), breaks in the nuclear envelope providing a direct connexion between the content of the nucleus and that of the endoplasmic reticulum (figure 26, plate 44).

Mesoblast cells in the early stages show the formation of numerous microvilli and pseudopodia which probably indicates increased motility of these cells (figure 27, plate 44).

From the 12th day of development in the mouse and from stage 21 in the chick the overall picture of the mesoblast cells changes completely. The cell membranes of the whole mesoblast usually become incomplete and in older limb buds are frequently absent so that there is a cytoplasmic continuity between cells, the tissue giving the impression of being syncytial in nature (figure 28, plate 44). There are wide intercellular spaces between the cells, the latter being connected with each other by means of elongated processes typical of mesenchymatous tissues. The vesicles found in the youngest stages are not present at this stage. There are no foldings of the outer nuclear membrane and no profiles of the endoplasmic reticulum appear to be attached to it. The endoplasmic reticulum is now found more frequently in the cytoplasm of these cells, often in close proximity to mitochondria. Golgi membranes remain scarce and form only small groups.

The epiblast

In the youngest embryos of both species the dorso-lateral ectodermal covering of the limb buds consists virtually of one layer of rather short cylindrical cells with or without an outer layer of flat peridermal cells. Between these cells there are intercellular spaces of considerable size. The ventro-lateral epidermis consists of two layers of cells and has fewer intercellular spaces; they are almost non-existent in the area of the future apical ectodermal ridge.

At these stages the external membranes form numerous finger-like microvilli which are usually evenly distributed on the free surface of the cell, and much denser in the near vicinity of the lateral junctions between the cells. In some sections microvilli are not found on the free surface but they are almost always found at the junctions between the cells. The microvilli are about 0·8 to 1 μm long and 0·1 μm wide (figure 29, plate 44).

Other cell membrane organelles which occur in these cells, but in much smaller numbers than the microvilli, are single, sporadically distributed cilia. Cilia are probably not present on every cell. There is usually not more than one cilium per cell. The cilia have the characteristic micro-structure as found in cilia from other material (e.g. *Paramecium*). They possess one well recognizable basal body (centriole) beneath the surface of the cell membrane, but without the other centriole alined along the axis, as described by Sotelo & Trujillo-Cenóz (1958) in chick neural epithelium. The cilium itself contains internal longitudinal fibrils continuous with the basal body and running parallel to the axis. The basal body is $\frac{1}{6}$ μm in diameter and $\frac{1}{4}$ μm long. The cilium at its base is about $\frac{1}{4}$ μm thick, tapering along its length which probably does not exceed 2 μm. In all but one of the observed cases (12 micrographs taken) the cilia were situated in the free cell membrane so that its basal body was close to a group of Golgi membranes lying below in the cytoplasm (figure 30, plate 44).

The junctions between adjacent cells of the epiblast in the early stages, as well as in later stages, are provided with junctional complexes at the sides of the cells. These structures consist of three distinct parts which are (beginning from the apical surface inwards): (1) the tight junction (zonula occludens), (2) the intermediate junction (zonula adherens), and (3) the desmosome (figures 31 to 33, plate 45). The Latin terminology was introduced by Farquhar & Palade (1963).

In cross-sections of the junctional complexes, the first part (the tight junction) appears to represent a fusion of adjoining membranes which, particularly in mouse, is often almost complete, with many electron-dense fibrils attached to the fusion. The fibrils involved in this part of the junctional complex run parallel to the cell membrane.

The second part, the intermediate junction (zonula adherens), does not differ to any great extent from the deeper cell membranes which do not belong to the junctional complexes. The cell membranes at this level are of approximately the same thickness as elsewhere in limb bud epithelial cells. The width of intercellular space is about 400 Å.

The third element of the junction, the desmosome, is similar to those described in many other epithelia. The intercellular space adjacent to a desmosome is only slightly wider (450 Å) than at the level of the intermediate junction.

In chick embryos no intermediate lamella could be found between the two membranes, but in the mouse such a structure could occasionally be detected (figure 32, plate 45). Where a cell membrane passes into the region of a desmosome the unit cell-membrane continues unchanged, but on each side it acquires a dense cytoplasmic component in the form of 200 to 300 Å thick plaques, separated from the cell membrane by a very narrow, less dense space about 60 Å in width. In the cytoplasm, outisde the dense plaques, the desmosome is formed by a bundle of fibres, which in cross-section appear as opaque dots about 75 Å in diameter. It is this part of the desmosome which, together with the dense plaques, give in cross-section its characteristic appearance (figure 33, plate 45).

In many transverse sections it is possible to distinguish what appear to be long filamentous elements which extend deep into the cytoplasm on either side of the desmosome, and which probably connect and run at right angles to the desmosomal longitudinal fibres. These elements probably should be interpreted as fibres seen in longitudinal aspect, but it was remarkable that these were obtained so frequently, each 60 Å wide and running in the plane of the section without links or discontinuities for distances up to $\frac{1}{2}$ μm. Alternatively, the filamentous elements could be recognized as sections of thin lamellae or sheets. The first interpretation, however, seems more likely to be true as the apparent length of the image of fine fibres may be increased if fibres run obliquely within the section so that their ends overlap. A similar problem in the interpretation of electron micrographs was considered by Huxley (1957). Moreover, Farquhar & Palade (1963) and Waddington & Perry (unpublished) noticed in other epithelia similar, although shorter, filamentous elements associated with desmosomes and interpret them as bundles of fibres.

In longitudinal sections through the desmosome region, i.e. in sections grazing the surface of the limb-bud epithelium, it appears that the first part of the junctional complex, viz. the tight junction (zonula occludens) is probably continuous, without breaks, and runs round each epidermal cell. In favourable cases it is possible to observe, just below the free surface of the cell, long stretches of this structure as an elongated dense belt of fibres running parallel to the cell surface (figure 34, plate 45). No separation between the cell membranes is distinguishable here or in transverse section due to the fusion of the two cell membranes.

In this projection desmosomes appear to be considerably elongated units, $\frac{1}{5}$ to $\frac{1}{10}$ μm wide and anything up to 2 μm long, situated between adjacent cells and about 1 to 2 μm below the external cell surface. These unit desmosomes form long chains consisting of three to six individual structures, in which each unit desmosome possesses its own separate dense plaque on each side, but the longitudinal fibrils are common for all units belonging to one chain of desmosomes. Such chains appear as intermittent structures with gaps between individual dense plaques and with only cell membranes and longitudinal fibrils running between them (figure 35, plate 45). In transverse sections through the gap in a chain between two unit

desmosomes there appear 'wings' of transversely sectioned fibrils without the dense plaque (figure 36, plate 45).

Figure 1, plate 40, shows diagrammatic reconstruction of the whole junctional complex, and separately a desmosome itself, together with the associated fibres.

In chick, but not so much in mouse embryos, certain other structures concerned with epidermal cell adhesion are frequently developed. These include complex interdigitating folds and processes (see figures 31 and 36, plate 45). Microvilli are also located below the free cell surface of the epithelium and below the level of the desmosome chains where they doubtless contribute to the adhesion of epithelial cells. At the points of adhesion between the internal microvilli there are either no junctional complexes, or only some of the three parts are present.

The dorsal and ventral epiblast cells do not differ to any extent in their morphology at the ultrastructural level except that the ventral epiblast cells leave fewer and smaller intercellular spaces.

Figure 2, plate 40, shows diagrammatically the ultrastructural details of the epiblast tissue of a young limb bud as observed in many micrographs taken from both of the species investigated.

The apical ectodermal ridge, which appears first in stage 18 chick embryos and 10 to 10½ day-old mouse embryos consists, particularly in the chick, of cells adhering very closely to each other, leaving almost no intercellular spaces. At first the most distally situated cells at the presumptive site of the apical ridge elongate, forming a single layer of columnar epithelium thus becoming thicker than the rest of the epithelium. Very soon this layer of cells is covered with an outer layer of flat cells. The number of cell layers in the later stages is 3 or 4 in both species, but the cells are considerably less elongated in the mouse than they are in the chick apical ridge. As soon as the epidermal ridge becomes established, its cells, particularly those situated deeper in the structure, contain numerous mitochondria, very many Golgi groups and fairly frequent profiles of endoplasmic reticulum. The mitochondria are often very elongated, up to 6 μm in length, which presumably indicates that these cells are metabolically very active (figure 37, plate 46).

In both stage 20 to 21 chick embryos and in 11- to 12-day-old mouse embryos, when the apical ectodermal ridge consists of three or four layers of cells it is possible to find between the cells single cilia which are usually bent, as they are covered by cells arriving there from the more distant parts of the epithelium probably by a sort of amoeboid movement (figure 38, plate 46). In later stages such cilia can be found in the form of remnants deeper between the apical ridge cells.

The fact that the cilia become covered and that they are found between the apical ridge cells indicates that the ridge may be formed partly by cell migration, but there is no doubt that it also develops by local mitotic activity.

In stage 23 to 25 chick embryos and in 12-day-old mouse embryos the ectodermal ridge reaches its maximum development. At this stage the structure differs considerably in the two species investigated. In the chick, sections cut transversely through the ridge, i.e. sections near and parallel to the axial plane, show a fan-shaped figure consisting of flat cells at its outer margin, then cuboidal cells in the

next layer or two, and columnar cells at its base with extremely narrow and elongated processes which converge centripetally towards the bottom-median line of the ectodermal ridge (figure 41, plate 47).

In 12-day-old mouse embryos, similarly cut sections show the epidermal ridge to be rather flat and lens-like in shape, consisting of flat and cuboidal cells only.

In longitudinal sections of the apical ridge, i.e. in sections tangential to the circumference of the limb bud in both species, all cells appear to be elongated in the direction of the length of the ridge. Also, the extremely elongated processes converging towards the median line in chick wing buds appear in this projection to be flat, blade-like extensions, and not finger-like processes (figures 42 and 43, plate 47).

During the formation of the apical ectodermal ridge its cells show a constantly increasing number of groups of Golgi membranes. This process is particularly conspicuous in 12-day-old mouse embryos where groups of Golgi membranes form large continuous systems distributed widely in the cytoplasm of these cells (figure 39, plate 46). Each Golgi group consists of the usual three elements characteristic of this organelle: (1) parallel layers of flattened sacs, (2) numerous small scattered vesicles, and (3) larger vesicles with electron lucent content. The last element is usually present only in old limb buds.

The increased number of Golgi complexes is accompanied by fairly numerous lysosomes and multivesicular bodies which seem topographically to be associated with the Golgi systems (figure 40, plate 46).

Once the ectodermal ridge has been established, the outer and also the intermediate ridge cells begin to show extensive necrotic changes which can be observed in light-microscope preparations. In electron micrographs such cells appear to contain one or more dense extranuclear necrotic centres in the cytoplasm side by side with the Golgi complexes, numerous lysosomes and multivesicular bodies. The nuclei of these cells, however, do not show any signs of pycnosis or other necrotic phenomena at the beginning of the process of degeneration.

The necrotic centres which range from 0·8 to 2 μm in diameter are surrounded by a single membrane and contain some electron-dense material, whose composition is mostly unrecognizable, side by side with mitochondria and numerous small vesicles (about 400 Å in diameter) (figure 44, plate 48). These structures resemble what Novikoff (1960) and Neapolitano (1963) described as cytolysomes. In the most advanced stages of cellular degeneration the nucleus eventually shows pycnosis or karyorrhetic changes which are followed by vacuolation of the cytoplasm (figure 45, plate 48).

In some instances it was possible to observe during the process of degeneration necrotic cells situated within normal cells of the ectodermal ridge. This clearly indicates that the degenerating cells are phagocytosed (figure 46, plate 48).

Acid phosphatase localization

In these investigations stage 24 chick and 11-, 12- and 13-day-old mouse embryos were used. Milaire (1961, 1963) has shown by means of histochemical methods that

at these stages the limb-bud ectodermal cells, particularly those of the apical ectodermal ridge, contain considerable amounts of acid phosphatase. On the other hand, in these cells, as stated above there are abundant Golgi groups, lysosomes and multivesicular bodies and when degeneration of the apical ridge begins there are numerous necrotic extranuclear centres. The electron-microscope investigations were undertaken to localize the acid phosphatase activity within the fine structure of the apical ridge cells and to correlate this with the degenerative processes.

In 11-day-old mouse embryos acid phosphatase activity is confined to the Golgi flattened sacs and to the small vesicles associated with them (figure 47, plate 49). Although the preservation and definition of the structural details of the cells, after the prolonged and rigorous procedure used, are not nearly as good as after the usual osmic fixation, the micrographs are considered good enough to permit the conclusion that the final product of the reaction (lead phosphate) is deposited exclusively in these two components of Golgi groups. All the other cell organelles, particularly the nuclei, endoplasmic reticulum, mitochondria and the large vesicles with electron lucent content associated with the Golgi apparatus, appear to be devoid of lead phosphate deposits, indicating the absence of acid phosphatase activity in these organelles.

In the 12-day-old mouse embryos ectodermal ridge the same localization in the Golgi apparatus was encountered, but in addition, larger cytoplasmic granules similar in size to lysosomes and multivesicular bodies, and also some of the same size of cytolysomes and extra-nuclear necrotic centres, appeared to be sites of acid phosphatase activity (figure 48, plate 49). A similar situation was observed in stage 24 wing-bud apical ridge cells in the chick.

In 13-day-old mouse limb buds the overall picture was similar to that in 12-day-old embryos. The only difference was that the extra-nuclear necrotic centres impregnated with lead phosphate were, on average, larger and more numerous. In addition, some nuclei of the outer flat cells of the apical ridge and occasionally the cell membranes, showed acid phosphatase activity (figure 49, plate 49).

The basement membrane

The epiblast is separated from the mesoblast by a basement membrane, which is an acellular structure present as a rule on the inner surface of various epithelia. It is found at the earliest stages of limb-bud development and its structure does not seem to change much as development proceeds. The only difference between the early and later stages is that earlier it is perhaps slightly thinner. It lies closely adhering to the basal cell membranes of the inmost epidermal cells. Its structure appears as a layer of about 300 to 400 Å thick with diffuse outlines and consists of short, probably fibre-like particles (figure 50, plate 49). In transverse sections the basement membrane is seen to run parallel to the inner surface of the epithelium, leaving a gap about 250 Å wide; it neither fills up smaller depressions in the cell membranes nor follows exactly the gaps formed by the terminal junctions between the cells.

In stage 22 to 26 chick wing buds, at the bottom median line of the apical ridge the basement membrane does not adhere to the flat blade-like extensions of the

cells, converging centripetally towards this line, and shows in this area discrete discontinuities (figure 51, plate 49).

In the mouse in corresponding stages there are no such flat extensions of the basal cells and no discontinuities in the basement membrane were found.

Discussion

For many years the study of limb development has been an important field in epigenetics. As was pointed out in the introductory remarks, not all problems of the interaction between the ectodermal and mesodermal components of limb buds are thoroughly understood. The most generalized hypothesis of limb development has been put forward by Zwilling (1961*a*) as a result of his extensive experimental studies. According to this hypothesis, which chiefly applies to amniote tetrapods, the first stimulus to the development of a limb primordium arises in the presumptive limb mesoderm which derives from the adjoining somatopleure. As soon as the first thickening becomes visible, the mesoderm induces the cells of the overlying ectoderm to elongate on the ventral side of the most distal area of the thickening and causes the lateral ectodermal cells to migrate towards this area, thus inducing the formation of the apical ectodermal ridge (see also Kieny 1960).

Once the apical ridge has been established (in the chick at stage 18 to 20, in the mouse on the 11th day of embryonic life) the two components, ectoderm and mesoderm, become an interdependent system. The mesoderm is believed to be responsible not only for the formation of the ectodermal ridge but also for its maintenance (Zwilling's maintenance factor). Moreover, the mesodermal component is also the site of the type specificity of the developing limb (Zwilling 1955). The ectodermal ridge, on the other hand, conditions the elaboration of the distal outgrowth and morphogenesis of the digits. By the 14th day in the mouse the ectodermal ridge disappears, as it does, although somewhat later, in the chick, and from then on the development of the limbs is entirely dependent on the morphogenetic changes taking place in the mesoblast itself. The latter gives rise to the blood vessels, to the connective tissue, together with the intercellular collagen fibres, to the cartilaginous structures of the preliminary skeleton and to all other components of the limb. Thus it is possible to distinguish roughly three periods in the development of a limb: (1) the period of initiating activity of the somatopleural mesenchyme, (2) the period of interaction between mesoblast and epiblast, and (3) the formation of the definite mesodermal derivatives in the limb mesoblast.

The findings in the present work, which is concerned with the first two periods, seem to confirm the fact that the first stimulus to the initiation of limb development arises in the mesoderm. In the earliest stages investigated there were found in the mesodermal cells frequent extensions of the outer nuclear membrane indicating increased cytodifferentiation in these cells. Very similar phenomena have been described in urodele notochord cells at an early stage of differentiation (Waddington & Perry 1962), and also in the early stages of chick notochord development (Jurand 1962). It is probably true to say, that in general, the continuity of the endoplasmic reticulum profiles with the nuclear membrane is a symptom associated with any active phase of cyto-differentiation.

Another feature at this stage is the polyribosomal condition (formation of clusters consisting of 5 to 10 ribosome granules) found in mesoblast and epiblast cells, which is assumed to be characteristic for cells producing specific proteins (Slayter, Warner, Rich & Hall 1963).

The granules encountered at very early stages in the cytoplasm of limb mesoderm cells, and which resemble the secretory granules usually found in various gland tissues (Kurosumi 1961), indicate that these cells may be secreting some substances whose activity is as yet unknown. However, it would probably be premature to say that the granules described here represent a secretion of the mesodermal cells, which when transferred, for instance, to the ectodermal cells induces morphogenesis there. This problem requires further investigation, perhaps using limb buds developing *in vitro* in the presence of an extract from the early limb-bud mesoderm.

The positive role of the apical ridge in the interaction of epiblast with mesoblast, i.e. in the second period of limb development, which has been so intensively discussed recently, cannot be proved or disproved by the results of this work. It is, however, possible to postulate that the epiblast is not completely passive in the morphogenesis of limb buds because the mesoblast cells do not show any special ultrastructural features of increased activity at this time, whereas the apical ridge at the time of its maximum development represents a highly complicated tissue with numerous subcellular systems, such as well-developed terminal junctions, microvilli, extensively developed Golgi systems and elongated mitochondria which are characteristic of metabolically active cells. That these complex intracellular structures persist even after the apical ridge is fully formed may suggest that the ridge cannot be merely a vestigial organ for evolutionary reasons homologous with the epithelial edge of fins (Glücksmann 1934).

The apical ridge is richer in *RNA* than other limb bud epithelial cells, which indicates high synthetic activity within its cells. This was also found by Hinrichsen (1956) who investigated the *RNA* content of the apical ridge in mouse hind-limb buds by means of the gallocyanin-chromalum method. Hinrichsen concluded that, since the concentration of *RNA* is highest in the apical ridge, this is probably the site of intensive protein synthesis and probably represents what is meant by the organizer of the limb. Taking into account other arguments also (some of which are detailed by Zwilling 1961*a*, *b*) it seems unlikely that the apical ridge plays no role in limb morphogenesis, as suggested by Amprino & Camosso (1955, 1959) and Bell, Kaighn & Fessenden (1959). That the presence of the elaborate subcellular organelles in the apical ridge is not merely associated with mitotic activity is indicated by the fact that the cells of the mesoblast do not have so many of these organelles although they have a far greater mitotic activity.

Description of plates 40 to 49

Figures 1 and 2 are pencil drawings, plates 41 and 42 and figures 17 and 18, plate 43, are photographs of light-microscope preparations (on which the scales are numbered), the remainder are electron micrographs (on which the scales all represent 1 μm). For abbreviations used on the plates see p. 405.

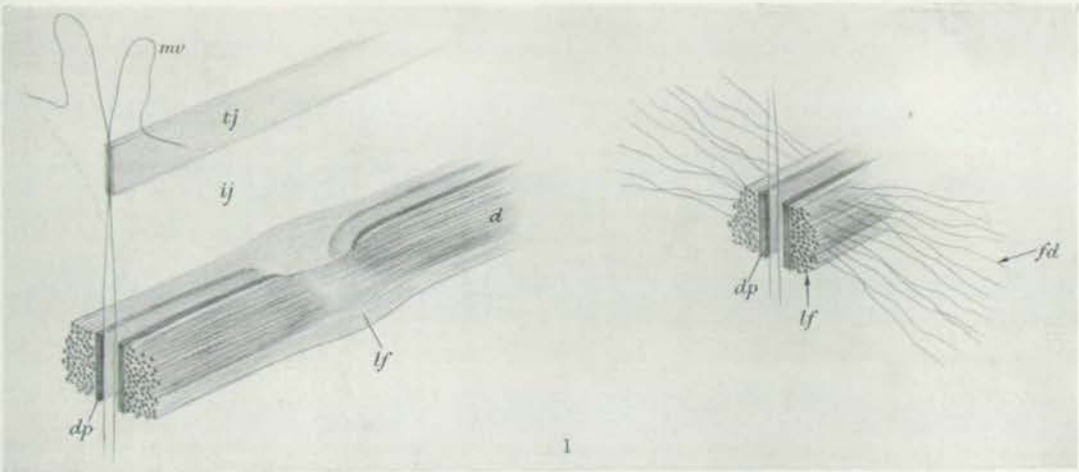

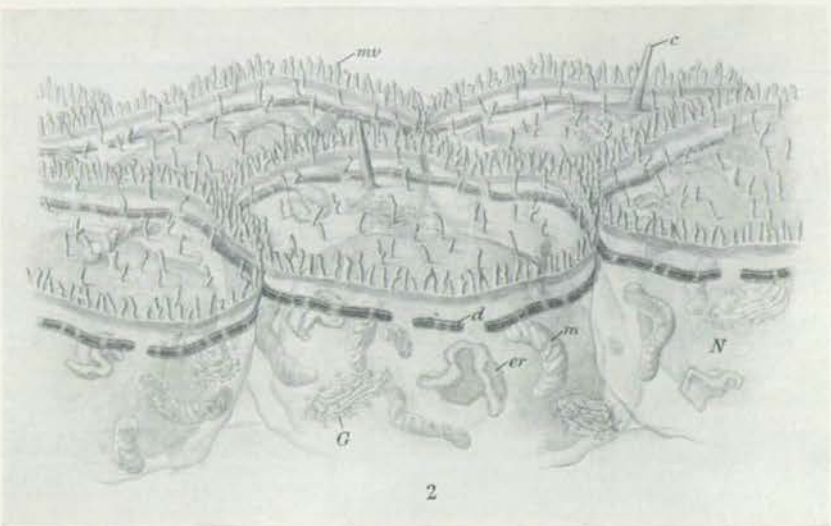

FIGURE 1. Diagrammatic reconstruction of the terminal junction in the chick wing bud epithelium in transverse section. The drawing on the left shows all three parts, i.e. the tight junction (*tj*), the intermediate junction (*ij*) and a part of the desmosome chain (*d*) represented by two units. The dense plaques (*dp*) are separate for each unit, but the units are connected by the bundles of longitudinal fibres (*lf*) continuous between the units.

The drawing on the right shows the reconstruction of a desmosome unit together with the associated cytoplasmic fibres (*fd*) running roughly at right angles to the bundles of the longitudinal fibres (*lf*). (Approx. magn. × 100000.)

FIGURE 2. Diagrammatic reconstruction of a few epithelial cells of an early limb bud showing the characteristic organelles, i.e. microvilli (*mv*), cilia (*c*), terminal junctions with chains of desmosomes (*d*), Golgi groups (*G*), endoplasmic reticulum (*er*), mitochondria (*m*) and nuclei (*N*). (Approx. magn. × 5000.)

(*Facing p.* 400)

FIGURE 3. Left column: sagittal sections through chick wing buds at stages 16, 18, 19, 21, 23, 25, 28 and 30 (stages after Hamburger & Hamilton 1951). (Magn. × 32.) Right column: sagittal sections through fore-limb buds of mouse embryos aged 9½, 10, 10½, 11, 12, 13 and 14 days. (Magn. × 24.)

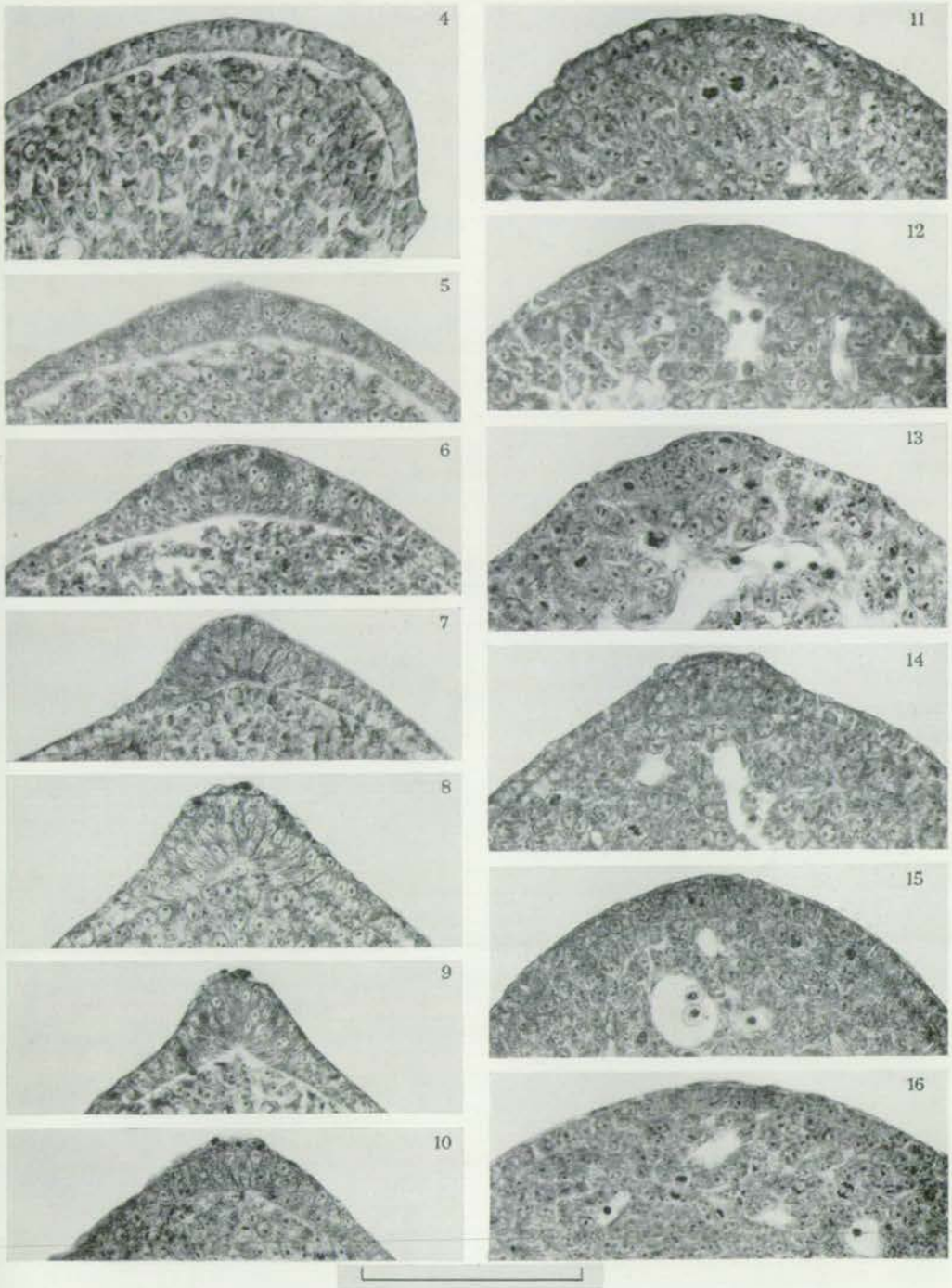

FIGURES 4 TO 10. The apical ectodermal ridge area in chick wing-buds at stages 16, 18, 21, 24, 26, 28 and 31. Note the necrotic cells in the ectodermal ridge in the figures 8, 9 and 10, and the differences in the size of the nucleoli in the apical ridge and in the mesoblast cells in figures 7 to 10. (Magn. ×310.)

FIGURES 11 to 16. The apical ectodermal ridge area in mouse embryos aged 9½, 10, 11, 12 13 and 14 days. Note the intensive mitotic activity in the apical ectodermal ridge in figures 12 to 14. (Magn. ×310.)

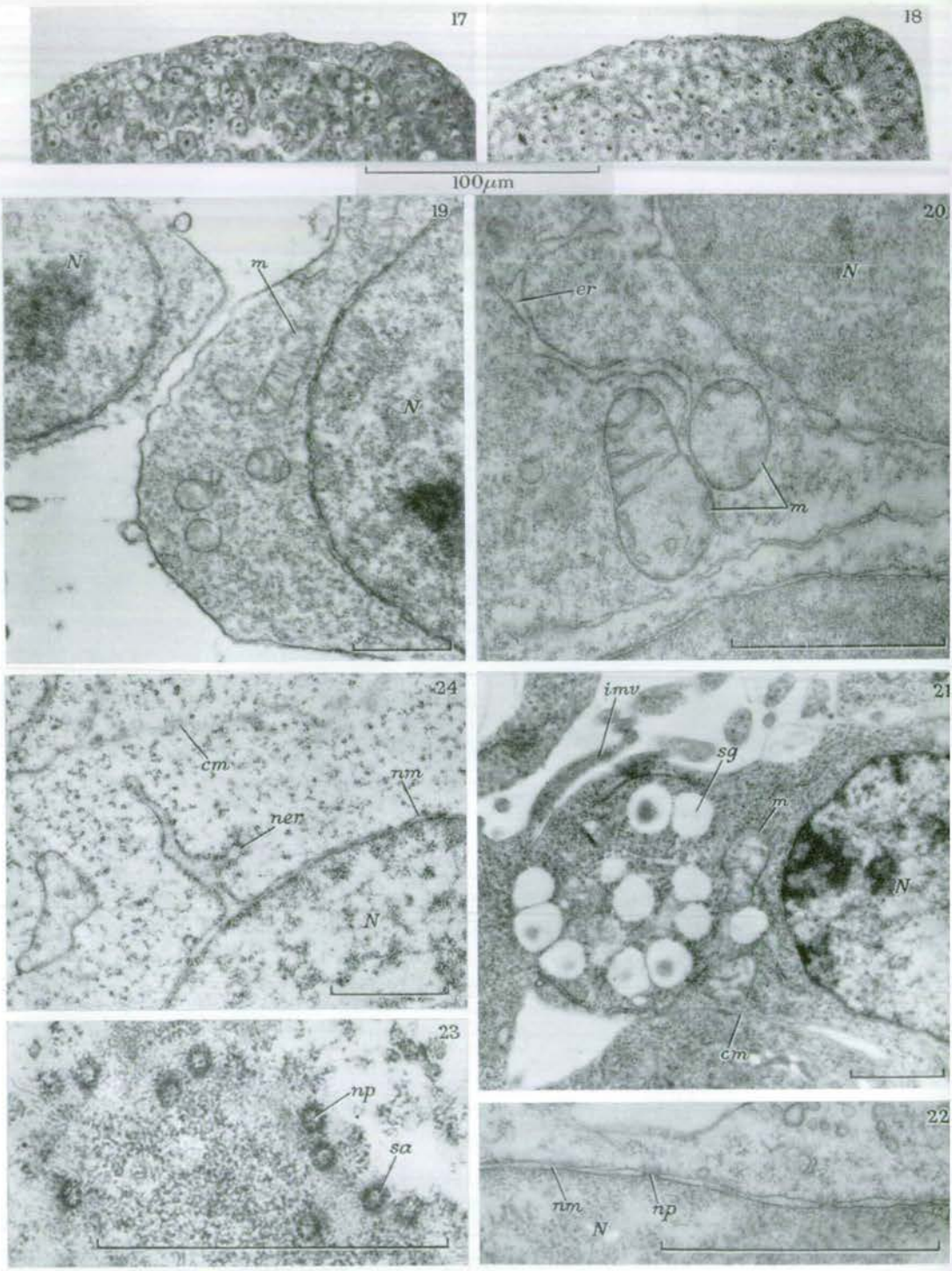

FIGURES 17 to 24

PLATE 43

FIGURE 17. Transverse section through the dorsal fore-limb bud epithelium together with, on the right, the apical ectodermal ridge in 12-day-old mouse. Note the flat cells on the outer surface of the epithelium. (Magn. × 350).

FIGURE 18. As figure 17; chick wing-bud at stage 24. (Magn. × 350.)

FIGURE 19. Mesoblast cells from fore-limb bud of 9½ day-old mouse embryo. Note the polysomal condition of the cytoplasm. *Os.P.U.* (Magn. × 14600).

FIGURE 20. Mesoblast cell from fore-limb bud 9½ day-old mouse embryo. Note characteristic mitochondria (*m*). *Os.P.U.* (Magn. × 31500.)

FIGURE 21. 9½-day-old mouse fore-limb bud. A mesoblast cell, its cytoplasm packed with secretory-like granules (*sg*). *G.Os.U.Z.* (Magn. × 13800.)

FIGURE 22. Chick, stage 22. Transverse section through the nuclear membrane (*nm*) with nuclear pores (*np*) visible. *Os.P.U.* (Magn. × 41250.)

FIGURE 23. Chick, stage 19. Tangential section through the nuclear envelope. 6–9 subannuli (*sa*) can be distinguished in the rim of the nuclear pores (*np*). *Os.P.U.* (Magn. × 52500.)

FIGURE 24. Ten-day-old mouse, fore-limb bud. Mesoblast cell with an endoplasmic reticulum profile continuous with the outer nuclear membrane (*ner*). *Os.P.U.* (Magn. × 17600.)

Plate 44

Figure 25. Ten-day-old mouse, fore-limb bud. Mesoblast cell showing a loop-like profile of the endoplasmic reticulum, continuous at both ends with the outer nuclear envelope (*nerl*). *Os.P.U.* (Magn. × 22500.)

Figure 26. Eleven-day-old mouse, fore-limb bud. Mesoblast cell showing a discontinuity in both nuclear membranes (*dnm*) which are linked with the endoplasmic reticulum profile. *Os.P.U.* (Magn. × 21400.)

Figure 27. Mesoblast cells with microvilli (*imv*) from fore-limb bud of 11-day-old mouse. *G.Os.U.Z.* (Magn. × 18000.)

Figure 28. Two nuclei (*N*) with no cell membrane between them from the mesoblast of a 12-day-old mouse fore-limb bud. *Os.P.U.* (Magn. × 18000.)

Figure 29. Microvilli (*mv*) of an outer epiblast cell. Chick, stage 19, wing bud. *Os.P.U.* (Magn. × 21750.)

Figure 30. Ten-day-old mouse, fore-limb bud. Cilium (*c*) and microvilli (*mv*) of an outer epiblast cell. *G.Os.U.Z.* (Magn. × 21000.)

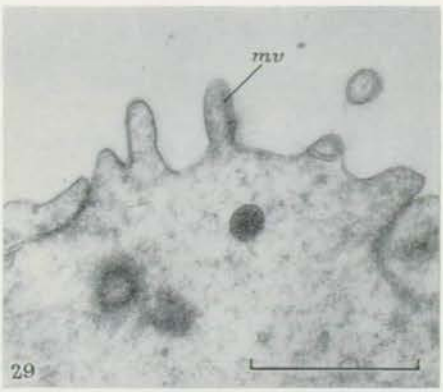

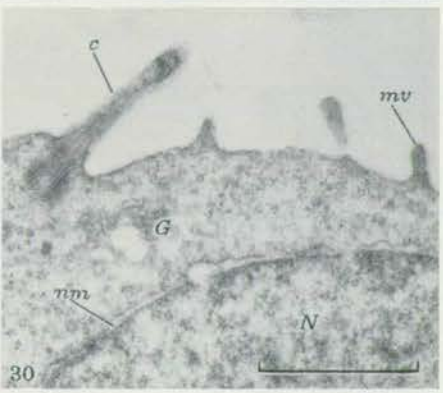

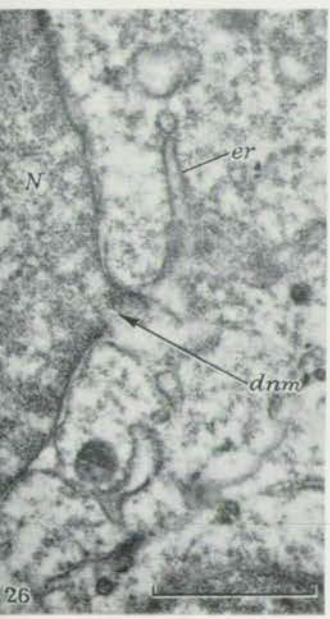

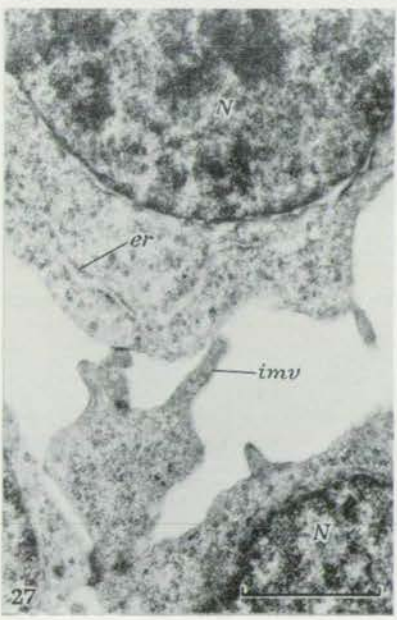

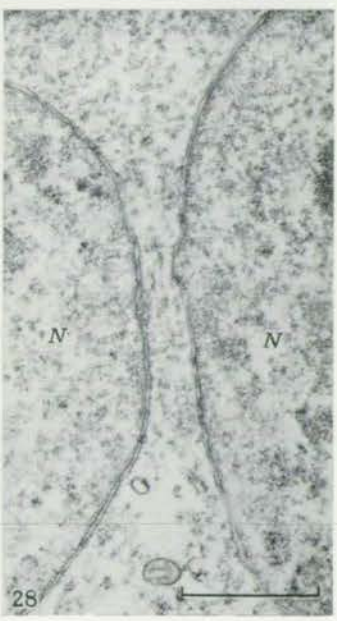

FIGURES 25 to 30

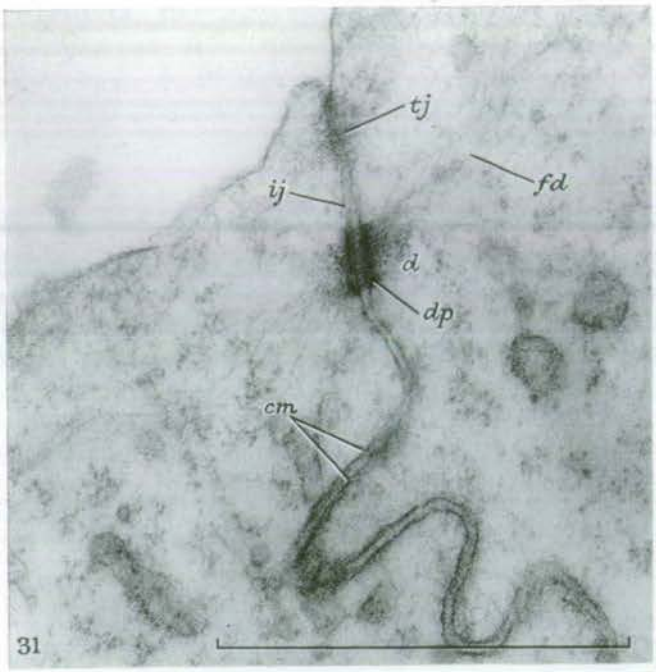

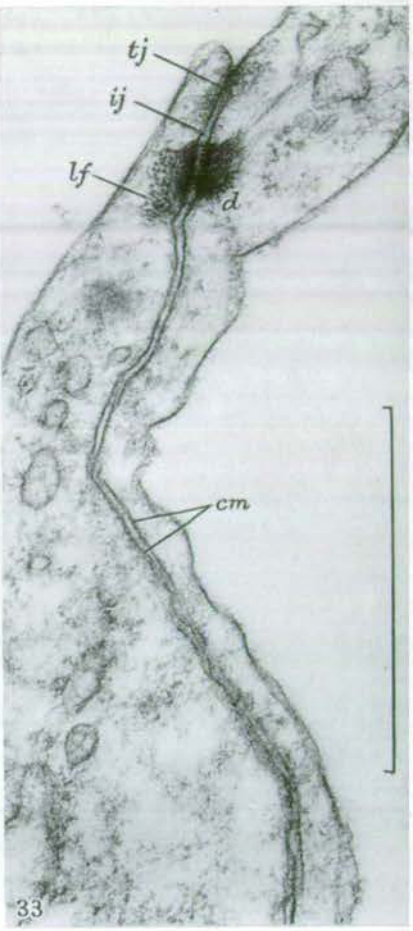

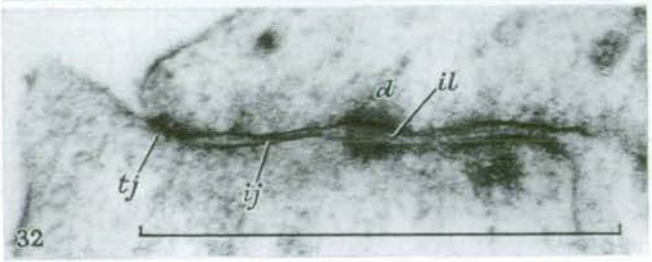

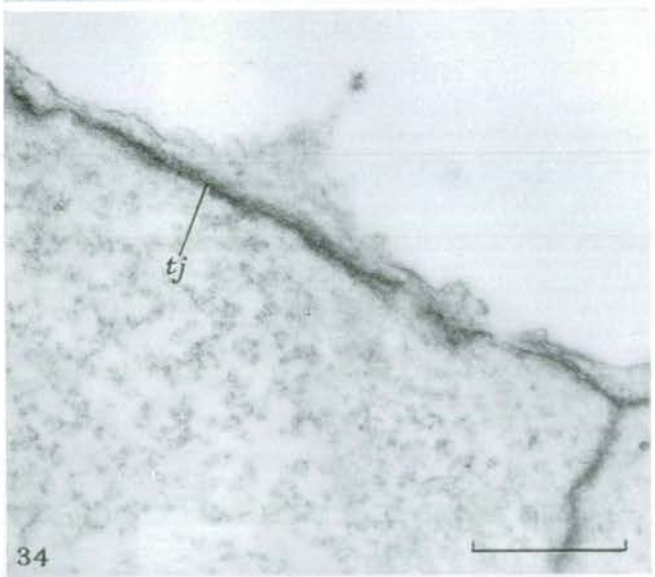

FIGURES 31 to 36

PLATE 45

FIGURE 31. Chick wing bud, stage 25. Transverse section through a terminal junction between two adjacent epiblast cells. The three parts are distinctly visible. *Os.P.U.* (Magn. × 20000.)

FIGURE 32. Twelve-day-old mouse, fore-limb bud. Transverse section through a terminal junction between two epiblast cells. The same three parts are visible as in figure 31, and in addition, the intermediate lamella (*il*) can be made out. *Os.P.U.* (Magn. × 63000.)

FIGURE 33 Chick wing bud, stage 25. Terminal junction similar to those in figures 31 and 34. Note cross-sections of the longitudinal fibres of the desmosome (*lf*). *Os.P.U.* (Magn. × 84000.)

FIGURE 34. Chick wing bud, stage 25. Longitudinal section through the tight junction at a plane parallel to the surface of the epithelium, seen in this projection as an elongated electron dense belt below the cell surface. *Os.P.U.* (Magn. × 20000.)

FIGURE 35. Chick wing bud, stage 25. Longitudinal section through a chain of five desmosome units between two epiblast cells. Note the bundles of longitudinal fibres (*lf*) common to all five units. *Os.P.U.* (Magn. × 27000.)

FIGURE 36. Chick wing bud. Stage 27. Transverse section passing between two desmosome units, showing the longitudinal fibres (*lf*) in cross-section, but without the dense plaques. *Os.P.U.* (Magn. × 27000.)

PLATE 46

FIGURE 37. Chick apical ectodermal ridge cell, stage 20. Mitochondrion about 6 μm long. *Os.P.U.* (Magn. × 16300.)

FIGURE 38. Eleven-day-old mouse embryo, apical ectodermal ridge. Note cilium (*c*) covered by the outer cell. *Os.P.U.* (Magn. × 34800.)

FIGURE 39. Twelve-day-old mouse embryo, apical ectodermal ridge cell. Note the extensive Golgi system (*G*). *Os.P.U.* (Magn. × 19200.)

FIGURE 40. Twelve-day-old mouse embryo, apical ectodermal ridge cell. Note the lysosome (*ly*) and the multivesicular body (*mvb*) in the neighbourhood of the Golgi group (*G*). *Os.P.U.* (Magn. × 21000.)

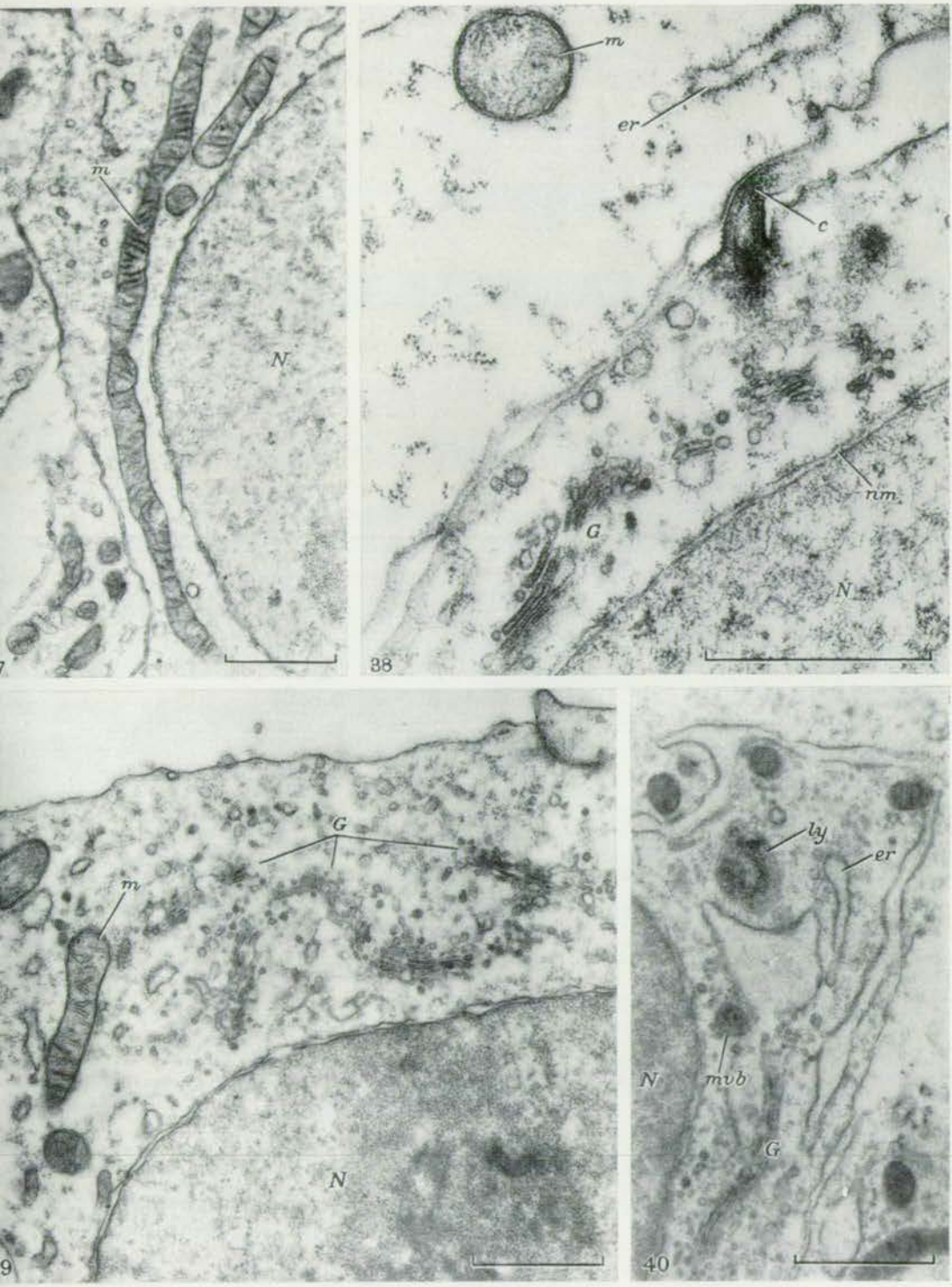

FIGURES 37 to 40

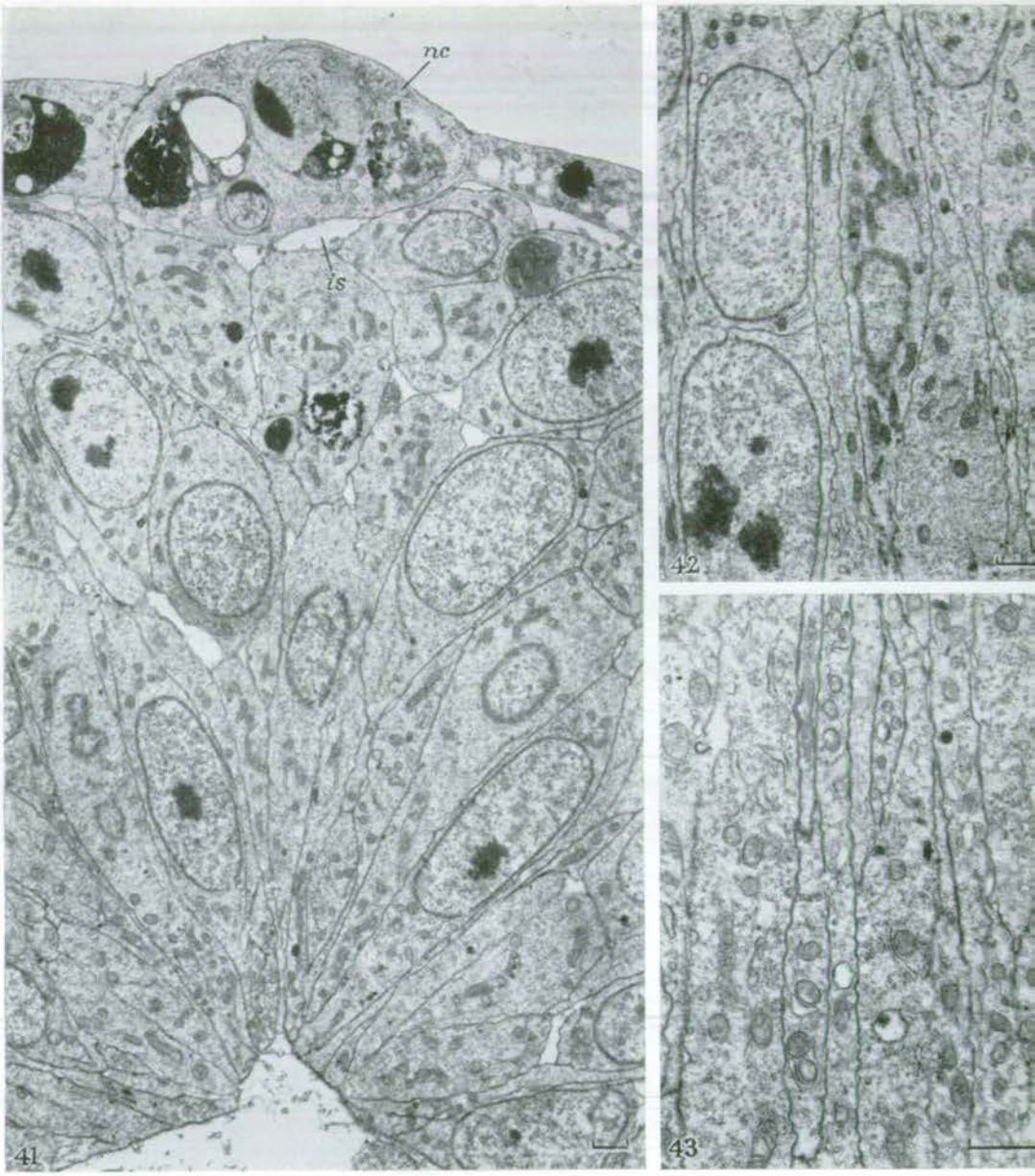

FIGURE 41. Chick, stage 25, wing bud. Low power electron micrograph of an exial transverse section through the apical ectodermal ridge. Note the necrotic cells (*nc*) at the top and the elongated cell processes converging towards the bottom median line. *Os.P.U.* (Magn. × 5000.)

FIGURE 42. Chick, stage 25. Longitudinal section through the outer layer of the apical ectodermal ridge. Note the elongation of the cells, which is parallel to the length of the apical ridge. *Os.P.U.* (Magn. × 6000.)

FIGURE 43. Chick, stage 25. Longitudinal section through the inner layers of the apical ectodermal ridge. Note the elongation of the processes parallel to the length of the apical ridge. *Os.P.U.* (Magn. × 9300.)

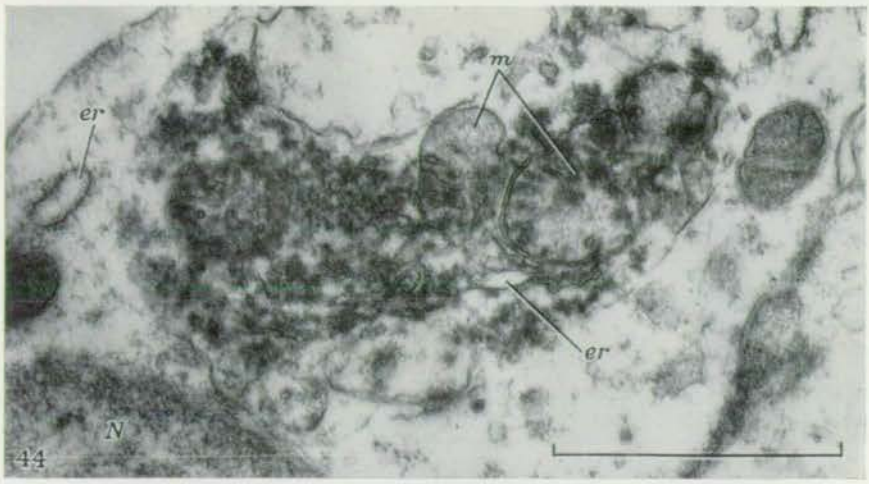

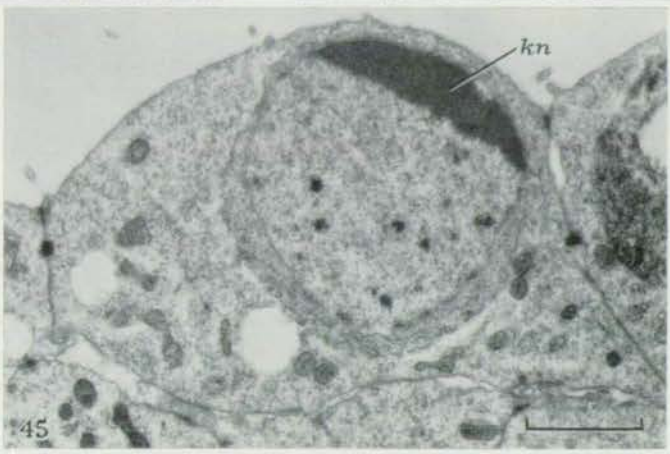

FIGURE 44. Twelve-day-old mouse embryo. Apical ectodermal ridge cell showing an extensive extranuclear necrotic centre (cytolysome) with mitochondria (*m*), endoplasmic reticulum (*er*) and dense unrecognizable material. *Os.P.U.* (Magn. ×37 800.)

FIGURE 45. Chick, stage 25, apical ectodermal ridge. Necrotic cell with the nucleus in a state of karyorrhexis (*kn*) and with vacuolated cytoplasm. *Os.P.U.* (Magn. ×15 300.)

FIGURE 46. Chick, stage 25, apical ectodermal ridge. Phagocytosis of a necrotic cell (*pc*). Note karyorrhexis of the nucleus and compare it with the normal appearance of the nucleus (*N*) of the host cell. *Os.P.U.* (Magn. ×15 750.)

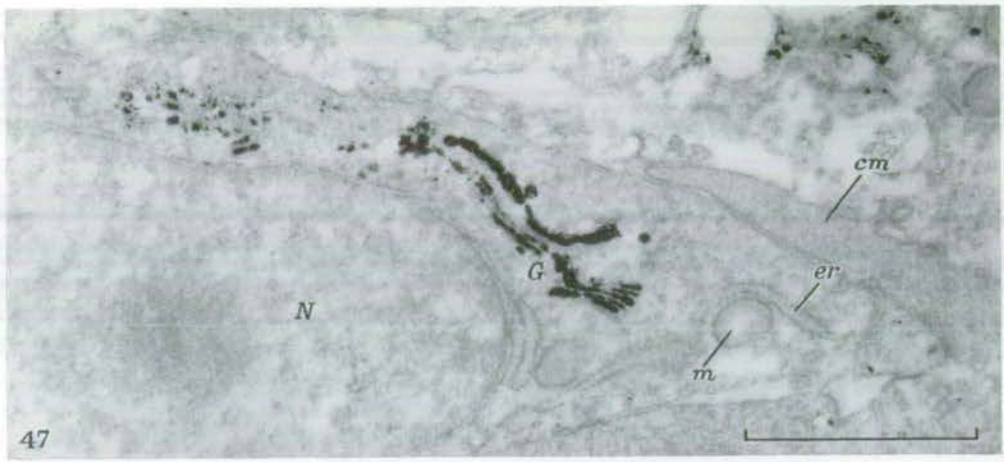

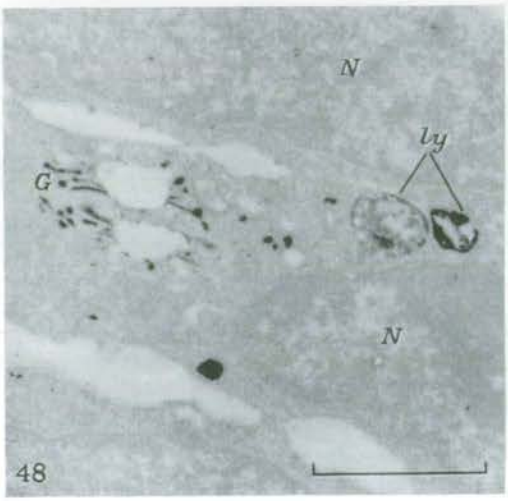

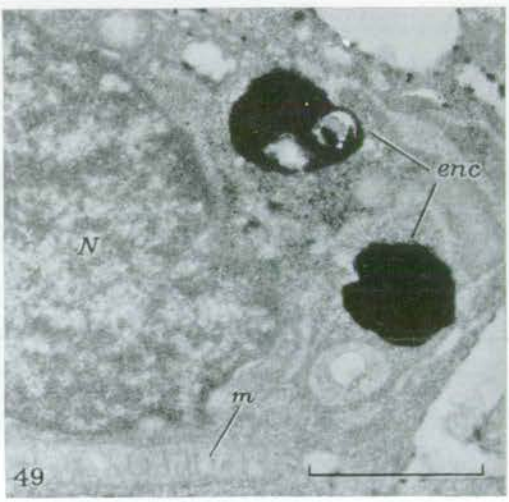

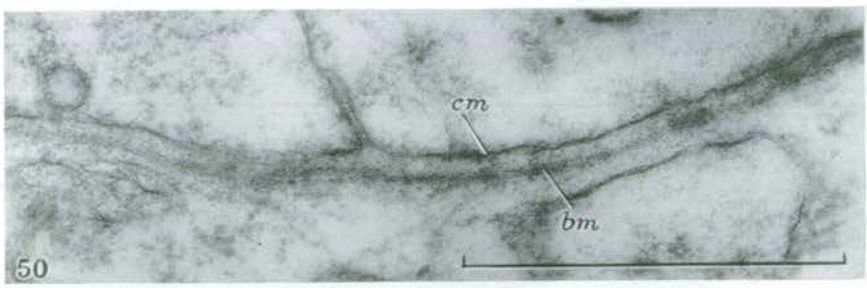

FIGURES 47 to 51

It is well known that during normal ontogeny in vertebrates cell death plays an important part in various morphogenetical processes. One of the cases is the process of necrosis in the apical ectodermal ridge. It is believed that cellular death of this kind is caused by nuclear changes, i.e. pycnosis and karyorrhexis (Glücksmann 1951). Present results indicate, however, that the cellular degenerations taking place in the apical ridge are seen outside the nucleus as profound changes in the cytoplasm, while the nucleus still remains unchanged. Golgi groups, lysosomes, multivesicular bodies, cytolysomes and extra-nuclear necrotic centres, as well as phagocytosed whole cells, appear successively as development proceeds. Necrotic changes in the nucleus appear much later when the extra-nuclear centres have enlarged so that they have occupied considerable areas of the cytoplasm. Eventually all of the organelles involved in the process of necrosis disappear simultaneously with the disappearance of the apical ridge itself. This course of events is unlike the cellular necrosis induced by means of cytotoxic substances, where the cells show nuclear changes first (Jurand 1961).

It is most striking that all the cytoplasmic organelles involved in the process of necrosis within the apical ridge show a strong positive reaction for acid phosphatase. It can be assumed therefore that these cell organelles are the sites of acid phosphatase activity. Milaire (1961, 1963) found acid phosphatase activity in all the cells of the epiblast but it was most strongly positive in the cells of the apical ridge. Milaire was of course unable by light microscopy to locate the intracellular sites of acid phosphatase activity. Evidence is accumulating in the literature that acid phosphatase as well as other phosphatases are often located in the Golgi apparatus and in the lysosomes and their analogues (Tice & Barrnett 1963; Meek & Lane 1964). However, more relevant seems to be the fact that increased acid phosphatase activity has been found histochemically by Brachet, Decroly-Briers & Hoyez (1958) in the Müllerian ducts of the male chick embryo during their involution between the 10th and 13th day of incubation. Brachet (1960) suggests that the acid phosphatase and other hydrolytic enzymes which are known to be located in lysosomes

---

DESCRIPTION OF PLATE 49

FIGURE 47. Eleven-day-old mouse embryo. Apical ectodermal ridge cell with the Golgi system (*G*) showing strongly positive reaction for acid phosphatase. Note that the other cell organelles are acid phosphatase negative. *G.Os.A.P.* (Magn. × 30400.)

FIGURE 48. Twelve-day-old mouse embryo. Apical ectodermal ridge cell showing positive reaction for acid phosphatase in the Golgi system (*G*) and in the lysosomes (*ly*). *G.Os.A.P.* (Magn. × 22800.)

FIGURE 49. 13-day-old mouse embryo. Apical ectodermal ridge cell showing positive reaction for acid phosphatase in two large extra-nuclear centres (cytolysomes, *enc*). *G.Os.A.P.* (Magn. × 22800.)

FIGURE 50. Chick, stage 25. Basement membrane (*bm*) closely adhering to the basal cell membranes (*cm*) of the epithelial cells. *Os.P.U.* (Magn. × 50300.)

FIGURE 51. Chick, stage 25. Basement membrane (*bm*) in the mediane line of the apical ridge showing discontinuities (*dbm*). *Os.P.U.* (Magn. × 19000.)

(de Duve 1959) are involved in the degeneration of the Müllerian duct when released into the cytoplasm from the lysosomes under the influence of testosterone, which begins to be produced at that time in the embryonic testes.

Milaire, in his most recent publication (1963), does not associate the increased acid phosphatase content with the cytolytic involution of the apical ectodermal ridge. It seems reasonable to assume, however, that the increasing acid phosphatase activity in this structure is closely related to the necrotic processes taking place in the apical ridge and consequently with its transient character. Such a character is particularly evident in mouse limb buds in which it exists for about 4 days. Its involution which proceeds rapidly after the ridge has reached its maximum structure seems to be already predetermined within the cytoplasm of the cells at the time when the ridge begins to be formed. This suggestion is based on the fact that the acid phosphatase activity, which is high in the extra-nuclear necrotic centres in later stages, is already evident in the Golgi system of young cells.

As regards the cilia found on the epithelial cells of early limb buds, they, no doubt, represent some kind of vestigial organelles here deprived of any biological importance. Such unexpected single cilia have also been encountered on free cell membranes of the neural epithelium in early chick embryos (Duncan 1957; Sotelo & Trujillo-Cenóz 1958) and, more recently, in various endocrine glands as remnants of ciliated ectoderm or entoderm (Barnes 1961; Salazar 1963; Evennett & Dodd 1964).

It is of interest that, in the course of the present work, cilia were found on several occasions in somewhat older limb buds between the cells of the apical ectodermal ridge, no doubt covered during the formation process by cells migrating on the epithelium towards the ridge. This observation agrees with the findings of Amprino & Camosso (1958) who have shown by carbon marking experiments that the epithelial cells do move towards the distal edge and 'pile up' at this region to form the ectodermal ridge. On the other hand, it may be, at least partly, that the cilia found between the ectodermal ridge cells have been covered during mutual shifting of cells within the ridge caused by local mitotic activity.

As far as the basement membrane is concerned, Bell *et al.* (1959) have suggested that it might be this structure and not the apical ridge which is important for the normal development of a limb bud. It would be particularly interesting to investigate the 'shiny' layer reported by Bell *et al.* (1959) and 'refractile layer' observed in the experiments of Bell, Gasseling, Saunders & Zwilling (1962), by means of electron microscopy in order to define more precisely what these terms mean and to provide more precise information as to whether these structures contain the basement membrane.

Balinsky (1957) showed that in grafting experiments carried out with *Amblystoma* the basement membrane, observed by electron microscopy, fails to develop or is greatly reduced when influenced by limb inductors such as olfactory organs or ear vesicles implanted under a non-limb epithelium, and that in these denuded areas limb rudiments can be found. He concluded from this result that for the normal inductive interaction between the constituents of limb buds the most important factor is a direct contact between them without the separating basement

membrane. In chick in natural conditions, as it was shown in the present paper, there are discontinuities of the basement membrane immediately under the apical ridge and it is possible that this allows a direct interaction between the apical ridge and the mesoblast.

The author wishes to thank Professor Waddington, F.R.S. and Dr G. G. Selman for their interest and encouragement as well as for reading and discussing the manuscript, and Miss A. P. Gray for invaluable editorial help.

Thanks are also due to Mr E. D. Roberts for skilful drawing of plate 40 and mounting the micrographs, and to Miss Patricia Collins for technical assistance.

References

Amprino, R. & Camosso, M. 1955 Ricerche sperimentali sulla morfogenesi degli arti nel pollo. *J. exp. Zool.* **129**, 453–493.

Amprino, R. & Camosso, M. 1958 Analisi sperimentali dello sviluppo dell'ala nell'embrione di pollo. *Roux Arch. EntwMech. Organ.* **150**, 509–541.

Amprino, R. & Camosso, M. 1959 Observations sur les duplications experimantales de la partie distale de l'ebauche de l'aile chez l'embryon de Poulet. *Arch. Anat. micr.* **48**, 261–305.

Balinsky, B. I. 1931 Zur Dynamik der Ektremitätenknospenbildung. *Roux Arch. EntwMech. Organ.* **123**, 565–648.

Balinsky, B. I. 1957 New experiments on the mode of action of the limb inductor. *J. exp. Zool.* **134**, 239–274.

Barnes, B. G. 1961 Ciliated secretory cells in the pars distalis of the mouse hypophysis. *J. Ultrastruct. Res.* **5**, 453–467.

Bell, E., Kaighn, M. E. & Fessenden, L. M. 1959 The role of mesodermal and ectodermal components in the development of the chick limb. *Devl Biol.* **1**, 101–124.

Bell, E., Gasseling, M. T., Saunders, J. W. Jr. & Zwilling, E. 1962 On the role of ectoderm in limb development. *Devl Biol.* **4**, 177–196.

Brachet, J., Decroly-Briers, M. & Hoyez, J. 1958 Contribution a l'étude des lysosomes au cours du dévelopment embryonnaire. *Bull. Soc. Chim. biol.* **40**, 2039–2048.

Brachet, J. 1960 *The biochemistry of development.* London: Pergamon Press.

Carter, T. C. 1954 The genetics of luxate mice. IV. Embryology. *J. Genet.* **52**, 1–35.

Caulfield, J. B. 1957 Effects of varying the vehicle for OsO_4 in tissue fixation. *J. biophys. biochem. Cytol.* **3**, 827–829.

Duncan, D. 1957 Electron microscope study of the embryonic neural tube and notochord. *Texas Rep. Biol. Med.* **15**, 367–377.

de Duve, C. 1959 Lyosomes, a new group of cytoplasmic particles. In *Subcellular particles* (Hayashi, T., ed.), New York: The Ronald Press Co. pp. 128–159.

Evenett, P. J. & Dodd, J. M. 1964 Fine structure of the thyroid gland of the *Xenopus* tadpole in different physiological states. *The 134th Conference of the Society of Experimental Biology, Nottingham.*

Farquhar, M. G. & Palade, G. E. 1963 Junctional complexes in various epithelia. *J. cell Biol.* **17**, 375–412.

Filatow, D. 1928 Über die Verpflanzung des Epithels und des Mesenchyms einer vorderen Extremitätenknospe bei Embryonen von Axolotl. *Roux Arch. EntwMech. Organ.* **113**, 240–244.

Glauert, A. M. & Glauert, R. H. 1958 Araldite as an embedding medium for electron microscopy. *J. biophys. biochem. Cytol.* **4**, 191–194.

Glücksmann, A. 1934 Über die Entwicklung der Amniotenextremitäten und ihre Homologie mit den Flossen. *Z. Anat. Entw. Gesch.* **102**, 498–520.

Glücksmann, A. 1951 Cell death in normal vertebrate ontogeny. *Biol Rev.* **26**, 59–86.

Gomori, G. 1952 *Microscopic histochemistry. Principles and practice.* Chicago: The University of Chicago Press.

Grüneberg, H. 1943 The development of some external features in mouse embryos. *J. Hered.* **34**, 88–92.

Hamburger, V. & Hamilton, H. L. 1951 A series of normal stages in the development of the chick embryo. *J. Morph.* **88**, 49–92.

Hinrichsen, K. 1956 Die Bedeutung der epithelialen Randleiste für die Extremitätenentwicklung. *Z. Anat. Entw. Gesch.* **119**, 350–364.

Holt, S. J. & Hicks, R. M. 1962 Combination of cytochemical staining methods for enzyme localization with electron microscopy. In *Symposia of the International Society for Cell Biology*, 1. *The interpretation of ultrastructure*. New York and London: Academic Press.

Huxley, H. E. 1957 The double array of filaments in cross-striated muscle. *J. biophys. biochem. Cytol.* **3**, 631–648.

Jurand, A. 1961 Further investigations of the cytotoxic and morphogenetic effects of some nitrogen mustard derivatives. *J. Embryol. exp. Morph.* **9**, 492–506.

Jurand, A. 1962 The development of the notochord in chick embryos. *J. Embryol. exp. Morph.* **10**, 602–621.

Kieny, M. 1960 Rôle inducteur du mesoderme dans la differenciation precoce du bourgeon de membre chez l'embryon de Poulet. *J. Embryol. exp. Morph.* **8**, 457–467.

Kölliker, A. 1879 *Entwicklungsgeschichte des Menschen und der höheren Tiere*. Leipzig: Wilhelm Engelmann.

Kurosumi, K. 1961 Electron microscopic analysis of the secretion mechanism. In *Int. Rev. Cytol.* **11**, 1–124.

Mangold, O. 1928 Das Determinationsproblem. II. Die paarigen Extremitäten der Wirbeltiere in der Entwicklung. *Ergbn. Biol.* **5**, 292–394.

Meek, G. A. & Lane, N. J. 1964 The ultrastructural localization of phosphatases in the neurones of the snail, *Helix aspersa*. *J. Micr. Soc.* **82**, 193–204.

Milaire, J. 1961 Le rôle de la cape apicale dans la formation des membres des Vertébres. *Ann. Soc. Zool. Belg.* **91**, 129–145.

Milaire, J. 1963 Étude morphologique et cytochimique du dévelopment des membres chez la Souris et chez la Taupe. *Arch. Biol. Paris*, **74**, 129–317.

Neapolitano, L. 1963 Cytolysomes in metabolically active cells. *J. Cell Biol.* **18**, 478–481.

Nicholas, J. S. 1955 Limb and girdle. In *Analysis of development* (Willier, B. H., Weiss, P. A. & Hamburger, V., ed.). Philadelphia & London: W. B. Saunders Co.

Novikoff, A. B. 1961 Lysosomes and related particles. In *The Cell*, **2** (Brachet, J. & Mirsky, A. E., ed.), New York and London: Academic Press.

Palade, G. E. 1952 A study of fixation for electron microscopy. *J. exp. Med.* **95**, 285–298.

Plumel, M. 1948 Tampon au cacodylate de sodium. *Bull Soc. Chim. biol., Paris*, **30**, 129–130.

Salazar, H. 1963 The pars distalis of the female rabbit hypophysis: an electron microscopic study. *Anat. Rec.* **147**, 469–497.

Saunders, J. W., Jr. 1948 The proximo-distal sequence of origin of the parts of the chick wing and the role of the ectoderm. *J. exp. Zool.* **108**, 363–404.

Slayter, H. S., Warner, J. R., Rich, A. & Hall, C. E. 1963 The visualization of polyribosomal structure. *J. Mol. Biol.* **7**, 652–657.

Sotelo, J. R. & Trujillo-Cenóz, O. 1958 Electron microscope study on the development of ciliary components of the neural epithelium of the chick embryo. *Z. Zellforsch.* **49**, 1–12.

Steiner, K. 1928 Entwicklungsmechanische Untersuchungen über die Bedeutung des ectodermalen Epithels der Extremitätenknospe von Amphibienlarven. *Roux Arch. EntwMech. Organ.* **113**, 1–11.

Tice, L. W. & Barnett, R. J. 1963 The fine structural localization of some testicular phosphatases. *Anat. Rec.* **147**, 43–64.

Waddington, C. H. 1956 *Principles of embryology*. London: George Allen & Unwin Ltd.

Waddington, C. H. & Perry, M. M. 1962 The ultrastructure of the developing urodele notochord. *Proc. Roy. Soc.* B, **156**, 459–482.

Zwilling, E. 1949 The role of epithelial components in the developmental of the 'wingless' syndrome in chick embryos. *J. exp. Zool.* **111**, 175–188.

Zwilling, E. 1955 Ectoderm–mesoderm relationship in the development of the chick embryo limb bud. *J. exp. Zool.* **128**, 423–441.

Zwilling, E. 1956 Reciprocal dependence of ectoderm and mesoderm during chick embryo limb development. *Amer. Nat.* **90**, 257–265.

Zwilling, E. 1961*a* Limb morphogenesis. In *Advances in morphogenesis* (1), pp. 301–330. New York and London: Academic Press.

Zwilling, E. 1961*b* Inductive mechanisms. In *Papers and discussions presented at the First International Conference on Congenital Malformations*, pp. 133–139. Philadelphia and Montreal: J. B. Lippincott Co.

Abbreviations on plates

bm	basement membrane
c	cilium
cm	cell membrane
d	desmosome
dbm	discontinuity in the basement membrane
dnm	discontinuity of the nuclear membrane
dp	dense plaques
enc	extra-nuclear necrotic centre
er	endoplasmic reticulum profile
fd	fibres associated with the desmosomes
G	Golgi complex
G.Os.A.P.	glutaraldehyde fixation, Gomori procedure for acid phosphatase localization adapted for electron microscopy, osmium postfixation, uranyl–zinc acetate counterstaining.
G.Os.U.Z.	glutaraldehyde–osmium tetroxide fixation, uranyl–zinc acetate staining
ij	intermediate junction
il	intermediate lamella
imv	interval microvillus
is	intercellular space
kn	karyorrhectic nucleus
lf	longitudinal fibres of the desmosome
ly	lysosome
m	mitochondrion
mvb	multivesicular body
mv	microvillus
N	nucleus
nc	necrotic cell
ner	endoplasmic reticulum profile continuous with the outer nuclear membrane
nerl	loop-like endoplasmic reticulum profile continuous with the outer nuclear membrane at two points
nm	nuclear membrane
np	nuclear pore
Os.P.U.	osmium tetroxide fixation, potassium permanganate with uranyl acetate staining
pc	phagocystosed cell
sa	subannuli
sg	secretory-like granules
tj	tight junction

PRINTED IN GREAT BRITAIN AT THE UNIVERSITY PRINTING HOUSE, CAMBRIDGE
(BROOKE CRUTCHLEY, UNIVERSITY PRINTER)

Early changes in limb buds of chick embryos after thalidomide treatment

by A. Jurand

J. Embryol. exp. Morph., Vol. 16, 2, pp. 289–300, October 1966
With 5 plates
Printed in Great Britain

Early changes in limb buds of chick embryos after thalidomide treatment

By A. JURAND[1]
From the Institute of Animal Genetics, Edinburgh

Since the first observations of hypoplastic and aplastic thalidomide deformities in infants (McBride, 1961; Lenz, 1962), the literature on this subject has grown to many hundreds of communications. Experimental investigations in almost all cases have been undertaken to show whether thalidomide and its metabolites have any teratogenic effects in experimental animals. Numerous review papers are available on this subject, e.g. Giroud, Tuchmann-Duplessis & Mercier-Parot (1962), Somers (1963), and Salzgeber & Wolff (1964).

Chick embryos did not seem for some time to be suitable for experimental production of typical thalidomide deformities. However, Kemper (1962*a*, *b*), Yang, Yang & Liang (1962). Boylen, Horne & Johnson (1963) and Leone (1963) have shown that thalidomide can produce a whole range of ectromelian deformities provided that it is introduced into the egg at a particular period of embryonic development. Certain controversy was created when Williamson, Blattner & Lutz (1963) demonstrated that certain insoluble and otherwise inert substances such as powdered glass, colloidal alumina and colloidal clay, when introduced into the amniotic cavity in chick embryos, caused thalidomide-like malformations.

More recently, Salzgeber & Salaün (1963*a*, *b*, 1965) established that thalidomide produces in the chick essentially the same kind of malformations as it does in human and rabbit embryos.

The present report gives an account of an investigation of short-term changes in chick embryos treated with thalidomide. This approach, if successful, would help to elucidate the mode of action of thalidomide on limb primordia when they are in the sensitive period of development.

MATERIAL AND METHODS

Thalidomide suspensions

Thalidomide (Distillers Co. Ltd.), well ground and dry-sterilized at 100 °C, was suspended in thin egg-white (10 or 20 mg/ml of medium). The egg-white was taken from non-experimental infertile fowl eggs. To these suspensions penicillin and streptomycin (2·5 mg of each per ml) were added.

[1] *Author's address:* Institute of Animal Genetics, West Mains Road, Edinburgh 9, Scotland.

Treatment of chick embryos

Fowl eggs (Brown Leghorn or Chunky Chick) were incubated at 38·5 °C for 60–64 h until the stage 17 or 18 of Hamburger & Hamilton (1951) was reached. The eggs were then opened through the air space by removing about 1–2 cm^2 of the calcareous shell together with the outer shell membrane. After the inner shell membrane had been pierced with a short-bevel hypodermic needle, 0·2 ml of thalidomide suspension was introduced into the egg-white in close proximity to the embryo, but not into the amniotic cavity. The same amount of suspension was also injected into the yolk sac just under the blastoderm in some eggs. These eggs were injected with a total of 0·4 ml of suspension. Since suspensions were used in two concentrations and some eggs were injected only in the egg-white and some in both egg-white and yolk, there were essentially four kinds of experimental embryos. The results obtained in all four experimental groups will be reported together, since embryos with all degrees of injury were found in each group. The degree of injury does not seem to be directly dependent upon the dose of thalidomide or upon the method of its application.

Control eggs were injected with thin albumen containing the same amount of calcium carbonate instead of thalidomide and with the same amounts of penicillin and streptomycin. Calcium carbonate has a low solubility in water like thalidomide and is probably harmless to avian eggs as it constitutes up to 98·5 % of the egg shell.

After injections the eggs were sealed with Parafilm (Lindsay and Williams, London) and incubated for 24 h at 38·5 °C. For further investigations only those embryos were selected which showed heart beat and were between stages 21 and 25 at time of fixation (Hamburger & Hamilton, 1951).

Light- and electron-microscopy techniques

For light-microscope observations the embryos were prepared according to the technique described previously (Jurand, 1965).

For electron-microscope investigations both osmic acid fixation (Jurand, 1962) and glutaraldehyde fixation followed by 1 % osmic acid postfixation were used. In the latter case 5 % glutaraldehyde solution was buffered with cacodylate buffer at pH 7·2 (Plumel, 1948) and 0·1 mg of calcium chloride was added for each ml of fixative. The embryos were fixed for 4 h in the glutaraldehyde solution at 2–4 °C. After rinsing with chilled buffered 7·5 % sucrose solution (3 times, 15 min each time) the forelimb buds were dissected and postfixed with 2 % osmic acid fixative (Jurand, 1962). Further preparation was done as described previously (Jurand, 1965).

To localize the acid phosphatase activity in the endothelial cells of the limb-bud axial artery, the procedure of Gomori (1952), as adapted to electron microscopy by Holt & Hicks (1962), was applied (for detailed description see Jurand, 1965).

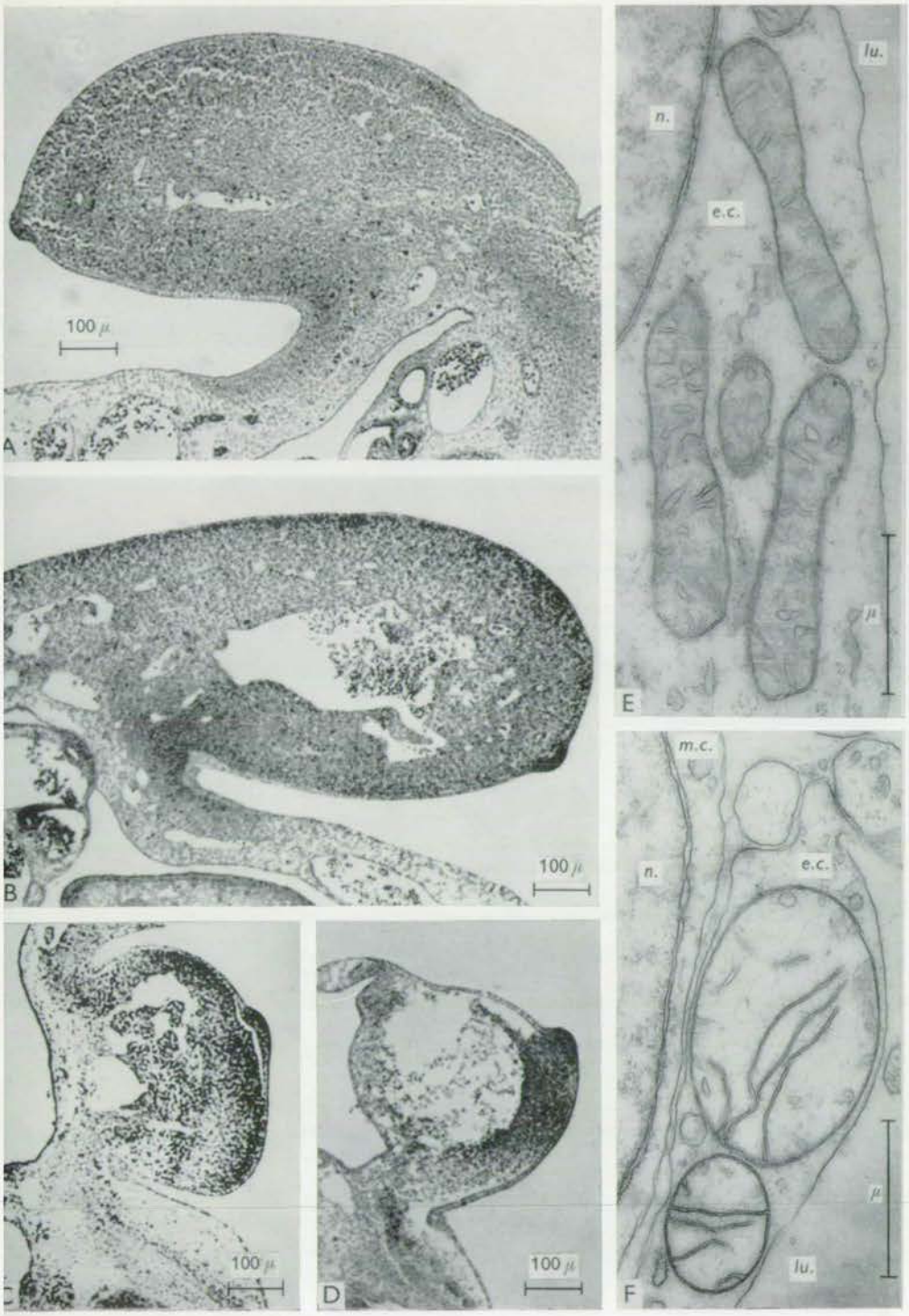
100 μ
A
100 μ
B
100 μ
C
100 μ
D
lu.
n.
e.c.
μ
E
m.c.
n.
e.c.
μ
lu.
F

RESULTS

Light microscopy

In normal conditions at stages 21–25, i.e. after 64–68 h of incubation, the axial artery is usually narrow and unbranched. Early injuries after thalidomide treatment appear in about 40 % of the embryos as distinct dilation of the limb-bud axial artery with or without necrotic changes in the surrounding mesoblast tissue. These changes, arbitrarily classified here into three groups, are easily observable with a low-power dissecting microscope. They are particularly visible in dehydrated specimens cleared with methyl benzoate, in whole mounts cleared in xylol and embedded in Canada balsam and also in specimens cleared by embedding in Araldite for electron-microscope purposes.

In histological sections taken from limb buds with distinct dilations of the axial artery, the endothelium of the blood vessels is very thin. The vessels are often convoluted, forming diverticula filled with blood corpuscles (Plate 1, figs. A, B). This kind of damage is classified as first-degree injury. In more affected limb buds (Plate 1, fig. C), the dilations of the axial artery are wider and a considerable number of necrotic cells are found in the mesoblast tissue adjacent to the dilated part of the blood vessel (second-degree injury).

In extreme cases the vast majority of the mesoblast tissue is completely destroyed, leaving extensive empty spaces without any blood vessels (third-degree injury). In these cases, however, there is usually a small concentration of more or less healthy looking mesoblast cells in the dorsal part of the limb bud just below the dorsal epiblast and extending into the area below the apical ectodermal ridge (Plate 1, fig. D).

Usually those embryos in which the limb buds show more prominent injury (second or third degree) are also retarded in general development.

Regardless of the degree of injury, the epiblast (together with the apical ectodermal ridge) never showed any visible abnormality, for instance in the form of discontinuities or necrosis.

Explanation of Plates

Abbreviations on Plates: *cly.*, cytolysome; *e.c.*, endothelial cell; *lu.*, lumen of the axial artery; *ly.*, lysosome; *m.c.*, mesoblast cell; *n.*, nucleus.

Plate 1

Fig. A. Sagittal section through a normal chick wing bud at stage 23. × 80.

Fig. B. Prominent dilation of the axial artery (first-degree injury), stage 22. × 80.

Fig. C. Scattered necrosis around the dilated artery (second-degree injury), stage 21. × 80.

Fig. D. Section through an embryo at stage 20, showing extensive damage of the limb bud mesoblast. Note the concentration of normal mesoblast cells in the dorsal and marginal area of the limb bud. × 80.

Fig. E. Mitochondria in a control endothelial cell. × 23000.

Fig. F. Swollen mitochondria in the endothelium after treatment (first-degree injury). × 23000.

Electron microscopy

Electron-microscope investigations were concerned mainly with the ultrastructure of the endothelial cells of the axial artery and of the adjacent mesoblast cells. The epiblast with the apical ectodermal ridge were also examined, but in these parts no divergence from normal ultrastructural patterns was observed.

Depending on the degree of injury, the endothelial cells show more or less distinct changes at the ultrastructural level. In the limb buds with markedly dilated axial artery but without extensive necrotic changes in the mesoblast (i.e. first-degree injury), the mitochondria in endothelial cells show considerable changes. In comparison with the controls, the affected mitochondria are markedly increased in size, rounded up, often partly or completely vacuolated and contain few cristae. The control mitochondria are elongated, with a much more electron-dense matrix and have the usual appearance of the metazoan type (Plate 1, figs. E, F; Plate 2, figs. A–C).

In many cases of first-degree injury the alteration of mitochondrial structure was confined to those in the endothelial cells; the adjacent mesoblast cells contained mitochondria of the same appearance as those in control endothelial cells (Plate 2, fig. B).

Also observed in the limb buds with first-degree injury was an increase in number of lysosomes in the endothelial cells. They formed groups of up to ten in one section and were frequently found near the Golgi apparatus (Plate 2, figs. C, D).

Morphologically, at least three types of lysosomes can be distinguished: (1) homogeneous type covered by a single membrane, (2) multivesicular body type (see Plate 4, fig. B), and (3) cytolysome type. The last type is usually found in more affected limb buds (Plate 2, fig. E).

In control endothelial cells only single droplets of the homogeneous type of lysosome were observed, and these very seldom.

In affected endothelial cells the lysosomes are often found close to vacuolated mitochondria, and in these cases the vacuole inside the mitochondrion is usually adjacent to the side where the lysosome is lying (Plate 3, fig. A). In some cases lysosomes, often containing myelin-like figures, were found embedded inside the injured mitochondria (Plate 3, fig. B).

PLATE 2

Fig. A. Vacuolated mitochondria. ×22000.

Fig. B. Swollen mitochondria confined to the endothelial cell (*e.c.*). Below, a mesoblast cell (*m.c.*) with normal mitochondria. ×15000.

Fig. C. Endothelial cell with Golgi apparatus and adjacent primary and secondary lysosomes. ×33000.

Fig. D. Group of lysosomes of various types in an endothelial cell. ×29000.

Fig. E. Cytolysomes in an endothelial cell. ×37000.

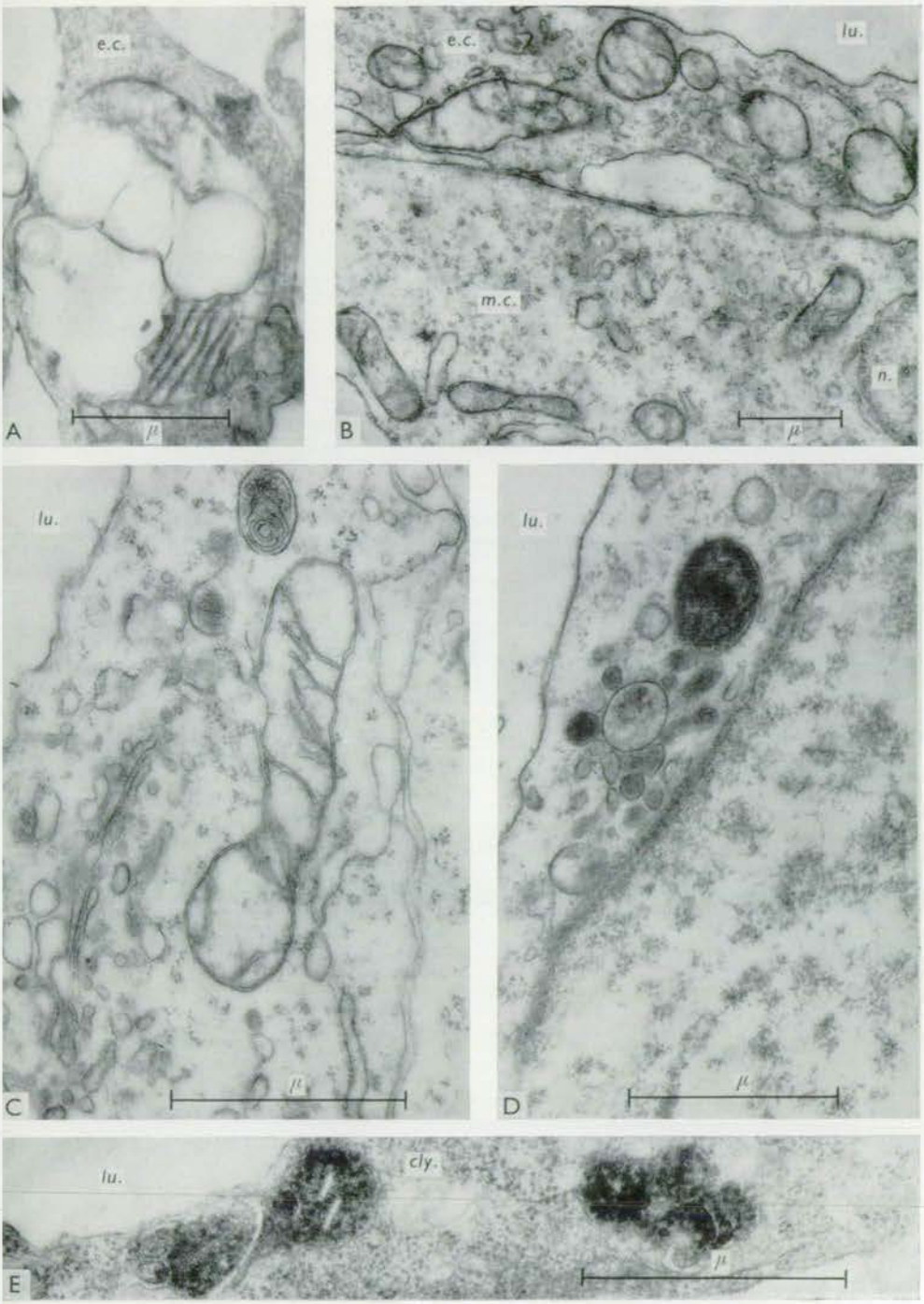
e.c.
A
μ
e.c.
lu.
m.c.
n.
B
μ
lu.
C
μ
lu.
D
μ
lu.
cly.
E
μ

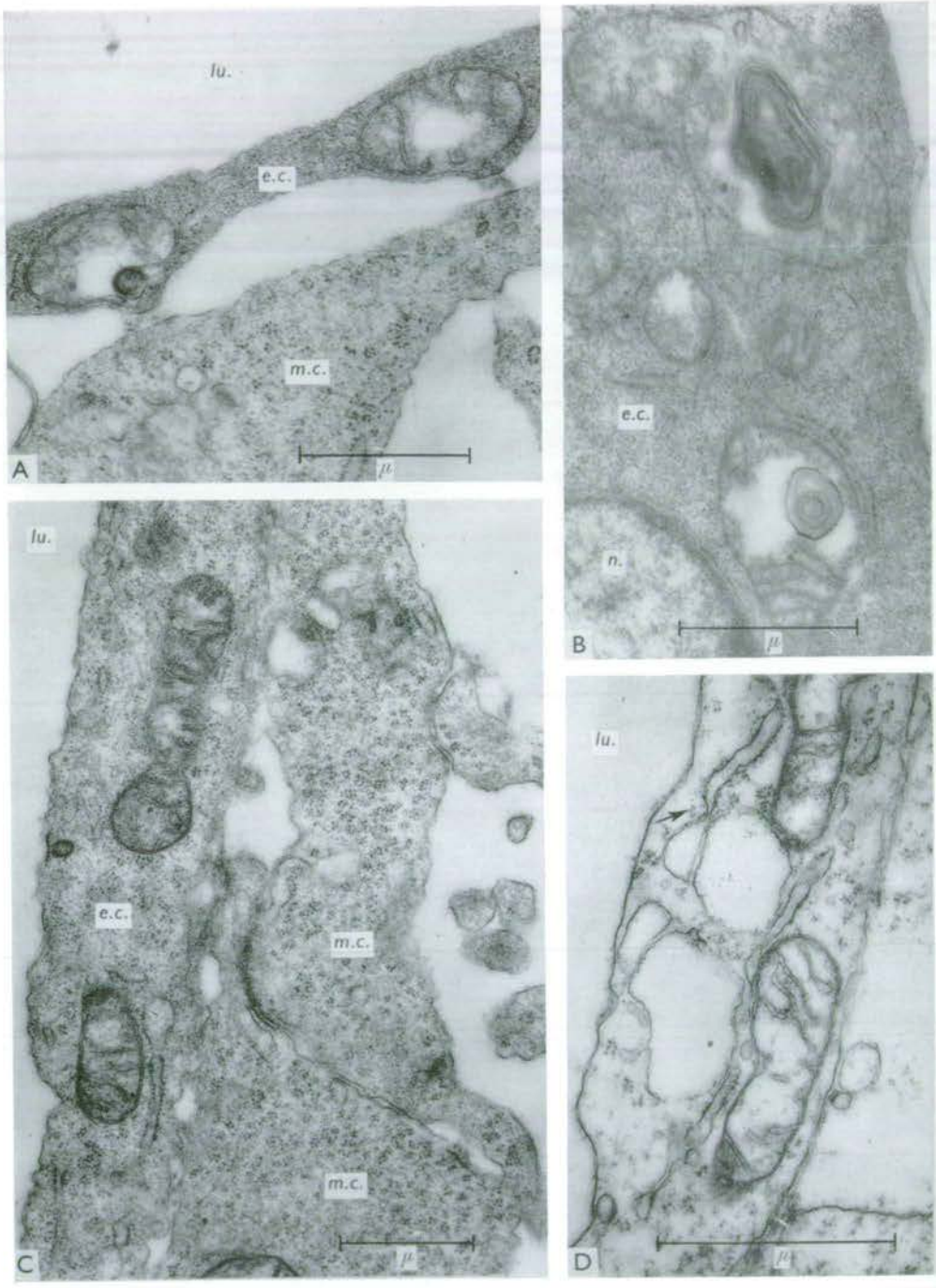
lu.
e.c.
m.c.
A
μ
B
n.
C
D

Another feature of the affected endothelium in these limb buds is the vacuolation of the cytoplasm. The vacuoles are often seen to be formed by dilation of endoplasmic reticulum cysternae (Plate 3, fig. D).

In limb buds which show the two higher degrees of injury the endothelial cells also display other characteristic properties. At first, when glutaraldehyde fixative is used, the cytoplasm of the endothelial cells becomes much more electron-dense than that of the adjacent mesoblast cells (Plate 3, fig. A). This difference is due to the increased number of ribosomes per unit volume; they are closely packed and uniformly fill the cytoplasm. In adjacent mesoblast cells the ribosomes are arranged in typical polysome groups scattered fairly loosely throughout the cytoplasm. Each polysome group consists of 6–9 units. In control limb buds there is no such difference in electron density between endothelial and mesoblast cells, although the same polysome arrangement of the ribosomes is also obvious only in the mesoblast cells (Plate 3, fig. C).

A subsequent ultrastructural feature of the affected endothelial cells is the formation of vesicular projections by these cells. They extend deep into the lumen of the blood vessel and are covered on the outside by the cell membrane and on the inside by a kind of vacuolar membrane (Plate 4, fig. A). In many cases such projections appear to lie loosely in the lumen of the blood vessel, but this is due to the fact that the point of attachment does not lie at the level of the section.

It was observed that these loop-like profiles of the vesicular projections, if sectioned at the point of attachment, have at the base a lysosome embedded in the endothelial cell (Plate 4, fig. B). This suggests that the lysosomes take part in the formation of these projections.

Frequently the vesicular projections are found to be formed by extremely thin endothelial cells (down to 50 mμ), and very often the continuity of the endothelium is broken at the point where such a vesicular projection is attached. Thus it may be that this is why the endothelium is weakened in the affected limb buds, and that in those with the higher degrees of injury this is the way discontinuities are formed in the endothelial lining (Plate 4, fig. C).

PLATE 3

Fig. A. In the upper part an endothelial cell (*e.c.*) with two mitochondria. Close to one of them a lysosome. Below, a mesoblast cell (*m.c.*). Note the difference between the electron density of the two cytoplasms and between the arrangement of their ribosomes. × 24000.

Fig. B. Two mitochondria with myelin figure bodies inside in endothelium. × 25000.

Fig. C. Control endothelium and mesoblast cells (see abbreviations). Note different arrangement of ribosomes and no difference in the electron density of the cytoplasms. Compare with fig. A on this Plate. × 19000.

Fig. D. Vacuolation of the endothelium cytoplasm. Note formation of vacuoles by dilation of the endoplasmic reticulum profiles (arrow). × 33000.

In the limb buds with considerable necrotic changes in the mesoblast adjacent to the abnormal axial artery (second-degree injury), the necrotic cells show enlarged lysosomes, numerous cytoplasmic vacuoles and abnormal mitochondria but the nuclei of these cells do not show any visible necrotic changes (Plate 4, fig. D). Probably the process of necrosis in the cytoplasm precedes any necrotic changes in the nucleus.

Experiments designed to show the localization of the acid phosphatase activity in the affected endothelial cells demonstrated that the Golgi apparatus and the lysosomes contain this enzyme (Plate 5, fig. A). In more affected limb buds, large accumulations of acid phosphatase-positive bodies were found in the cytoplasm of these cells. They can be classified as cytolysomes or extranuclear necrotic centres (Plate 5, fig. B).

In these experiments it could also be demonstrated that the lysosomes found at the point of attachment of the vesicular projections show a considerable concentration of acid phosphatase (Plate 5, fig. C). This suggests that the formation of these projections is due to the enzymic activity of the lysosomes. The vesicular projections themselves also contain some acid phosphatase, but the specificity of the reaction on membranous structures is rather uncertain.

Similarly, at the points of extreme flattening, the endothelial cells show considerable acid phosphatase activity (Plate 5, fig. D).

DISCUSSION

Only after the thalidomide disaster did the methods of experimental embryology and applied pharmacology find more intensive application in the appropriate evaluation of drugs with respect to their potentially dangerous side-effects for developing embryos. The co-operation of embryologists with other specialists in the field is the most advisable way to achieve the necessary progress in overcoming drug-induced embryopathies in man (see Töndury, 1962).

Many of the present discussions concern the methods of examination and the extent to which they should be adopted. Admittedly it is not a simple and easy problem, because of the diversity of the potential side-effects, the differences in sensitivity of various laboratory animals, and because of the difficulties in applying the obtained results to the biological conditions in man. For these reasons there obviously cannot be any standardized testing procedure. It seems,

PLATE 4

Fig. A. Vesicular projection formed by a thinned endothelial cell (*e.c.*). ×54000.

Fig. B. Multivesicular type body lysosome at the point of attachment of the vesicular projection. ×55000.

Fig. C. Thinned endothelial cells with vesicular projections. Note the discontinuity in the endothelial lining (arrow). ×38000.

Fig. D. Necrotic changes in a mesoblast cell (*m.c.*). Note numerous vacuoles, lysosomes, and one extracellular necrotic centre. Nucleus and nucleolus normal. ×9000.

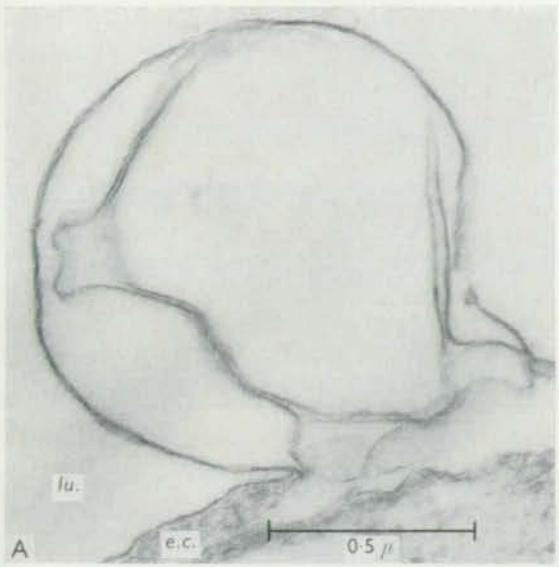
lu.
e.c.
0·5 μ
A

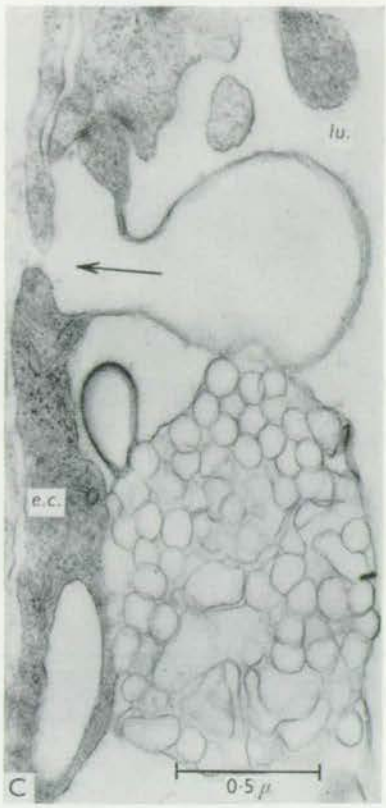
lu.
e.c.
0·5 μ
C

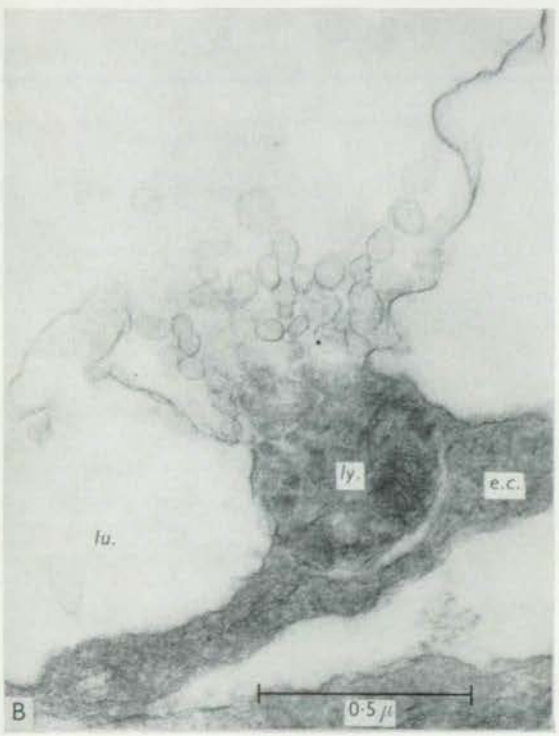
ly.
e.c.
lu.
0·5 μ
B

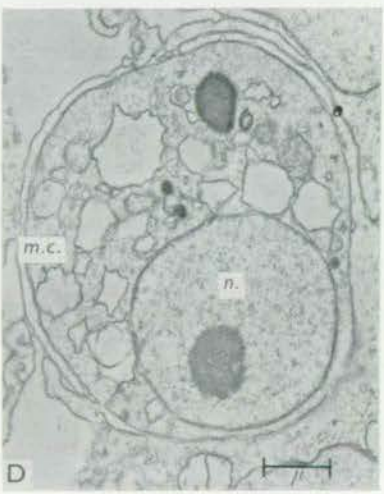
m.c.
n.
D

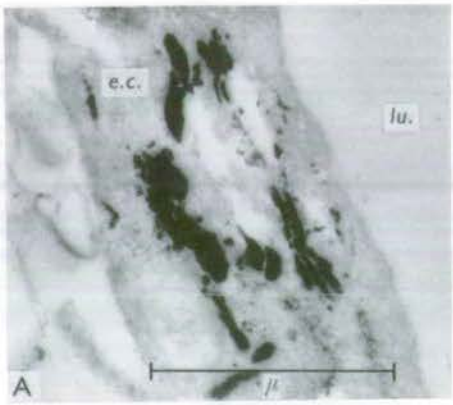
e.c.
lu.
A
μ

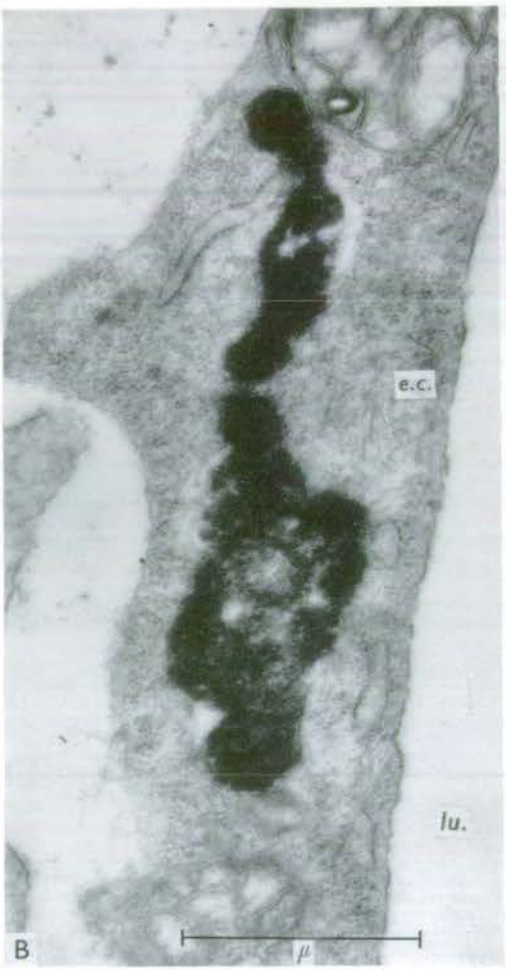
e.c.
lu.
B
μ

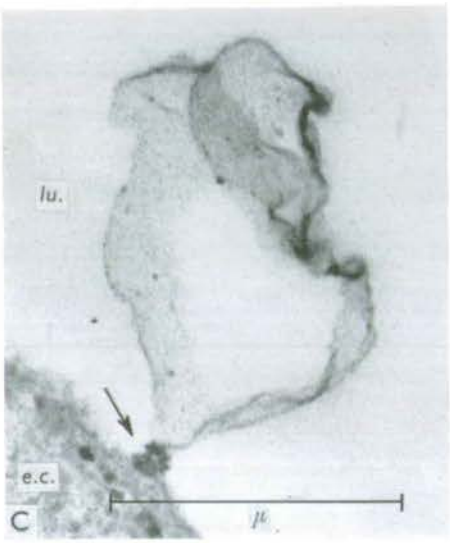
lu.
e.c.
C
μ

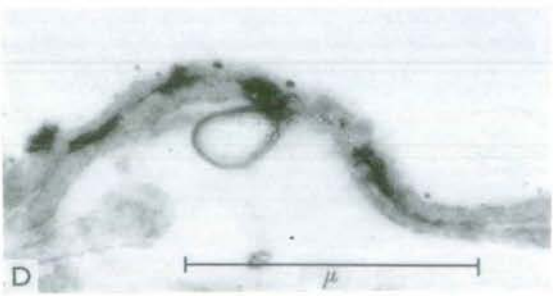
D
μ

however, that the first step should be to examine the early effects at the onset of organogenesis rather than to wait for later gross abnormalities. The early effects, if spotted shortly after the administration of the drug to pregnant females or to fertilized fowl eggs, might give quick and reliable indications. The late congenital malformations in newborns do not always reveal all embryopathic properties of the drug under examination, because many embryos, particularly those suffering the most serious injuries, die shortly after treatment.

The results presented here suggest that the primary cause of thalidomide abnormalities is an injury of the endothelial lining of the axial limb artery. This effect by itself may not lead to any developmental abnormalities, but it probably has an influence on the developmental potentialities of the non-vascular part of the mesoblast tissue. This possibility is indicated by the fact that in the embryos with more prominent injury of the axial artery numerous necrotic cells are found in the areas of the future skeleton blastemas.

In extreme cases, the injury leads to a complete cytolysis of the central core and the ventral part of the mesoblast, but always with the exception of the dorsal region near the apical ectodermal ridge (see Plate 1, fig. D). For some reason the mesoblast cells in this region show greater resistance than the rest of the mesoblast. These observations may explain the mechanism of some of the malformations obtained by Salzgeber & Salaün (1965). Taking phocomelia as an example, one can assume that this malformation occurs due to the fact that the cellular material for the formation of the more distal parts of a limb has greater chance to remain undamaged than that of the proximal parts.

The epiblast is undoubtedly insensitive to thalidomide, and all malformations induced by this drug are due to the selective sensitivity of the mesoblast. It is worth mentioning that McBride, whose note published in 1961 was one of the earliest on thalidomide malformations in human babies, correctly interpreted the primary cause of these deformities by emphasizing that it is the mesenchyme, particularly the prospective bone tissue, which is injured.

At the ultrastructural level the thalidomide injury has several aspects. The mitochondria in the endothelial cells appear to be the most sensitive cell organelles and become morphologically abnormal even in the limb buds which show the first degree of injury. This is not surprising, since it has long been known that mitochondria swell and undergo fragmentation in adverse physiological

---

PLATE 5

Fig. A. Positive acid phosphatase reaction in the Golgi cysternae. Note droplets in the course of detachment (primary lysosomes). × 32000.

Fig. B. Acid phosphatase-positive large cytolysome. × 31000.

Fig. C. Vesicular projection with acid phosphatase-positive lysosome at its base (arrow). × 38000.

Fig. D. Extensive acid phosphatase activity between two extremely thinned endothelial cells. × 38000.

conditions (Novikoff, 1961; Hartroft, 1964). Regardless of the damaging factor, whether it is dietary deficiency (Hartroft, 1964), starvation (Gansler & Rouiller, 1956), addition of toxic substances to tissue cultures (Frederic, 1958), irradiation with X-rays (Okada & Peachy, 1957; Manteufel & Meissel, 1965), or treatment with drugs, the same syndrome of changes is always observed in mitochondria. They become larger and more spherical, and they show only abnormally short peripheral parts of disrupted cristae. Considerable loss of electron opacity is followed by extensive vacuolation.

The question arises whether the changes in mitochondria imply that thalidomide interferes selectively with the metabolic activities in the endothelium, causing lesions of the vascular system of a developing limb. Indeed, this seems to be the case, because the changes in mitochondria initially are restricted to the endothelial cell. Accordingly, the necrotic changes in the mesoblast outside the axial artery should be regarded as secondary.

Pliess (1962) attempted to explain the mode of action of thalidomide by suggesting that the drug interferes with the normal biochemical processes governing the course of development of mesodermal structures. Kemper (1962) saw in chick embryos some similarities between thalidomide-induced abnormalities and those caused by B-type antivitamins (e.g. 4-deoxypyridoxol, antivitamin B_6). Woollam & Millen (1963) suggested that teratogenic agents in general have an effect on the enzymic processes in cells during organo-genesis and cause anoxia and general disturbance in the intracellular metabolism. In fact, it has been shown that certain thalidomide metabolites (monohydroxy derivatives) affect *in vitro* the activity of glutamine synthetase and of glutamate dehydrogenase from rat brain (Williams, 1963).

The suggestion that thalidomide interferes with the intracellular metabolism was also made by Villa & Eridani (1963), who observed certain anti-mitotic properties of thalidomide. These properties are not specific for any particular stage of cell division, however, and should be ascribed to a general antimetabolic activity of the drug. They are probably therefore responsible for the general retardation of development.

In the light of the findings reported here, the mitochondrial lesions apparently being the primary effect, anoxia inside the endothelial cells may be the first result, followed by a chain of changes leading to an extensive necrosis of the mesoblast tissue.

On the other hand, it may be that the primary effect is the increase of the lysosome population and that all other changes, particularly those in mitochondria, follow later. This possibility should be taken into account since mitochondria are known to be extremely sensitive to the hydrolytic activity of lysosomal enzymes, particularly to that of phosphatases. When treated *in vitro* with lysosome preparations they lose their oxidative phosphorylation capacity and show extensive membrane damage. Also, their proteins undergo hydrolysis (see Tappel, Sawant & Shibko, 1963).

The increased number of lysosomes in endothelial cells, and in advanced cases in the mesoblast cells, suggest a potential increase of destructive processes. Necrosis, which is the end result of these processes, is characterized by autodigestion of different parts of the cell, probably by hydrolytic enzymes released from lysosomes (Bessis, 1964).

Lysosomes appear first near the Golgi complexes in the form of small vesicles (primary lysosomes) which are probably produced by pinching off from the Golgi flat cysternae. Due to the toxic activity of thalidomide, they are produced in increased numbers and consequently grow to reach the size of cytolysomes measuring 0·5–2 μ (extranuclear necrotic centres, Jurand, 1965). Necrotic changes in the nucleus (pycnosis, karyorrhexis) follow later as the last stage of cell death. This fact is in agreement with the observation that nuclei separated from cells are much more resistant to the activity of lysosomal enzymes than other cellular organelles (Tappel *et al.* 1963).

A course of events very similar to that described in this paper was recently reported for duodenal crypt cells in mice after X-irradiation (Hugon & Borgers, 1965). Also, cellular degeneration processes occurring in natural conditions during embryogenesis proceed in a similar way, e.g. in the limb-bud apical ectodermal ridge in the chick and in the mouse (Jurand, 1965).

The higher electron density of the cytoplasm of the endothelial cells in experimental limb buds in comparison with the control endothelium (see Plate 3, figs. A and C) suggests that these cells react specifically to the treatment. The mesoblast cells do not differ from the control cells to any significant degree at the ultrastructural level.

Fig. C on Plate 3 also demonstrates that in normal conditions there is a marked difference between the monosomal arrangement of ribosomes in the endothelial cells and the typically polysomal arrangement in the mesoblast cells. The same situation is also evident in the experimental limb buds (see Plate 3, fig. A). This phenomenon might be of general interest. Specifically, due to their low synthetic activity, the endothelial cells, which are already differentiated, contain ribosomes in the form of monosomes. On the other hand, the mesoblast cells, which are about to begin the process of differentiation into various mesodermal derivatives, contain polysomes consisting of 6–9 units. Apparently these cells have initiated the synthesis of new specific proteins.

SUMMARY

Thalidomide in suspension in thin egg-white introduced into chicken eggs preincubated for 64–68 h causes dilation of the axial limb-bud artery in 24 h after treatment. In some cases there are necrotic cells in the mesoblast outside the dilated artery. In the most extreme degree of injury the mesoblast is almost completely destroyed except for a small group of mesoblast cells located in the dorsal area of the limb bud.

At the ultrastructural level the mitochondria in the endothelial cells of the dilated artery become swollen and vacuolated. Lysosomes are found in markedly increased numbers, and the cytoplasm undergoes vacuolation.

The injured endothelial cells become extremely thinned (down to 0·05 μ) and form vesicular projections protruding into the lumen of the artery. At these points gaps are found in the continuity of the endothelial cells.

In more heavily affected limb buds both endothelial and mesothelial cells undergo necrosis by accumulation of lysosomes and formation of cytolysomes, while their nuclei still appear to be normal.

Golgi apparatus, lysosomes, and cytolysomes show considerable acid phosphatase activity.

Possible intrepretations of the above observations are discussed.

RÉSUMÉ

Modifications precoces observées dans les bourgeons de membres après traitement par la thalidomide

La thalidomide, en suspension dans l'albumine, injectée dans des œufs de Poule de 64–68 heures d'incubation, provoque, 24 heures après traitement, la dilatation de l'artère axiale du bourgeon de membre. Dans certains cas, on observe des cellules nécrotiques dans le mésoblaste en dehors de l'artère dilatée. Dans les cas d'altérations les plus intenses, le mésoblaste est presque totalement détruit à l'exception d'un petit groupe de cellules mésodermiques localisées dans la partie dorsale du bourgeon de membre.

A l'échelle ultrastructurale, les mitochondries présentes dans les cellules endothéliales de l'artère dilatée, prennent un aspect gonflé et vacuolisé. On trouve des lysosomes en nombre accru et le cytoplasme devient vacuolaire.

Les cellules endothéliales altérées s'amincissent (inférieur à 0·05 μ) et forment des vésicules faisant saillie dans la lumière de l'artère. A ces endroits, les cellules endothéliales sont séparées par des lacunes.

Dans les cas où les bourgeons de membres sont très atteints, les cellules endothéliales et mésothéliales subissent la nécrose par suite de l'accumulation de lysosomes et de formation de cytolysomes, alors que leur noyau paraît encore normal.

L'appareil de Golgi, les lysosomes et les cytolysomes montrent une activité phosphatase acide intense.

La discussion porte sur l'interprétation possible de ces observations.

The author wishes to express his gratitude to Professor C. H. Waddington, F.R.S., for reading and criticizing the manuscript, to Mr J. D. Amundson of the Oak Ridge National Laboratory for the skilful editorial work, and to Miss Patricia Collins for her technical assistance.

This work was supported by a grant from the Distillers' Company to the University of Edinburgh.

Separate thanks are due to Dr W. P. Kennedy of the Distillers' Company for providing a sample of thalidomide.

REFERENCES

BESSIS, M. (1964). Studies on cell agony and death: An attempt at classification. In *Cellular Injury* (ed. A. V. S. de Reuck and J. Knight), pp. 287–328. Ciba Foundation Symposia. London: Churchill.

BOYLEN, J. B., HORNE, H. H. & JOHNSON, W. J. (1963). Teratogenic effects of thalidomide and related substances. *Lancet* i, 552.

FREDERIC, J. (1958). Recherches cytologiques sur le chondriome normal ou soumis à l'expérimentation dans des cellules vivantes cultivées *in vitro*. *Archs Biol., Liège* **69**, 167–350.

GANSLER, H. & ROUILLER, C. (1956). Modifications physiologique et pathologique du chondriome. Etude au microscope électronique. *Schweiz. Z. allg. Path. Bakt.* **19**, 217–43.

GIROUD, A., TUCHMANN-DUPLESSIS, H. & MERCIER-PAROT, L. (1962). Influence de la thalidomide sur le développement foetal. *Bull. Acad. natn. Méd.* **146**, 343–5.

GOMORI, G. (1952). *Microscopic Histochemistry. Principles and Practice*. Chicago: University of Chicago Press.

HAMBURGER, V. & HAMILTON, H. L. (1951). A series of normal stages in the development of the chick embryo. *J. Morph.* **88**, 49–92.

HARTROFT, W. S. (1964). Electron microscopy of liver and kidney cells in dietary deficiencies. In *Cellular Injury* (ed. A. V. S. de Reuck and J. Knight), pp. 248–81. Ciba Foundation Symposia. London: Churchill.

HOLT, S. J. & HICKS, R. M. (1962). Combination of cytochemical starving methods for enzyme localization with electron microscopy. In *The Interpretation of Ultrastructure*, pp. 193–211. Symposia of the International Society for Cell Biology, vol. 1. New York and London: Academic Press.

HUGON, J. & BORGERS, M. (1965). Etude morphologique et cytochimique des cytolysomes de la crypte duodénale de souris irradiée par rayous X. *J. Microscopie* **4**, 643–56.

JURAND, A. (1962). The development of the notochord in chick embryos. *J. Embryol. exp. Morph.* **10**, 602–21.

JURAND, A. (1965). Ultrastructural aspects of early development of the fore-limb buds in the chick and the mouse. *Proc. R. Soc.* B **162**, 387–405.

KEMPER, F. (1962*a*). Thalidomid und Entwicklung von Hühner-embryonen. *Arzneimittel-Forsch.* **6**, 640–1.

KEMPER, F. (1962*b*). Thalidomide and congenital abnormalities. *Lancet* ii, 836.

LENZ, W. (1962). Thalidomide and congenital abnormalities. *Lancet* i, 45.

LEONE, V. G. (1963). Contributo allo studio degli effetti della talidomide sullo sviluppo embrionale del pollo. *Rc. Ist. lomb. Sci. Lett.* B **97**, 366–72.

MCBRIDE, W. G. (1961). Thalidomide and congenital abnormalities. *Lancet* ii, 1358.

MANTEUFEL, V. M. & MEISSEL, M. N. (1965). The role of the mitochondrial apparatus of lymphocytes in their response to ionizing radiation. *Izv. Akad. Nauk SSSR*, ser. Biol. no. 6, 884–97.

NOVIKOFF, A. B. (1961). Mitochondria (Chondriosomes). In *The Cell* (ed. J. Brachet and A. E. Mirsky), vol. I, pp. 299–421. New York and London: Academic Press.

OKADA, S. & PEACHY, L. D. (1957). Effect of gamma irradiation on the desoxyribonuclease. II. Activity of isolated mitochondria. *J. Biophys. Biochem. Cytol.* **3**, 239–48.

PLIESS, G. (1962). Thalidomide and congenital abnormalities. *Lancet* i, 1128–9.

PLUMEL, M. (1948). Tampon au cacodylate de sodium. *Bull. Soc. Chim. biol.* **30**, 129–30.

SALZGEBER, B. & SALAÜN, J. (1963*a*). Malformations de membres obtenus chez l'embryon de Poulet après traitement par la thalidomide. *C. r. hebd. Séanc. Acad. Sci., Paris* **256**, 2719–22.

SALZGEBER, B. & SALAÜN, J. (1963*b*). Action teratogène de la thalidomide sur l'embryon de Poulet à différents stades du développement. *C. r. hebd. Séanc. Acad. Sci., Paris* **257**, 273–5.

SALZGEBER, B. & SALAÜN, J. (1965). Action de la thalidomide sur l'embryon de Poulet. *J. Embryol. exp. Morph.* **13**, 159–70.

SALZGEBER, B. & WOLFF, E. (1964). Experimental production of malformations of the limbs by means of chemical substances. In *International Review of Experimental Pathology*, vol. III, pp. 329–63. Ed. G. W. Richter and M. A. Epstein. New York and London: Academic Press.

SOMERS, G. F. (1963). Thalidomide and congenital malformations. *Congr. de l'Union Thérap. Intern. VIII*, pp. 41–9.

TAPPEL, A. L., SAWANT, P. L. & SHIBKO, S. (1963). Lysosomes: distribution in animals, hydrolytic capacity and other properties. In *Lysosomes*, pp. 78–113. Ed. A. V. S. de Reuck and M. P. Cameron. Ciba Foundation Symposia. Boston: Little, Brown and Co.

TÖNDURY, G. (1962). Die Embryologie im Dienste der Krankheitsforschung. Möglichkeiten, Grenzen und Verantwortung in der embryologichen Forschung. *Verh. schweiz. Naturf. Ges.* 142 Jahresvers. der S.N.G. pp. 39–49.

VILLA, L. & ERIDANI, S. (1963). Cytological effects of thalidomide. *Lancet* ii, 725.

WILLIAMS, R. T. (1963). Teratogenic effects of thalidomide and related substances. *Lancet* i, 723–4.

WILLIAMSON, A. P., BLATTNER, R. Y. & LUTZ, H. R. (1963). Abnormalities in chick embryos following thalidomide and other insoluble compounds in the amniotic cavity. *Proc. Soc. exp. Biol. Med.* **112**, 1022–5.

WOOLLAM, D. H. M. & MILLEN, J. W. (1963). The action of drugs on the embryo. *Proc. R. Soc. Med.* **56**, 597–600.

YANG, TSU-JU, YANG, TZU-SZU & LIANG, HSÜ-MU (1962). Induction of limb deformities in chicken embryos by thalidomide. *Bull. Inst. Zool. Academia Sinica* **1**, 107–12.

(*Manuscript received 23 March 1966*)

The effect of hydrocortisone acetate on the development of mouse embryos

by A. Jurand

J. Embryol. exp. Morph. Vol. 20, 3, pp. 355–66, November 1968
With 4 plates
Printed in Great Britain

The effect of hydrocortisone acetate on the development of mouse embryos

By A. JURAND[1]
From the Institute of Animal Genetics, Edinburgh

Hydrocortisone (Kendall's compound F, 17-hydroxycorticosterone, Cortisol) and cortisone (Kendall's compound E, 17-hydroxy-11-dehydrocorticosterone) have been widely used in medicine for about 20 years, first as adrenal hormones in substitution therapy. Since the discovery of Hench, Kendal, Slocumb & Polley (1949) that cortisone is beneficial against a wide range of rheumatic diseases and against all forms of arthritis, many more types of diseases have been added in later years to the list of ailments curable with cortisone, namely bronchitis, bronchial asthma, pulmonary tuberculosis, colitis, various inflammatory conditions and certain skin, blood and eye diseases. Hydrocortisone is used against the same diseases as cortisone; in fact, it is believed that cortisone becomes pharmacologically active only after conversion to hydrocortisone in the liver (Cope, 1964). Particularly in the inflammatory conditions cortisone must be converted to hydrocortisone to become antiphlogistic (Applezweig, 1962).

The biochemical mode of action of these drugs was not understood for many years. More recently, hydrocortisone in particular has been used extensively in investigations in the field of cell biology, particularly in investigations of protein synthesis. In general, it is believed that at the cellular level hydrocortisone influences many metabolic processes. First, it has a cell-stabilizing effect which can be expressed for instance in its antihaemolytic activity. It stabilizes lipoprotein membranes in general, and in particular prevents lysosomes from releasing the hydrolytic enzymes contained inside these organelles (de Duve, Wattiaux & Wibo, 1961). The latter effect may explain the mechanism of the protective properties of hydrocortisone against cell damage induced by such factors as irradiation with ultraviolet light or X-rays or intoxication with bacterial toxins or chemical agents (Weissmann & Dingle, 1961; Weissmann & Fell, 1962; Weissmann & Thomas, 1963).

However, hydrocortisone does not always protect cells from injury or alleviate damage. On the contrary, in some cases it delays the repair of cellular injury. This paradoxical phenomenon is most probably due to occasional stimulation of the synthesis of enzymes deaminating amino acids, which is followed by delayed protein synthesis (Kenney, 1962*a*, *b*; Segal & Kim, 1963; Schimke,

[1] *Author's address:* Institute of Animal Genetics, West Mains Road, Edinburgh, 9, Scotland.

Sweeney & Berlin, 1964). In other cases stimulation of the synthesis of othe enzymes may be more constructive, e.g. it may enhance the formation of glycoge by activating the enzymes responsible for glycogenesis (Jacobson, 1964).

It was found, moreover, that the induction of enzyme synthesis is brough about following an increase in nuclear RNA synthesis (Kenney, Greenman Wicks & Albritton, 1965). This was confirmed by Sekeris & Lang (1964), wh were able to show that in the rat liver messenger RNA synthesis is increased The increase in DNA-dependent RNA synthesis, and subsequently in protei synthesis, after administration of cortisone and hydrocortisone modifies th intracellular enzymic environment. The newly synthesized enzymes may the impair the later synthesis of specific proteins that are essential for growth an differentiation in developing systems. I would suggest that this is one mechanism by which these hormones cause foetal mortality, stunting and decrease in th viability of neonates.

In medicine, the effects of cortisone are not too disappointing. For example Bongiovanni & McPadden (1960), summarizing the clinical literature, cite tha about 10% of 260 human pregnancies resulted in still-born and prematur infants after cortisone medication at various stages of pregnancy.

As far as animal experimentation is concerned, except for investigations o the influence of cortisone and hydrocortisone on the growth rate of chic embryos (Sames & Leatham, 1951) and on the uranoschitic activity of thes hormones, there has been only one report of malformations caused by cortison (Moscona & Karnofsky, 1960). Hydrocortisone has not been investigated i this respect.

This paper attempts to deal with the embryopathogenic properties of hydr cortisone acetate, mainly with regard to limb development in mice.

MATERIAL AND METHODS

The pregnant mice used in the present investigations were of the JBT strai inbred by brother–sister litter-mate matings for twenty-four generations wit the retention of sublines. This strain was derived from the outbred JC strai selected for genes *a*, *b* and *bt*. The day on which the copulation plug was foun was considered the first day of pregnancy.

The hydrocortisone acetate used was obtained in pure crystalline form fro Calbiochem, Los Angeles, or in the form of Hydrocortistab Boots (hydrocort sone acetate injection B.P.) for intra- and peri-articular injections. In each cas the drug was prepared as a suspension in 0·9% saline solution and was injecte subcutaneously under slight ether anaesthesia, usually in three doses on th 10th, 11th and 12th days of pregnancy. The dose applied was estimated to b just below the 'embryonic LD 50' for the hormone. The 'embryonic LD 50' fo hydrocortisone acetate is defined as the total dose which, if administered sub cutaneously on the 10th, 11th and 12th days of pregnancy kills about 50% o

ıe implanted embryos by the 14th day of pregnancy. The 'embryonic LD 50' f hydrocortisone acetate is 84 mg/kg (i.e. 28 mg/kg on each of the three injection ays). The surviving embryos show the abnormalities to be described. To crease the proportion of the surviving embryos a slightly lower dose of 5 mg/kg was injected.

The animals were sacrificed by cervical dislocation on the 14th day of pregancy (291 pregnant females, 1382 surviving embryos) or on the 18th day of egnancy (104 pregnant females, 407 surviving embryos). Dissected uteri were ked *in toto* in 5% trichloroacetic acid containing 1·37% lanthanum acetate, ıd the embryos were dissected at least 3 h later. Some embryos after immediate ssection from the uterus were fixed with 3% glutaraldehyde buffered at pH 7·2 ith cacodylate buffer (Plumel, 1948).

The embryos were first examined macroscopically and any gross abnormalities corded. Selected whole embryos or isolated limb buds were prepared for stological examination in the usual way and stained with methyl green–ronine. This staining method works particularly well after 3% glutaraldehyde ation.

In order to determine the possible influence of hydrocortisone on growth te, the experimental and control embryos were fixed on the 14th day of egnancy, dissected, weighed, and the averages compared.

Limb buds showing necrotic changes and haemorrhages as well as those with crotic areas in the innermost parts of cartilage condensations were also epared for electron microscope examination. For this purpose the 14-day-old mbryos were dissected and fixed in 1% osmic acid solution buffered with ronal-acetate buffer at pH 7·2 (Palade, 1952) in Caulfield's modification (1957) r 45 min at 2–4 °C. During the dehydration procedure the limb buds were ssected and embedded in Araldite, using a slow rotary shaker (Jurand & eland, 1965).

Control material was collected in the same manner from 152 untreated egnant females which were only slightly etherized on the days corresponding the injection days. In addition, all relevant information contained in a evious paper (Jurand, 1965) was used for comparison.

RESULTS

Macroscopical observations

Fourteen-day-old embryos. 150 experimental and 163 control 14-day-old mbryos were used for testing the influence of hydrocortisone on the growth e. There was no significant difference in body weight between the experimental d control embryos:

	Number of embryos	Average weight
Control embryos	163	0·103 g
Experimental embryos	150	0·105 g

Macroscopically, 26% of the surviving 14-day-old experimental embryo showed one or more abnormalities. For convenience, the effects are classifie into three groups according to the degree of damage and to the presumed ord of events.

Primary effects are those which include macroscopically visible dilatation the venous marginal blood sinus (marginal vein) of any of the foot plat without any other macroscopically visible abnormalities (Plate 1, figs. A and E

Secondary effects comprise macroscopically visible necrotic areas in the lim bud mesoblast, usually localized in the marginal area of the foot plate (Plate fig. C) or extensive haemorrhages present in the same marginal areas of t limb buds (Plate 1, fig. D). These two types of damage can be present in one more limb buds without any obvious preference for localization in the fo or hind-limb buds. To this group of effects also belong changes similar to tho in the limb buds but located in the tail tip (Plate 1, fig. E), necrosis of t maxillary processes (Plate 1, fig. F), facial fissures (Plate 1, fig. G) and su epidermal blisters located usually on the temporal region of the head (Plate fig. A) or, less frequently, on the back, limbs or other regions of the body.

Malformations of limbs without any macroscopically visible necrotic chang or haemorrhages resulting in an abnormal outline of foot plates are regard as tertiary effects (Plate 1, figs. C, E; Plate 2, fig. A). Such deformations a regarded as regulatory effects of healing after previous localized necro injuries.

Numerical data on macroscopically detectable effects are shown in Table

To the tertiary effect group belong also histologically detectable, sharp demarcated necrotic changes of the innermost areas of the limb skeletal co densations (Plate 2, figs. E, F). Such changes very frequently accompany t secondary effects, i.e. necrotic injuries and haemorrhages located in the dis parts of the limb mesoblast, but they are often found also in macroscopica quite normal-looking embryos. It is worth noting that in embryos where t

---

PLATE 1

Fig. A. Control 14-day-old mouse embryo hind-limb bud. × 16.

Fig. B. Dilation of the marginal venous sinus in a 14-day-old mouse embryo hind-limb b after treatment with hydrocortisone acetate. × 16.

Fig. C. Experimental 14-day-old mouse embryo with an extensive necrosis of the margi region in the left forelimb bud. Note also the malformation of the hind-foot plate. × 1

Fig. D. Experimental 14-day-old mouse embryo with an extensive haemorrhage in distal part of the forelimb bud. × 14.

Fig. E. Tail-tip haemorrhage and distinct malformation of the right hind-foot plate in experimental 14-day-old mouse embryo. × 12.

Fig. F. Bilateral extensive necrotic blisters of the maxillary processes resulting in a w hare lip: 14-day-old mouse embryo. × 10.

Fig. G. Bilateral facial clefts. × 10.

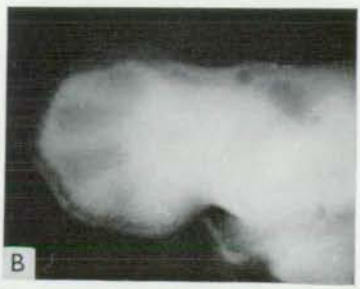

facing p. 358

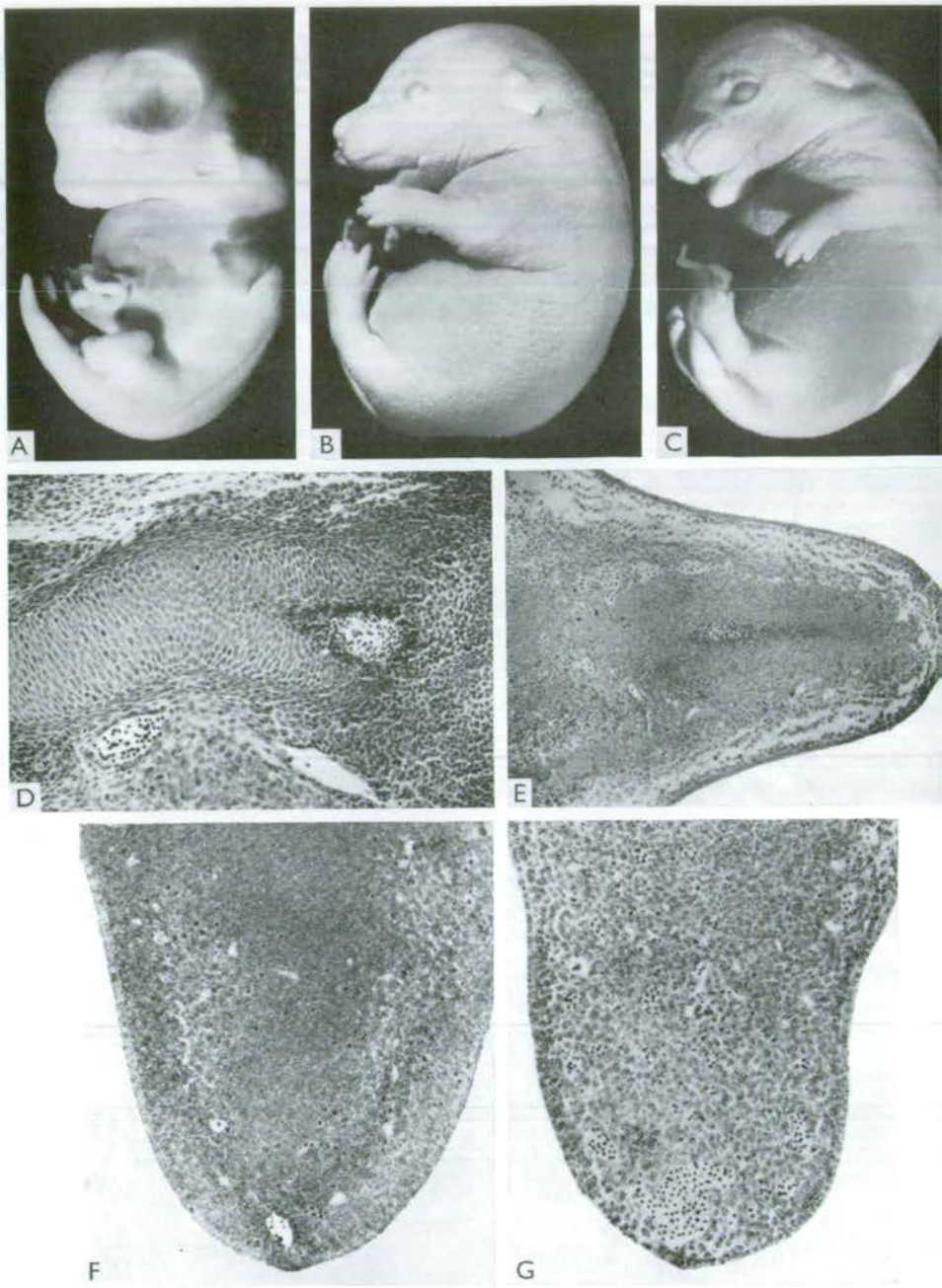
A
B
C
D
E
F
G

keletal condensations show necrotic changes, the non-limb cartilage condensations are not affected by necrosis.

Table 1. *Macroscopically detectable changes in* 14*-day-old embryos (total,* 1382 *embryos)*

	No. of embryos*	%
Dilatation of the venous blood sinus	201	14·5
Distal limb bud mesoblast necrosis	110	7·9
Distal limb bud haemorrhages	149	10·7
Tail-tip haemorrhages	125	9·04
Necrosis of the maxillary processes	25	1·8
Subepidermal blisters	180	13·0
Malformations of foot plates	68	4·9
Micromelia	130	9·4

* In many cases embryos showed several of the above abnormalities and so were recorded ore than once.

Eighteen-day-old embryos. In the 407 embryos (from 104 pregnant females) this group the frequency of those with deformations of limbs is lower than the 14-day-old embryo group. There were forty-two embryos (10·3%) with icromelia (Plate 2, figs. C, D), but only twenty-four with abnormal digits ·8%). The latter figure indicates that embryos with necrotic changes and with aemorrhages in the mesoblast of the foot plates probably do not survive from e 14th to the 18th day. On the other hand, cleft palate was found in 214 of ese embryos (i.e. 52·7%). The appearance of the cleft palate was exactly like at shown in the paper by Fainstat (1954).

Light and electron microscopy of the abnormalities

The primary effect, i.e. the dilatation of the venous marginal sinus (Plate 2, gs. F, G), is more frequent in the hind-limb buds and is characterized by scontinuities in the endothelial lining of this blood vessel. The limb buds with

PLATE 2

g. A. Experimental 14-day-old mouse embryo with subepidermal blister in the temporal gion. Note also the malformation of the hind-foot plate. × 7.

g. B. Control 18-day-old mouse embryo. × 4.

g. C. Experimental 18-day-old mouse embryo with micromelia. × 4.

g. D. Necrotic area in the central part of the cartilage condensation of femur in a 14-y-old experimental embryo. × 110.

g. E. Necrosis of the central part of the third-toe cartilage condensation in 14-day-old perimental embryo. × 80.

g. F. Axial section through a control hind-limb bud (14-day-old mouse embryo). × 110.

g. G. Axial section through an experimental hind-limb bud with an extensive dilation of marginal venous sinus. × 110.

a dilated sinus also sometimes show increased vascularization in other regio of the mesoblast.

At the electron-microscope level, the endothelial cells of dilated venou sinuses contain far more numerous Golgi groups with many primary an secondary lysosomes around them than are normally seen in the endotheli cells of untreated animals (Plate 3, figs. A, B). Some of these cells were foun to contain extranuclear necrotic centres (Plate 3, fig. C).

Histological examination of the necrotically changed limb buds (secondar effects) showed that the injury is usually situated at the distal margin of th foot plate and only in a small proportion of cases was the necrotic area locate in other than marginal parts of the limb mesoblast. Regardless of the locatio such areas are as a rule sharply delineated from the healthy mesoblast tiss and represent virtually empty-looking spaces sparsely scattered with blood cel cells containing pycnotic nuclei, necrotic cells and cell debris (Plate 3, figs. D, E

In the extensive haemorrhages the shape of the affected limb buds appea to be abnormal, as the margin of such foot plates becomes thickened due to th presence of the haemorrhage. This is particularly clear in median sections, whi appear to be much less pointed than those of the control embryos (Plate fig. F). The haemorrhages consist of dense masses of blood cells (Plate 3, fig. G The venous marginal sinus is usually absent in the areas occupied by extensi necrosis or haemorrhages. However, it must be pointed out that even in lim buds with extreme injuries of these types the epidermal covering is always inta and its cells appear to be completely unaffected (see Plate 3, figs. D, E, G).

Histological examination of the limb buds in 14-day-old embryos has al shown that, regardless of whether there were any macroscopically visible chang or not, most of the experimental limb buds that were examined contain necrotic areas inside the skeletal cartilage condensations (Plate 2, figs. E, F These areas are found almost exclusively in the condensations of the lim skeleton and are very rarely encountered in the blastemata of other parts the embryonic skeleton.

PLATE 3

Fig. A. Electron micrograph of a control endothelium cell fragment. ×18000.

Fig. B. Electron micrograph of an experimental endothelium cell showing abundance Golgi groups with primary lysosomes in the vicinity. ×18000.

Fig. C. Experimental endothelium cell with the extranuclear necrotic centre (*nc*). ×52

Fig. D. Histology of the distal marginal necrotic area in the forelimb bud mesoblast. N completely unaffected epiblast with the apical ectodermal ridge and the cell debris ins the necrotic area. ×85.

Fig. E. Histology of the distal marginal necrotic area in an experimental hind-limb b mesoblast. Note the unaffected epiblast and the cell debris inside the necrotic area. ×1

Fig. F. Extensive distal haemorrhage in an experimental forelimb bud. ×42.

Fig. G. Higher power showing the nucleated blood cells in the mesoblast haemorrha ×170.

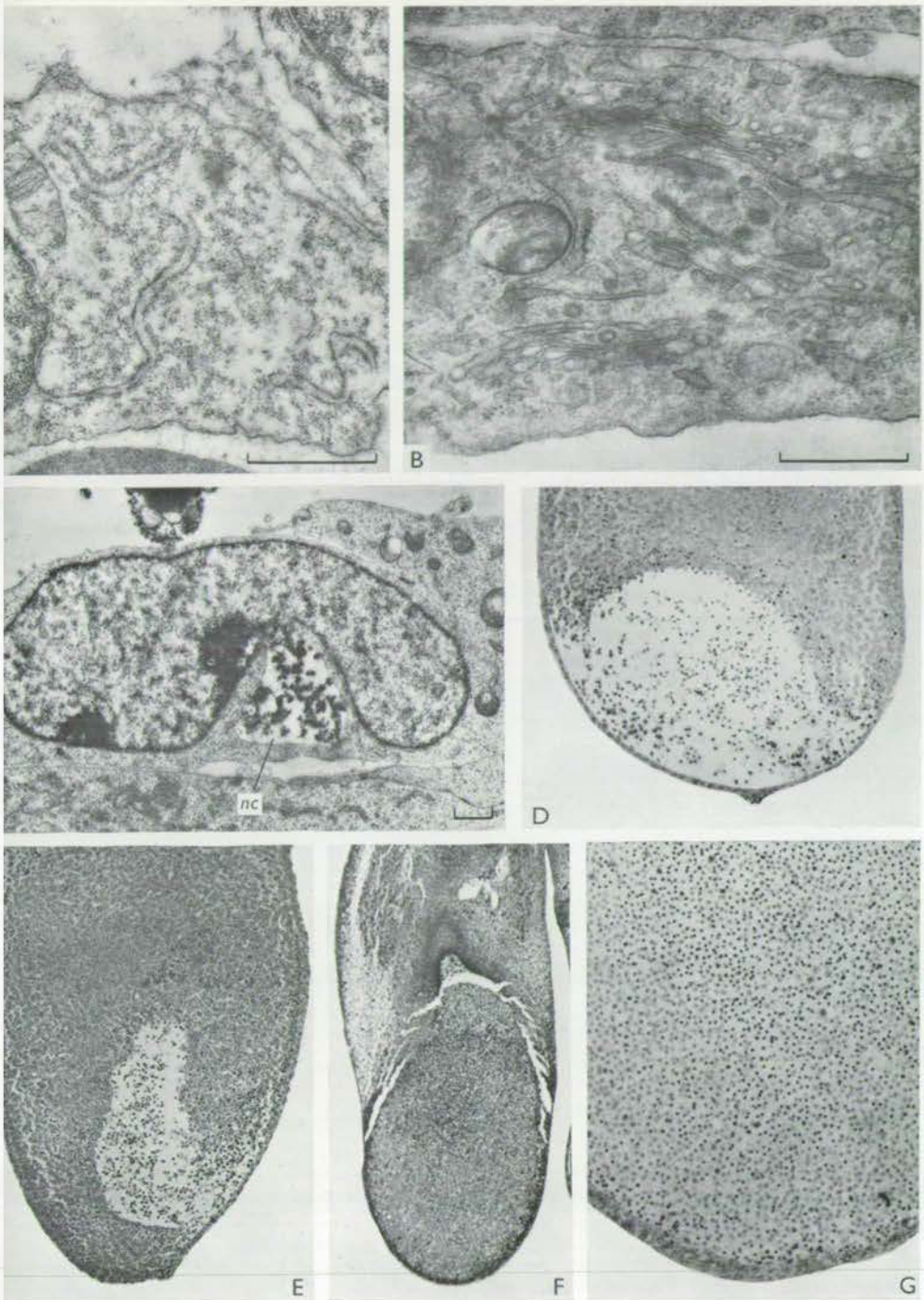

facing p. 360

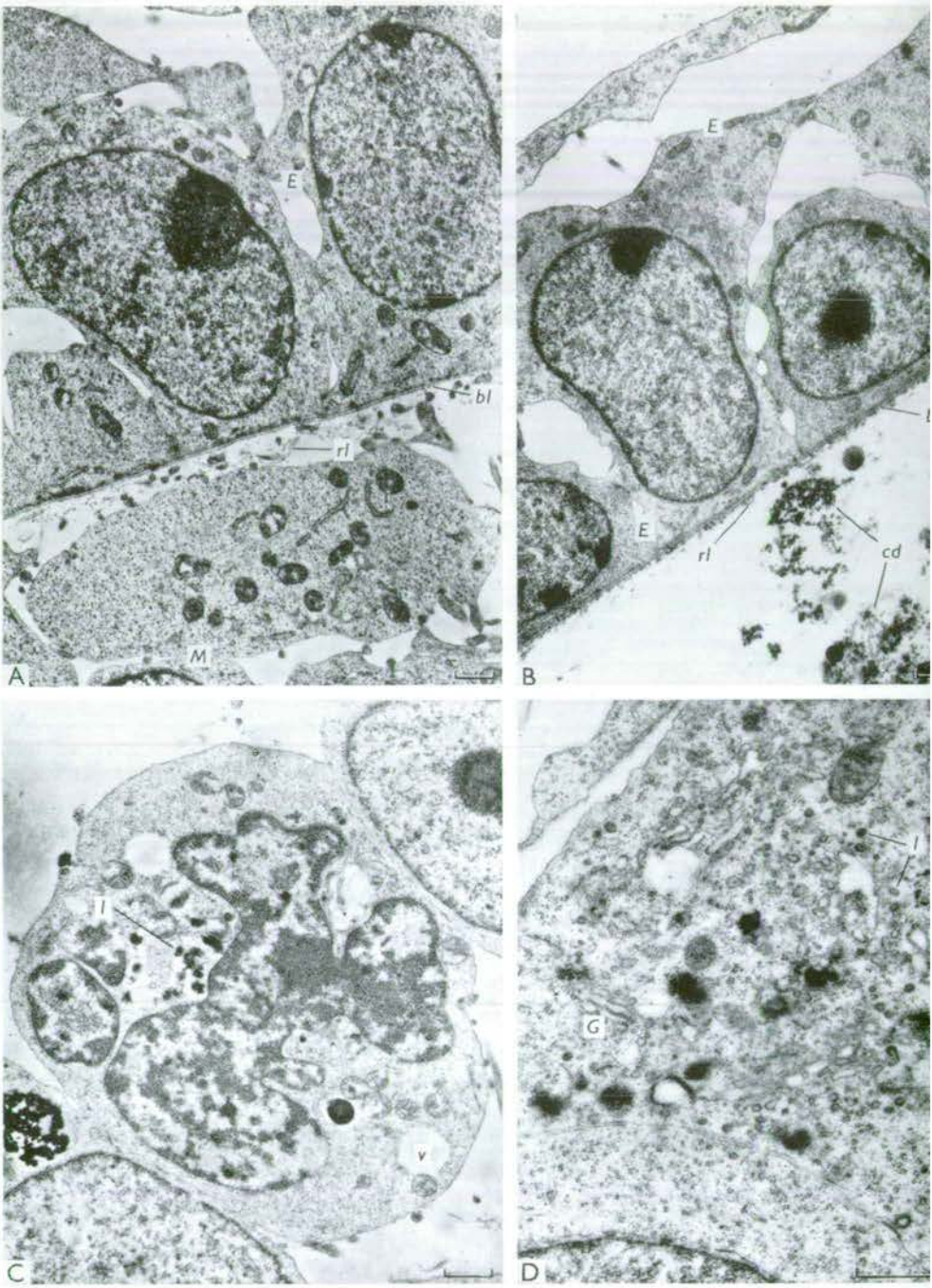
E
bl
rl
M
A
E
E
rl
cd
B
l
v
C
l
G
D

Like the histological survey of the lesions, the electron-microscope examination confirmed that the epidermal covering in the necrotically changed limb buds or in those containing extensive haemorrhages consists of cells with the same ultrastructural features as those in control embryos (Plate 4, figs. A, B). The necrotic cells in the mesoblast adjacent to the necrotic areas or to the haemorrhages contain in the cytoplasm large lysosomes and cytolysomes, but the nuclei of these cells do not show any apparent abnormality (Plate 4, fig. C). Necrotic cells of the same type were found in the necrotic areas within the cartilage condensations (Plate 4, fig. D).

DISCUSSION

In animal experiments cortisone is known to cause a general retardation of embryonic development (Moscona & Karnofsky, 1960) and also to be specific in producing cleft palate (Walker & Fraser, 1957; Fraser, 1961). As far as hydrocortisone is concerned, it is undoubtedly also a very potent embryotoxic drug, although relatively non-toxic for adult animals, including pregnant females. The high embryotoxicity of hydrocortisone is further emphasized by the fact that, due to the partial barrier effect of the placenta, the mean value for hydrocortisone concentration in human blood is 10·8 μg/100 ml (Sweat, 1955), whereas in the human amniotic fluid it is only 2 μg/100 ml (Cope, Hurlock & Caldwell, 1955). In other words, although the concentration of hydrocortisone behind the placenta is lower, the embryos become affected much more than the mothers.

On the whole, the embryotoxic effect of hydrocortisone in mice is very similar to that of cortisone on pregnancy in rabbits, as described by Courrier & Cologne (1951) and by DeCosta & Abelman (1952).

The present investigations on the embryotoxicity of hydrocortisone acetate have confirmed its relatively high cleft-palate specificity, as is the case with cortisone, and this is in agreement with the fact that cortisone is active

---

PLATE 4

Fig. A. Electron micrograph showing a control limb-bud epiblast (*E*) and the underlying mesoblast cells (*M*) separated by the basal lamina (*bl*) and the reticulin layer (*rl*). × 5200.

Fig. B. Electron micrograph of an area similar to that in fig. A but with a necrotic region in the mesoblast after treatment with hydrocortisone. Note that the epiblast (*E*), together with the basal lamina (*bl*), remains unaffected, while the necrotic region is full of cell debris (*D*). Also note change in the ultrastructure of the reticulin layer (*rl*). × 5200.

Fig. C. Extranuclear necrosis of a mesoblast cell from a region adjacent to the marginal necrotic area in the limb bud mesoblast. Note lysosomes (*l*) and vacuolation of the cytoplasm × 6500.

Fig. D. Electron micrograph of an early cytoplasm necrosis of a chondroblast at the necrotic area within a toe-cartilage condensation. Note numerous Golgi groups (*G*) and abundance of lysosomes (*l*). × 13000.

pharmacologically after conversion into hydrocortisone (Cope, 1964). Virtual everything that is true for one of these hormones is true also for the other. In t mice in the present experiments, however, hydrocortisone acetate did not cau any noticeable retardation of growth, as judged by the average weights of l day-old experimental and control embryos.

The abnormalities described in this paper, such as dilatation of the margir venous sinus in both fore- and hind-limb buds, necrosis of the distal portio of the limb mesoblast, distally located haemorrhages in the limb mesoblast a necrotic changes in the central portions of skeletal cartilage condensatio together with occasional micromelia, indicate that hydrocortisone is capable changing the normal metabolic balance in the developing limb mesoblast. must be stressed that similar abnormalities in limb development in the form shortened humeri and femora and missing phalanges have been reported the chick by Moscona & Karnofsky (1960). In general, the present investigatio have shown that the mesoblast of the limb bud, particularly in its distal portic is much more sensitive to hydrocortisone activity than is the epiblast, whi remains virtually unaffected. Ragan *et al.* (1949) have also shown that t mesodermal components of healing wounds in rabbits are those which a inhibited after treatment with cortisone.

As to the mechanism and origin of these abnormalities it is feasible to assu that in all the observed cases the primary changes take place in the endothel cells of the marginal venous sinuses. From electron-microscope examination seems that injury to these cells involves in the first instance an overproducti of lysosomes and possibly at the same time an increased synthesis of thc hydrolytic enzymes not contained in the lysosomes. At an early stage in ce where there was a very moderate dilatation of the marginal sinus there is increase in the number of Golgi groups with primary and secondary lysosom in their vicinity. When there are large numbers of lysosomes and they ha increased in size to reach the diameter of cytolysomes, the cells become necrot It must be remembered, however, that there are many authors who descri hydrocortisone as a stabilizing agent for lysosomes (de Duve *et al.* 196 Jacobson, 1964). Necrosis of cells preceded by an increase in the number a size of lysosomes is confined at first to the cytoplasm of the affected cells, wh their nuclei remain completely unaffected. Similar observations were made experiments with chick embryos treated with thalidomide, but in that case t endothelium of the axial artery was the primary site of the injury (Jurand, 196 Cellular necrosis and disruption of the endothelial lining of either arteries venous sinuses leads most probably to disturbances of the local blood circulatic

Extensive well-delimited necrotic areas and haemorrhages in the distal p tions of limb-bud mesoderm at the site of the marginal venous sinuses shou be regarded as secondary changes caused by an inadequate blood supply d to impaired blood circulation. The necrotic areas in the central parts of li cartilage condensations seem to be caused by the decrease in food and oxyg

upplies due to their deep location within a tissue which itself is not vascularized. n circumstances in which there is a deficiency of food and oxygen, the innermost arts of an unvascularized cartilage will suffer first. On the other hand, the sions in the central parts of cartilage condensations might be caused directly y the interference of hydrocortisone in the synthetic activity of the cartilage lls, for it is known that cortisone inhibits the synthesis of chondroitin sulphate Layton, 1951; Boström & Odebald, 1953). This mechanism, however, could ot explain why the necrotic areas are located exactly at the centres of the fected cartilage condensations.

Moscona & Karnofsky (1960) have reported defects in ossification of the ng bones of the extremities in the chick after cortisone treatment which may ave been caused by prior necrosis inside the cartilage condensations.

In attempting to interpret the mechanism of hydrocortisone embryotoxicity, should be pointed out that in the more recent literature there are consistent dications that, on one hand, it acts as an anti-inflammatory drug and is protec- ve against cell injury by various agents, but, on the other hand, it can also delay e repair of cellular injury. This paradoxical situation is probably the result stimulation of DNA-dependent messenger RNAs and of other RNAs involved the synthesis of specific proteins in general and enzymes in particular. The d result of such a stimulation will depend on whether it leads predominantly cell repair, or whether the synthesis of deaminases and proteolytic enzymes stimulated, when it will result in the delay of cell repair or even in cell injury d death.

Another feature of hydrocortisone injury is the occurrence of subepithelial isters on the skin, accompanied occasionally by local necrosis. They occur referentially in certain regions of the body, e.g. the temporal region on the ead, the mandibular processes and, dorsally, on the proximal parts of the mbs. In some cases the regions seem to contain single-whisker primordia where intensive protein synthesis probably takes place. This detail may be related the growth-inhibiting syndrome after cortisone administration described by arnofsky, Ridgway & Patterson (1951) in chick embryos, where complete hibition of feather formation was observed.

In conclusion it should be pointed out that, although hydrocortisone is widely ed in medicine and is regarded as a safe drug from the point of view of its de effects, nevertheless its embryotoxicity in animal experiments is quite nsiderable.

SUMMARY

Hydrocortisone acetate injected into mice subcutaneously (25 mg/kg) on the 0th, 11th and 12th days of pregnancy causes in the limb buds of 14-day-old mbryos dilatation of the venous marginal sinuses (primary effect) (14·4%), tensive distal mesoblast necrosis (7·9%), distal haemorrhages (10·7%), and equent necrotic centres in the limb skeleton blastemas (secondary effects).

Similar injuries are found in the tail tip. In some embryos the foot plates sho deformations, possibly due to missing digits, which seems to be the effect healing of previous injuries (tertiary effect).

Other macroscopically visible malformations included: micromelia in abo 9·4% of embryos and necrosis of the maxillary processes with facial fissur (1·8%). In addition, the affected embryos show subepidermal blisters on t skin in the temporal region of the head and on the back. Cleft palate was fou in 52·7% of 18-day-old embryos.

RÉSUMÉ

L'effet de l'acétate d'hydrocortisone sur le développement de l'embryon de Souris

L'acétate d'hydrocortisone injecté aux Souris par voie sous-cutanée (25 m kg) le 10e, 11e et 12e jour de la gestation provoque dans les bourgeons de membr d'embryons de 14 jours une dilatation des sinus veineux marginaux (ef primaire) (14,4%), une nécrose étendue du mésoblaste distal (7,9%), c hémorragies distales (10,7%), et des centres de nécrose abondants dans blastèmes du squelette de membre (effets secondaires). Des altérations identiqu ont été observées à l'extrémité de la queue. Chez certains embryons, les palet pédieuses montrent des déformations qui sont peut-être dues à l'absence doigts et vraisemblablement provoquées par la cicatrisation de lésions antérieu (effet tertiaire).

D'autres malformations sont visibles macroscopiquement: la micromé chez 9,4% des embryons, la nécrose des bourgeons maxillaires avec des fissu faciales (1,8%). Les embryons affectés présentent en outre des ampoules so épidermiques de la peau dans la région temporale de la tête et sur le dos. D fissures palatines ont été observées chez 52,7% des embryons âgés de 18 jou

The author wishes to express his gratitude to Professor C. H. Waddington, F.R.S., reading the manuscript, and to Miss A. P. Gray for the invaluable editorial help.

Thanks are also due to Miss Helen Tait for technical assistance and her care of the mo colony, as well as to Mr G. Hutchinson and Mr F. Johnston for printing the micrograp and to Mr E. D. Roberts for mounting them.

This work was supported by a grant from the Distillers' Company to the University Edinburgh.

REFERENCES

Applezweig, N. (1962). *Steroid Drugs*. New York, Toronto, London: The Blakis Division, McGraw-Hill Co. Inc.

Bongiovanni, A. M. & McPadden, A. J. (1960). Steroids during pregnancy and possi foetal consequences. *Fert. Steril.* **11**, 181–6.

Boström, H. & Odebald, E. (1953). The influence of cortisone upon the sulphate excha of chondroitin sulphuric acid. *Ark. Kemi.* **6**, 39–42.

Caulfield, J. B. (1957). Effects of varying the vehicle for OsO_4 in tissue fixation. *J. biop biochem. Cytol.* **3**, 827–9.

Cope, C. L. (1964). *Adrenal Steroids and Disease*. London: Pitman.

OPE, C. L., HURLOCK, B. & SEWELL, C. (1955). The distribution of adrenal cortical hormone in some body fluids. *Clin. Sci.* **14**, 25–36.
OURRIER, R. & COLOGNE, A. (1951). Cortisone et gestation chez la Lapine. *C. r. hebd. Séanc. Acad. Sci., Paris* **232**, 1164–6.
ECOSTA, E. J. & ABELMAN, M. A. (1952). Cortisone and pregnancy. *Am. J. Obstet. Gynec.* **64**, 746–67.
E DUVE, C., WATTIAUX, R. & WIBO, M. (1961). Effects of fat-soluble compounds on lysosomes *in vitro*. *Biochem. Pharmac.* **8**, 30.
AINSTAT, T. (1954). Cortisone-induced congenital cleft palate in rabbits. *Endocrinology* **55**, 502–8.
RASER, F. C. (1961). The use of teratogens in the analysis of abnormal developmental mechanisms. In *First International Conference on Congenital Malformations*, pp. 179–86. Ed. Dr Morris Fishbein. Philadelphia and Montreal: J. B. Lippincott Co.
ENCH, P. S., KENDAL, E. C., SLOCUMB, C. H. & POLLEY, H. F. (1949). The effect of a hormone of the adrenal cortex (17-hydroxy-11-dehydrocortosterone: compound E) and of pituitary adrenocorticotropic hormone on rheumatoid arthritis. *Proc. Staff Meet. Mayo Clin.* **24**, 181–97.
COBSON, W. (1964). Cellular injuries caused by folic acid antagonists and some corticosteroids. In *Cellular Injury*, pp. 136–61. Ed. A. V. S. de Reuck and J. Knight. *Ciba Fdn Symp.* London: Churchill.
RAND, A. (1965). Ultrastructural aspects of early development of the forelimb buds in the chick and the mouse. *Proc. R. Soc.* B **162**, 387–405.
RAND, A. (1966). Early changes in limb buds of chick embryos after thalidomide treatment. *J. Embryol. exp. Morph.* **16**, 289–300.
RAND, A. & IRELAND, M. J. (1965). A slow rotary shaker for embedding in viscous media. *Stain Technol.* **40**, 233–4.
ARNOFSKY, D. A., RIDGWAY, L. P. & PATTERSON, P. A. (1951). Growth inhibiting effect of cortisone acetate on the chick embryo. *Endocrinology* **48**, 596–616.
ENNEY, F. T. (1962*a*). Induction of tyrosine-α-ketoglutarate transaminase in rat liver. III. Immunochemical analysis. *J. biol. Chem.* **237**, 1610–14.
ENNEY, F. T. (1962*b*). Induction of tyrosine-α-ketoglutarate transaminase in rat liver. IV. Evidence for an increase in the rate of enzyme synthesis. *J. biol. Chem.* **237**, 3496–8.
ENNEY, F. T., GREENMAN, D. L. WICKS, W. D. & ALBRITTON, W. L. (1965). RNA synthesis and enzyme induction by hydrocortisone. In *Advances in Enzyme Regulation*, vol. III (edited by George Weber), pp. 1–11. Oxford: Pergamon Press.
AYTON, L. L. (1951). Cortisone inhibition of mucopolysaccharide synthesis in the intact rat. *Archs Biochem. Biophys.* **32**, 224–6.
OSCONA, M. H. & KARNOFSKY, D. A. (1960). Cortisone-induced modifications in the development of the chick embryo. *Endocrinology* **66**, 533–49.
LADE, G. E. (1952). A study of fixation for electron microscopy. *J. exp. Med.* **95**, 285–98.
UMEL, M. (1948). Tampon au cacodylate de sodium. *Bull. Soc. Chim. biol.* **30**, 129–30.
AGAN, C., HOWES, E. L., PLOTZ, C. M., MEKER, K. & BLUNT, J. W. (1949). Effect of cortisone on production of granulation tissue in the rabbit. *Proc. Soc. exp. Biol. Med.* **72**, 718–21.
MES, G. L. & LEATHAM, J. (1951). Influence of desoxycorticosterone acetate and cortisone acetate on body weight of chick embryos. *Proc. Soc. exp. Biol. Med.* **78**, 231–2.
HIMKE, R. T., SWEENEY, E. W. & BERLIN, C. M. (1964). An analysis of the kinetics of rat liver tryptophan pyrrolase induction: the significance of both enzyme synthesis and degradation. *Biochem. biophys. Res. Commun.* **15**, 214–19.
GAL, H. L. & KIM, Y. S. (1963). Glucocorticoid stimulation of the biosynthesis of glutamic-alanine transaminase. *Proc. natn. Acad. Sci. U.S.A.* **50**, 912–8.
KERIS, C. E. & LANG, N. (1964). Stimulation of messenger RNA synthesis in rat liver by cortisol. *Life Sci.* **169**–73.
VEAT, M. L. (1955). Adrenocorticosteroids in peripheral adrenal venous blood of man. *J. clin. Endocrin.* **15**, 1043–56.

WALKER, B. E. & FRASER, F. C. (1957). The embryology of cortisone-induced cleft pala
J. Embryol. exp. Morph. **5**, 201–9.
WEISSMANN, G. & DINGLE, J. (1961). Release of lysosomal protease by ultraviolet irradiati
and inhibition by hydrocortisone. *Expl Cell Res.* **25**, 207–10.
WEISSMANN, G. & FELL, H. B. (1962). The effect of hydrocortisone on the response of foe
rat skin in culture to ultraviolet irradiation. *J. exp. Med.* **116**, 365–80.
WEISSMANN, G. & THOMAS, L. (1963). Studies on lysosomes. II. The effect of cortisone
the release of acid hydrolases from large granule fraction of rabbit liver induced by
excess of vitamin A. *J. clin. Invest.* **42**, 661–9.

(*Manuscript received 11 April 1968*)

Second group of publications

Structure of the mate-killer (mu) particles in *Paramecium aurelia*, stock 540

by G.H. Beale and A. Jurand

J. gen. Microbiol. (1960), **23**, 243–252
With 4 plates
Printed in Great Britain

Structure of the Mate-Killer (mu) particles in *Paramecium aurelia*, stock 540

By G. H. BEALE and A. JURAND
Department of Animal Genetics, University of Edinburgh, Scotland

(*Received* 16 *March* 1960)

SUMMARY

The mate-killer (mu) particles in the cytoplasm of *Paramecium* aurelia, stock 540, variety (syngen) 1, were studied by: Feulgen-staining; phase-contrast microscopy; fluorescence under ultraviolet irradiation after staining with acridine orange; electron microscopy (including the 'silver-Feulgen' technique). The appearance of the particles following treatment with DNAase and RNAase was observed. It was found that the mu particles were capsulated rod-shaped structures, 2–10 μ long and about 0·3 μ in diameter (excluding the capsule); they appeared to reproduce by transverse fission without formation of cross-walls. There was an external double membrane and the internal material consisted largely of DNA, which was not limited to particular zones but spread throughout the interior of the particle. RNA was also present. The relationships of the particles to other micro-organisms is discussed, and it is concluded that they do not differ from bacteria in any important respect.

INTRODUCTION

Ever since the discovery of the 'killer' strains of *Paramecium aurelia* by Sonneborn (1938) there has been discussion about the nature and homologies of the cytoplasmic kappa particles responsible for the peculiar killing properties of these paramecia. At one time kappa particles were considered to be gene-like elements in the cytoplasm or plasmagenes (Sonneborn, 1947), but this view became less plausible as knowledge of the particles increased. For example Preer (1948) showed that they could be stained and seen with the light microscope, and were as large as some bacteria. Moreover, Sonneborn (1948) showed that at least one kind of kappa particle could be experimentally transmitted from one paramecium to another by infection through the external medium. These and other findings strengthened the belief, which had been firmly held all along by certain critics (e.g. Altenburg, 1946), that the particles were to be regarded as symbiotic micro-organisms rather than plasmagenes. Their exact position remains, however, uncertain, as can be seen from the discussion of Preer & Stark (1953) and the recent exhaustive review of Sonneborn (1959).

Characterization of a micro-organism would ideally require a thorough description of both morphological and physiological properties, but since kappa and similar particles cannot as yet be grown anywhere except within the cytoplasm of a paramecium, we are restricted to morphological and cytochemical studies. In this paper we give an account of the structure of one type of cytoplasmic particle called mu,

occurring in *Paramecium aurelia*, stock 540 (variety or syngen 1). This stock was originally collected in Mexico, and was kindly made available to us by Dr T. M. Sonneborn. It is a mate-killer having the same general properties as the mate-killers earlier described by Siegel (1953) in variety 8. As found there, when conjugation between a mate-killer and a normal (sensitive) organism takes place, nuclear exchange proceeds normally, but one half of the ex-conjugants (those which receive cytoplasm from the sensitive conjugant) die after two fissions or less, whilst the other half (which receive cytoplasm, and hence mu particles, from the mate-killer conjugant) give rise to fully viable clones. The mechanism causing the death of the sensitive organisms is unknown, but it has been shown by Siegel (1954) that contact of the surfaces of mate-killer and sensitive paramecia for a minimum of about 2 hr. is required. Exchange of the internal contents, either nuclei or cytoplasm, is not an essential part of the killing process. A brief account of the stock 540 mate-killer, including some genetical information, was given previously (Beale, 1957). Out of 60 stocks of *P. aurelia* variety 1 collected from many different parts of the world, stock 540 is the only mate-killer.

METHODS

Cultures. The paramecia were grown on baked lettuce or dried grass infusions containing *Aerobacter aerogenes*. Abundant mu particles were obtained by allowing the cultures of paramecia to starve for 3–4 days at room temperature in dilute buffered saline. Under such conditions the particles continue to multiply whilst the paramecia do not. The ciliates were concentrated by drawing the culture fluid through a Berkefeld candle, and subsequent centrifugation of the organisms from the fluid which remained behind.

Light microscopy. The fixatives most commonly used were methanol + acetic acid (3:1), and 1 % (w/v) osmic acid buffered to pH 7·2. Time of fixation was 1 hr. For Feulgen staining the material was hydrolysed with N-HCl for 5 min. at 60°, and stained for 1½ hr. (whole mounts) or 2½ hr. (sections) at room temperature in dilute buffered saline. Azure A staining (see DeLamater, 1951) was by a procedure essentially the same as for the Feulgen procedure, except that in place of Feulgen reagent, staining was with azure A for 3–4 hr. at room temperature. Paraffin sections were cut at 2–7 μ thickness.

Preparations of mu particles for phase-contrast observations were made by gently crushing a few living paramecia on a slide with a coverglass and observing the particles directly (method of Preer & Stark, 1953).

For the demonstration of translucent capsules surrounding the particles, a method based on that described by Duguid (1951) was used. A dense suspension of paramecia was crushed between a slide and coverslip. The coverslip was then removed and placed on a drop of water on a clean slide. Indian ink was infiltrated into the preparation and the particles which adhered to the coverslip were observed by phase-contrast microscopy, with an oil-immersion objective.

Fluorescence of particles stained with acridine-orange was studied by a technique based on that described by Anderson, Armstrong & Niven (1959). The particles on a slide were washed with 0·01 M-acetate buffer (pH 5), stained for 2 hr. with acridine orange (2·5 mg. in 1 ml. of the same buffer), thoroughly washed with buffer, and examined under ultraviolet (u.v.) radiation under the microscope with a dark ground

condenser (Zeiss). An Osram high-pressure mercury vapour lamp (type HBO 200) was used as source of u.v. radiation.

Electron microscopy. The preferred fixative was 1 % (w/v) osmic acid, buffered to pH 7·2 with veronal + acetate at 1/9 the concentration recommended by Palade (1952). For special purposes methanol + acetic acid (3:1) was also used as fixative. The time of fixation was 1 hr. at room temperature, after which the suspensions of whole paramecia were dehydrated, embedded in methacrylate and sectioned at about 250 A. on a Porter-Blum Servall microtome. A Siemens Elmiscope I electron microscope was used.

Enzyme treatments. (*a*) *DNAase.* After fixation of whole paramecia with osmic acid or methanol + acetic acid and thorough rinsing in water and buffer (0·003 M-tris buffer at pH 7·6; 0·02 M-$MgSO_4.7H_2O$), the suspensions of organisms were divided into two parts (tris buffer, even though it causes considerable distortion, was used in place of phosphate buffer here since a precipitate formed when the latter is used with the DNAase preparation containing $MgSO_4$). One part was treated with a solution of crystalline DNAase (Nutritional Biochemicals Corp.; 1 mg./10 ml. buffer) for 2 hr. at 37·5°. The second part was left in buffer for the same time and at the same temperature, as a control. Following DNAase treatment samples were stained by the Feulgen method and examined in the light microscope to check the effectiveness of the digestion; the remainder were prepared for electron microscopy as described above.

(*b*) *RNAase.* After fixation with methanol + acetic acid (3:1) and thorough rinsing in 1/10 Ringer solution buffered to pH 6·8 with 0·004 M-phosphate, the suspensions of whole paramecia were treated with a 1 % (w/v) solution of crystalline RNAase (Light) for 3 hr. at 37°. Effectiveness of the digestion was checked by staining samples by the methyl-green pyronin method, and observing with the light microscope the absence of pyronin-stained material in the cytoplasm.

'*Silver-Feulgen*' *method* (based on a technique of Bradfield, 1954; see also Jurand, Deutsch & Dunn, 1959). After osmic fixation for 1 hr. and hydrolysis in N-HCl at 60° for 5 min. the material was washed with distilled water until no reaction took place with a 3 % (w/v) $AgNO_3$ solution, then treated for 1–3 hr. at 40–48° with a 1·5 % (w/v) aqueous solution of hexamethylenetetramine containing 0·25 % (w/v) $AgNO_3$ buffered with borate to pH 8·3. The paramecia were then washed in 1·5 % (w/v) hexamethylenetetramine, rinsed with water, then with 5 % (w/v) sodium thiosulphate and again with water. The material was then dehydrated and embedded in methacrylate.

RESULTS

Light microscope observations

Feulgen and azure-A staining. In mounts of whole paramecia the mu particles appeared as clouds of stained material (Pl. 1, fig. 2*a*); usually individual particles could not be distinguished. When the paramecia were sectioned, the individual particles were seen more clearly (Pl. 1, fig. 1) and were then revealed as Feulgen-positive rod-shaped structures, with no internal differentiation. After 3–4 days starvation of the paramecia, the particles were extremely numerous and occupied almost the entire cytoplasm. With less severe starvation of the paramecia the particles were aggregated in one or two large colonies, in a manner similar to that

described previously by Siegel (1954) for the mu particles in other stocks. Following DNAase treatment of mate-killer paramecia, no Feulgen-positive material remained in the cytoplasm, nor, of course, in the nucleus (Pl. 1, fig. 2*b*). (The darker material in Pl. 1, fig. 2*b*, is due to browning produced by osmic acid, not to the Feulgen reaction.)

Phase-contrast observations. The mu particles were not seen inside living unstained paramecia, but when the latter were gently crushed, causing the contents to flow out, the particles became easily visible in phase contrast, as previously recorded for the kappa particles in other stocks by Preer & Stark (1953). Stock 540 mu particles became characteristically orientated flat on the glass slide (Pl. 1, fig. 3*a*), and were not washed off with distilled water or culture fluid, nor were they removed when the coverslip was taken off, the fluid allowed to dry and the preparation re-wetted. Some of the particles likewise adhered to the coverslip. These treatments left the particles adhering to the glass surface, and it was therefore possible to obtain a homogeneous preparation of mu particles since most other cytoplasmic structures were washed away with water. Solutions of higher ionic strength (2%, w/v, NaCl or N-HCl) caused the particles to become detached from the glass. As seen in phase contrast, the particles were usually about 2μ in length, but varied between 2 and 10μ. A constriction was frequently seen, but no internal structural details were discerned. The refractile bodies described by Preer & Stark (1953) in kappa particles were not present in the mu particles. It will be noticed in Pl. 1, fig. 3*a*, that the particles never appear to come into direct contact with one another, and this is a general rule. Even after DNAase treatment, which removed all Feulgen-positive material (this constitutes the bulk of the internal contents of the particles; see below) the appearance of the latter in phase contrast remained unchanged; and the same was found after RNAase treatment. The particles therefore possess a rigid envelope made of some substance other than nucleic acid. The presence of translucent material or capsules surrounding the particles was clearly shown by the indian ink technique (see Pl. 1, fig. 3*b*). Considerable variation in the thickness of the capsule was found in different particles, but it was commonly about 0·2μ thick.

Fluorescence following acridine-orange staining. Cells of higher organisms, and also bacteria, when stained with acridine orange at particular pH values and examined under u.v. radiation, show differential fluorescence of DNA- and RNA-containing regions (see Anderson *et al.* 1959). For example these authors report that, at pH 5, RNA fluoresced red and DNA green or greenish yellow in the bacteria *Salmonella typhi* and *Escherichia coli*.

Preparations of unfixed and of methanol + acetic acid fixed mu particles on glass slides obtained by crushing the paramecia were stained with acridine orange and examined under u.v. radiation. The fluorescence of the mu particles was always weak, notwithstanding use of longer and stronger staining procedures than those recommended by Anderson *et al.* For comparison we sometimes included in the same preparations bacteria (*Aerobacter aerogenes*) and cytoplasm and nuclei of Paramecium, and found that these fluoresced brightly as expected.

At pH 5 the mu particles fluoresced a pale yellowish colour. When they had been pretreated with DNAase and then stained with acridine orange, fluorescence was somewhat more orange, and when the pretreatment was with RNAase, the

fluorescence became more greenish, than in the preparations not treated with enzymes. It is therefore concluded that the particles contained RNA and DNA, but the reason for the faintness of the fluorescence is not known. In any case no internal differentiation of RNA- and DNA-containing regions was demonstrated by this method.

Electron microscope observations

Ultra-thin sections of mu particles in the cytoplasm of osmic acid-fixed paramecia, as seen with the electron microscope, are shown in Pl. 1 and 2, figs. 4–8. The particles are seen to be bounded by a double membrane, have a diameter of about 0·3μ, are usually quite straight, and contain material which appears more dense than the cytoplasm of the paramecia. Within the dense material there is an arrangement of irregular vacuole-like areas, within which dense granules are frequently seen. Sometimes a section was obtained which showed a rather regular row of these 'vacuoles', each one containing a dense central spot, but usually the pale regions were irregularly distributed and might be close against the external membrane. A single large vacuole was often found at one end of a particle (Pl. 2, fig. 8). In particles which showed a median constriction, and were apparently about to undergo transverse fission, no internal cross-wall was seen (Pl. 1, fig. 4). Around the outside of the particles a pale area was commonly (though not always) found, corresponding to the capsule as seen in phase contrast by the indian ink technique (see especially Pl. 1, fig. 6). (Mitochondria and other cytoplasmic inclusions showed no such surrounding pale area.) Where the particles were concentrated in one or two large groups in the cytoplasm, the latter appeared generally less dense in that region than where there were few or no particles. A number of normal paramecia (not mate-killers) were sectioned and examined in the electron microscope; none was found to contain the mu particles as described above.

Effect of enzyme treatment on appearance of particles in the electron microscope. In Pl. 3, figs. 9*b* and 10*b*, are shown preparations of paramecia treated with DNAase before embedding and sectioning. Pl. 3, fig. 10, shows material fixed with osmic acid (and washed with tris buffer) and Pl. 3, fig. 9, material fixed with methanol + acetic acid (and washed with phosphate buffer). In each case samples of DNAase-treated material were stained by the Feulgen method and confirmation was obtained that all Feulgen-positive material had been removed from the mu particles and from the macronucleus. Further, DNAase-treated material was stained with pyronin; it gave positive reactions. Thus it was confirmed that DNAase treatment removed DNA but not RNA, and that the fixatives used did not interfere with subsequent digestion by DNAase.

The DNAase-treated material was compared with controls which were treated according to the same procedure of fixation, washing in buffer, etc., but not treated with enzyme (Pl. 3, figs. 9*a*, 10*a*). This was important since the appearance of the particles in the electron microscope was markedly affected by such treatments, as can be seen by comparison of Pl. 3, figs. 9*a*, 10*a* with Pl. 1, figs. 4–6. We have never considered it worth while to make comparisons between preparations made at different times, since there is no doubt that slight variations in the kind of buffer, times and temperatures of washing, etc., have profound effects on the appearance of the material in the electron microscope. The effect of the DNAase treatment was

clearly to remove the greater part of the electron-dense material from both osmic-acid-fixed and methanol + acetic-acid-fixed mu particles. Some electron-dense material remained round the outer margin and a few irregular granules within. In the methanol + acetic acid-fixed preparations, the contents of the particles were shrunken away from the membrane; DNAase treatment resulted in some swelling (Pl. 3, figs. 9*b*, 10*b*). From these observations it is concluded that most of the electron-dense material inside the particles contained DNA, which was not restricted to any central 'nuclear' region.

The effects of treatment with the RNAase preparation were also studied, and were quite clear in spite of the severe distortion brought about by the methanol + acetic acid fixation and rinsing in Ringer solution, etc. (see Pl. 4, fig. 13*a*). RNAase treatment resulted in the disappearance of the pale vacuole-like regions, so that the particles became uniformly opaque (Pl. 4, fig. 13*b*). A superficial resemblance may be noted between the particles in Pl. 4, fig. 13*b* (RNAase treated), and Pl. 3, fig. 9*a* (controls for DNAase experiment), but this is due to the fact that in Pl. 3, fig. 9*a*, the pale areas in the particles were much decreased in size on account of the tris buffer used. It is tentatively concluded that RNA is present in the 'pale' regions, and that the structure of the latter is destroyed by RNAase, allowing the electron-dense material to flow in. It is not excluded, of course, that RNA is present also in the electron-dense regions before treatment with RNAase.

'*Silver-Feulgen*' *reaction.* As described in the 'Methods' section, some mate-killer paramecia were hydrolysed with N-HCl and impregnated with silver nitrate. The idea behind this method is that products of hydrolysis of DNA (aldehydes), which re-colorize Schiff's reagent in the normal Feulgen technique, would also be expected to reduce silver nitrate to metallic silver, which could then be detected in the electron microscope. Some paramecia were therefore hydrolysed and impregnated with silver nitrate, then embedded, sectioned and observed in the electron microscope. The mu particles in these preparations were found to contain a massive electron-dense deposit—('silver granules'), especially in a zone just inside the outer double membrane, and to a lesser degree in the interior of the particles (Pl. 4, fig. 11). Other cytoplasmic structures such as mitochondria showed no such concentration though there was a background of electron-dense granules randomly distributed throughout (though much less dense than in the mu particles). The macronucleus, as expected, showed a dense accumulation of electron-dense granules. Unhydrolysed material when treated with silver nitrate in the same way showed no differential accumulation of silver granules in the mu particles or elsewhere, but merely a random deposition. That reduction of silver to the metallic form was in fact brought about by the hydrolysis products of DNA was shown by studying the effect of DNAase on preparations subsequently treated with silver nitrate. Pl. 4, figs. 12*a*, 12*b*, shows a comparison of DNAase-treated and control particles, and clearly reveals an almost complete absence of silver granules in the enzyme-treated particles, in spite of severe distortion of the structure of the particles due to the various chemical treatments.

DISCUSSION

From these observations it is concluded that the mu particles in *Paramecium aurelia* stock 540 (mate-killer) are rod-shaped structures varying in length between 2 and 10μ, width about 0·3μ, and surrounded by a double membrane and capsule. In a general way they resemble the kappa particles of other stocks of *P. aurelia* described by Dippell (1958) and Hamilton & Gettner (1958), but there are differences in detail. The mu particles studied here differ from the kappa particles by being longer and thinner, in lacking the refractile bodies found in a proportion of kappa particles (so-called 'brights'), and in the presence of a capsule. The kappa particles are more or less uniformly distributed throughout the cytoplasm whilst the mu particles form large clusters; it seems likely that this clumping is connected with the presence of the capsular material, since it will be remembered that the cytoplasm of paramecia is a fluid medium constantly circulating in the living organisms. The mu particles, like kappa particles, contain DNA and this substance is not confined within central 'nuclear' bodies, but spread throughout the particles. RNA is also present, as also reported for kappa by Dippell (1959*a*, *b*).

The mu particles resemble certain bacilli in size and shape and it is with these organisms that we should compare the particles most closely. The most striking difference is in the localization of the 'nuclear' material. With many bacteria, even though no chromosomes can be seen, the 'nuclei' are localized in a definite zone in the centre of the cell, containing Feulgen-positive material. In electron micrographs this zone appears less dense than the rest of the bacterial contents, but within this less dense zone extremely electron-dense material may sometimes be seen and the latter has been considered to be identical with the Feulgen-positive material seen in the light microscope (Maaløe & Birch-Andersen, 1956). These workers consider that in bacteria fixed with osmic acid or formaldehyde aggregates of DNA are objects which appear dark in electron micrographs. This would be in conformance with the results of our studies on the effect of treatment of the mu particles with DNAase, which led to a considerable decrease or elimination of electron-dense material within the particles in both osmic acid and methanol+acetic-acid-fixed material. What is unusual about the contents of the mu particles is that the DNA-containing material seems to occupy practically the whole of the interior of the particle, extending even to the external double membrane.

Concerning the 'silver-Feulgen' technique, several different interpretations are possible (as indeed is true also of the classical Feulgen reaction itself). We have found that some structures in paramecia which are unlikely to contain DNA, e.g. parts of the pellicle, may also cause a reduction to metallic silver in hydrolysed material. However, our results with DNAase treatment showed that the silver deposit within the mu particles was in fact due to the presence within them of DNA hydrolysis products. The fact that so high a density of silver granules was found just within the outer double membrane is not clearly understood but we assume is due to the reduction of silver ion immediately on entering the particle, so that a concentration gradient is set up. It seems unlikely that there is localization of DNA around the outside of the particles.

Doubtless objections could be raised against the various interpretations of individual cytochemical reactions which are described here, and particularly

with regard to enzyme treatments of material examined by electron microscopy. However, when the results of all the tests are considered, a consistent picture is obtained. All the different techniques studied (Feulgen staining; fluorescence of acridine-orange-stained particles; DNAase treatment of particles observed in the electron microscope; the 'silver-Feulgen' technique) have given the same result, namely that the DNA in the particles is spread throughout them. This kind of distribution is not typical of many bacteria which have been examined cytochemically (as earlier noted by Preer & Stark, 1953). Nevertheless, it is known that the appearance of bacterial 'nuclei' is much affected by the nutritional and ionic conditions before and during fixation and staining (Robinow, 1956), and the habitat of the mu and kappa particles is after all very different from that of the saprophytic bacteria normally studied. The mu particles also differ from many bacteria in their structure during division. Sections of dividing bacteria often show a cross-wall developing between the two halves (see for example Bradfield, 1956); in the constricted mu particles, which one assumes are in the process of fission, no such cross-walls were seen. However, this distinction is unlikely to be critical and many bacteria may well be found to divide by constriction rather than transverse septum formation. Finally, the mu particles apparently lack the cytoplasmic membrane, distinct from the cell wall, often seen in electron micrographs of bacteria.

Whether the mu (and kappa) particles should be classified amongst the bacteria depends entirely on what definition is placed on that group. Doubtless the obligatory intracellular habitat of the particles has led to a nutritional situation where it is unnecessary for them to maintain the metabolic machinery of free-living forms. They would not require many of the enzymes located in the 'cytoplasm' of bacteria, and this might result in a greater proportion of the structure being occupied by nuclear material (as pointed out by Sonneborn, 1959). We therefore conclude that the mu particles are bacteria which have become adapted to life in the cytoplasm of paramecia.

We wish to thank Dr K. Deutsch for his collaboration with electron microscopy during the early stages of this work; also Drs T. M. Sonneborn and J. P. Duguid for criticism of the manuscript, and the last mentioned for drawing our attention to the indian ink technique. One of us (A. J.) is a Research Worker of the British Empire Cancer Campaign.

REFERENCES

Altenburg, E. (1946). The symbiont theory in explanation of the apparent cytoplasmic inheritance in *Paramecium*. *Amer. Nat.* **80**, 661.

Anderson, E. S., Armstrong, J. A. & Niven, J. S. F. (1959). Fluorescence microscopy: observation of virus growth with amidoacridines. In *Virus Growth and Variation. Symp. Soc. gen. Microbiol.* **9**, 224.

Beale, G. H. (1957). A mate-killing strain of *Paramecium aurelia*, variety 1, from Mexico. *Proc. R. phys. Soc. Edinb.* **26**, 11.

Bradfield, J. R. G. (1954). Electron microscope observations on bacterial nuclei. *Nature, Lond.* **173**, 184.

Bradfield, J. R. G. (1956). Organization of bacterial cytoplasm. In *Bacterial Anatomy. Symp. Soc. gen. Microbiol.* **6**, 296.

DeLamater, E. D. (1951). A new cytological basis for bacterial genetics. *Cold Spr. Harb. Symp. quant. Biol.* **16**, 381.

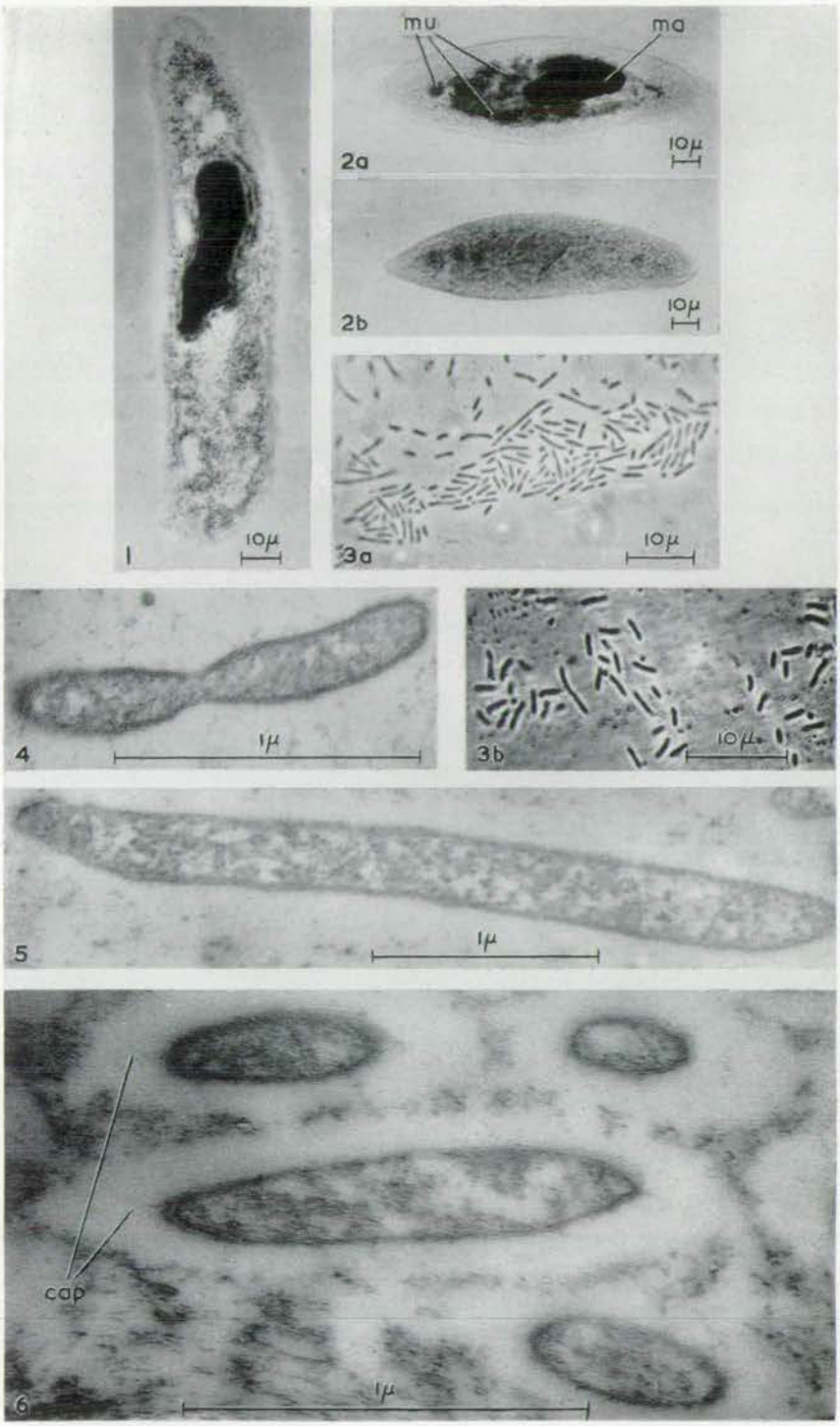

G. H. BEALE AND A. JURAND

(*Facing p.* 252)

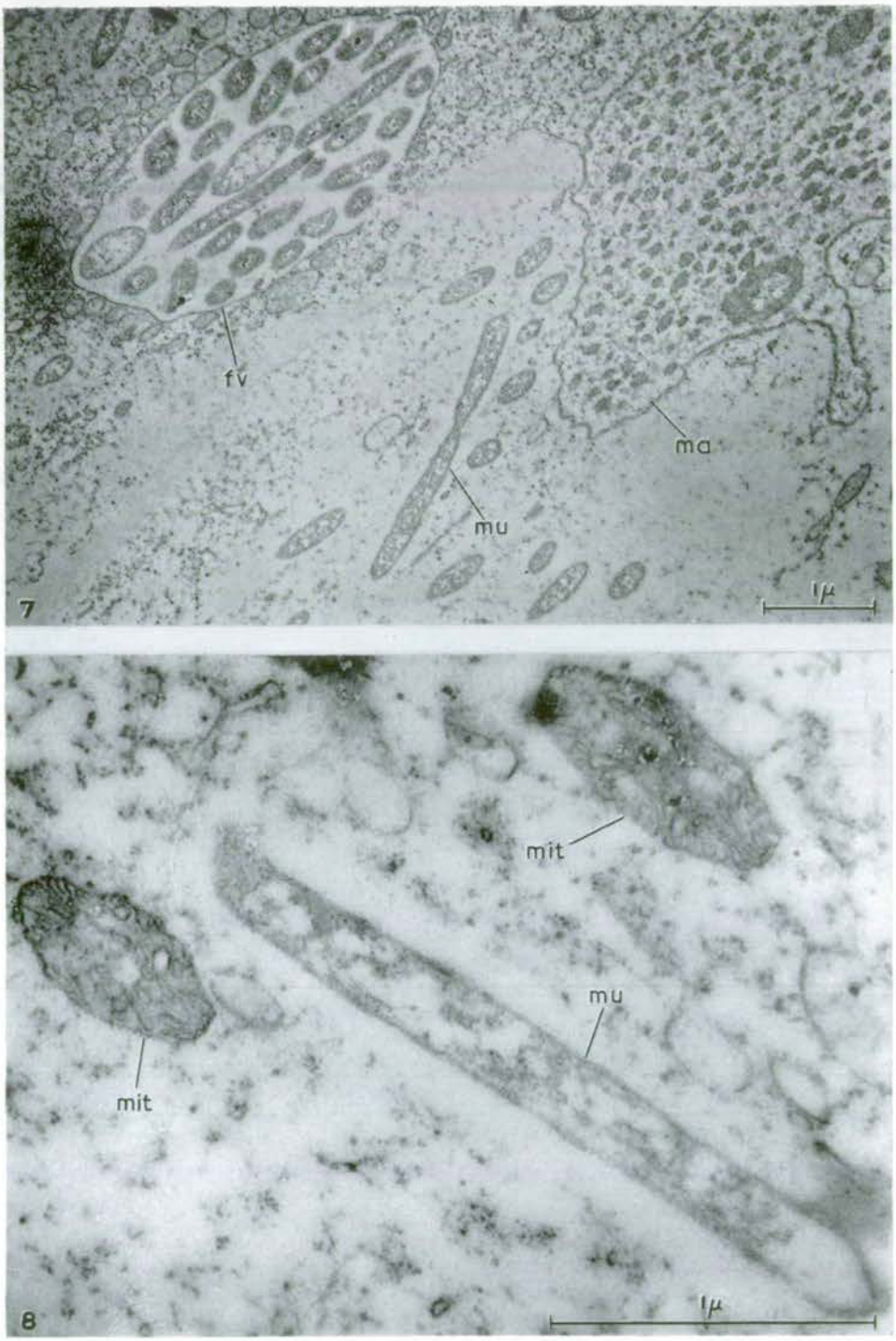

G. H. BEALE AND A. JURAND

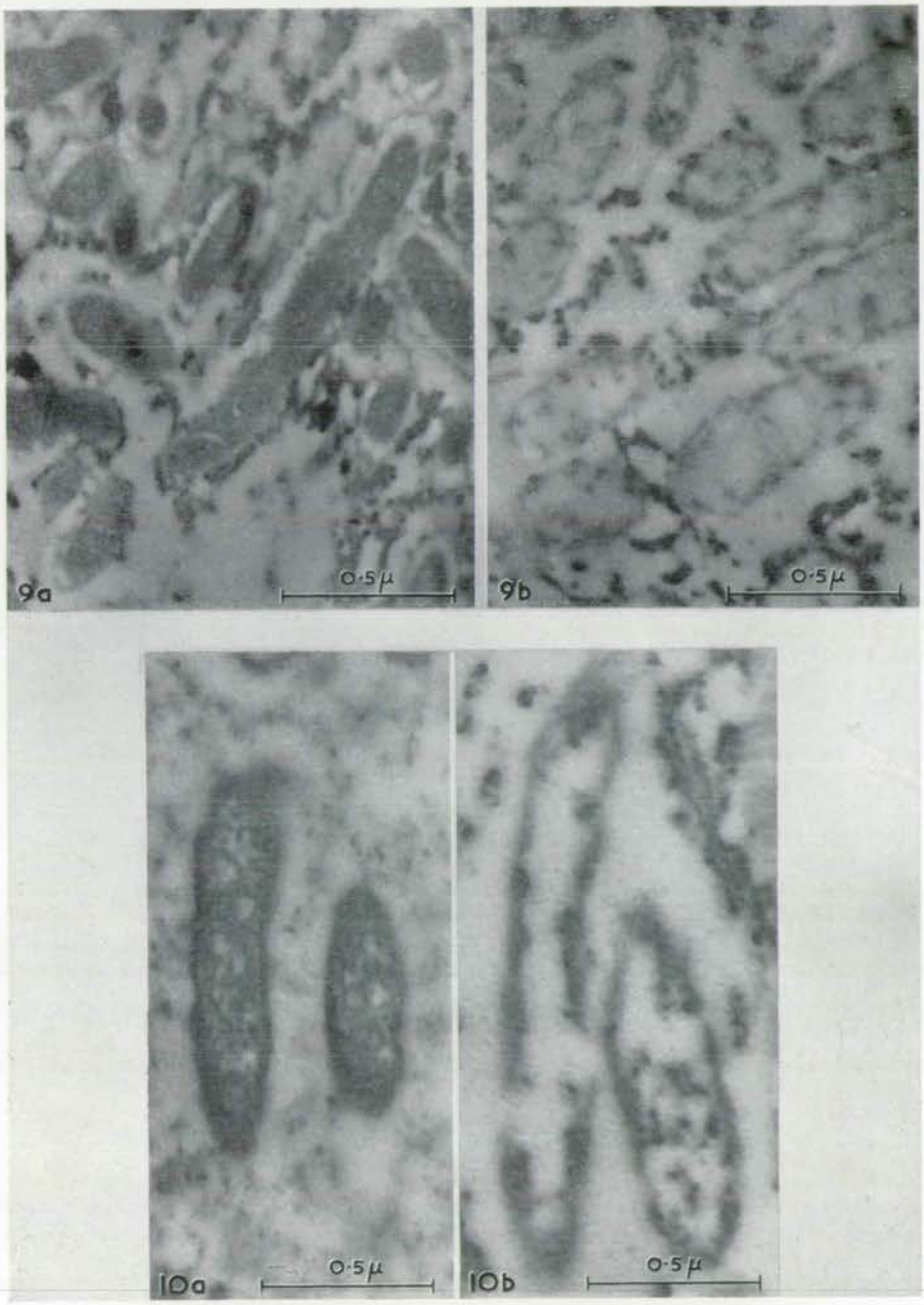
9a
0·5μ
9b
0·5μ
10a
0·5μ
10b
0·5μ

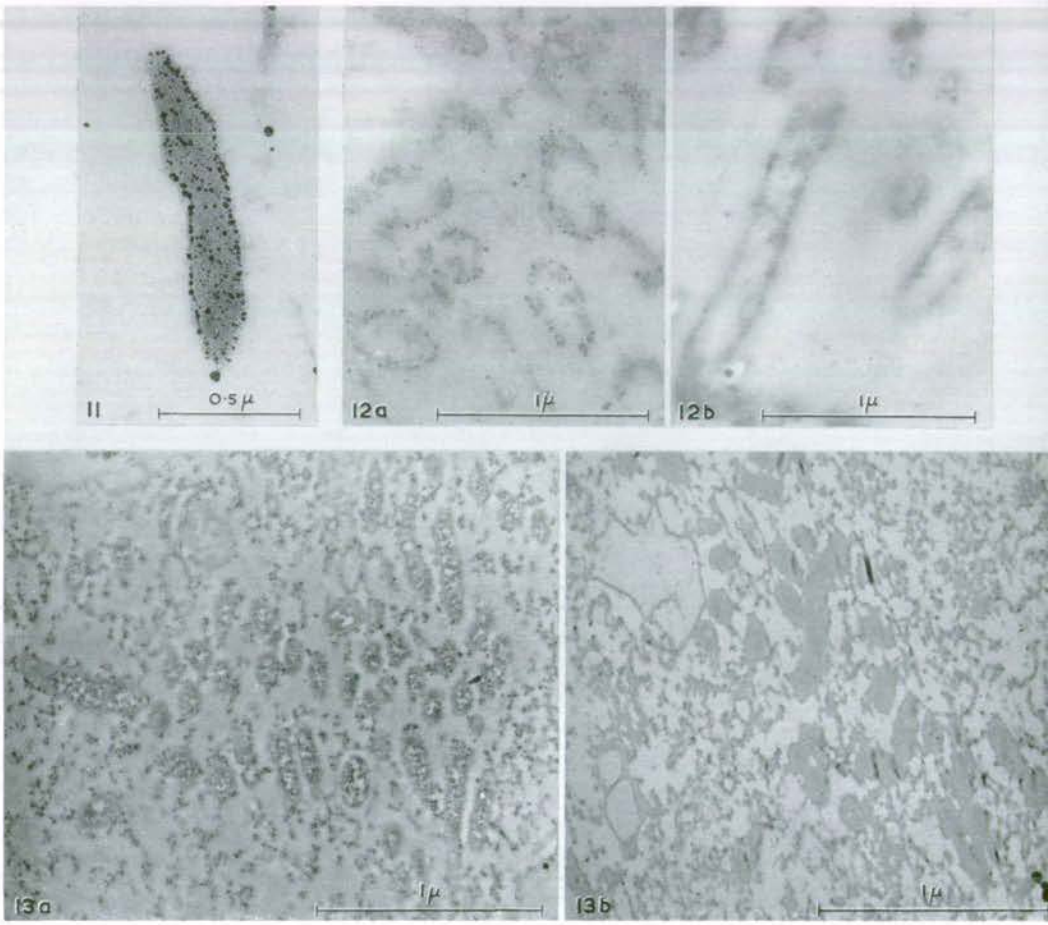

G. H. BEALE AND A. JURAND

DIPPELL, R. V. (1958). The fine structure of kappa in killer stock 51 of *Paramecium aurelia*. *J. biophys. biochem. Cytol.* **4**, 125.

DIPPELL, R. V. (1959*a*). Cytological observations on kappa in killer stock 51 of *Paramecium aurelia*. *Anat. Rec.* **134**, 554 (abstract).

DIPPELL, R. V. (1959*b*). The distribution of DNA in kappa particles of *Paramecium* in relation to the problem of their bacterial affinities. *Science*, **130**, 1415 (abstract).

DUGUID, J. P. (1951). The demonstration of bacterial capsules and slime. *J. Path. Bact.* **63**, 673.

HAMILTON, L. D. & GETTNER, M. E. (1958). Fine structure of kappa in *Paramecium aurelia*. *J. biophys. biochem. Cytol.* **4**, 122.

JURAND, A., DEUTSCH, K. & DUNN, A. E. G. (1959). Application of the silver-Feulgen reaction in electron microscopy. *J. R. micr. Soc.* **78**, 46.

MAALØE, O. & BIRCH-ANDERSEN, A. (1956). On the organization of the 'nuclear material' in *Salmonella typhimurium*. In *Bacterial Anatomy. Symp. Soc. gen. Microbiol.* **6**, 261.

PALADE, G. E. (1952). A study of fixation for electron microscopy. *J. exp. Med.* **100**, 641.

PREER, J. R. (1948). The killer cytoplasmic factor kappa. Its rate of reproduction, the number of particles per cell, and its size. *Amer. Nat.* **82**, 35.

PREER, J. R. & STARK, P. (1953). Cytological observations on the cytoplasmic factor 'kappa' in *Paramecium aurelia*. *Exp. Cell Res.* **5**, 478.

ROBINOW, C. F. (1956). The chromatinic bodies of bacteria. *Bact. Rev.* **20**, 207.

SIEGEL, R. W. (1953). A genetic analysis of the mate-killer trait in *Paramecium aurelia*, variety 8. *Genetics*, **38**, 550.

SIEGEL, R. W. (1954). Mate killing in *Paramecium aurelia*, variety 8. *Physiol. Zoöl.* **27**, 89.

SONNEBORN, T. M. (1938). Mating types, toxic interactions and heredity in *Paramecium aurelia*. *Science*, **88**, 503.

SONNEBORN, T. M. (1947). Recent advances in the genetics of *Paramecium* and *Euplotes*. *Advanc. Genet.* **1**, 263.

SONNEBORN, T. M. (1948). Symposium on plasmagenes, genes and characters in *Paramecium aurelia*. *Amer. Nat.* **82**, 26.

SONNEBORN, T. M. (1959). Kappa and related particles in *Paramecium*. *Advanc. Virus Res.* **6**, 229.

EXPLANATION OF PLATES

Figs. 1–3. Light microscope preparations. Figs. 4–13. Electron microscope preparations. *mu*, mu particles; *ma*, macronucleus; *fv*, food vacuole; *cap*, capsule.

PLATE 1

Fig. 1. Paraffin section of *P. aurelia*, stock 540 mate-killer, fixed with osmic acid, hydrolysed with N-HCl, stained with azure A, examined in phase contrast.

Fig. 2*a*. Whole mount, fixed and stained as in fig. 1.

Fig. 2*b*. As fig 2*a*, but treated with DNAase before applying stain. The osmic acid causes some browning (dark in photograph), but the organism is completely unstained.

Fig. 3*a*. Unstained mu particles outside paramecium, flat on glass slide, observed in phase contrast. Note separation of particles.

Fig. 3*b*. Unstained mu particles lying flat on coverslip (or hanging vertically). Mounted in indian ink to show capsules. The indian ink particles are in Brownian movement, and produce grey background due to 10 sec. exposure of photographic plate.

Fig. 4. EM section through a mu particle, fixed with osmic acid, showing constriction.

Fig. 5. Longitudinal section through a long mu particle.

Fig. 6. Group of mu particles showing capsules in EM.

Plate 2

Fig. 7. Comparison of mu particle with bacteria (*Aerobacter aerogenes*) in food vacuole. Note pale ('nuclear') areas in the bacteria are more concentrated towards the centre than corresponding areas in the mu particles.

Fig. 8. Mu particle with capsule, compared with mitochondria.

Plate 3

Fig. 9*a*. Mu particles fixed with methanol + acetic acid, treated with tris buffer. Control for fig. 9*b*.

Fig. 9*b*. As fig. 9*a*, but treated with DNAase.

Fig. 10*a*. As figs. 9*a* and 9*b*, but fixed with osmic acid instead of methanol + acetic acid.

Fig. 10*b*. As fig. 10*a*, but treated with DNAase.

Plate 4

Fig. 11. Mu particle prepared by 'silver Feulgen' technique.

Fig. 12*a*. Mu particles fixed with osmic acid, hydrolysed with N-HCl and silvered. Control for fig. 12*b*.

Fig. 12*b*. As fig. 12*a*, but treated with DNAase before silvering.

Fig. 13*a*. Mu particles fixed with methanol + acetic acid, rinsed in dilute buffered Ringer solution. Control for fig. 13*b*.

Fig. 13*b*. As fig. 13*a*, but treated with RNAase.

An electron microscope study of food vacuoles in *Paramecium aurelia*

by A. Jurand

An Electron Microscope Study of Food Vacuoles in *Paramecium aurelia*

A. JURAND

Institute of Animal Genetics, University of Edinburgh, Scotland, U. K.

SYNOPSIS. The food vacuoles of *Paramecium aurelia*, when examined in the electron microscope, are seen to be surrounded by small secondary vacuoles 0.05 - 0.2 μ in diameter. Similar small vacuoles also surround the deepest part of the buccal cavity. Young food vacuoles, *i.e.* those containing well preserved bacteria, are encircled by a smooth vacuolar membrane. In older food vacuoles the vacuolar membrane in a transverse section often appears more wavy with small gulfs and protuberances. It is suggested that the small surrounding vacuoles are formed by the vacuolar membrane of older vacuoles by means of a process similar to pinocytosis. There is no evidence, however, that formation of small surrounding vacuoles takes place by pinocytosis in young food vacuoles. Examination of the cytoplasmic membrane of the deepest parts of the buccal cavity shows a similar process of vacuole formation by pinocytosis.

FOOD vacuoles are digestive organelles common in Protozoa, and similar structures have also been observed occasionally in some groups of Metazoa. Protozoan food vacuoles have been extensively studied in many species, particularly in *Paramecium* and *Amoeba*. In *Paramecium* as in all Ciliata the food vacuoles form an essential part of the feeding apparatus and are analogous to the stomach and intestines in higher organisms. Due to this analogy, which is not merely a superficial one, they were called gastrioles by Volkonsky(20), since the use of the term vacuole for different structures often led to confusion.

After being formed at the bottom of the buccal cavity the food vacuoles are separated from the surrounding cytoplasm by a semi-permeable, or rather selectively permeable, vacuolar membrane. It is believed that this membrane resembles cell membranes in both structural and biological properties(10). In the Ciliata it has physiological functions similar to those of the endodermal epithelium of the alimentary canal in higher organisms. In any case, the vacuolar membrane has its own morphological existence and is not merely an interface between the cytoplasmic continuous phase and the "dispersed" phase of the liquid contents of the food vacuole. This view is based on the observations of King and Beams(9) who were able to show that food vacuoles of *Paramecium* retain their shape outside the cell for more than half an hour. Similarly, Dogiel and Issakova-Keo(4) observed the extrusion through the pharynx of entire, although morphologically changed vacuoles, as a result of treatment with some inorganic salts. In spite of the defects of these experiments, as pointed out by Mast (12), they demonstrated the existence of the vacuolar membrane. Furthermore, evidence has been made available which indicates that the vacuolar membrane is mechanically very resistant, for the food vacuoles do not readily fuse during ultracentrifugation of *Paramecium* cells(9).

In *Amoeba proteus*, on the other hand, where food vacuoles are formed in the outer layers of the cytoplasm (*i.e.* in the plasmalemma), the vacuolar membrane seems to have properties more similar to those of the interfacial surfaces of colloidal systems(1).

The observations reported here were obtained by means of electron microscopy. They are thought to be of value not only in elucidating the morphological properties of the food vacuole membrane but also in their bearing on physiological properties of the latter, confirming that it is not merely an interface between the vacuole and cytoplasm. In addition, light is thrown on the nature of the so-called neutral red granules first described by Provazek(16).

MATERIAL AND METHODS

Paramecium aurelia, variety 1, obtained from dried grass medium cultures grown on *Aerobacter aerogenes* in the laboratory were used in the experiments. The cells were fixed from growing cultures or after 3-5 days' starvation in buffered diluted Ringer solution (pH 7). After fixation with buffered (pH 7.1) 1% osmic acid solution for 1 hour, the cells were centrifuged at low

Reprinted from THE JOURNAL OF PROTOZOOLOGY.
J. PROTOZOOL. 8(2), 125-130 (1961).
Printed in U.S.A.

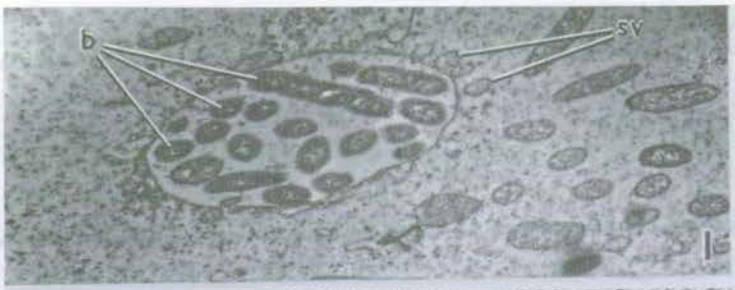

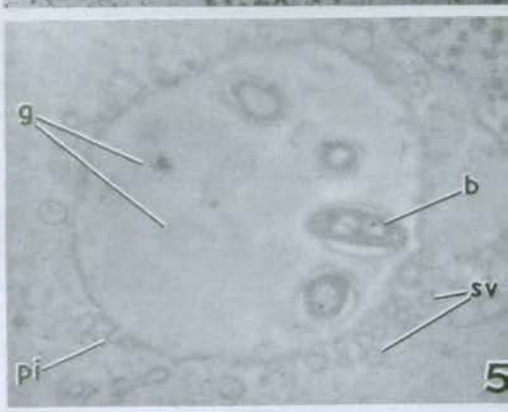

1μ

peed (<1000 rpm), dehydrated and embedded in a ethacrylate mixture in the usual way. Ultra-thin ections were cut on a Porter-Blum Servall microtome nd viewed in a Siemens Elmiskop.

RESULTS

Sections through the food vacuoles show round or val spaces containing bacteria varying in numbers nd appearance, presumably depending on the age of ne vacuole and also to some extent on the amount of ood available in the medium. Estimates of the age f the vacuoles may be made from the state of diges- on of the bacterial contents.

In newly-formed food vacuoles bacteria densely fill ne internal space of the vacuole and are well pre- erved, usually showing nuclear bodies surrounded by ytoplasm (Fig. 1). This stage probably corresponds o that at which the food vacuoles are contracted, hich is known in light microscopy as the acid phase. t the next stage, a rapid swelling follows, but most f the bacteria are still unchanged in appearance (Fig.). In older vacuoles the bacteria show various stages f digestion and often the cell walls become separated way from the internal contents (Figs. 3, 4). In tarved *Paramecium*, and occasionally in fed ones, nly a few bacteria are seen in a section of an old vac- uole, the rest being filled with "ghosts" and small ragments of digested bacterial cells (Figs. 5, 6).

The internal contents of the vacuoles (apart from he bacteria) always have a lower electron density han that of the surrounding cytoplasm. The vacuolar nembrane in the young vacuoles of growing animals ed *ad libitum* shows as a continuous slightly wavy ine. In older vacuoles containing bacteria, but in the ater stages of digestion, the vacuolar membrane ap- pears to be much more wavy often showing character- stic small outwardly directed loops; this presumably esults in a greater absorbing area (Figs. 7, 8). The oops differ in shape; in some cases they are bottle-like vith comparatively narrow necks and wide round am- poules (Figs. 9, 10).

In the cytoplasm around the younger food vacuoles nd close up against their membranes there are al- ways present small vacuoles ranging in size from 0.05- 0.2 μ. They are seldom found deeper in the cyto- plasm. Those that seem to be deeper, especially in groups, presumably belong to other food vacuoles which lay above or below the level of the section. Ap- parently similar small vacuoles are also present around the older food vacuoles with the wavy outline. The electron density of these small vacuoles is similar to that of the loops and small sacs. Further, the small vacuoles surrounding the older food vacuoles can be seen, especially at higher magnifications to have mem- branes similar to those of the food vacuoles. Some of the small vacuoles contain irregular inclusions (Fig. 11).

Loops similar to those of the food vacuoles were found to be formed also by the cytoplasmic membrane at the bottom of the buccal cavity, which in its most aboral parts (*i.e.*, in the cytostome area) is also densely surrounded by small vacuoles (Figs. 12, 13).

DISCUSSION

Careful examination of the electron-micrographs described above gives the impression that the small vacuoles surrounding the young food vacuoles and present in large numbers round the deepest part of the buccal cavity are probably identical with the di- gestive granules stainable with the vital stains, par- ticularly with neutral red, first described by Provazek (16). This assumption is based on the size of the small vacuoles and their tendency to accumulate around the food vacuoles and in the deepest part of buccal cavity; also on the fact that there are no other granules detectable by electron microscopic examina- tion present in those places.

The neutral red granules which now are seen to be small vacuoles are believed by many authors to ori- ginate in the cytoplasm. Volkonsky(20) suggests that they appear in great numbers in response to the stimu- lus of feeding. Their nature, function and origin have long been a matter for discussion among protozoolo- gists. One group has suggested that these cytoplasmic granules contain digestive enzymes ("Fermentträger" of Provazek), are attracted to the vacuolar membranes by surface tension(6) and eventually enter the food vacuoles(16, 15, 17, 2, 6, 19 and many others). Other workers however, assert that in *Paramecium* and other ciliates the digestive granules accumulate

Explanation of lettering: b—bacteria (Aerobacter aerogenes); sv—secondary vacuoles; m—mitochondria; rc—expanding and cracking bacterial cell wall; g—"ghosts" of digested bacteria; pi—pinocytic loops in the vacuolar membrane or in the cyto- plasmic cell membrane in the buccal cavity; pc—pellicular chambers; vm—vacuolar membrane; in—inclusions.

Fig. 1. Young food vacuole filled with bacteria (b) sur- rounded by few secondary vacuoles (sv). Fig. 2. Young food vacuole in the stage of swelling. Note the large number of secondary vacuoles (sv) placed close to the vacuolar membrane. Fig. 3. Older food vacuole filled with bacteria showing first signs of digestion. Note the expanding and cracking of the bac- terial cell wall (rc). The secondary vacuoles are in small quan- tity. Fig. 4. Old food vacuole at the end of the digestive pe- riod. Vacuolar membrane is wavy, number of secondary vacu- oles negligible. Fig. 5. Older food vacuole with four bacteria (b) and a few digestive remnants (g) at this level with a number of secondary vacuoles. Note pinocytic sac (pi) at the left upper part of the vacuolar membrane. Fig. 6. Food vacu- ole at its last period of existence filled with "ghosts" of digested bacteria (g) and abundant secondary vacuoles around it (sv).

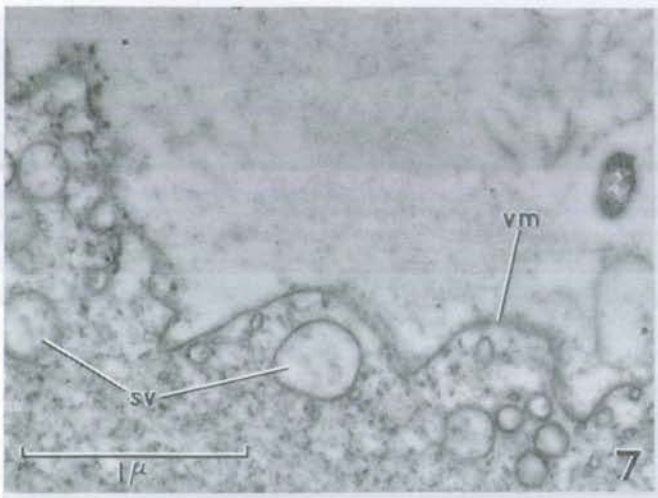
vm
sv
1μ
7

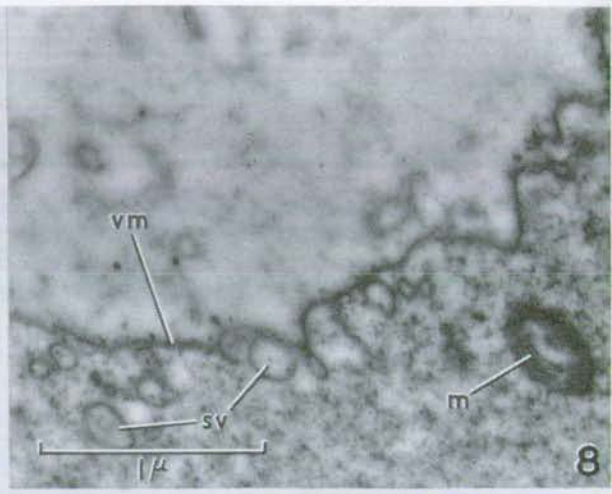
vm
sv
m
1μ
8

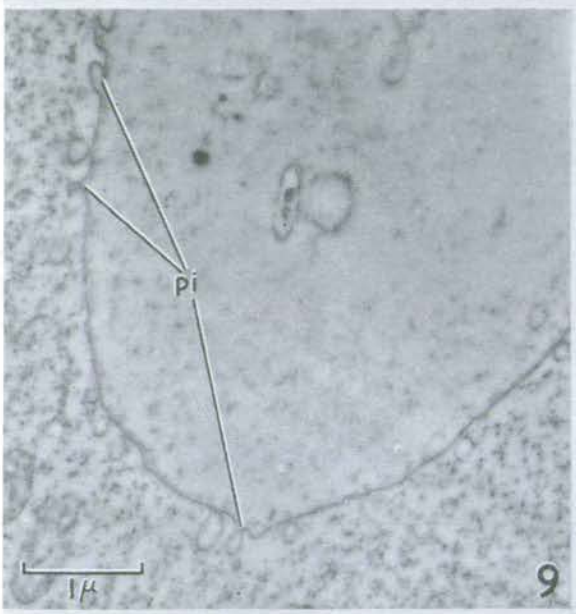
pi
1μ
9

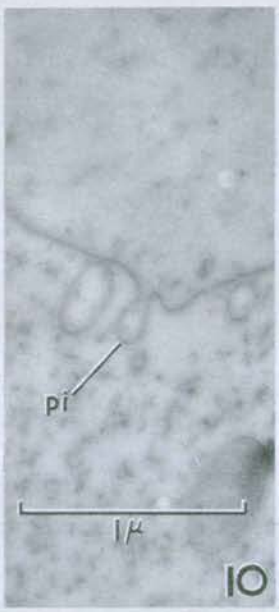
pi
1μ
10

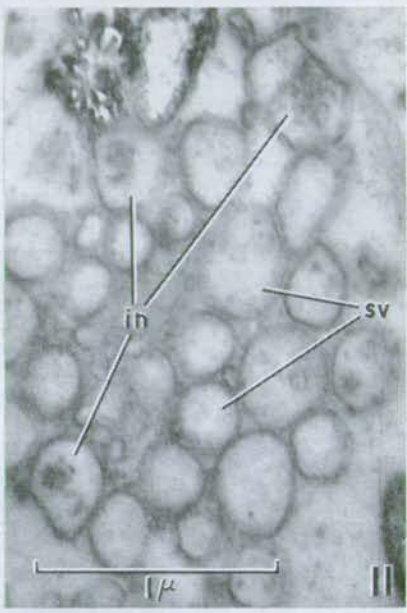
in
sv
1μ
11


sv
m
1μ
12

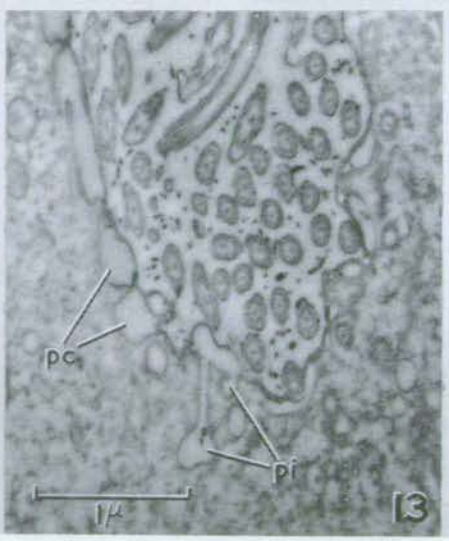
pc
pi
1μ
13

around the food vacuoles but do not enter them (8,5, 14 and 12). Khainsky even suggests that the digestive granules are formed in the food vacuoles and pass through the vacuolar membrane into the cytoplasm during the process of digestion.

Thus the origin and nature of the digestive granules still remain obscure. From the present investigations, however, one can conclude that the small vacuoles seen in the electron-micrograph, at least round the older food vacuoles, may originate from the food vacuoles themselves by means of a process similar to pinocytosis, a phenomenon first described and named by Lewis (11) in rat omentum cell cultures *in vitro*. According to his observations the surrounding liquid medium is trapped by irregular folds of cell membrane which form small vacuoles. Later this phenomenon was extensively investigated experimentally in many species of *Amoeba* (13,7,3).

The suggestion that we have to do with a similar process in *Paramecium* food vacuoles is based on two facts. Firstly, as shown in Figs. 9 and 10, the fact that there is a comparatively long and narrow constriction in a small vacuole connecting it with food vacuole indicates that the former is probably in the process of separation from the food vacuole rather than in the process of uniting or entering it. Secondly, as shown in Fig. 11, the small secondary vacuoles often contain small solid particles which possibly represent fragments of disintegrated, not yet completely digested bacteria.

The above facts show the occurrence of pinocytosis in Ciliata and the formation of small secondary digestive vacuoles adjacent to the vacuolar membrane of older food vacuoles. No evidence, however, has been found that the small vacuoles surrounding young food vacuoles originate in the same way and it is therefore considered that the small vacuoles although morphologically very similar may be of two types, one originating in the cytoplasm and identical with neutral red granules, and the other originating from the vacuolar membrane of the older food vacuoles.

Small secondary vacuoles are abundantly present around the deepest aboral parts of the buccal cavity. It is assumed that here also they are identical with neutral red granules, but they seem to originate here at least partly, by means of a process similar to pinocytosis which occurs in the cytoplasmic membrane at the bottom of the pellicular chambers covering the whole external surface of the *Paramecium* cell and also the inner surface of the feeding apparatus.

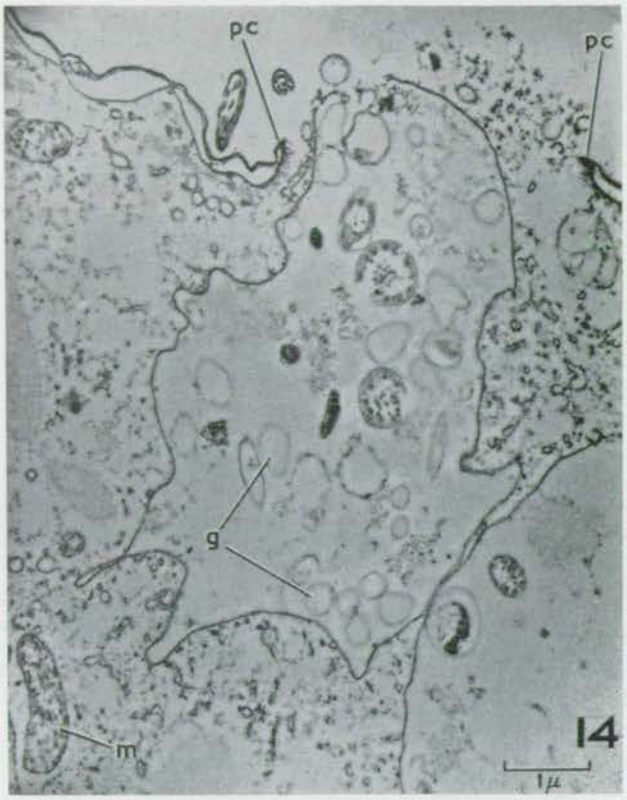

Fig. 14. Section through cytopyge, showing an old food vacuole at the time of excretion.

The process similar to pinocytosis which is described above indicates that the vacuolar membrane of older vacuoles is capable of playing the rôle of an active component of the food vacuole and that it is not merely an interface between the cytoplasm and the contents of the food vacuole.

The process of the formation of small secondary vacuoles by the vacuolar membrane in older vacuoles is thought to have some significance in the physiology of assimilation of the digested food. Their function is probably to increase the absorbing surface of the true food vacuoles and therefore to permit more rapid assimilation by the organism of large quantities of the digestion products.

The dynamics of the food vacuole membrane has been recently described in *Pelomyxa* by Roth (18). According to his observations young vacuoles of *Pelomyxa* have also a smooth vacuolar membrane and the pinocytic function of this membrane begins later, when digestion has started to take place. Roth interprets these morphological changes as evidence that the

Fig. 7. Fragment of a vacuolar membrane of an older food vacuole showing an increased activity. Fig. 8. Similar picture in a slightly older food vacuole. Fig. 9. Older food vacuole with several examples of protuberances suggesting pinocytosis (pi). Fig. 10. Fragment of Fig. 7a in higher magnification. Fig. 11. Secondary food vacuoles (sv) with inclusions (in).

Fig. 12. Deepest part of the buccal cavity surrounded densely with secondary vacuoles (sv). Fig. 13. Deepest part of the buccal cavity with two protuberances suggesting pinocytosis (pi) formed by cytoplasm membrane at the bottom of a pellicular chamber (pc).

membrane of older food vacuoles is a very active site in the digestive process, and finally concludes that pinocytosis is undoubtedly connected with the increased surface area for diffusion. This is in agreement with the interpretation arrived at in the present paper.

APPENDIX

After the paper on food vacuoles in *Paramecium aurelia* was sent for publication a rather rare electron micrograph of an ultra-thin section through the cytopyge was obtained. The photogaph (Fig. 14) shows an old food vacuole at the time of excretion. It is burst on the exterior side and shrunken, presumably due to release of a part of its contents, consisting of ghostly (g) remainders of bacteria in a very late stage of digestion. Close to this vacuole there was another one, also old, which can be partly seen in the lower right corner of the photograph. It is round, being still inside the cell, and has a well preserved vacuolar membrane. Alongside the food vacuole partially plugging the cytopyge a certain amount of cytoplasm can be seen escaping from the cell.

The section through the edges of the cytopyge shows that the pellicular membranes have not been torn by the glass knives as the extreme pellicular chambers (pc) in the cell membrane are closed and rounded up in a similar manner on both sides of the section through the opening of the cytopyge. × 16.000.

I am grateful to Dr. G. H. Beale, for reading the manuscript and helpful discussion. I would like to express my thanks to Mr. D. C. Barker of Department of Zoology, University of Edinburgh for the facilities in the Electron Microscopy Unit. I wish to mention my thanks to Miss Anne R. Wightman for printing the photographs and to Mr. E. D. Roberts for mounting them.

REFERENCES

1. Beams, H. W. & King, R. L. 1941. Some physical properties of the protozoa. In: *Protozoa in Biological Research*, Columbia University Press, New York.

2. Bozler, E. 1924. Über die Morphologie der Ernährungsorganellen und die Physiologie der Nahrungsaufnahme von *Paramecium caudatum* Ehrb. *Arch Protistenk.* **49**, 163-215.

3. Chapman Anderson, C. & Nilsson, J. R. 1960. Electron micrographs of pincytosis channels in *Amoeba proteus*. *Exptl. Cell Res.* **19**, 631-633.

4. Dogiel, V. & Issakova-Keo, M. 1927. Physiologische Studien an Infusorien. II. Der Einfluss der Salzlosungen auf die Ernährung von *Paramecium Biol. Zbl.* **47**, 577-586.

5. Dunihue, F. W. 1931. The vacuome and neutral red reaction in *Paramecium caudatum*. *Arch. Protistenk.* **75**, 476-497.

6. Fortner, H. 1926. Zur Frage der diskontinuirlichen Excretion bei Protisten. *Arch. Protistenk.* **56**, 295-320.

7. Holter, H. & Marshall, J. M. 1954. Studies on pinocytosis in the *Amoeba Chaos chaos*. *Compt. Rend. Lab. Carlesberg*, Ser. Chim. **29**, 7-26.

8. Khainsky, A. 1911. Zur Morphologie und Physiologie einiger Infusorien (*Paramecium caudatum*) auf Grund einer neuen histologischen Methode. *Arch. Protistenk.* **21**, 1-60.

9. King, R. L. & Beams, H. W. 1937. The effect of ultracentrifuging on *Paramecium*, with special reference to recovery and macronuclear reorganization. *J. Morphol.* **61**, 27-49.

10. Kitching, J. A. 1956. Food Vacuoles. *Protoplasmatologia* III. D. 3b.

11. Lewis, W. H. 1931. Pinocytosis. *Bull. Johns Hosp.* **49**, 17-28.

12. Mast. S. O. 1947. The food vacuole in *Paramecium*. *Biol. Bull.* **92**, 31-72.

13. Mast. S. O. & Doyle, W. L. 1934. Ingestion of fluid by Amoeba. *Protoplasma* **20**, 555-560.

14. Müller, W. 1932. Cytologische und vergleichend-physiologische Untersuchungen über *Paramecium multimicronucleatum* und *Paramecium caudatum*, zugleich ein Versuch zur Kreutzung beider Arten. *Arch. Protistenk.* **78**, 361-462.

15. Nierenstein, E. 1905. Beiträge zur Ernährungsphysiologie der Protisten. *Z. allg. Physiol.* **5**, 435-510.

16. Provazek, S. 1897. Vitalfärbung mit Neutralrot an Protozoen. *Z. wiss. Zool.* **63**, 187-194.

17. Rees, C. W. 1922. The micro-injection of *Paramecium*. *Univ. Cal. Publ. Zool.* **20**, 235-242.

18. Roth. L. E. 1960. Electron microscopy of pinocytosis and food vacuoles in *Pelomyxa*. *J. Protozool.* **7**, 176-85.

19. Volkonsky, M. 1929. Les phenomènes cytologiques au cours de la digestion intracellulaire de quelques Ciliés. *Compt. rend. soc. biol.* **101**, 133-135.

20. ——— 1934. L'aspect cytologique de la digestion intracellulaire. *Arch. exper. Zellforsch.* **15**, 355-372.

Studies on the macronucleus of *Paramecium aurelia*.I.

(with a note on the ultra-violet micrography)

by A. Jurand, G.H. Beale and M.R. Young

Studies on the Macronucleus of *Paramecium aurelia*. I. (with a note on Ultra-violet Micrography).

A. JURAND, G. H. BEALE and M. R. YOUNG

Institute of Animal Genetics, University of Edinburgh, Edinburgh, Scotland, and National Institute for Medical Research, London

SYNOPSIS. This is a description of structures seen in EM preparations of the macronucleus of *Paramecium aurelia*, using both starved and growing organisms, the latter at timed stages after fission. The effects of treatment with RNA-ase, DNA-ase and of the "silver-Feulgen" reaction are described, and comparisons made between structures in the macronucleus and the micronucleus. The appearance of macronuclei in thin (2 μ) paraffin sections, stained by the Feulgen, azure A and pyronin-methyl green methods, and upon examination by ultra-violet micrography, is also considered. From these observations it is concluded that the macronucleus contains a large number of structures, 0.5 μ in diameter, consisting of an outer RNA-containing region and central elements containing DNA. These bodies, which are usually thought to be "nucleoli" by other workers, are now considered to be the most likely candidates for the genetic "sub-nuclei" which have been postulated from genetic work.

FROM the genetic work of Sonneborn(10) it is known that the macronucleus of *Paramecium aurelia* contains the elements which determine the phenotype of the organism, and that a considerable number of sets of genes must be present in each macronucleus. The question of whether the latter are organised in "sub-nuclei" within the macronucleus or are distributed in a disorganised manner has not however been

Reprinted from THE JOURNAL OF PROTOZOOLOGY,
J. PROTOZOOL. 9(2), 122-131 (1962).
Printed in U.S.A.

satisfactorily answered, though *a priori* it would seem most likely that a regular organised system of replicating sets of genetic units must exist and this view is now rather generally accepted(10,8). The electron- and light-microscope studies to be described here were carried out with the aim of obtaining information on this question. In this paper we describe the structure of the macronucleus during the various stages of asexual growth; in a subsequent one we will consider the development of new macronuclei after conjugation and autogamy, and discuss the relevance of our results to the work of others, both with *Paramecium* and with other ciliates.

MATERIALS AND METHODS

All our observations were made on individuals belonging to stock 60, syngen (variety) 1, *P. aurelia*, grown on bacterized lettuce or grass media.

Preparation of animals at timed stages after fission. Paramecia in an actively growing condition were isolated singly into depression slides containing culture fluid pre-heated to 27-29°C, and immediately returned to the incubator. Every 30 min the slides were quickly examined and the times of first appearance of two fission products from a single individual noted. At known times—0, 1, 2, 3, 4 hr—after fission, samples of animals were transferred to fixative. Under good conditions the interfission period was a little longer than 4 hr, but sometimes, due to poorer culture fluid or the state of the animals etc., it was between 5 and 6 hours.

Preparations of sections of single animals for electron microscopy. Paramecia at timed stages were fixed for ½ hr at room temperature in 1% (w/v) osmic acid buffered to pH 7.2 with veronal-acetate. In later preparations the modification of adjusting isotonicity with sucrose(2) was used, and gave improved results. In all cases the osmotic pressure of the fixative was made equivalent to 0.1% saline. After fixation, single cells were washed in 1/10 Ringer solution buffered to pH 6.8 with 0.004 M-phosphate, then dehydrated by transferring them individually with a micro-pipette through graded alcohols (35, 70, 95, 100% (twice)), and embedded in methacrylate mixture. It was found that the single paramecia were easily visible at the bottoms of the capsules containing polymerised methacrylate.

Alternatively, some paramecia were fixed in methanol-acetic acid (3:1) for 1 hr, then rinsed in 100% alcohol and embedded in methacrylate.

The material was sectioned at about 600 Å* with a Porter-Blum-Servall microtome and examined in a Siemens Elmiscope I electron microscope.

Preparations of small groups of paramecia for light microscopy. Paramecia at timed stages were fixed in 1% buffered osmic acid as above, or alternatively in ethanol-acetic acid (3:1), for 30-60 min at room temperature. The osmic-fixed material was dehydrated by passage through graded alcohols. By means of a micro-pipette groups of 10-40 animals at the same stage were then transferred into gelatin capsules half-filled with benzene, care being taken to carry over as little alcohol as possible. The capsules were then placed in an oven at 60°C for 5-10 min, and warm wax (M.P. 54°C) added. After 12-16 hr, when the benzene and traces of alcohol had evaporated, melted wax was again added so as to top up the capsules. After a further 1-2 hr in the oven the capsules were taken out and allowed to cool to room temperature. Removal of the gelatin capsules was done by soaking them in water at room temperature for 20-30 min, causing the gelatin to swell up and become easily detachable from the wax. The wax blocks were carefully sectioned at 2 μ, using only the rounded bottom portions where nearly all the paramecia had accumulated. Apart from the fact that the small round sections did not form ribbons, the technique was quite satisfactory as a means of obtaining paraffin sections of small groups of paramecia all at a given stage. The sections were stained by the Feulgen procedure (using 5 min hydrolysis in N HCl at 60°C), with azur A (Delamater(3)) and methyl green-pyronin.

Enzyme treatment of fixed paramecia. These techniques, involving treatment of fixed whole paramecia with DNA-ase and RNA-ase, were as described previously(1,5).

"Silver-Feulgen" method. This method, which gives an indication of the distribution of DNA in EM sections, was also used as previously described(1).

RESULTS

Electron microscope observations of the macronucleus. Ultra-thin sections through the macronucleus show the latter to contain large numbers of electron-dense bodies of two distinct size classes, as previously observed by others, e.g., Sonneborn(11) (Fig. 1). The first, of diameter about 0.1 μ will be referred to hereas "small bodies," and the second, of diameter ~0.5 μ (but showing considerable variation) will be referred to as "large bodies." After fixation in osmic acid, the electron density of the small and large bodies appears to be about the same, but after fixation in alcohol-acetic acid the large bodies appear much less dense than the small bodies (Figs. 2a and b). Presumably a large part of the density of the large bodies in osmium-fixed material is due to uptake of osmium whereas the density of the small bodies is due to their intrinsic composition.

At different stages the large bodies show considerable variations in size and shape. In partially starved animals the bodies are compact round structures with "hollow" centres (Fig. 3). In animals at stages just before or just after fission the appearance of the large bodies is similar to those in starved animals except that the centres are dense throughout (Fig. 4, 5). At this stage there is a conspicuous "halo," devoid of small bodies, surrounding the large bodies. During actual fission of the animals the large bodies may appear to be elongated in the direction of the separation of the two daughter cells, but are otherwise unaltered. About mid-way between two fissions (2-3 hr after previous fission at 28°C with good growth) the large bodies are strikingly different: the outlines are extremely irregular, sometimes apparently detached fragments are seen (though such "fragments" may of course be merely sections through a lobe joined to the main body), and the halo is practically absent (Figs. 6a, 6b). At a somewhat later stage, about three quarters of the time through the interfission period doubl

* Based on data in D. C. Pease, (1960) "Histological techniques for electron microscopy," p. 131. Academic Press, New York and London.

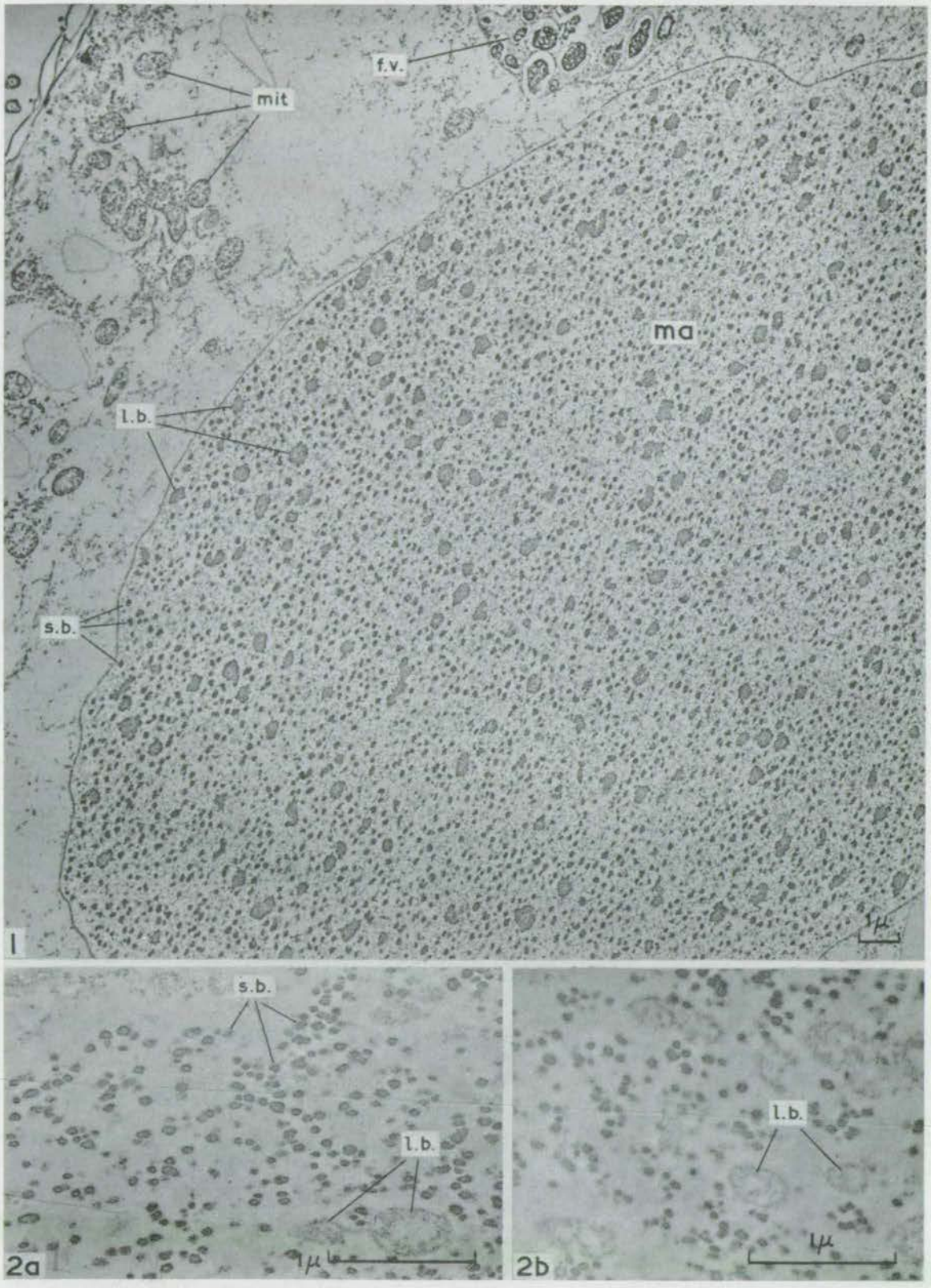

Explanation of lettering: ma—macronucleus; l.b.—large bodies; s.b.—small bodies; mit—mitochondria; f.v.—food vacuole; mi—micronucleus; o—outpocketing of micronuclear membrane. Fixation in osmic acid unless otherwise specified.

Fig. 1. Section showing large area of macronucleus from "young" paramecium (ca. 48 hr after autogamy). Figs. 2a, 2b. Macronucleus fixed with alcohol-acetic acid, showing reduced density of large bodies. Boundary between cytoplasm and macronucleus across upper left corner of 2a, no membrane visible.

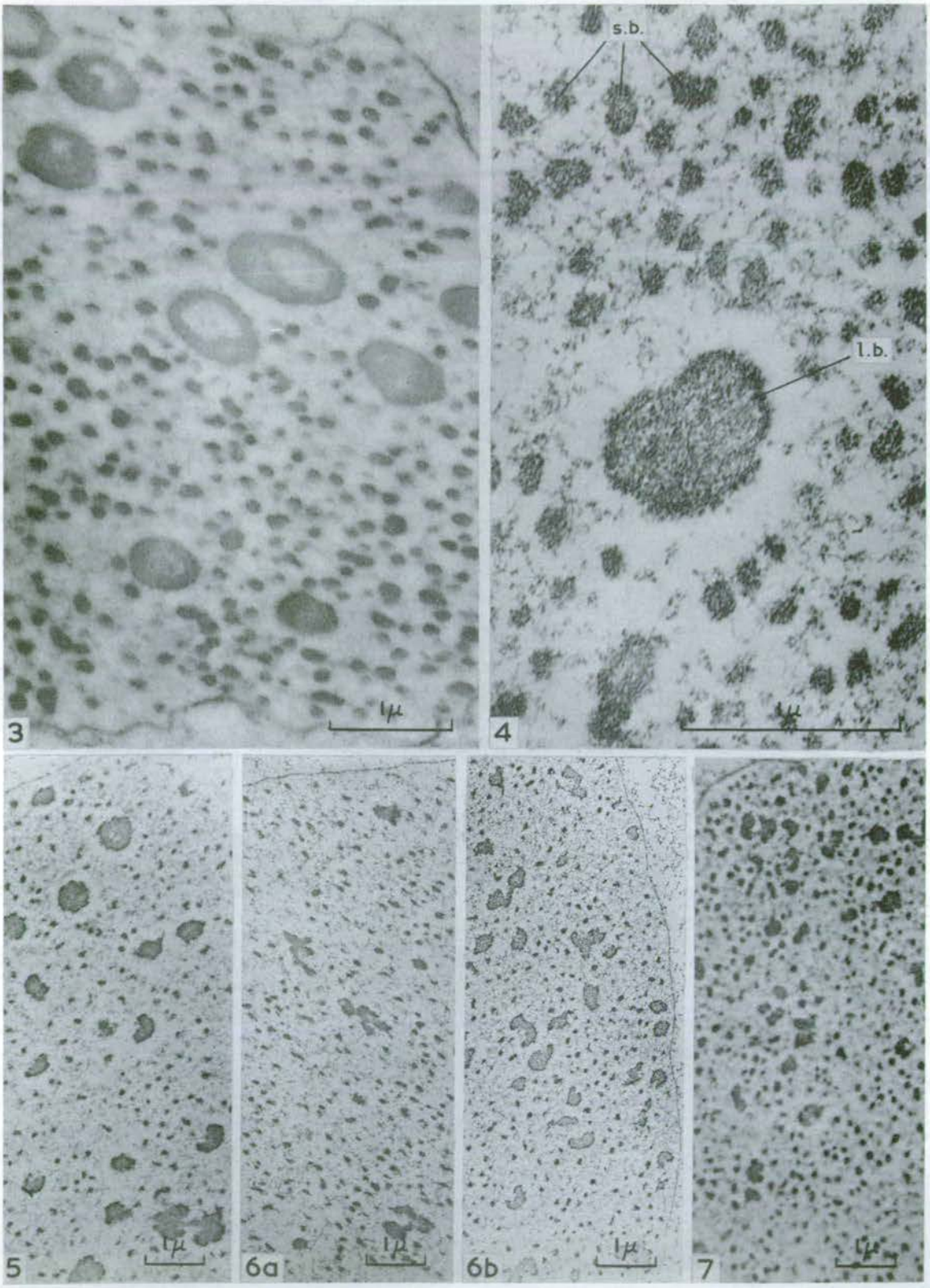

Fig. 3. Macronucleus of starved paramecium. Fig. 4. Detail of large body showing "halo." Figs. 5-7. Macronuclei in various stages of growing animals: Fig. 5—Fission stage; Figs. 6a, 6b—mid-way between two fissions; Fig. 7—¾ of time through interfission period.

large bodies are often seen, though here again in the absence of a complete set of serial sections it is impossible to be certain that the two portions are not joined together at some other level (Fig. 7). It should be added that at the various stages in the middle of the interfission period, the large bodies in a single macronucleus are by no means identical in appearance, and the above description is based on general impressions of a large number of nuclei at certain stages. Evidently the behaviour of the large bodies is not very well synchronised.

As for the small bodies, no regular sequence of changes in size or shape at different stages has been observed.

"Aged" paramecia, i.e., those from clones which have been prevented from undergoing conjugation or autogamy for a prolonged period (e.g., 47 days or 230 fissions) develop macronuclei in which the large bodies appear clumped together in irregular masses (Fig. 8), in a manner apparently similar to that recorded by Kimball(6) following treatment with ultra-violet light. Very "young" paramecia, i.e., those in clones derived from recent ex-conjugants or ex-autogamous animals, are noteworthy only for the relatively small size of the large bodies (Fig. 1).

The membrane around the macronucleus can be seen in osmium-fixed preparations, but does not appear in material fixed with alcohol and acetic acid (Figs. 2a and b). The membrane is double and often has conspicuous pores (Figs. 9a and b). Tangential sections (Fig. 10) show the pores to be about 40 mμ in diameter, though at different stages the size of the latter varies considerably. They are least conspicuous in starved animals, and appear much stretched out during fission when the macronucleus extends across the constriction between the two halves.

In an attempt to identify some of the constituents of the macronucleus as seen by electron microscopy, we treated some paramecia with RNA-ase and others with DNA-ase. RNA-ase was found to have little or no effect on the appearance of the macronuclear structures. DNA-ase clearly reduced the electron density of the large bodies while leaving that of the small bodies unaltered (Fig. 11). (In a separate paper(5) evidence has been described showing that, contrary to general belief, fixation with osmium does not necessarily interfere with the subsequent action of DNA-ase.) Other paramecia were treated by the "silver-Feulgen" method, and under favourable conditions there was seen to be a marked accumulation of fine "silver granules" in the large bodies (Fig. 12). Elsewhere within the macronucleus there was a relatively sparse deposition of silver, which was not concentrated within the small bodies, though to a slight extent around their surfaces. In view of possible non-specific deposition of silver, the indications derived from the "silver-Feulgen" method should be considered only in a confirmatory sense.

Electron microscope observations on the micronucleus. For comparative purposes some observations were made on the micronuclei which were occasionally to be seen in our preparations. Characteristically the micronucleus consists of a dense central region, apparently "hollow" in resting cells, and surrounded by a region of much lower electron density (Fig. 13) (as noted also by Sonneborn(11)). These regions correspond to the chromatin and vesicle, respectively, of the micronucleus of *P. aurelia* as seen in stained light microscope preparations. At least in a superficial way the micronucleus is similar to the large bodies of the macronucleus, though the diameter of the former is about 4 times that of the latter (Fig. 14). The micronuclear and macronuclear membranes appear to differ in that no obvious pores can be seen in the former, which is also distinguished by the possession of outpocketings (Fig. 14) similar to those found in the nuclear membranes of higher animals. Such outpocketings have not been seen to arise from the macronuclear membrane.

Light microscope studies of the macronucleus. When whole mounts of *P. aurelia* are stained by the Feulgen or Azure A methods the macronucleus appears very opaque and practically no details can be made out. Only at early stages in the development of the Anlagen can any specially stained areas be distinguished, as will be described in a later paper (see also (4)). Paraffin sections cut at 5 μ show an appearance of Feulgen-negative "vacuoles," approximately 1 μ in diameter, each one containing a Feulgen-positive granule in the centre. Between these "vacuoles" one sees an opaque, stained, "matrix" (Fig. 15). Similar sections stained by the methyl green-pyronin method show that the "vacuoles" are pyronin-positive, with central methyl green-stained spots. Thinner paraffin sections (2 μ) (Fig. 16a and b) however reveal that the macronucleus is composed of a mass of Feulgen-positive granules or rod-shaped structures, each surrounded by Feulgen-negative, pyronin-staining material. These Feulgen-positive structures are near to the limits of resolution with the light microscope and can only be interpreted with caution. However it appears that they are elongated structures not of uniform thickness, and one possibility is that they are made up of rows of granules of varying sizes. Careful scrutiny reveals the existence of pairs of parallel structures in which the individual granules within a particular "rod" correspond quite precisely (Fig. 16a and b). Comparisons of nuclei at different stages in the fission cycle have not shown any obvious differences in these structures, corresponding to the variations in the "large bodies" seen in the EM. Presumably this is because of reaching the limits of resolution obtained with the light microscope. The appearance of Feulgen-

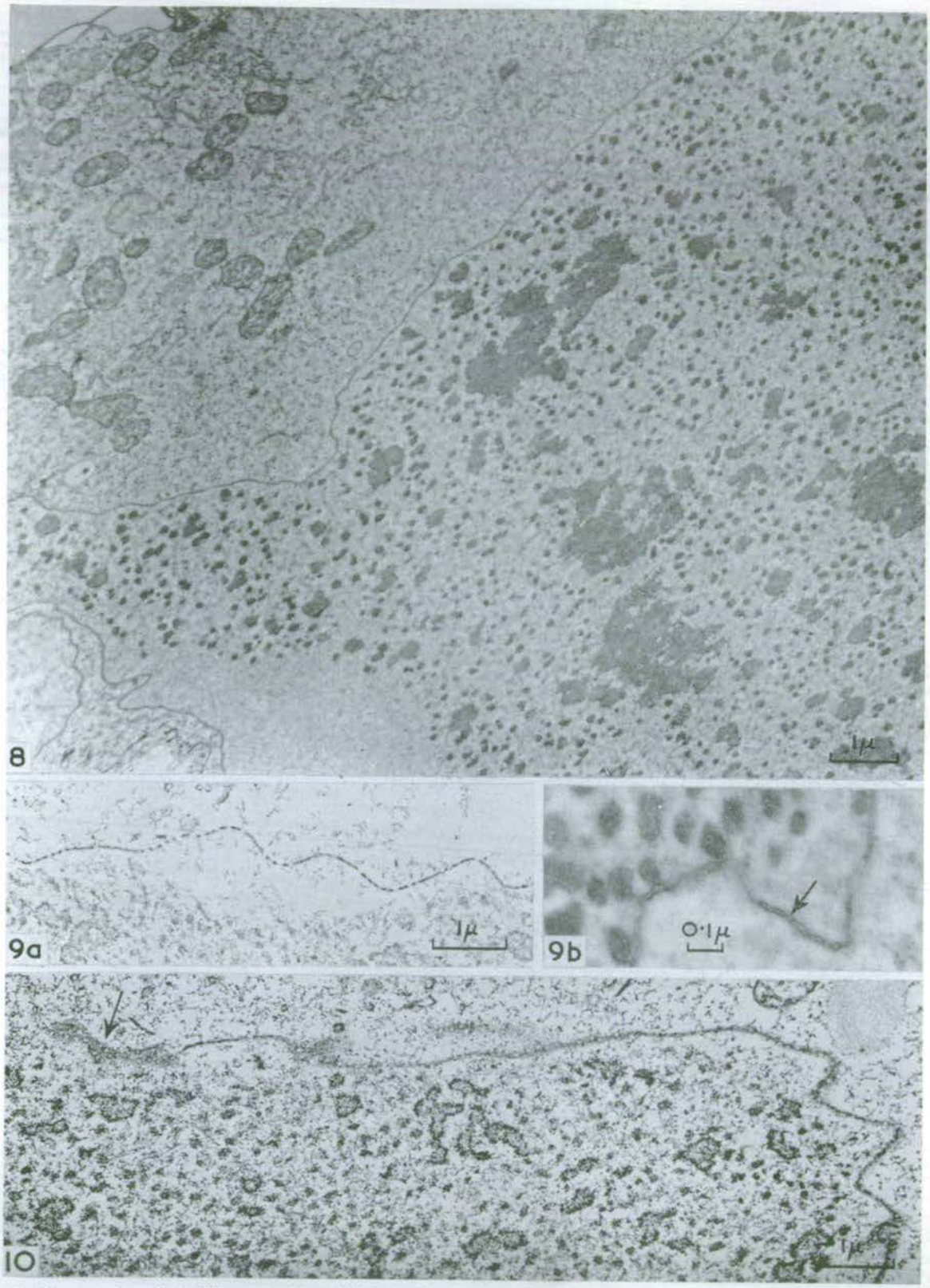

Fig. 8. Macronucleus in "old" paramecium (47 days after previous autogamy). Figs. 9a, 9b, 10. Details of macronuclear membrane. In Fig. 10 arrow indicates tangential section showing pores.

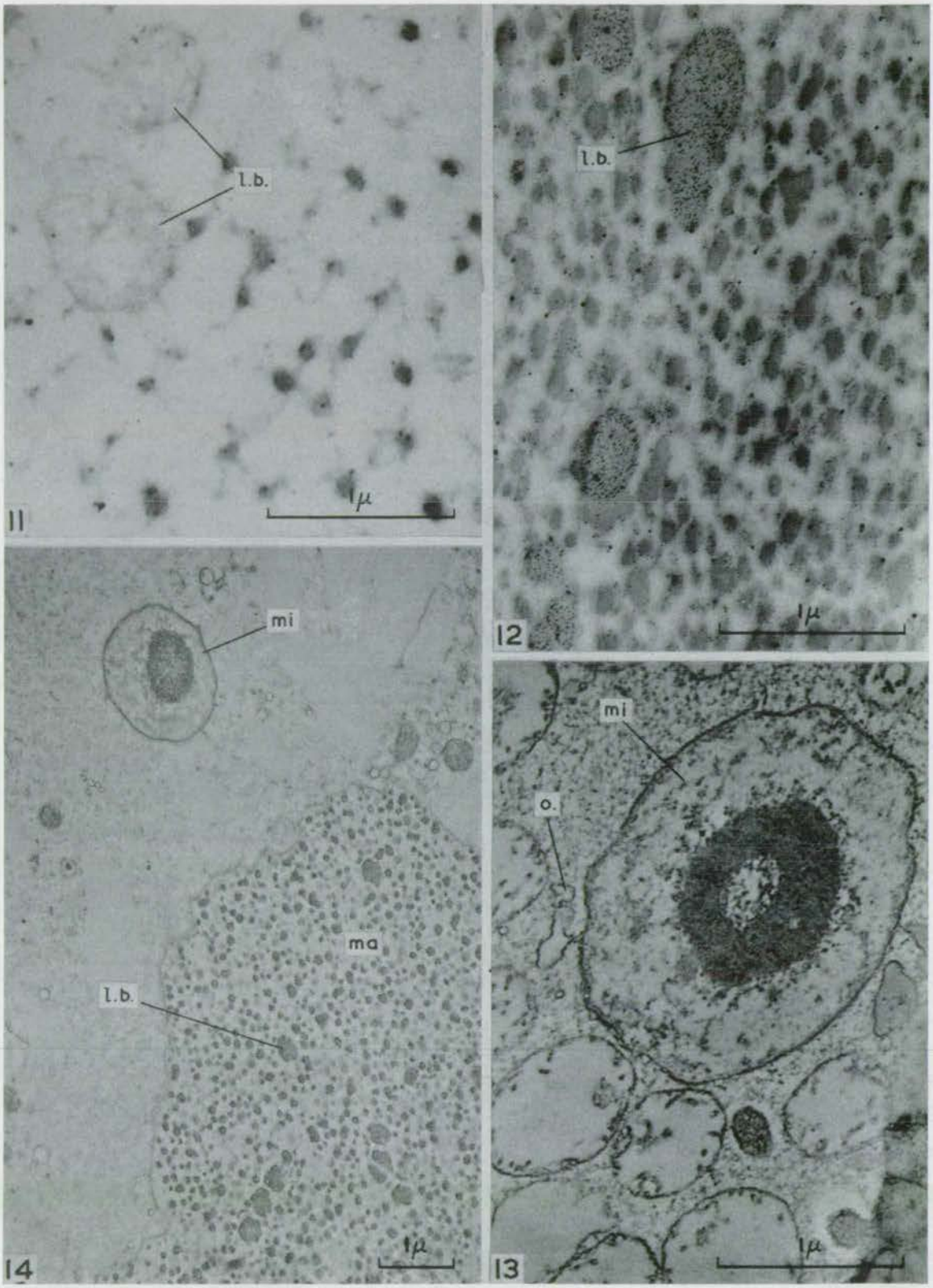

Fig. 11. Macronucleus after DNA-ase treatment. Fig. 12. Macronucleus after "silver-Feulgen" treatment. Note concentration of "silver granules" in large bodies. Fig. 13. Micronucleus. Fig. 14. Micronucleus for comparison with size of bodies in macronucleus.

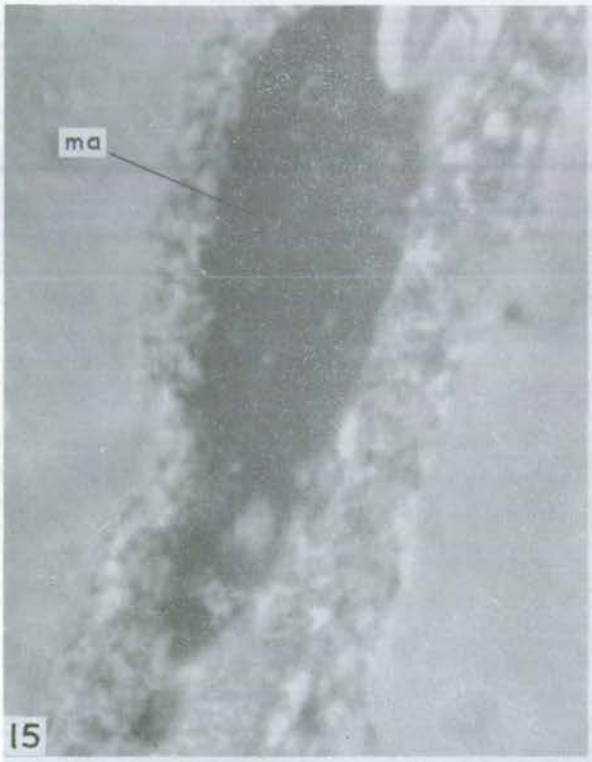

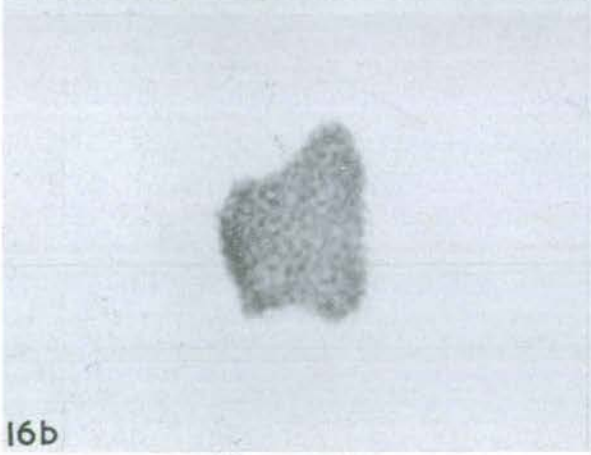

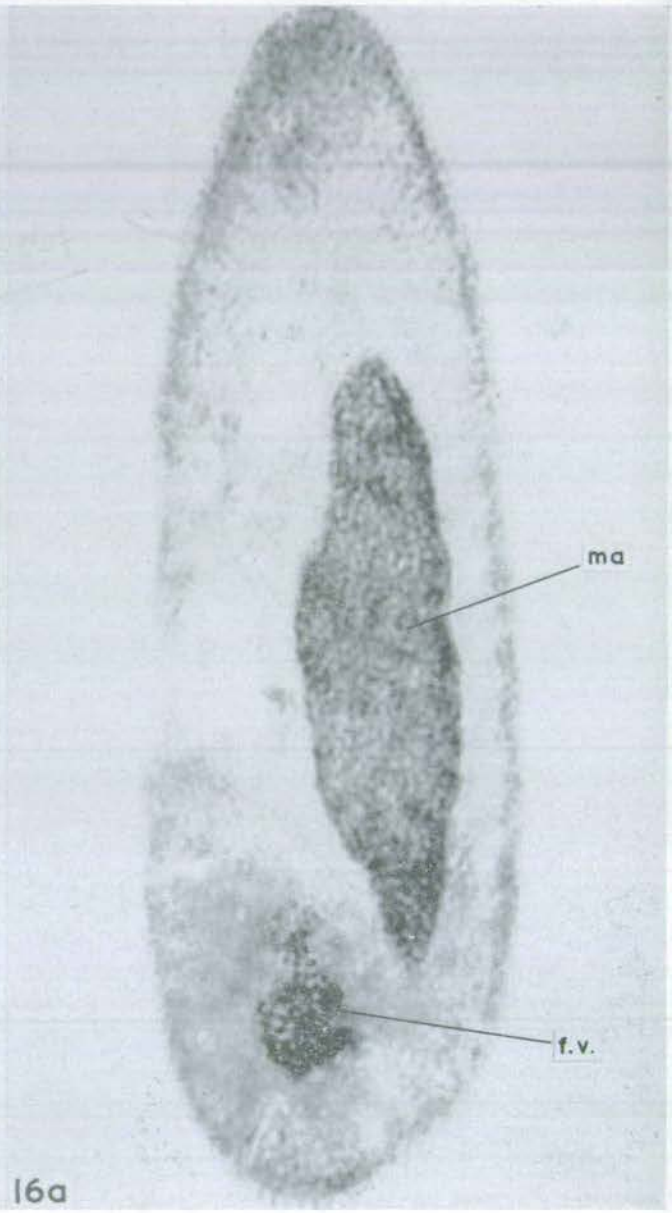

Fig. 15. 5 μ paraffin section stained with Azure A, × 5,000. Fixed in acetic alcohol. Figs. 16a, 16b. 2 μ paraffin section stained with Azure A, × 2,200.

negative "vacuoles" with central stained bodies in the thicker (5 μ) sections is assumed to be due to the vertical positioning of some Feulgen-positive elongated structures each surrounded by a hollow cylinder of Feulgen-negative material, and the "matrix" is an illusion due to the mass of Feulgen-positive bodies lying horizontally or obliquely (see *Addendum*).

DISCUSSION

In considering the composition of the various structures seen in EM preparations of the macronucleus, information may be utilised from the various treatments applied to such preparations, as with the nucleases and the "silver Feulgen" reaction, from comparisons of macronuclear and micronuclear structures, and finally by comparisons of EM and stained light microscope preparations. Such considerations lead us to believe that the electron-dense "large bodies" in EM preparations are DNA-containing structures, each surrounded by an RNA-containing zone probably coinciding with the "halo" often seen. The "small bodies" do not contain either DNA or RNA. This interpretation may seem at variance with the common finding of electron microscopists that nucleoli are electron-dense structures and chromosomes are usually described as "poorly visible." However all the evidence

obtained here supports our interpretation. We thus find ourselves in disagreement with the views of those who have proposed that the "large bodies" are nucleoli and the "small bodies" are chromosomes (e.g., Bretschneider, cited Kimball(7); Nanney & Rudzinska(8)). Similarly we cannot agree with the inter-

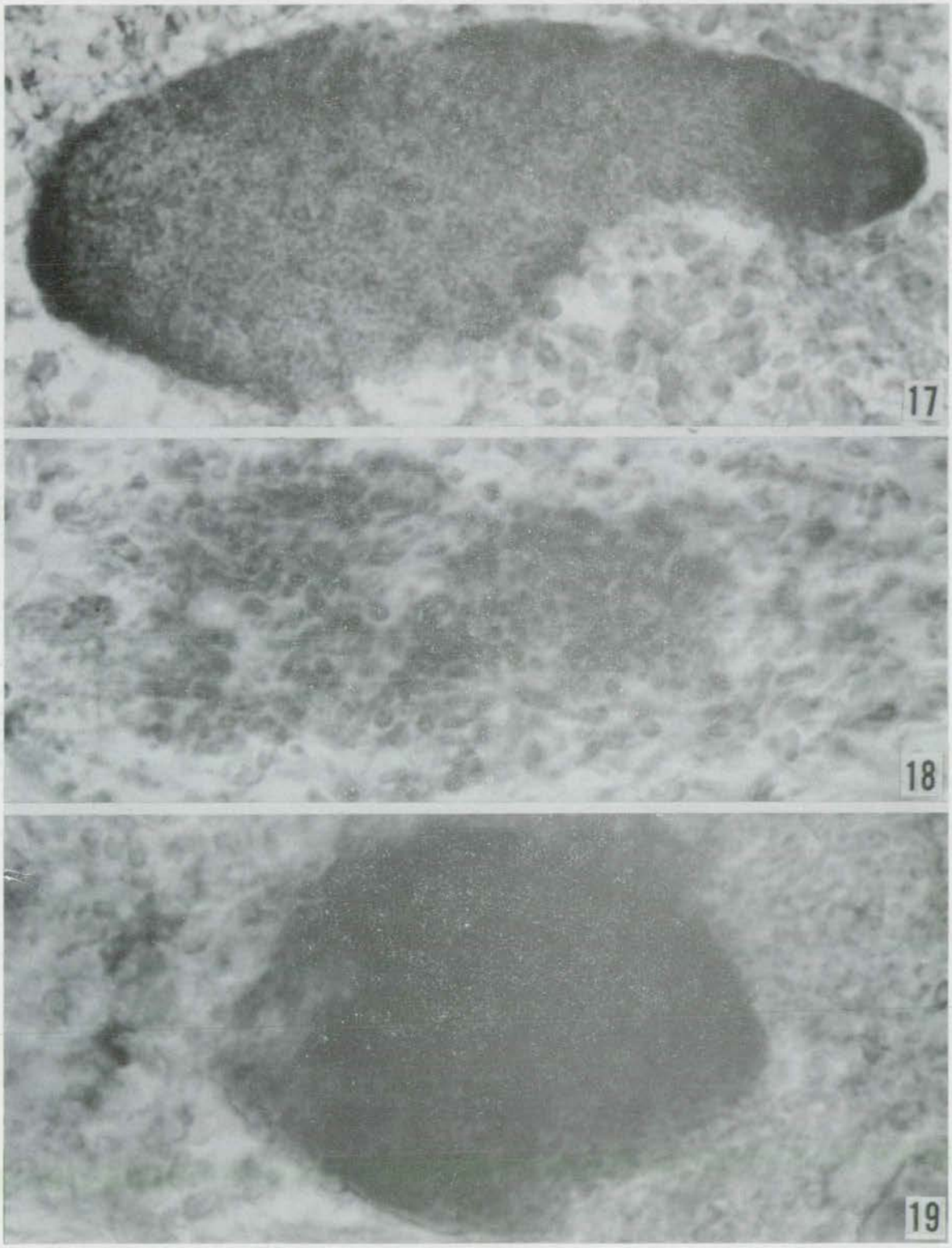

Fig. 17. Ultra-violet micrograph of RNA-ase treated macronucleus of *P. aurelia*. Fig. 18. As Fig. 17, but treated with DNA-ase. Fig. 19. As Fig. 17, but untreated with either nuclease. All × 4675. Photographed at 2570 Å.

Fixed OsO_4.

pretation of light microscopists that the Feulgen-negative, pyronin-positive bodies of diameter ~1 μ should be regarded as nucleoli, and that the mass of minute granules which can be seen when the cells are crushed chromosomes.

We would tentatively propose that the DNA of the macronucleus is concentrated within the "large bodies" seen in EM preparations, i.e., in the central regions of the RNA-containing "vacuoles" seen in light microscope preparations. These are the only candidates for the genetic "sub-nuclei" postulated by Sonneborn(10). Further discussion will be deferred until presentation of the results of studies of the development of the macronuclar Anlagen, to be given in a later paper.

We wish to acknowledge the help of Mr. D. C. Barker in the use of the electron microscope, and also of Mr. J. Nelson for cutting the 2 μ paraffin sections.

ADDENDUM: *A note on ultra-violet micrography.*

Some further information on the macronuclear structure of *P. aurelia* was obtained by ultra-violet micrography. Concentrated paramecia were fixed in OsO_4 as previously described and samples treated with ribonuclease and deoxyribonuclease. The material was then embedded in wax, sectioned at ca. 2 μ and mounted on quartz slides. The wax was dissolved away with xylol and the sections immediately covered with a small drop of pure castor oil, covered by a quartz cover-slip and sealed with wax. The Beck-Barnard ultra-violet microscope was used. Preparations were searched with a visual light (pointalite) phase-contrast system and specimens photographed in monochromatic light of the cadmium spark spectrum using the wavelength 2570 Å to obtain the maximum absorption of the nucleic acid in the macronucleus. A Zeiss 1.66 mm focal length quartz monochromatic objective corrected for 2570 Å immersed in glycerine, with a $\times 5$ quartz eyepiece, was used to obtain the absorption records. The source was a condensed spark between rotating cadmium disc electrodes. Using direct illumination an exposure of 2 seconds was required.

The prints are shown in Figs. 17-19. Very little structure can be made out in the sections untreated with either nuclease (Fig. 19), but the RNA-ase- and DNA-ase-treated preparations are strikingly different (Figs. 17, 18). The u-v absorption prints of RNA-ase-treated nuclei gave pictures similar to the Feulgen-stained preparations described earlier (Fig. 16), except that the u-v prints show more detail. There is a mass of very fine filaments and granules of diameter approximately 0.2 μ, and these presumably contain DNA. The DNA-ase-treated nuclei, by contrast, show an irregular collection of larger bodies of diameter approximately 0.6 μ, presumably containing RNA, some being elongated structures at least 2.5 μ long. These bodies are clearly separated one from another, and each contains a non-dense core. Finally, the outline of the macronucleus—i.e., the boundary between macronucleus and cytoplasm—is not clearly seen in the DNA-ase-treated preparation.

The u-v absorption prints thus confirm that the macronucleus consists of a large number of elongated bodies, each consisting of a DNA-containing core and an RNA-containing periphery. The diameter of the cores appears to be less than that of the "large bodies" seen in electron microscope preparations, but in view of the considerable variation in the sizes of the latter bodies at different stages, we do not place any significance on this size discrepancy. The u-v absorption prints also show that there is a DNA-containing "matrix" surrounding the above-described macronuclear bodies, and this matrix would appear to be particularly evident near to the outer boundary of the macronucleus.

REFERENCES

1. Beale, G. H., & Jurand, A. 1960. Structure of the mate-killer (mu) particles in *Paramecium aurelia*, stock 540. *J. gen. Microbiol.* **23**, 243-52.

2. Caulfield, J. B. 1957. Effects of varying the vehicle for OsO_4 in tissue fixation. *J. Biophys. Biochem. Cytol.* **3**, 827-9.

3. Delamater, E. D. 1951. A new cytological basis for bacterial genetics. *Cold Spr. Harbor Symp. Quant. Biol.* **16**, 381.

4. Jones, K. Macronuclear development in *Paramecium aurelia*. (In preparation.)

5. Jurand, A. 1961. Activity of nucleases on *Paramecium* cells fixed with osmium tetroxide. *Exptl. Cell Res.* **25**, 80-6.

6. Kimball, R. F. 1949. The effect of ultra-violet light on the structure of the macronucleus of *Paramecium aurelia*. *Anat. Rec.* **105**, 543.

7. ——— 1953. The structure of the macronucleus of *Paramecium aurelia*. *Proc. Natl. Acad. Sci.* **39**, 345-7.

8. Nanney, D. L., & Rudzinska, M. A. 1960. Chap. 3 in "The Cell," vol. 4, ed. J. Brachet and A. E. Mirsky. Academic Press, New York and London, pp. 109-50.

9. Palade, G. E. 1952. A study of fixation for electron microscopy. *J. Exptl. Med.* **100**, 641-

10. Sonneborn, T. M. 1947. Recent advances in the genetics of *Paramecium* and *Euplotes*. *Adv. Genet.* **1**, 264-358.

11. ——— 1953. Electron micrographs of ultra-thin sections of the nuclei of *Paramecium aurelia*. *Microbial Genetics Bull.* **7**, 24.

Studies on the macronucleus of *Paramecium aurelia*. II.

Development of macronuclear anlagen

by A. Jurand, G.H. Beale and M.R. Young

. Protozool. 11(4), 491-497 (1964).

Studies on the Macronucleus of *Paramecium aurelia*. II. Development of Macronuclear Anlagen

A. JURAND, G. H. BEALE and M. R. YOUNG*

Institute of Animal Genetics, Edinburgh 9, Scotland

YNOPSIS. The development of the macronuclear Anlagen f *Paramecium aurelia* was studied by means of electron, light nd ultra-violet microscopy of timed stages following conjuation. In the youngest Anlagen, no differentiated structures ould be made out, and staining reactions gave little or no ndications of the presence of DNA or RNA. As development roceeds, a number of conspicuous "sponge-like" RNA-containing bodies surrounded by a "matrix" containing DNA can be seen. Eventually these RNA bodies develop DNA centres and apparently disintegrate, yielding the "large bodies" characteristic of the mature macronucleus, and the "small bodies" then also appear. The relation of these observations to interpretations of the structural elements in the macronucleus is discussed.

THE first paper of this series(10) contained an account of the structure of the macronucleus of *Paramecium aurelia* based on observations by light, ultra-violet (UV) and electron (EM) microscopy. Attention was concentrated on the electron-dense "large bodies," (or "nucleoli," as usually denoted) which are structures approximately 0.5 μ in diameter but varying considerably at different stages of the cell cycle and under different environmental conditions, and which consist of an RNA-containing cortex and an elongated DNA-containing core. In the absence of any other suitable candidates for the macronuclear genetic sub-units postulated by Sonneborn(18) and others, the possibility that the "large bodies" might be such sub-units was considered. In the work to be described here an attempt is made to follow the development of the mature macronucleus from the early Anlagen formed during conjugation. We had hoped to trace this development back to the micronuclei of the conjugating cells, since the EM structure of the dense central part of the 'resting' micronuclei superficially resembled the structure of the macronuclear large bodies, though the micronuclei were much the larger of the two. The various micronuclear events during conjugation, however, have not been followed by us in detail, and this paper will deal only with a series of stages from early Anlagen to the mature macronucleus.

MATERIALS AND METHODS

Stock 60 (syngen 1) of *P. aurelia* was used. To obtain ex-conjugants at timed stages, sexually reactive cultures of opposite mating type were mixed in depression slides and allowed to form pairs for about 1 hr at 27°C. The pairs were then transferred individually to drops of nutrient medium and allowed to complete conjugation and the post-conjugational processes. Under these conditions conjugation usually lasted 5½ hr (sometimes less), and the first fission of the ex-conjugants usually occurred about 18 hr after commencement of conjugation. The times stated for the various stages mentioned in the "Results" section are calculated from the time of mixing of reactive cultures to the moment of fixation.

Fixation, embedding and sectioning of single ex-conjugant paramecia for electron microscopy was carried out as previously described(10). In addition, samples at all stages were

* At National Institute of Medical Research, Mill Hill, London.

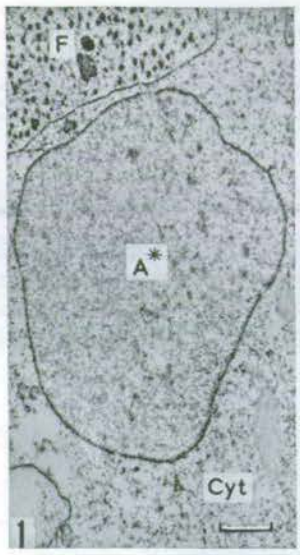

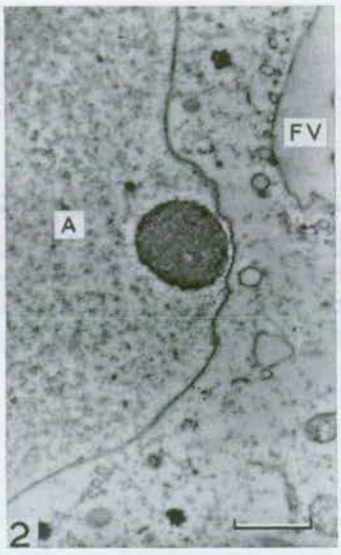

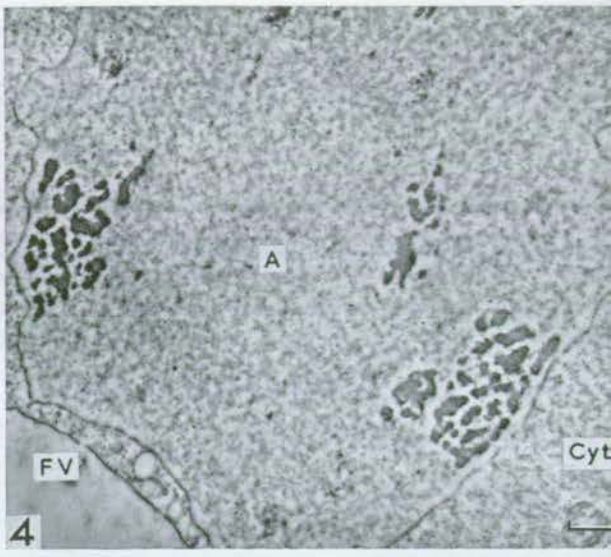

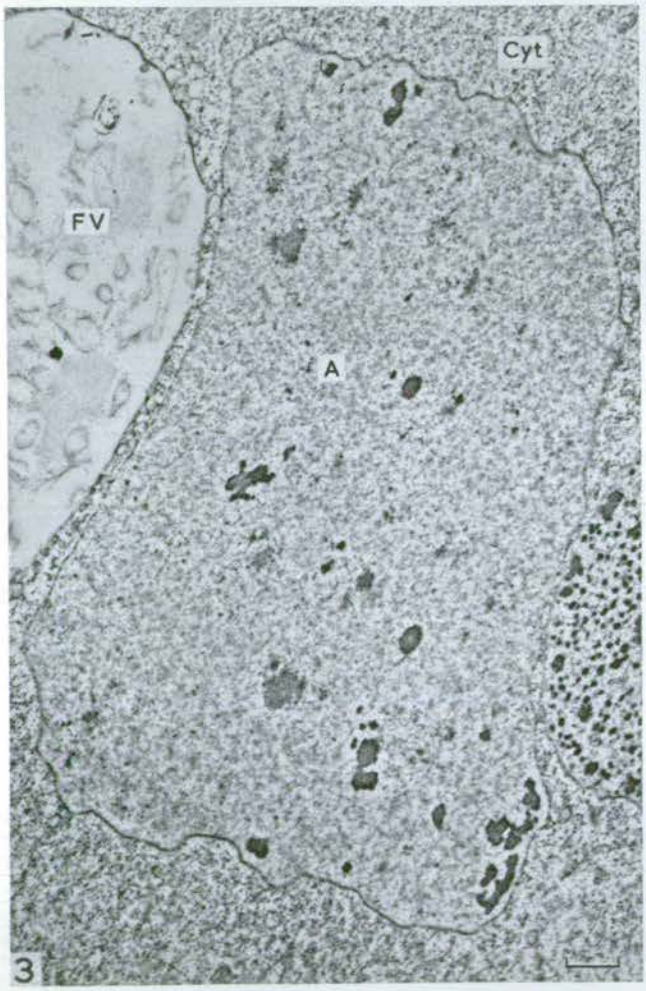

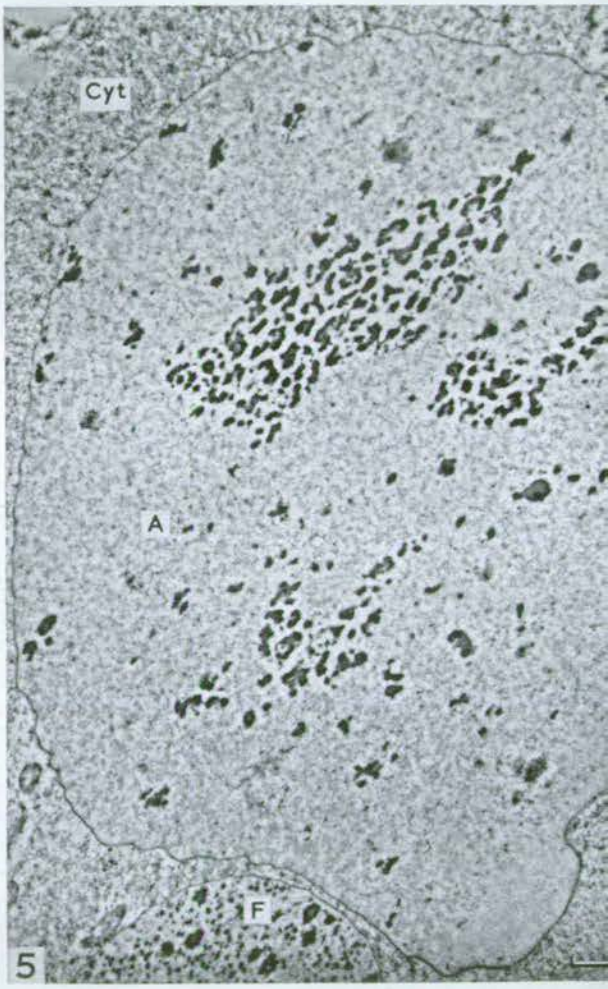

Figs. 1-5. Electron micrographs of developing Anlagen of *Paramecium aurelia*. A, Anlagen; F.V., food vacuole; Cyt, cytoplasm; F, fragment of old macronucleus. Fig. 1. Five hr after start of conjugation. × 6,600. A*, possible Anlage, see te Fig. 2. 10 hr. × 10,000. Fig. 3. 12 hr. × 6,600. Fig. 4. hr. × 6,600. Fig. 5. 17 hr. × 6,600.

embedded in wax, stained with Feulgen, Azure-A or methyl-green-pyronin, and examined by light microscopy, also as previously described. Since fixation of single paramecia was found to give EM preparations inferior to those of animals fixed in bulk, the EM photographs shown here were taken of paramecia fixed in bulk. These cultures were prepared as follows. About 100 ml of cultures of each of the two mating types in a sexually reactive state were mixed in large flat glass vessels (3 l Thompson flasks) at 27° giving shallow cultures of conjugating animals. After 1 hr the cultures were examined to confirm that at least 50% of the animals had formed pairs, and then about 100 ml of bacterized medium (pre-heated to 27°) was added. The excess food prevented any further animals from initiating conjugation at later times, but did not affect conjugations which had started earlier. At appropriate intervals the organisms were concentrated and fixed. For the material which was to be fixed at later stages, additional bacterized medium was added when necessary to ensure that the animals continued to grow at the maximum rate. Paramecia treated in this way varied to some extent in regard to their cytological stage of development at a given fixation time, but after previous study in single animals of the structures occurring at various precisely known times after start of conjugation, it was possible to identify and photograph particular stages in the bulk preparations. The material was prepared for UV absorption micrography as described previously(10).

RESULTS

The observations are illustrated by 10 photographs of EM preparations (Figs. 1-10), 2 light-microscope photographs of stained preparations (Figs. 11, 12), and 4 UV micrographs (Figs. 13-16). A series of stages can be recognized, and will be described in order.

Stage 1. In the earliest stage at which the Anlagen are recognizable they are roundish structures, 5-7 μ in diameter, which stain very faintly with Fuelgen, Azure-A or methyl green and in EM micrographs show practically no differentiated structures.

In Fig. 1 we show an EM picture of a cell recorded as being fixed 5 hr after commencement of conjugation. At this time in stock 60 of *P. aurelia* it is known that the syncaryon has usually formed and may have just divided, yielding presumptive micro- and macronuclear Anlagen(9). The exact stage of the nucleus shown in Fig. 1 cannot, however, be specified.

Stage 2—12 hr. At this stage the Anlagen, which have now grown to a diameter of 10-15 μ, stain faintly and uniformly with Fuelgen, Azure-A or methyl green. EM preparations show the appearance of sporadic dense bodies, variable in size and shape, but usually larger than the "large bodies" of mature macronuclei (compare the "large bodies" in the old macronuclear fragments with the dense bodies in the Anlage in Fig. 3). A slightly earlier stage, showing one very conspicuous dense body, is shown in Fig. 2. At these stages no "small bodies" (like those abundantly present in mature macronuclei) are seen, though the background is finely granular. UV absorption micrographs show a practically uniform appearance throughout the Anlagen at this time (Fig. 13).

Stage 3—15-20 hr. EM pictures now reveal the presence in each Anlage of a few prominent "sponge-like" aggregates of electron-dense material (Figs. 4, 5, 6 and 7). The electron-dense "small bodies" of the mature macronucleus are not seen at this stage. Treatment with ribonuclease resulted in a decrease in electron density of the sponge-like structures, but they were still visible (Fig. 7). Following staining with methyl-green pyronin at this stage, a small number of conspicuous pink areas are seen by light microscopy (Fig. 11), and staining with Fuelgen or Azure-A gives a corresponding group of unstained "vacuoles" (Fig. 12). U.V. absorption micrography shows one or a small number of dense bodies, and in some cases the "sponge-like" structure can be made out (Fig. 15).

The background to these aggregates is positively stained by Fuelgen, Azure-A or methyl green, but much less strongly than in the mature macronucleus.

Stage 4—21-30 hr. By this stage, which follows the first fission of the ex-conjugants, the Anlagen (or young macronuclei as they may now be called) contain a large number of electron-dense "small bodies," differing from those in the mature macronucleus only by the smaller size of the former (cf. "small bodies" in Anlage and in fragments of old macronucleus in Fig. 8). There are also present structures resembling the "large bodies" of mature macronuclei, but the number of such bodies is very small by comparison with those in the mature macronucleus.

At approximately the same stage, some EM preparations show curious and very complex structures (Figs. 9 and 10). They appear to be large aggregates in the process of disintegration. It is possible that they represent the last stage of development of the above mentioned "sponge-like" bodies, which may be breaking up into smaller elements each comprising a single "large body" of the type found in the mature macronucleus. Figs. 9 and 10 show that the smaller electron-dense components of these complex "disintegrating" agglomerates are often surrounded or partly surrounded by electron-dense "rinds," and fragments of the latter are scattered about in the vicinity.

Light microscope preparations at this stage show that the "matrix" of the Anlagen is fairly densely stainable with methyl-green, Fuelgen or Azure-A, though still not so densely as in the mature macronucleus. There are also large pyronin-positive areas which now contain methyl-green (or Azure-A) staining centers. UV absorption micrographs of these very late Anlagen are almost uniformly dark (Fig. 16), like those of mature macronuclei(10).

Later stages. Shortly after the stages shown in Figs. 8-10 and 16, the Anlagen rapidly develop into structures indistinguishable from mature macronuclei, the

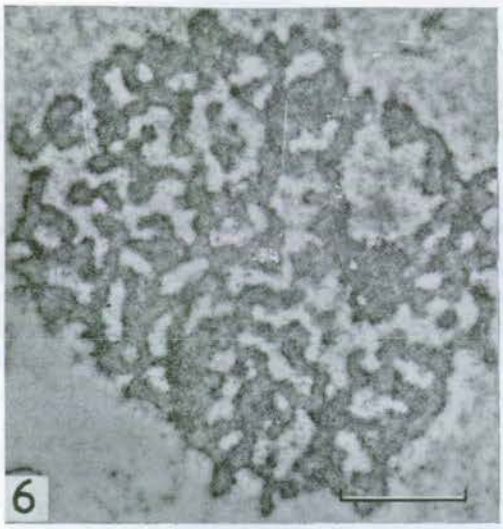

6

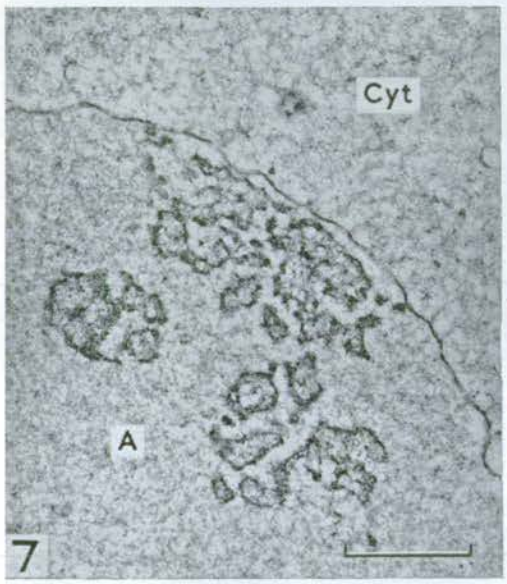

7

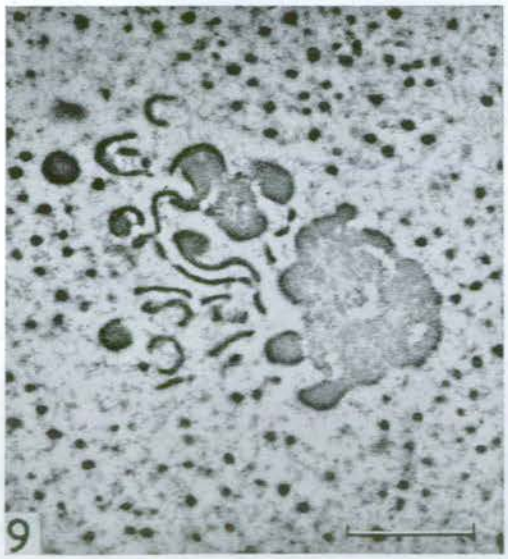

9

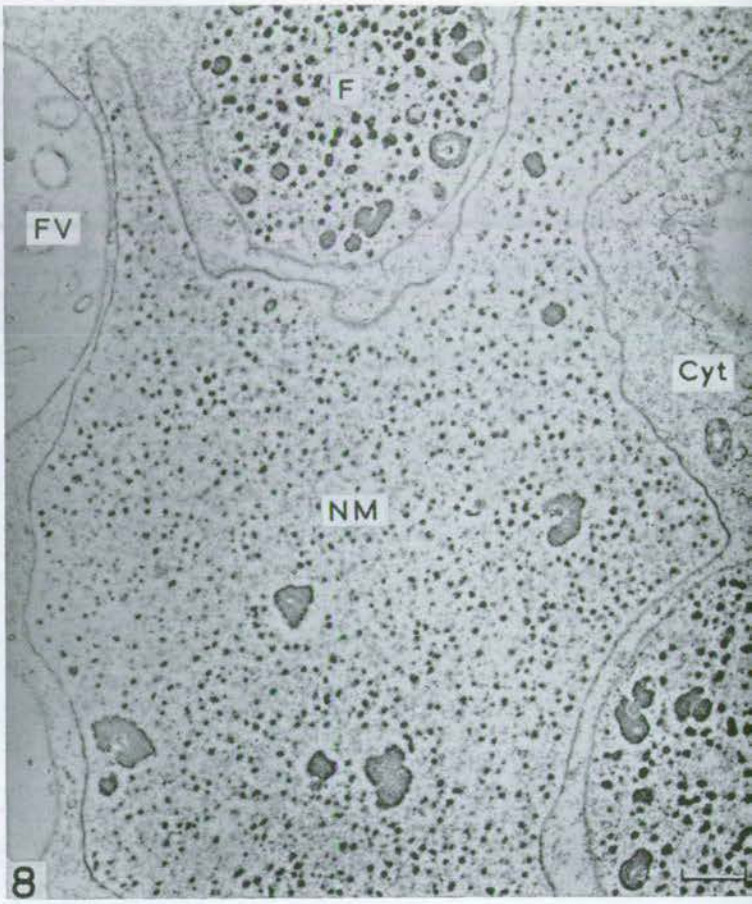

8

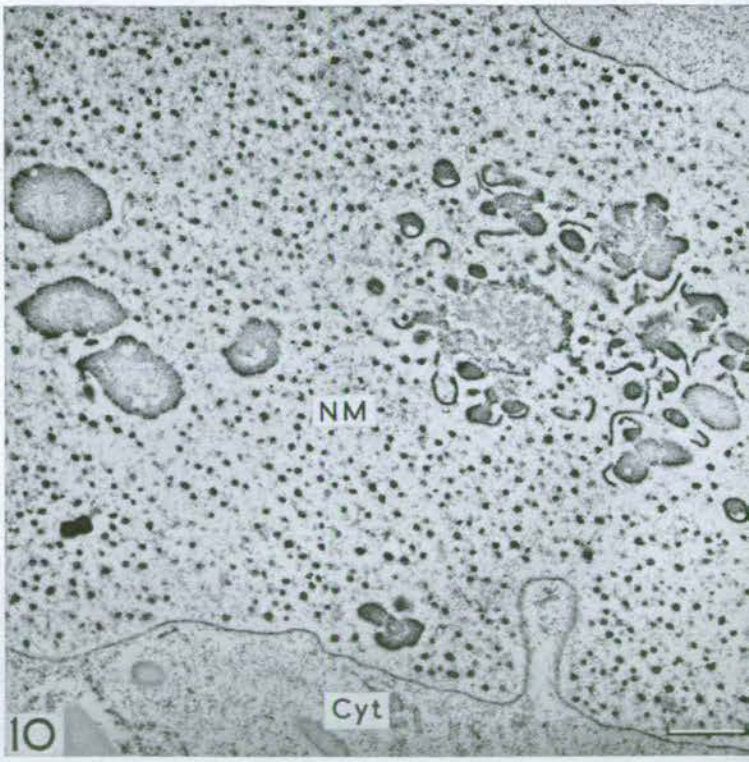

10

structure of which was described in our first paper (10).

DISCUSSION

The above-described observations may be interpreted in the following way. Initially the Anlagen are roundish bodies showing no differentiated structures by any technique used by us, and apparently containing very little DNA or RNA as judged by staining reactions. It must therefore be assumed that the genetic elements ("chromosomes"), derived from the micronuclei, are in an extremely diffuse condition at this stage. At about 12 hr after beginning of conjugation the Anlagen contain DNA distributed diffusely throughout, though no electron-dense "small bodies" are present. Shortly afterwards the large sponge-like bodies, rich in RNA, but lacking DNA centers, have appeared. Such structures had previously been observed in the developing Anlagen of *P. bursaria* by Ehret and Powers(3), who considered that there was a series of cycles of fusions of smaller "nucleoli" into the large aggregates. At about 30 hr, *i.e.*, after the first post-conjugational fission, at which the two Anlagen of *P. aurelia* segregate without dividing, the large RNA-containing aggregates now each have a DNA center as judged by staining of light microscope preparations, and appear to be in a state of "distintegration," as judged by the EM pictures. Possibly there are two (or even more) such disintegration processes occurring at stages 3, 4, etc. At stage 4, the "small bodies" characteristic of mature macronuclei, (but smaller than in the old macronuclear fragments) have now appeared, and there is a diffuse background of DNA. After this stage the macronuclei rapidly gain their mature appearance, the large sponge-like aggregates disappear, many typical "large bodies" are formed—each containing RNA with a DNA center, and there is a background consisting of very many "small bodies." The whole macronucleus now stains very intensely with nuclear stains.

In planning this work we had hoped to demonstrate some sort of continuity between structures in the micronuclei and certain components (especially in the "large bodies") in the mature macronuclei. This hope has obviously not been realized: the developing Anlagen pass through a very complicated series of stages at which structures unlike those in either the micronucleus or the macronucleus are present; and on the other hand the Anlagen lack the characteristic structures of the two types of nuclei.

In our earlier paper(10) we tentatively put forward the unconventional view that the electron-dense "large bodies," (usually called "nucleoli") might be the macronuclear sub-units postulated on genetic evidence by Sonneborn(18). We also at first drew the conclusion that most or even all the macronuclear DNA was contained within these "large bodies." However, our own UV absorption pictures, which were obtained after the earlier paper(10) was already in press, and published as an addendum to that paper, did not support this view, for they indicated that a DNA-containing matrix surrounding the "large bodies" was probably present. Further, Dippell and Sinton(1) have now published other evidence in favor of such a matrix, making use of a treatment described earlier by Kimball and Gaither(13). This involved irradiation of paramecia with an intense beam of UV causing the "large bodies" in the macronucleus to fuse into one or a few vacuolated masses. After such treatment Dippell and Sinton(1) found that the area outside these masses stained positively for DNA, and when examined by electron microscopy, were seen to contain many "small bodies." In a further note, Dippell(2) states that localization of tritiated thymidine in untreated cells and in early fusion stages led to a similar interpretation. We therefore must accept that there is a DNA-containing matrix between the "large bodies," but in our view it has still not been definitely proved that the DNA is entirely concentrated within the "small bodies." Such proof might be provided if the "small bodies" would be digested away by DNA-ase treatment, but in our earlier study we were unable to demonstrate this. It is to be hoped that future work will clarify this point.

It is relevant here to refer to the observations of Fauré-Fremiet, Rouiller and Gauchery(5), who made an electron microscope study of the macronucleus of *Euplotes eurystomus*. These workers found that the "small bodies" (denoted "DNA-microsomes") passed through a regular cycle of disaggregation and reaggregation in the two reorganization bands which appear at the two ends of the macronucleus of this organism, and migrate towards the center where they finally fuse and disappear. However, as the cited authors point out: "on ne saurait conclure que chaque granule désoxyribonucléique représente un chromosome." Gall(6) showed that the reorganization bands were the sites of a doubling in the concentration of DNA. Finally, Kimball and Prescott(14) found, by a technique involving use of ^{3}H-thymidine, that there

Figs. 6-10. Electron micrographs of later stages in Anlagen development. A, Anlage; Cyt, cytoplasm; F.V., food vacuole; F, fragment of old macronucleus; NM, new macronucleus (or late Anlage). Fig. 6. Detail of RNA-containing sponge-like body in Anlage at 21 hr stage. × 15,000. Fig. 7. As Fig. 6, but treated with ribonuclease for 3 hr after fixation. × 15,000. Fig. 8. New macronucleus (or late Anlage) at 30 hr stage, showing numerous "small bodies." × 7,500. (Assumed earlier stage than Figs. 9 and 10.) Fig. 9. Detail of RNA-containing aggregate apparently "disintegrating," 30 hr stage. × 15,000. Fig. 10. New macronucleus (or late Anlage) showing "disintegrating RNA-rich aggregates and numerous small bodies; 30 hr stage. × 9,000.

was a complete mixing of DNA in the macronucleus in preparation for division. The view of Grell(7), according to which the chromosomal structures in macronuclei multiply by endomitosis was not confirmed by Fauré-Fremiet, Rouiller and Gauchery(5). It seems more likely that replication of the chromatin bodies involves a cycle of dispersion and reaggregation, but if this is so, no evidence for it has been found so far in *P. aurelia*. According to Kimball and Barka(12), DNA synthesis occurs during the second half of the interfission period in this ciliate. During this time no obvious changes in the "small bodies" were observed by us in our earlier study(10), though if a proportion of "small bodies," randomly spread throughout the macronucleus, were dispersing and/or reaggregating at a given moment, this would be difficult to observe. Possibly during the early Anlage stages such a dispersion takes place, and this is presumably a period of massive DNA synthesis.

It might be hoped that further information on the problem of the homologies of the macronuclear elements would be gained by a study of ciliate species known to contain, in their micronuclei, a relatively small number of conspicuous chromosomes. Such a form is *Tetrahymena pyriformis*, in which Ray(16) found the diploid chromosome number to be ten. Roth and Minick(17) and Elliott *et al.*(4) have carried out EM studies of the macronucleus of this ciliate, show-

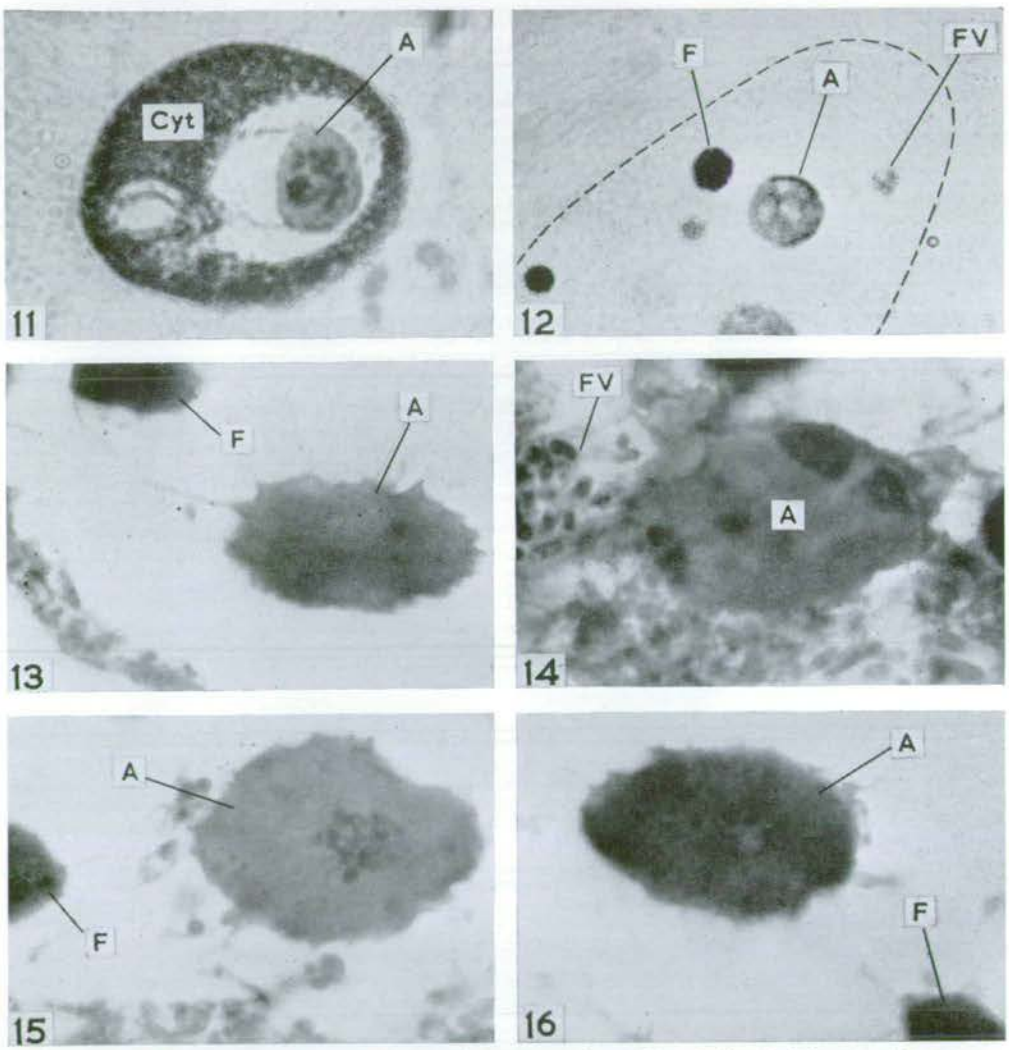

Fig. 11. Light-microscope photograph of 2 μ section of a cell at 22 hr stage stained with methyl green-pyronin. Cyt, cytoplasm; A, Anlage. The dark areas in the Anlage are stained with pyronin and presumed to contain RNA. × 1,000.

Fig. 12. Light-microscope photograph of 2 μ section of a cell at 19 hr stage, stained with Azure A. A, Anlage; F, fragment of old macronucleus; F.V., food vacuole. The Anlage is stained with Azure A except in 3 areas corresponding to the pyronin-positive bodies in Fig. 11. × 1,000.

Figs. 13-16. UV (2,750 Å) absorption micrographs. A, Anlage; F, fragment of old macronucleus; F.V., food vacuole. All × 3,300. Fig. 13. 12 hr stage. Fig. 14. 16 hr stage, showing a few dark areas corresponding to RNA-containing bodies in Fig. 11. Fig. 15. 18 hr stage, showing one "sponge-like" aggregate. Fig. 16. 24 hr stage, showing almost uniform absorption throughout.

ing the presence of a number of peripheral crescent-shaped "nucleoli" (or "large bodies"), and a mass of "chromatin bodies" (or "small bodies" in our terminology). In general the homologies of these elements seem to be no clearer in *Tetrahymena* than in *Paramecium*, however. The situation in various other ciliates in reviewed by Grell(8) and Pitelka(15).

To sum up, we must regretfully concede that our new observations on the structure of the Anlagen in *P. aurelia* do not throw any light on the problem of the genetic sub-units in the macronucleus. Indeed our earlier proposal that the electron-dense "large bodies" might be the genetic sub-units was founded on the thought that the "large bodies" were the only structures within the macronucleus having the complex organization required for such genetic sub-units. The "small bodies" could hardly be considered to have such complexity. While it is conceivable (though in our opinion unlikely) that they might be "chromosomes"(11), it is extremely improbable that the "small bodies" are equivalent to genetically complete nuclei. Thus if we have to abandon the "large-body" hypothesis of genetic sub-units, the reality of the genetic sub-units themselves becomes more nebulous.

Nevertheless it is hoped that the additional details pertaining to Anlage development which we have described will be of value for the eventual construction of a satisfactory theory of macronuclear structure in *Paramecium*. For the moment we find ourselves unable to propose one.

REFERENCES

1. Dippell, R. V. & Sinton, S. E. 1963. Localization of macronuclear DNA and RNA in *Paramecium aurelia*. *J. Protozool.* **10** (Suppl.), 22.

2. Dippell, R. V. 1963. Nucleic acid distribution in the macronucleus of *Paramecium aurelia*. *J. Cell Biol.* **19**, 20A.

3. Ehret, C. F. & Powers, E. L. 1955. Macronuclear and nucleolar development in *Paramecium bursaria*. *Exptl. Cell Research* **9**, 241-57.

4. Elliott, A. M., Kennedy, J. R. & Bak, I. J. 1962. Macronuclear events in synchronously dividing *Tetrahymena pyriformis*. *J. Cell Biol.* **12**, 515-31.

5. Fauré-Fremiet, E., Rouiller, Ch. & Gauchery, M. 1957. La réorganisation macronucléaire chez les *Euplotes*. Etude au microscope électronique. *Exptl. Cell Research* **12**, 135-44.

6. Gall, J. G. 1959. Macronuclear duplication in the ciliated Protozoan *Euplotes*. *J. Biophys. Biochem. Cytol.* **5**, 295-308.

7. Grell, K. G. 1949. Die Entwicklung der Makronucleusanlage im Exkonjuganten von *Ephelota gemmipara*. *Biol. Zentr.* **68**, 289-312.

8. ——— 1962. Morphologie und Fortpflanzung der Protozoen (einschliesslich Entwicklungsphysiologie und Genetik). *Fortschr. Zool.* **14**, 1-85.

9. Jones, K. 1956. Nuclear differentiation in *Paramecium*. Ph.D. Thesis, Aberystwyth University.

10. Jurand, A., Beale, G. H. & Young, M. R. 1962. Studies on the macronucleus of *Paramecium aurelia*. I (with a note on ultra-violet micrography). *J. Protozool.* **9**, 122-31.

11. Kimball, R. F. 1953. The structure of the macronucleus of *Paramecium aurelia*. *Proc. Natl. Acad. Sci. U.S.* **39**, 345-7.

12. Kimball, R. F. & Barka, T. 1959. Quantitative studies on *Paramecium aurelia*. II. Feulgen microspectrophotometry of the macronucleus during exponential growth. *Exptl. Cell Research* **17**, 173-82.

13. Kimball, R. F. & Gaither, N. 1951. The influence of light upon the action of ultraviolet on *Paramecium aurelia*. *J. Cellular Comp. Physiol.* **37**, 211-33.

14. Kimball, R. F. & Prescott, D. M. 1962. Deoxyribonucleic acid synthesis and distribution during growth and amitosis of the macronucleus of *Euplotes*. *J. Protozool.* **9**, 88-92.

15. Pitelka, D. R. 1963. *Electron Microscopic Structure of Protozoa*. Pergamon, Oxford.

16. Ray, C. 1956. Meiosis and nuclear behaviour in *Tetrahymena pyriformis*. *J. Protozool.* **3**, 88-96.

17. Roth, L. E. & Minick, O. T. 1961. Electron microscopy of nuclear and cytoplasmic events during division in *Tetrahymena pyriformis*. *J. Protozool.* **8**, 12-21.

18. Sonneborn, T. M. 1947. Recent advances in the genetics of *Paramecium* and *Euplotes*. *Advances in Genet.* **1**, 264-358.

The fine structure of the parasitic suctorian

Podophrya parameciorum

by A. Jurand and R. Bomford

THE FINE STRUCTURE OF THE PARASITIC SUCTORIAN *PODOPHRYA PARAMECIORUM*

rtur JURAND and Robert BOMFORD
stitute of Animal Genetics, West Mains Road, Edinburgh, 9

OURNAL DE MICROSCOPIE — Vol. 4, n° 4 - 1965 - pp. 509 à 522

JOURNAL DE MICROSCOPIE

Le « Journal de Microscopie », créé en 1962, est publié par les soins de la Société Française de Microscopie Electronique avec le concours du Centre National de la Recherche Scientifique.

Le « Journal de Microscopie » paraît tous les deux mois (soit six numéros par an) et publie des articles originaux portant sur la microscopie et ses applications (microscopie classique, électronique, ionique, X, etc...; applications à la cristallographie, à la biologie, à la métallographie, etc...). Le journal accepte des articles en *anglais* et en *allemand*.

ABONNEMENT

	1962, 1963, 1964, 1965 (par volume)		1966	
Laboratoires et Firmes	100, - F	21, - US $	140, - F	30. - US $
Particuliers, *à titre strictement privé*	80, - F	17, - US $	100, - F	21. - US $
Membres de la S.F.M.E., *à titre strictement privé*	50, - F	10,50 US $	65, - F	14. - US $
Numéro séparé	20, - F	4,50 US $	30, - F	7. - US $

La souscription doit être envoyée à la :
Société Française de Microscopie Electronique
Ecole Normale Supérieure — Laboratoire de Botanique
24, rue Lhomond — Paris 5e.

Le paiement peut être fait :

par chèque bancaire, ou par virement postal (C.C.P. Paris 10 797-33), établi **au nom de la Société Française de Microscopie Electronique.**

Tous ces prix sont nets de toute remise.

J. Microscopie (1965), **4**, 509-522.

THE FINE STRUCTURE OF THE PARASITIC SUCTORIAN *PODOPHRYA PARAMECIORUM*

Artur JURAND and Robert BOMFORD *
Institute of Animal Genetics, West Mains Road, Edinburgh, 9

INTRODUCTION

Many instances of parasitism on other ciliates by members of the suctorian family Podophryidae have been recorded; the described species being assigned either to the genus *Podophrya* or the genus *Sphaerophrya* (3, 11, 12, 15, 25).

The organism used for this work, parasitic on *Paramecium bursaria*, so closely resembles that previously described (25) as *Podophrya parameciorum incursella* that, despite the fact that the stalked cyst stage observed in this species has not been detected in our material, and that the adult in our stock reaches a greater size (40 μ as compared to 24 μ), it has been included in this species.

The life history as so far observed thus consists of two stages: a free-swimming ciliated larva and a non-ciliated adult with sucking tentacles. In addition, in cultures which have been allowed to starve, and in which all the host organisms have lysed, unattached individuals of *P. parameciorum*, spherical in shape, smaller than the feeding adult, and without tentacles may be found.

Our observations have been confined to the adult stage and the following features have been given special attention; the position of the parasite in the host and its effect on the host; the structure and cytochemical properties of the macronucleus; and the structure of the tentacles and their associated elements.

* The junior author is a holder of a post-graduate award for research training from the Medical Research Council of Great Britain.

MATERIALS AND METHODS

The culture of *P. parameciorum* used was derived from infected in dividuals of *P. bursaria* collected in Elf Loch, Edinburgh, in June, 1964 The density of *P. bursaria* in the collections made at this time range from 40 paramecia/ml to over 600/ml. Over 75 % of the parameci isolated from the collections (46 out of 60 individuals) were infected Further collections were made from Elf Loch in the following months and the density of *P. bursaria* fell so that only a few individuals coul be recovered from a 5 ml sample. Under these conditions no infecte paramecia were found.

The cultures of *P. parameciorum* were maintained in test tubes i the light at room temperature and fed once a week with uninfecte *P. bursaria*. Various different stocks of *P. bursaria* could be used, bu *Paramecium aurelia* and *Paramecium caudatum* were not attacked In this respect our material resembles the stock of *P. parameciorur* previously described (25).

To obtain sufficient material for light and electron microscop 2 litre cultures of *P. bursaria* were innoculated with a test-tube full c infected paramecia. After about a week 100 % of the paramecia in th mass culture were found to be infected with *P. parameciorum*. Th culture was harvested by filtration through absorbent cotton wool (t remove debris) followed by centrifugation in an oil-testing centrifuge

For light microscopy the organisms were fixed in a 5 % solution c trichloro-acetic acid with 1.37 % lanthanum acetate for 1 hour. Afte dehydration by resuspension in alcohols (35 %, 70 %, 95 %, and thre changes of 100 %, with ten minutes in each strength) they were re suspended twice in benzene, used as a clearing agent, and then trans ferred to a preheated solid watchglass half filled with paraffin wax a a temperature of 54 °C. The benzene was evaporated overnight in th oven at 56 °C. The resulting suspension in paraffin wax was transferre into tin foil moulds and kept for about ten minutes in the oven befor cooling so that the organisms could form a layer at the bottom of th mould. Sections were cut at a thickness of 3-4 μ, mounted on slides an stained with Feulgen reagent or methyl green - pyronin.

For electron microscopy the organisms were fixed in a 1 % solutio of osmic acid buffered to pH 7.2 with veronal-acetate and with sucros added to make the osmotic pressure equivalent to 0.2 % saline solution After 30 minutes fixation and dehydration with alcohols (see preparatio for light microscopy) the organisms were embedded either in metha

crylate mixture or in Araldite. Ultra-thin sections were cut on a Porter-Blum Servall microtome, mounted on collodion-carbon coated grids and, in the case of Araldite-embedded material, stained for 20 minutes with a 1 % potassium permanganate solution containing 2.5 % uranyl acetate. The sections were examined and photographed using the Philips EM 75 or AEI EM 6 electron microscopes.

RESULTS

1. THE POSITION OF THE PARASITE IN THE HOST

The adult *P. parameciorum* lies in a pouch formed by an invagination of the paramecium pellicle (Pl. I, fig. *a* and *d*), frequently but not always in the gullet region. Larvae, produced by budding, are released to the exterior (Pl. I, fig. *b*), and the parasite may also divide by transverse fission within the host, the product of the division remaining in the pouch (Pl. I, fig. *c*). Amongst 48 infected *P. bursaria* isolated from Elf Loch the greatest number of *P. parameciorum* within a single paramecium was 6, the average being between two and three.

The parasite is connected to the paramecium via the tentacles (Pl. II), and elsewhere in the pouch the surfaces of two organisms remain apart.

2. THE EFFECT OF THE PRESENCE OF THE PARASITE ON THE HOST

P. parameciorum does not paralyse its host, in contrast to some sessile Suctoria which paralyse their prey (21). This lack of paralysis is perhaps the only justification for describing the association between *Podophyra parameciorum* and *Paramecium bursaria* as one between parasite and host rather than predator and prey. The majority of paramecia in an infected culture do however finally lyse.

Usually a depletion of the paramecium cytoplasm may be seen around the point of attachment of a tentacle (Pl. II, in the lower part, *Par*) from whence, presumably, it has been removed by the parasite. In the lower right hand corner of Pl. I, fig. *d*, may be seen the micro- and macronuclei of the infected paramecium (*Par ma* and *Par mi*). Their contents appear to have been destroyed in the regions nearest to the parasite although the nuclear membranes, at least in the plane of the section, remain intact. Similar effects have been seen in many other

sections. This suggests that *P parameciorum* actively secretes enzymes into the host at some stage during the feeding process, which thus does not merely consist of the sucking out of intact host material.

3. *GENERAL STRUCTURE OF P. PARAMECIORUM*

The surface of the organism is covered by two membranes (Pl. II), the outer called the alveolar pellicle and the inner the plasma membrane by previous authors (13, 19). The outer membrane comes into contact with the inner at intervals of 0.5 to 1.0 μ, and at some of these points of juncture a small pit is formed (Pl. II, *pt*). These pits resemble the cuticular pores described in *Epistylis anastatica* (4).

The details of the structure of the two surface membranes cannot be seen in any of the micrographs we have included in this paper. However from other excluded micrographs the following details may be gathered. The alveolar pellicle consists of two unit membranes each 6 mμ thick with the space between them 7 mμ wide, and the plasma

FIGURE 1. Diagrammatic representation of the alveolar pellicle of Podophrya parameciorum showing the double unit membrane of the outer pellicular membrane and a single unit plasma membrane with the adjacent dense layer of the cytoplasm.

membrane of a single unit membrane. The latter is a continuation of the inner of the two unit membranes of the alveolar pellicle as shown in Figure 1. Beneath the plasma membrane there lies a strip of electron-dense cytoplasm.

The contractile vacuole and pore are similar to those of *Tokophrya infusionum* (18).

Description of the mitochondria is complicated by the fact that it is difficult to distinguish those that belong to the parasite from those that have just been ingested from the host. However all the bodies of mitochondrial form seen in the cytoplasm of *P. parameciorum* have the typical protozoan mitochondrial structure (*e.g. mit,* at the upper left corner of Pl. II).

No food vacuoles of normal appearance have been observed. To the left of the tentacle in Pl. II, may be seen the cell body of an alga (*A*) from the host (*P. bursaria* contains symbiotic algae) lying unenclosed in the cytoplasm of the parasite. This fortunate chance of being able to identify part of the parasite's meal allows us to suggest that the material ingested by the parasite may indeed not be organised into conventional vacuoles.

STRUCTURE OF THE NUCLEI OF P. PARAMECIORUM

P. parameciorum possesses a single massive macronucleus about 10 μ in diameter (Pl. I, fig. *d* and Pl. III, fig. *a*) and a smaller micronucleus 3 μ in diameter (Pl. III, fig. *b*).

In electron micrographs of equatorial sections through the macronucleus (Pl. III, fig. *a*) three components may be distinguished according to their electron density. In the centre of the nucleus lies a region of medium electron density (r_1), from which radial spokes project towards the periphery of the nucleus and may reach the nuclear membrane. The fact that this region forms a core in the centre of the nucleus has been verified by examining serial sections under the light microscope. Between the radial spokes lie strips of heavily stained material, arranged more or less radially (r_2) which frequently come directly into contact with the nuclear membrane. The heavily stained regions are separated from the region of medium electron density by a narrow zone of low electron density (r_3).

Material stained with Feulgen and methyl green-pyronin has been examined under the light microscope in order to identify some of the constituents of the three regions of the macronucleus. Feulgen- stained macronuclei are coloured only at the periphery, the stained areas being in the form of radially arranged strips (Pl. III, fig. *c*). It is considered

that these represent the regions of maximum electron density seen i electron micrographs. In methyl green-pyronin preparations these strip appear purple and the spaces between them pink. The central core c the nucleus is also pink (Pl. III, fig. *d*). This central region and its radia spokes might represent the nucleolar material of the macronucleus although in preparations stained with pyronin alone it is no more deepl coloured than the Feulgen-positive areas of the macronucleus.

It is of interest to note that the micronuclei of both host and parasit stain a clear blue with methyl green-pyronin. This indicates that the contain little or no RNA, a fact in agreement with the suggeste inertness of the genetic material contained in the micronuclei of ciliate (6, p. 35).

5. *THE STRUCTURE OF THE TENTACLES AND THEIR ASSOCIATED ELEMENTS*

The general structure of the tentacles resembles that of the suckin tentacles of other Suctoria (13, 16, 19, 20).

The tentacle (Pl. III, fig. *e*) is covered by the pellicle and plasm membrane except at the terminal knob region *(tkr)* where only on

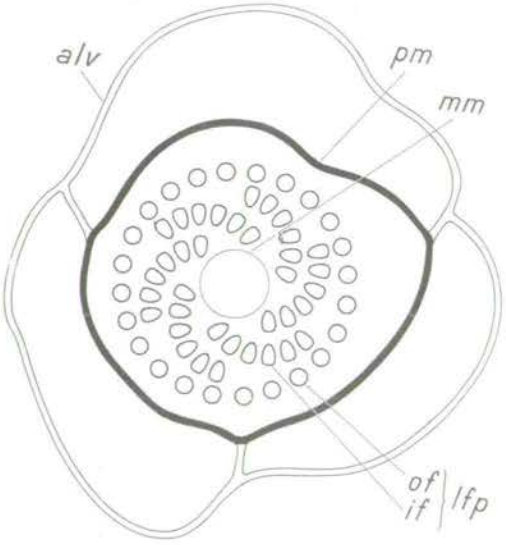

FIGURE 2. Diagrammatic representation of the cross-section of a tentacle surrounde by the alveolar pellicle *alv* and plasma membrane *pm* and containing the longi tudinal fibrillar partition *lfp* composed of inner and outer fibres, *if* and *of*. At th centre a membrane *mm* surrounds host material when this is present.

membrane is present. Previous authors (11, 17) have stated that this single membrane at the tentacle tip is a continuation of the plasma membrane. Our observations however indicate that in *P. parameciorum* the membrane of the tentacle tip is continuous with the outer unit membrane of the pellicle (Figure 1).

The interior canal of the tentacle is divided into an inner and outer tube by longitudinal fibres, which continue for some distance into the cytoplasm (*lfp*, Pl. II, and Pl. III, fig. *e*). Whether these fibres terminate in any organised structure comparable to the kinetosome of a cilium has not been determined; and their arrangement at the distal end of the tentacle is also unclear. In the unattached tentacle they do not seem to penetrate as far as the exposed surface membrane at the tentacle tip (Pl. III, fig. *e*).

Transverse sections of the tentacle (Plate IV, fig. *a* and *b*) reveal that the longitudinal fibrillar partition is made up of a circle of 24 to 27 fibres (outer fibres, *of*) themselves of circular outline, and inside this circle at regular intervals project inward six curved fibrillar bands (inner fibres, *if*), each consisting of a row of six fibres of a more triangular outline. The diameter of either sort of fibre is about 15 mμ. When

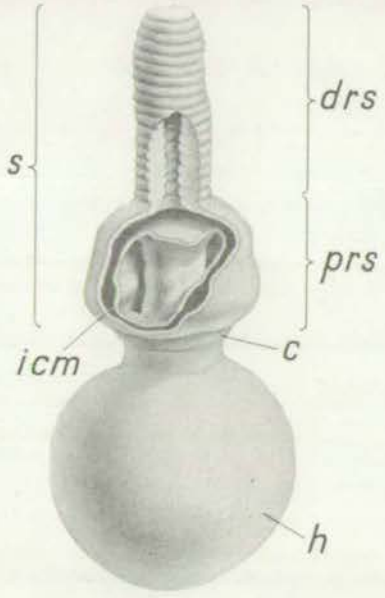

FIGURE 3. A three-dimensional reconstruction of a missile-shaped body composed of a head *h*, collar *c* and shaft *s*. The shaft is divided into a distal striated region *drs* and a proximal region *prs*. The inner curved membrane *icm* passes across the canal running along the shaft.

the tentacle is active in feeding the host material located in the inner tube is separated from the cytoplasm of the tentacle by a thin membrane (Pl. IV, fig. *b*, *mm*). The proposed cross-sectional structure of the tentacle is represented diagramatically in Figure 2. It is unknown whether the six fibrillar bands point in a clockwise or counterclockwise direction when the tentacle is viewed from a defined direction.

Associated with the tentacles are 'missile-shaped' bodies (Pl. III, fig. *e*, *msb*), similar to those previously described in *T. infusionum* (19). Under a high magnification (Pl. IV, fig. *c* and *d*) these seem to consist of a round head *(h)* usually with an electron-dense region at one side, a collar region *(c)* and a shaft *(s)*. The distal region of the shaft *(drs)* is striated, with a clearly defined lightly staining strip along the middle. The proximal region of the shaft *(prs)* is not striated and a lightly staining central strip is visible in some sections, but is not as clearly defined as in the distal region.

The distal and proximal regions of the shaft are divided by two curved membranes *(cm)* lying transversely to the shaft, the ends of which are directed backwards towards the head and appear to join up with the collar region. The diameter of the head is about 100 mμ, and the total length of the head and shaft about 350 mμ.

A diagrammatic interpretation of the structure of these bodies is given in Figure 3. One of the most difficult points to decide was whether the lightly-staining central strips in the shaft, interpreted as canals along the shaft, are continous from one end to the other, or whether they are interrupted by the inner of the two transverse membranes *(icm)* as shown in the diagram. The latter possibility was considered more likely, after the careful examination of this region in sections of over 40 different bodies.

The bodies may be found throughout the cytoplasm in considerable numbers, several scores having counted in a single section. When located in the vicinity of a tentacle the shaft is always found to be pointing towards the tentacle base (Pl. III, fig. *e*). They also occur within the tentacle, always in the outer tube outside the fibrillar partition (Pl. III, fig. *e*) or in the tip (Pl. III, fig. *e* and Pl. IV, fig. *e*). In the tip of the tentacle the neck of the bodies is opposed to the surface membrane, and in Pl. IV, fig. *e* a puff of material may be seen outside the tentacle at the point of attachment of the missile-shaped body to the membrane.

The possible function of these bodies is discussed below.

DISCUSSION

1. *STRUCTURE OF THE MACRONUCLEUS*

The internal structure of the macronucleus shows a degree of organisation and compactness not present in most of the ciliate macronuclei whose ultrastructure has so far been investigated (8, 9, 14, 23). In so far as a common pattern emerges from the cited studies, it is of a nucleus composed of a large number of randomly-distributed elements falling into two classes, called by most authors 'large bodies' and 'small bodies'. The diameter of the large bodies ranges from 0.5 μ to 0.75 μ and the small bodies grom 0.05 μ to 0,2 μ. The small bodies are usually held to be chromatin and the large bodies nucleoli, but there is some disagreement on this point (8). The only other suctorian whose macronucleus has been studied with the electron microscope is *T. infusionum* (17, 22). The macronucleus of this species contains a single class of body, Feulgen-positive, about 0.5 μ in diameter and sometimes arranged in longitudinal rows. They are thus larger than the small bodies described in other ciliate macronuclei.

The two Suctoria thus appear to differ from the other investigated ciliates by the relatively aggregated state of the components of their macronuclei. It is tempting to suppose that this might be related to their habit of unequal macronuclear division by budding. However, the state of aggregation of the macronuclear components can be effected by the physiological state of the organism (27, 24) which makes comparative statements somewhat unreliable.

In the developing macronuclear anglen of the suctorian *Ephelota gemmipara* chromosomes may be detected (5) and it has also been claimed that there are chromosomes in the mature macronucleus of *Tocophrya sp.* (6) on the basis of phase contrast observations. The macronucleus of *P. parameciorum* appears very similar to that of *Tocophrya sp.* under the phase contrast. However the electron micrographs of the macronucleus (Pl. III, fig. *a*) certainly do not contain any structures that might be interpreted as individually resolvable chromosomes, although the electron dense zones might be interpreted as aggregations of chromosomal material. On the contrary, the micronucleus (Pl. III, fig. *b*) does contain electron dense strands that correspond very well with appearance expected of individual chromosomes.

2. *THE CROSS-SECTIONAL STRUCTURE OF THE TENTACLES*

The cross-sectional structure of the tentacles is known in two other species of Suctoria apart from *P. parameciorum*. In *T. infusionum* (19) there are about 49 longitudinal fibres making up what we have called the fibrillar partition. These are arranged in a pattern similar to that found in *P. parameciorum*. As far as can be judged from Figure 3 of the cited reference an outer circle of about 22 fibres encloses seven inwardly directed rows of fibres, with 5 fibres in each row. In *Ephelota gemmipara* (16) the cross-sectional structure of the sucking tentacles resembles in principle that described above, but the outer circle takes the form of a continuous membrane, striated longitudinally, and there are many more inward projections, between 26 and 28. These also appear as continuous membranes rather than as rows of fibres. *E. gemmipara* also possesses prehensile tentacles of a quite different structure.

It is thus clear that the sucking tentacles of Suctoria are built on a common plan, although the details of this are not so rigid as those, for example, of the cilium.

3. *THE FUNCTIONING OF THE TENTACLES AND THE MISSILE-SHAPED BODIES*

It has been suggested (19) that the longitudinal division of the tentacle into an inner and outer tube provides separate channels for material passing into and out of the suctorian. It is supposed that there is an outward flow of material, including the missile-shaped bodies, along the outer tube and an inward flow of material from the prey along the inner. Our observations give support to this interpretation of tentacle function. (See missile-shaped bodies in the outer tube in Pl. III, fig. *e*, and in Pl. II mitochondria mit_2, possibly from the prey, in the inner tube.)

The same author proposes that the missile-shaped bodies may be identical with the dark granules seen under phase contrast during feeding in *Podophrya collinsi* (7); and that they are to be regarded as offensive organelles analogous to trichocysts, secreting substances concerned with the process of tentacle adhesion or the digestion of the prey cytoplasm.

The fact that these bodies have now been encountered in another suctorian indicates that, they are a regular suctorian organelle. Also their location around the tentacle strongly suggests that they play a part in the feeding process.

It is difficult at present to come to any firm conclusion about the possible homology between the missile-shaped bodies and trichocysts. Trichocysts have been observed in most ciliates with the exception of Suctoria (10). On *a priori* grounds it might therefore be expected that bodies equivalent to trichocysts would come to light in the Suctoria. However the most extensive comparative study of trichocysts (10) has not revealed any of them smaller than 3 μ in length, which is about ten times the size of a missile-shaped body. Nor does the electron-microscopical work (2, 26) on trichocysts offer much support for a detailed resemblance between trichocysts and missile-shaped bodies.

The missile-shaped bodies are to be found in the terminal knob region of unattached tentacles (Pl. III, fig. *e*) where the distal striated part of the shaft may penetrate through the surface membranes (Pl. IV, fig. *e*), giving rise to the previously mentioned puffs of material. This might suggest that the missile-shaped bodies are responsible for secreting onto the tip of the tentacle a substance necessary for adhesion to the prey.

However, the dark bodies of *P. collinsi* were observed to move outwards along the tentacle just after the moment of attachment of the tentacle, and also again just prior to its detachment (7). If he missile-shaped bodies are identical with the dark bodies this observation would suggest that they perform some other function than rendering the tentacle adhesive, perhaps concerned with the breakdown of the prey pellicle that must accompany tentacle attachment and detachment.

It would help to clarify the situation if the fate of the missile-shaped bodies in the tips of the tentacles could be determined after tentacle attachment. Signs of them may be detected in feeding tentacles (*e.g.* the 3 dark bodies at the upper right hand end of the tentacle in Pl. II), but we have not obtained a clear enough picture to determine whether they have retained their full structure in this situation. We have never seen any trace of them beyond the end of the tentacle in the cytoplasm of the paramecium.

Acknowledgements

The authors would like to thank Mr. E.D. Roberts, who drew the text figures and Prof. G.H. Beale, F.R.S. for reading and criticising the manuscript.

SUMMARY

The ultrastructure of a suctorian parasitic on the Ciliate *Paramecium bursaria Podophrya parameciorum incursella*, is described.

Particular attention is paid to the structure and histochemical properties of the macronucleus, and the organisation of the sucking tentacles and certain « missile-shaped » bodies found in the cytoplasm in association with the tentacles.

RÉSUMÉ

L'ultrastructure d'un Acinétien, parasite du Protozoaire cilié *Paramecium bursaria Podophrya parameciorum incursella*, est décrite.

On remarque surtout la structure et les propriétés histochimiques du « macronucleus », l'organisation des tentacules suceurs, et certains corps « en forme de fusée » qu'on trouve dans le cytoplasme et associés aux tentacules.

BIBLIOGRAPHIE

1. BEALE G.H., 1954. The genetics of *Paramecium aurelia*. Cambridge University Press.
2. EHRET C.F. and DE HALLER G., 1963. Origin, development and maturation of organelles and organelle systems of the cell surface in *Paramecium*. *J. Ultrastructure Res. Suppl.*, **6**, 1-42.
3. FAURE-FREMIET E., 1945. *Podophyra parasitica* nov. sp. *Bull. biol. Fr. Belg.*, **79**, 85-97.
4. FAURE-FREMIET E., FAVARD P. et CARASSO N., 1962. Etude au microscope électronique des ultrastructures d'*Epistylis anastatica*. *J. Microscopie*, **1**, 287-312.
5. GRELL K.G., 1949. Die Entwicklung Macronucleusanalge im Exkonjugaten von *Ephelota gemmipara* R. Hertwig. *Biol. Zbl.*, **68**, 289-312.
6. GRELL K.G., 1953. Die Struktur des Macronucleus von *Tokophrya*. *Arch. Protistenk.*, **98**, 466.
7. HULL R.W., 1961. Studies on suctorian Protozoa; The mechanism of ingestion of prey cytoplasm. *J. Protozool.*, **8**, 351-359.

8. JURAND A., BEALE G.H. and YOUNG M.R., 1962. Studies on the macronucleus of *Paramecium aurelia* I. (with a note on ultraviolet micrography). *J. Protozool.*, **9**, 122-131.

9. KLUS S.B.C., 1962. Electron microscopy of the macronucleus of *Euplotes eurytomus*. *J. Cell Biol.*, **13**, 462-465.

10. KRÜGER F., 1936. Die Trichocysten der Ciliaten im Dunkelfeldbild. *Zoologica, Stuttgart*, **34**, 1-82.

11. LOPEZ-OCHOTERENA E., 1962. Protozoarios ciliados de Mexico. I. *Stylonichia mytilus* Ehremberg, 1838 y *Sphaerophrya sol* Metchnikoff, 1864. Un caso de parasitismo entre protozorios. *Acta Zool. Mex.*, **6**, 1-6.

12. PEREZ REYES R. and LOPEZ-OCHOTERENA E., 1963. *Sphaerophrya sol* (Ciliata : Suctoria) parasitic in some Mexican Ciliates. *J. Parasitol.*, **49**, 697.

13. POTTAGE R.H., 1959. Electron microscopy of the adults and migrants of the suctorian Ciliate *Discophrya piriformis*. In *Proc. XVth Intern. Congr. Zool. London*, 472-473.

14. RANDALL J.T. and JACKSON S.F., 1958. Fine structure and function in *Stentor polymorphus*. *J. Biophys. Biochem. Cytol.*, **4**, 807-830.

15. REUKAUF E., 1939. Sphaerophrya-infection bei *Paramecium bursaria*. *Mikrokosmos, Stuttgart*, **33**, 11-14.

16. ROUILLER C., FAURE-FREMIET E. and GAUCHERY M., 1956. Les tentacules d'*Ephelota;* Etude au microscope électronique. *J. Protozool.*, **3**, 194-200.

17. RUDZINSKA M.A., 1956. Further observations on the fine structure of the macronucleus in *Tokophrya infusionum*. *J. Biophys. Biochem. Cytol.*, **2** (4), suppl. 425-430.

18. RUDZINSKA M.A., 1958. An electron microscope study of the contractile vacuole in *Tokophrya infusionum*. *J. Biophys. Biochem. Cytol.*, **4**, 195-202.

19. RUDZINSKA M.A., 1962. The fine structure of the feeding apparatus in *Tokophrya infusionum*. *Proc. 5th Intern. Congr. Electron Microscopy*, Academic Press, **2**, UV-12.

20. RUDZINSKA M.A. and PORTER K.R., 1954. Electron microscope study of intact tentacles and disc in *Tokophrya infusionum*. *Experientia*, **10**, 460-462.

21. RUDZINSKA M.A. and PORTER K.R., 1954. The fine structure of *Tokophyra infusionum* with emphasis on the feeding mechanism. *Trans. N.Y. Acad. Sci.*, **16**, 408-411.

22. RUDZINSKA M.A. and PORTER K.R., 1955. Observations on the fine structure of the macronucleus of *Tokophrya infusionum*. *J. Biophys. Biochem. Cytol.*, **1**, 421-428.

23. SESHACHAR B.R., 1964. Observations on the fine structure of the nuclear apparatus of *Blepharisma intermedium* Bhandary (Ciliata; Spirotricha). *J. Protozool.*, **11**, 402-409.

24. VIVIER E., 1963. Etude au microscope électronique des nucléoles dans le macronucleus de *Paramecium caudatum*. In Progress in Protozoology. (*Proc. Ist Intern. Congr. Protozool.*) ed. Ludnik, J., Lom, J. and Varra, J. Prague. 421.

25. YANKOVSKY A.B., 1963. Pathology of the Infusoria II. Life cycles of Suctoria parasitic in *Urostyla* and *Paramecium*. *Cytologia.*, **5**, 428-439. (In Russian).

26. YUSA A., 1963. An electron microscope study on regeneration of trichocysts in *Paramecium caudatum*. *J. Protozool.*, **10**, 253-262.

Manuscrit reçu le 23 mars 1965.

Plate I

Fig. a, b and *c*. — 3 µ paraffin wax sections stained with methyl-green pyronin.

Fig. a. — *Podophrya (Pod)* embedded in *Paramecium (Par)*. Also visible are the macronucleus and micronucleus of the *Paramecium (Par ma)* and *(Par mi)*, and the macronucleus of *Podophrya (Pod Ma)*; × 640.

Fig. b. — *Podophrya (Pod)* inside a *Paramecium (Par)* in the process of liberating a larva *l* to the exterior; × 400.

Fig.c. — Two *Podophrya* in a single *Paramecium;* × 400.

Fig. d. — *Podophrya (Pod.)* In a pouch formed by an invagination of the pellicle of the *Paramecium (Par)*. Notice the macronucleus of *Podophrya (Pod ma)*, and the marconucleus and micronucleus of the infected *Paramecium, (Par ma)* and *(Par mi)*, which show degeneration at the side nearest to the parasite; × 9 000.


Par
Pod
Par ma
Par mi

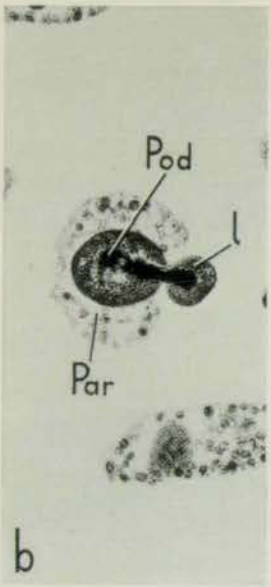
Pod
l
Par
b


c

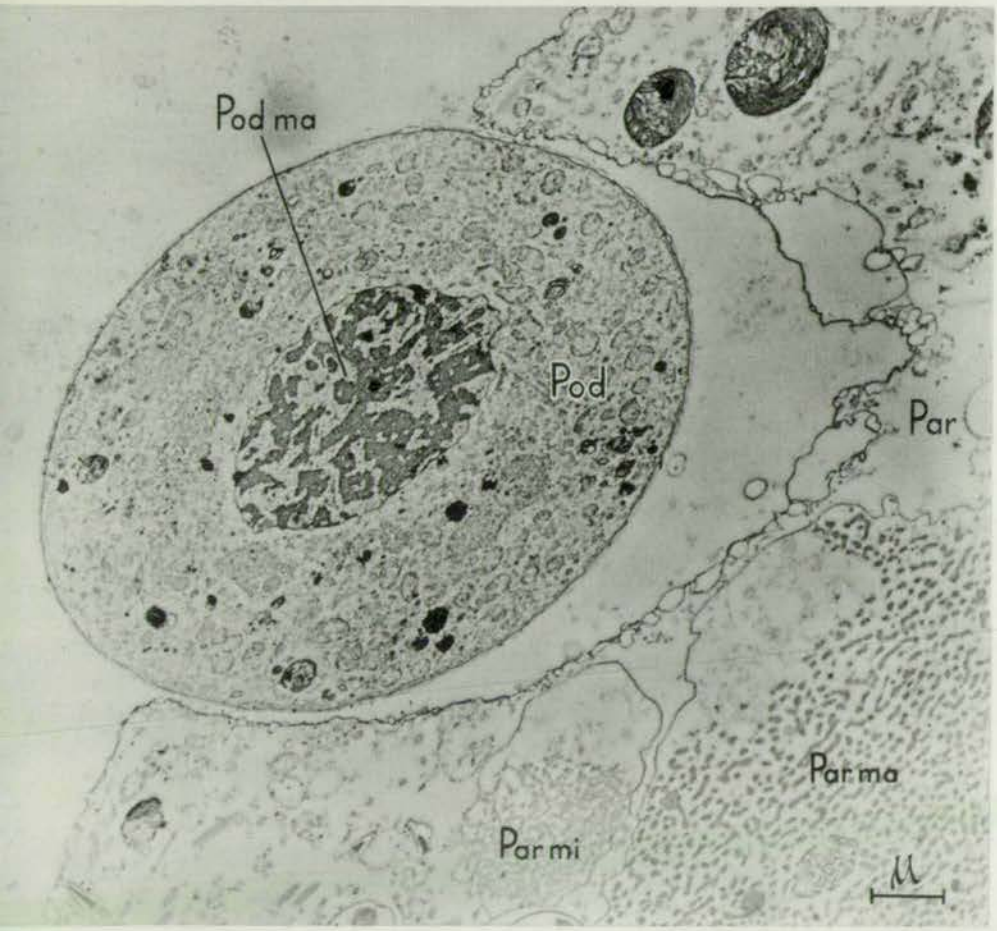
Pod ma
Pod
Par
Par ma
Par mi
μ

Plate II

Podophrya (*Pod*) attached to a *Paramecium* (*Par*), by means of a tentacle *T*, containing a longitudinal fibrillar partition *lfp* and, inside this, mitochondria mit_1 which presumably are being sucked out of the *Paramecium*. In the cytoplasm of the *Podophrya* may also be seen an alga *A* from the *Paramecium*, and mitochondria mit_2 which may belong either to the parasite or the host. The surface of the *Podophrya* is covered by an alveolar cuticle *alv* and plasma membrane *pm* and is interrupted at intervals by pits *pt;* × 56 000.

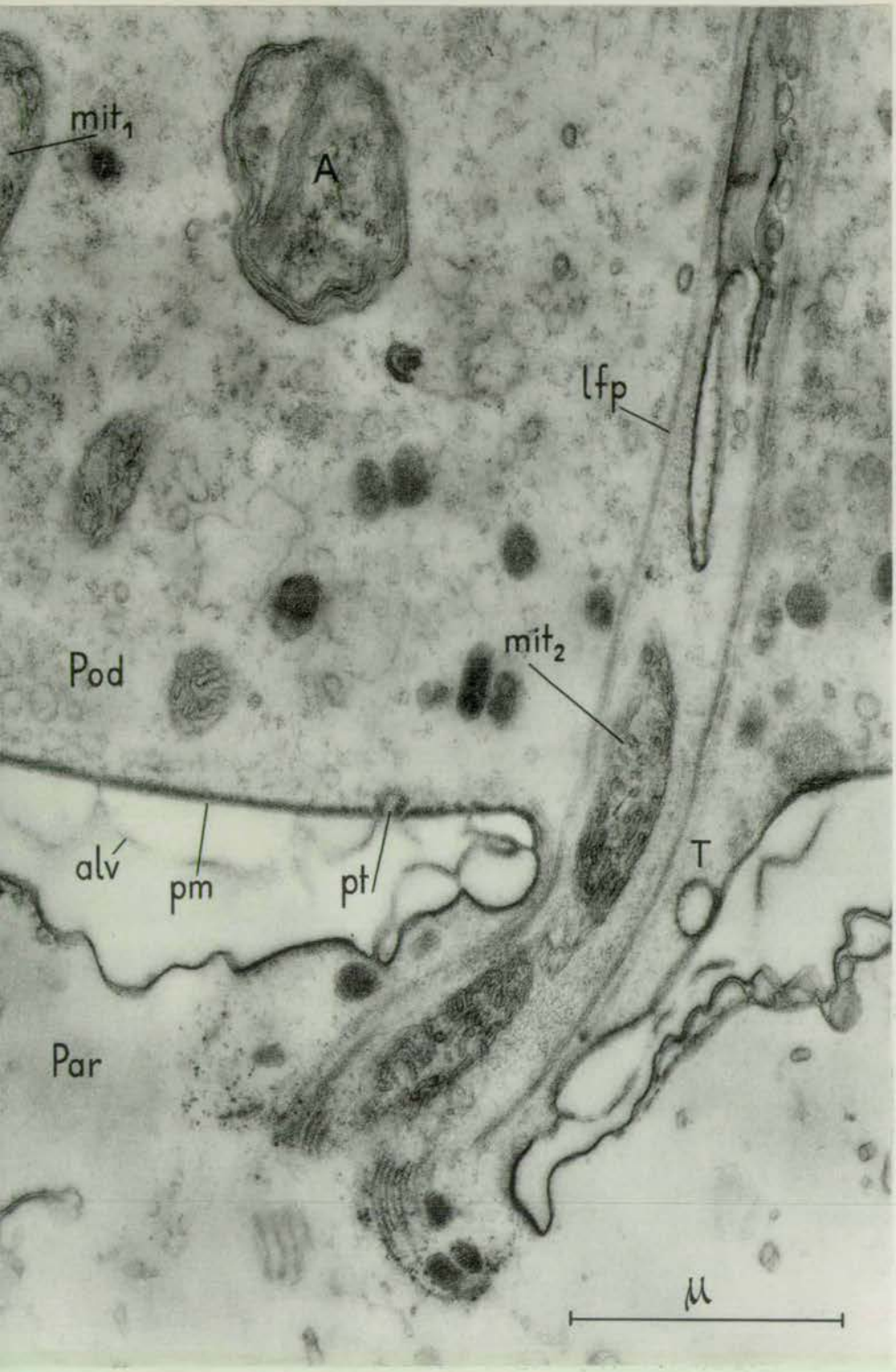
mit1
A
lfp
Pod
mit2
alv
pm
pt
T
Par
μ

Plate III

Fig. a. — Equatorial section through macronucleus of *Podophrya*. Note the three regions, r_1, r_2 and r_3, distinguished by their electron densities; × 7 200.

Fig. b. — Tangential section through micronucleus of *Podophrya;* × 44 000.

Fig. c and *d.* — Macronucleus of *Podophrya* under the light microscope; × 1 040.

Fig. c. — Stained with Feulgen reagent, periphery of nucleus only coloured.

Fig. d. — Stained with methyl-green pyronin, periphery and centre stained.

Fig. e. — Longitudinal section through tentacle of *Podophrya* showing longitudinal fibrillar partition *lfp*, terminal knob region *tkr*, and missile-shaped bodies *msb;* × 28 000.

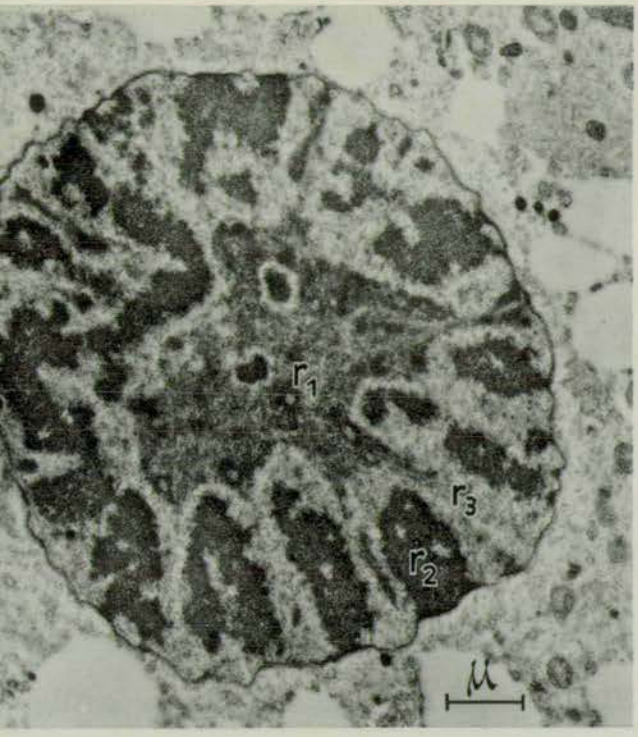
r1
r3
r2
μ

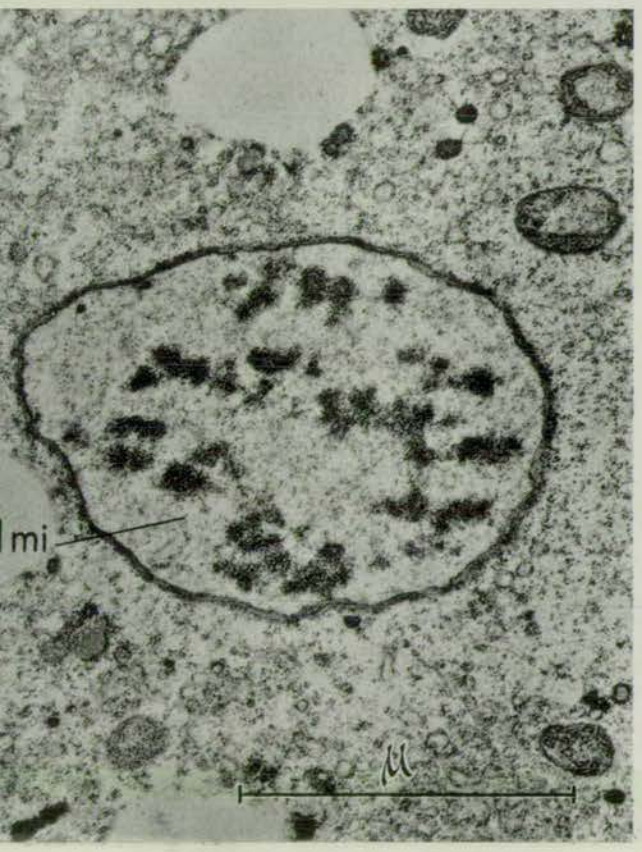
mi
μ

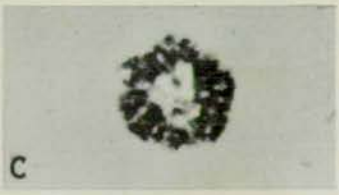
c

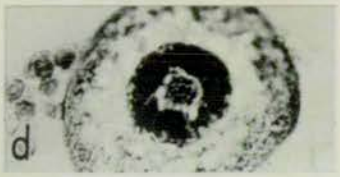
d

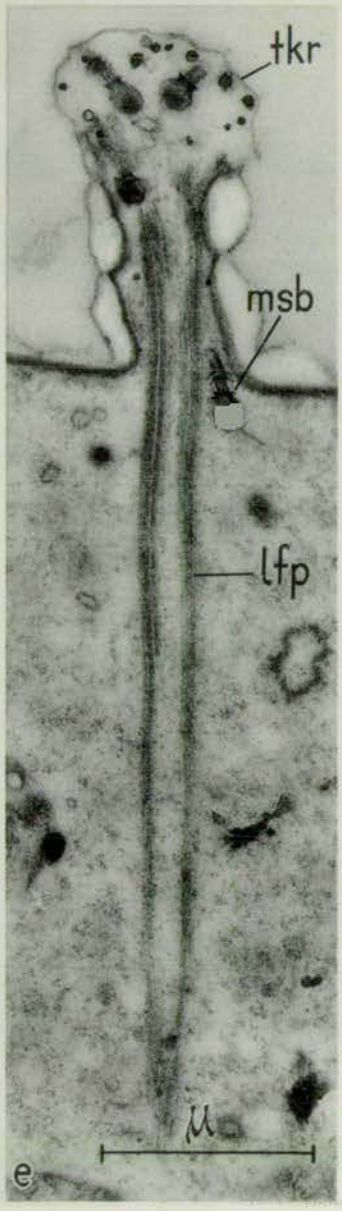
tkr
msb
lfp
μ
e

Plate IV

Fig. a and *b*. — Transverse sections of tentacles of *Podophrya* showing inner fibres *if* and outer fibres *of*. The tentacles are lying in the space between the *Podophrya* (*Pod*) and *Paramecium* (*Par*).

Fig. a. — Tentacle not feeding; × 80 000.

Fig. b. — Tentacle feeding, as indicated by the presence of host material in the centre surrounded by a thin membrane *mm;* × 60 000.

Fig. c and *d*. — Missile-shaped bodies, showing the head *h*, collar *c*, shaft *s*, proximal region of shaft *prs*, distal region of shaft *drs* and curved membranes *cm;* fig. *c*, × 80 000; fig. *d*, × 100 000.

Fig. e. — Section through terminal knob region *tkr* of the tentacle of *Podophrya* showing missile shaped body apparently discharging material (marked by arrow) to the exterior; × 36 000.

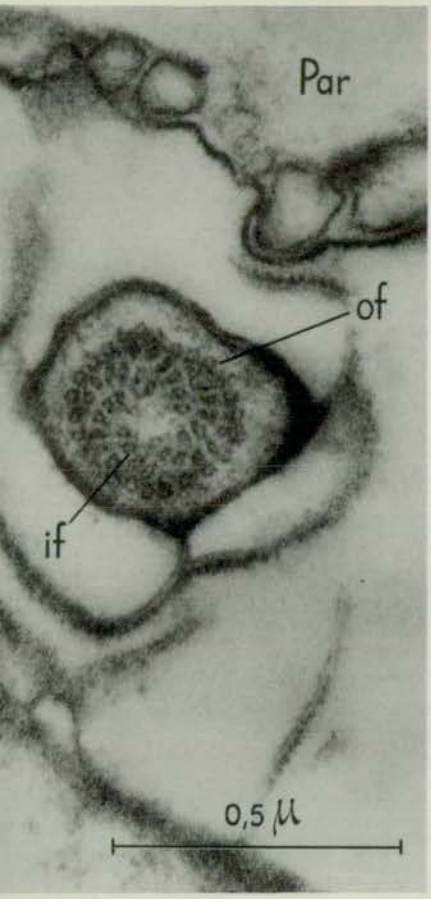
Par
of
if
0,5 μ

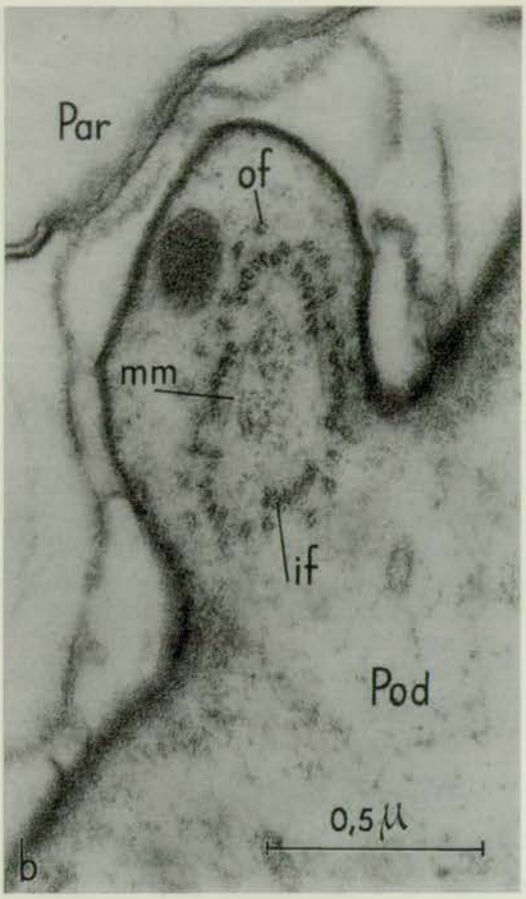
Par
of
mm
if
Pod
0,5 μ
b

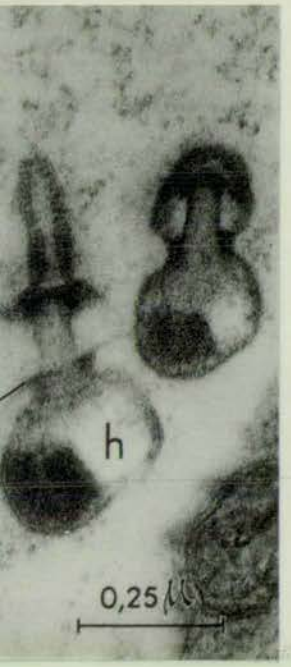
h
0,25 μ

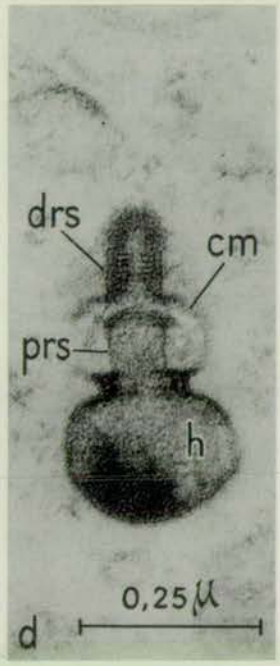
drs
cm
prs
h
0,25 μ
d

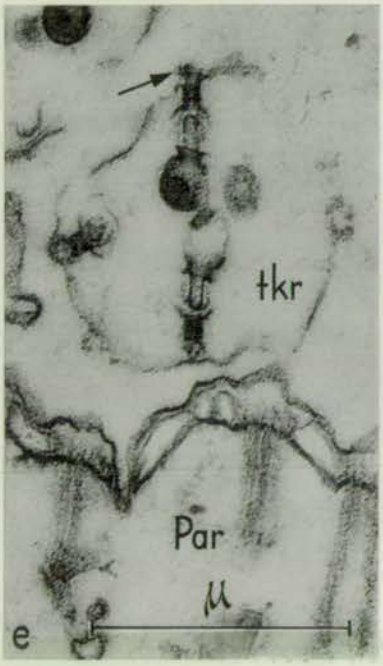
tkr
Par
μ
e

INSTRUCTIONS AUX AUTEURS

MANUSCRITS. Les manuscrits doivent être envoyés à la Société Française de Microscopie Electronique, 24, rue Lhomond, PARIS (5e).

Bien que la langue officielle soit le *français*, le journal accepte des articles en *anglais* ou en *allemand*.

Les manuscrits doivent être dactylographiés en double interligne.
Les mémoires ne peuvent en général dépasser 20 pages imprimées, soit 50 000 caractères environ. Les lettres à l'éditeur : deux pages imprimées, soit 5 000 caractères.

ILLUSTRATIONS PHOTOGRAPHIQUES. Les photographies sont reproduites sur des planches hors texte par phototypie sur papier kromekôte laqué; celles-ci sont placées à la fin de l'article; la justification des planches est de 140 × 210 mm. Elles sont numérotées en chiffres romains; si une planche comporte plusieurs micrographies, celles-ci sont désignées par les lettres : a, b, c, etc... à l'intérieur de chaque planche. Il est demandé aux auteurs de faire parvenir deux jeux des photographies : un jeu où les photographies sont assemblées et lettrées selon les désirs de l'auteur, un second jeu non noté et non lettré. Le montage des planches et le lettrage sont faits par les éditeurs, ceci afin de rendre plus homogène la présentation des documents. Le journal offre quatre planches hors texte gratuites par mémoire. Les lettres à l'éditeur ne comportent qu'une planche gratuite. Les planches supplémentaires sont aux frais de l'auteur au prix de 250 F chacune.

FIGURES AU TRAIT. Les figures et schémas au trait ainsi que leurs légendes sont reproduits dans le texte et leur place doit être indiquée sur le manuscrit. Elles sont numérotées en chiffres arabes.

BIBLIOGRAPHIE. Les références des auteurs cités dans le texte sont placées à la fin de l'article et disposées par ordre alphabétique. Elles peuvent alors être numérotées pour faciliter les renvois du texte à la bibliographie.

Le Journal, le volume, la première et la dernière page ainsi que le titre de l'article doivent être indiqués.

La ponctuation doit être placée selon le modèle :

1. FAURÉ-FREMIET E., 1961. Le cytoplasme stomo-pharyngien des Ciliés cyrtophores. *C.R. Ac. Sc.*, 253, 357-362.
2. GIBBONS I.R. et GRIMSTONE A.V., 1960. On flagellar structure in certain flagellates. *J. Biophys. Biochem. Cytol.*, 7, 697-716.
3. WIESENBERGER E., 1958. Die Anwendung Mikrochemischer Nachweisverfahren in der Elektronenmikroskopie. *Quatrième Congrès International de Microscopie Electronique*, Springer éd., Berlin, I, 769-779.

RÉSUMÉS. Il est demandé deux résumés : *un résumé en français* et *un autre en anglais* qui sont placés à la fin de l'article. Chacun de ces résumés ne doit pas dépasser une quinzaine de lignes soit 1 000 caractères environ. Il n'est pas demandé de résumé pour les lettres à l'éditeur.

TIRÉS A PART. En même temps que l'envoi de son manuscrit, il est demandé à l'auteur de préciser le nombre de tirés à part désiré. Ceux-ci lui sont facturés au prix coûtant. Pour des raisons techniques dues au procédé de reproduction par phototypie, le nombre de tirés à part ne peut être inférieur à 200. Au-delà de ce nombre les tirés à part sont fournis par multiple de 100.

Three different types of mate-killer (mu) particle in *Paramecium aurelia* (syngen 1)

by G.H. Beale and A. Jurand

J. Cell Sci. 1, 31–34 (1966)
Printed in Great Britain

THREE DIFFERENT TYPES OF MATE-KILLER (MU) PARTICLE IN *PARAMECIUM AURELIA* (SYNGEN 1)

G. H. BEALE AND A. JURAND
Institute of Animal Genetics, Edinburgh

SUMMARY

A new rapid method for staining endosymbiotic particles in *Paramecium* is described. Two new strains of mu particle in *P. aurelia* syngen 1 are compared with the previously known mu particles of stock 540 by light and electron microscopy. Morphologically the three types of particle differ only in size, but each converts its host *Paramecium* into a mate-killer of a specific type. Each of the three particles appears to require the presence of different genes of *Paramecium*.

INTRODUCTION

The bacterium-like endosymbionts called mu particles, which grow in the cytoplasm of *Paramecium*, and cause the latter to become a 'mate-killer', were first described by Siegel (1953), working with *P. aurelia*, syngen 8. Later a similar type of particle was found in stock 540 of syngen 1 (Beale, 1957), and some details of these mu particles as observed by light and electron microscopy have been described (Beale & Jurand, 1960). Current interest in these particles centres around two problems: (1) the homologies of the particles with other micro-organisms; and (2) the dependence of the particles on the genetic apparatus of the host paramecia. For the further study of these problems it is desirable to obtain a number of different types of particle in stocks of the same syngen of *P. aurelia*, capable of being intercrossed for genetic analysis. Making use of a new, rapid method for staining the particles, whereby a large number of stocks can be screened in a short time, all the old stocks of syngen 1, as well as some newly collected material, have been examined. This search has resulted in the discovery of a number of new endosymbionts, some of which are now described.

MATERIALS AND METHODS

Three stocks of *P. aurelia*, all mate-killers, were studied: stock 540, collected in Mexico in 1956 (kindly supplied by Dr T. M. Sonneborn); stock 548, collected at Lake Malibu near Los Angeles in 1962; and stock 551, collected in Golden Gate Park, San Francisco, in 1964. In addition, sensitive stock 513, lacking cytoplasmic endosymbionts, was used for testing the mate-killing effects of the other stocks.

The paramecia were grown in the standard bacterized lettuce medium (Sonneborn, 1950).

Staining of mu particles was carried out as follows. The paramecia were placed in a

small drop on a slide, as much of the fluid as possible was withdrawn by a micro-pipette, the paramecia were lightly fixed by exposure to OsO_4 vapour for a few seconds, and immediately stained with a small drop of full-strength lacto-orcein (1 g synthetic orcein, 22 ml lactic acid, 36 ml glacial acetic acid, 42 ml distilled water). A coverslip, with vaseline smeared around the edges, was placed over the drop of stained paramecia and lightly pressed down, flattening but not disrupting the animals. The preparations were examined under phase contrast with a ×100 oil-immersion objective. This method has been found to show clearly all types of endosymbionts (mu, kappa, etc.) as well as the micronuclei, which are ordinarily difficult or impossible to identify in temporary preparations. The method has the advantage of making a clear distinction between symbiotic particles in the cytoplasm of the paramecia, and bacteria in the food vacuoles.

For electron microscopy, the paramecia were fixed in 1% osmium tetroxide (with acetate-veronal buffer at pH 7·2, and 10 mg/ml $CaCl_2$ for better preservation of membranes) and embedded in Araldite. After sectioning, the material was stained with 1% aqueous $KMnO_4$ solution containing uranyl acetate.

RESULTS AND DISCUSSION

The three types of mu particle—540, 548 and 551 mu—are illustrated in Figs. 1–3 (light microscope) and Figs. 4–6 (electron micrographs). Particles of type 540 mu consist of rod-like structures, approximately 0·3 μ wide and varying greatly in length, from about 2–20 μ or more. Starvation of the paramecia results in a great increase in the total numbers of mu particles per cell, and causes production of the very long forms. In actively growing paramecia, the number of particles is smaller, long forms are absent and the particles are usually clumped together (as found also by Siegel (1953) for the mu particles of syngen 8). The two other types, 548 mu and 551 mu, are much shorter (1–1·5 μ and 1·5–2 μ long, respectively) than 540 mu particles, and neither 548 mu nor 551 mu develop the long forms of 540 mu. The type 548 mu forms clumps but 551 mu does not.

Electron microscopy shows that all the particles have a conspicuous outer membrane. The internal contents are rather undifferentiated. From previous work (Beale & Jurand, 1960) it has been shown that 540 mu particles contain DNA (as well as RNA), spread throughout the particles; and the better electron-microscope techniques now available show the presence of extremely fine filaments throughout the particles. Certainly nothing like the differentiated nuclear structures of certain bacteria can be seen here. No obvious differences in the contents or outer membranes of the three types of particle can be seen.

Nevertheless each of the particles has distinct properties. Each converts its host paramecium into a mate-killer, as shown by the fact that conjugation between any of the three and the sensitive stock 513 results in death of the ex-conjugant deriving cytoplasm from the 513 parent. Of the three mate-killers, stock 548 has the most pronounced effect; even at the moment of separation of the ex-conjugants, the sensitive one can be seen to be already much reduced in size, and death occurs within a few

hours. Stock 540 mate-killer usually causes death of the sensitive ex-conjugant only after about 12 h, and sometimes a fission of the 'doomed' cell may take place. Stock 551 mate-killer has a still more delayed effect, causing death only after 1–2 days, and occasionally the clones from the sensitive ex-conjugant recover completely. This variation in intensity of mate-killing effect recalls some earlier findings by Levine (1953) with three syngen 8 mate-killers, which could be arranged in a 'peck-order' of mate killing. However, the interrelations of the three types of syngen 1 mate-killers described here differ in that conjugation between any two of them (548 × 551, 540 × 548, 540 × 551) results in death of *both* ex-conjugants (except that occasionally 551 fails to kill the others). This mutual killing effect has a parallel in the effects of various symbiotic particles (kappa) studied by Sonneborn (1939) and Preer (1948) in syngen 2. Here killing does not occur as a consequence of mating, but is due to the excretion of a lethal agent from the kappa-bearing *Paramecium* into the culture fluid, and subsequent action of this liberated killing agent on a sensitive animal. It was found that the killers of stock 7 were sensitive to killing by stock 8, and vice versa. Thus, in this case at least one type of particle does not confer on a *Paramecium* immunity to killing by another type, and the same is true of the three types of mu particle now described.

The genetic basis of ability to maintain mu particles in stocks 540, 548 and 551 is at present under study. It has previously been reported (Gibson & Beale, 1961) that stock 540 contains two dominant genes (M_1 and M_2), either of which is capable of maintaining the mu particles. When these genes were replaced by the two recessive alleles m_1 and m_2 from stock 513, all mu particles were destroyed. Crosses have now been made between the two other mate-killer stocks (548 and 551) and the sensitive stock 513. In each case mu particles were maintained in F_1 and segregation of animals with and without mu particles occurred in F_2. Hence it is likely that both 548 and 551 contain one or more dominant genes necessary for maintenance of these mu particles. Further, cultures of stock 540 lacking mu particles (and therefore not mate-killers) have been obtained by various environmental treatments (extremes of temperature, penicillin treatment, etc.), and crossed with stocks 548 and 551 containing mu particles. In F_2 segregation of animals with and without particles was again found. Hence, the genes in stocks 548 and 551 supporting growth of their respective mu particles are different from the genes M_1 and M_2 which support the 540 mu particles. These results indicate that there is a high degree of specificity in the interrelations of the mu particles and the genotype of the host cell.

It is now becoming clear that quite a high proportion of wild strains of *P. aurelia* contain endosymbiotic particles. By making random collections and staining the paramecia by the method described here, many new particle-containing strains have been found (which may or may not be killers or mate-killers). Not uncommonly it has been found that after cultivating the paramecia in bacterized lettuce or grass medium for a short period in the laboratory (even with slow growth rates of the paramecia), the symbionts rapidly disappear, due presumably to the specific nutritional requirements of some symbionts.

These facts—the abundance of different types of endosymbionts in natural populations of *P. aurelia*, the remarkable adaptation between the particles and the host

genotype, and the ease with which some particles are lost from the paramecia—make it seem likely that in nature there is potentially a vast array of micro-organisms (presumably free-living bacteria) capable of establishing themselves in *Paramecium*, and that infection and loss may occur repeatedly. Occasionally permanent symbiotic systems are established, and these are the systems available for study.

REFERENCES

Beale, G. H. (1957). A mate-killing strain of *Paramecium aurelia*, variety 1, from Mexico. *Proc. R. phys. Soc. Edinb.* **26**, 11–14.

Beale, G. H. & Jurand, A. (1960). Structure of the mate-killer (mu) particles in *Paramecium aurelia*, stock 540. *J. gen. Microbiol.* **23**, 243–52.

Gibson, I. & Beale, G. H. (1961). Genic basis of the mate-killer trait in *Paramecium aurelia*, stock 540. *Genet. Res.* **2**, 82–91.

Levine, M. (1953). The diverse mate-killers of *Paramecium aurelia* variety 8: their interrelations and genetic basis. *Genetics, Princeton* **38**, 561–78.

Preer, J. R. (1948). Microscopic bodies in the cytoplasm of 'killer' *Paramecium aurelia*. *Genetics, Princeton* **33**, 349–404.

Siegel, R. W. (1953). A genetic analysis of the mate-killer trait in *Paramecium aurelia*, variety 8. *Genetics, Princeton* **38**, 550–60.

Sonneborn, T. M. (1939). *Paramecium aurelia:* mating types and groups; lethal interractions: determination and inheritance. *Am. Nat.* **73**, 390–413.

Sonneborn, T. M. (1950). Methods in the general biology and genetics of *Paramecium aurelia*. *J. exp. Zool.* **113**, 87–143.

(*Received* 8 *October* 1965)

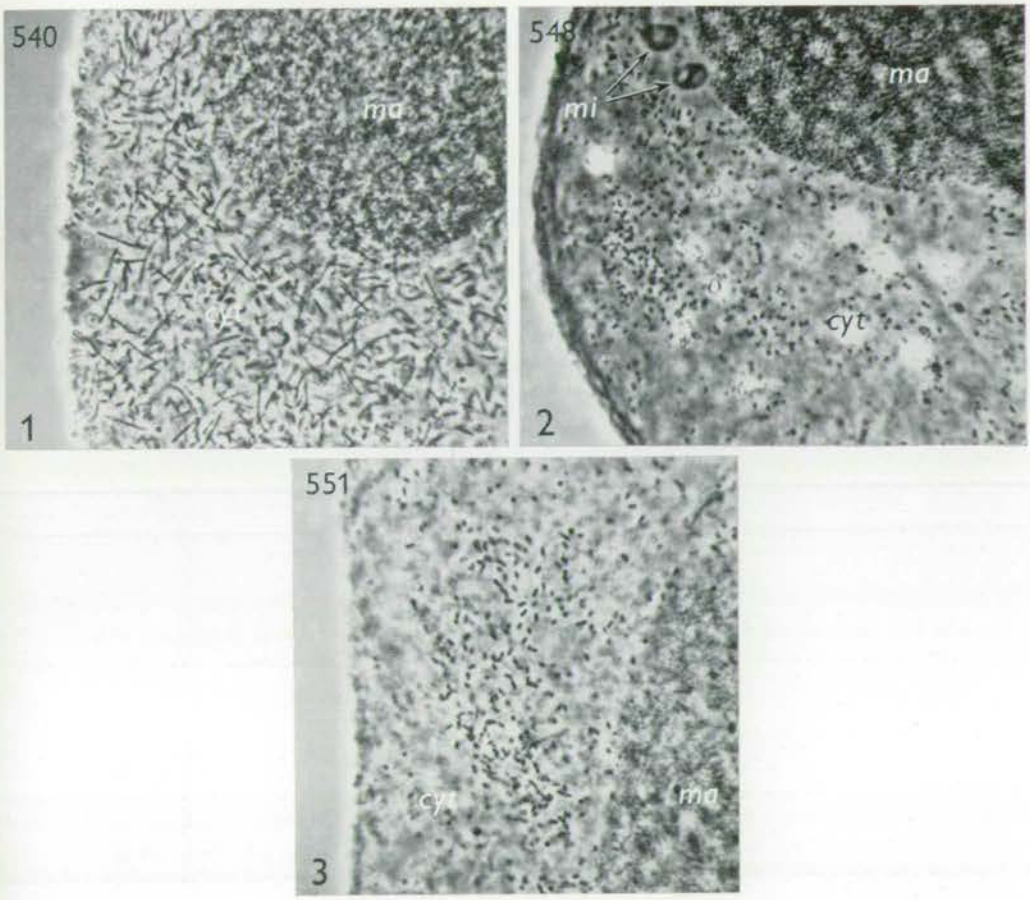

Figs. 1–3. Three types of mu particle (540, 548, 551 respectively) as seen by phase-contrast microscopy of preparations stained by method described in text. The particles are seen scattered throughout the cytoplasm. *cyt*, cytoplasm; *ma*, macronucleus; *mi*, micronucleus. × 800.

(*Facing p.* 34)

Figs. 4–6. Electron micrographs of the three types of mu particle (540, 548 and 551 respectively), surrounded by cytoplasm of *Paramecium*.

Changes in the ultrastructure of salivary gland cytoplasm in *Sciara ocellaris* (Comstock, 1882) due to microsporidian infection

by A. Jurand, L.C.G. Simoes and C. Pavan

J. Insect Physiol., 1967, *Vol.* 13, *pp.* 795 *to* 803. *Pergamon Press Ltd. Printed in Great Britain*

CHANGES IN THE ULTRASTRUCTURE OF SALIVARY GLAND CYTOPLASM IN *SCIARA OCELLARIS* (COMSTOCK, 1882) DUE TO MICROSPORIDIAN INFECTION*

A. JURAND,† L. C. G. SIMÕES, and C. PAVAN‡

Biology Division, Oak Ridge National Laboratory, Oak Ridge, Tennessee

(*Received* 2 *September* 1966)

Abstract—The effects of infection by a microsporidian, *Thelohania* sp., on the ultrastructure of the cytoplasm of salivary gland cells in *Sciara ocellaris* were investigated. Cytoplasm of uninfected cells contains a dense ribosomal population studding large condensations of lamellar and vesicular endoplasmic reticulum, numerous scattered Golgi areas, and typical metazoan mitochondria. In infected cells of salivary glands the ultrastructural integrity of the cytoplasm is profoundly changed due to depletion of ribosomes, disarrangement of endoplasmic reticulum, and to decrease in size and increase in number of mitochondria. The overall electron opacity of the infected cytoplasm is decreased due to a decrease in ribosomal population and to formation of cytoplasmic vacuoles.

The implications of the various features observed in both normal and infected cells are discussed, and possible suggestions are made regarding alteration of the metabolic functions due to infection.

INTRODUCTION

RECENTLY DIAZ and PAVAN (1965), PAVAN and BASILE (1966a, b), and PAVAN and PERONDINI (in preparation) described cases of infections in Sciaridae that induce profound changes in the infected cells of various tissues. Two types of infections were described. In one the infective agent is a protozoon, *Thelohania* sp., of the order Microsporidia. It settles in the cytoplasm of cells in different tissues and proliferates there. In some specimens the cells of salivary glands are found to be infected by *Thelohania* sp. and another unidentified micro-organism, probably also a microsporidian. In the other type of infection a DNA virus is found, exclusively in the nucleus. In both types of infection, however, the infected cells, including the nucleus and the chromosomes, increase enormously in size.

In general, the increase in size of the chromosomes is determined by two processes: (a) a more extensive polyteny (an endomitotic process in which the

* Research sponsored by the U.S. Atomic Energy Commission under contract with the Union Carbide Corporation.

† Present address: Institute of Animal Genetics, West Mains Road, Edinburgh.

‡ Present address: Departmento de Biologia, Universidade de São Paulo.

chromatids multiply but the daughter chromatids do not separate and the cell does not divide), and (b) more intensive DNA-dependent RNA synthesis by the chromosomes in the infected cells. These two phenomena are responsible for chromosomes becoming much thicker and longer than the polytene chromosomes of nearby normal cells (ROBERTS *et al.*, 1966).

There are also cases in which the cells infected by Microsporidia contain nuclei that become polyploid because the chromosomes divide but the nuclei do not. Polyteny and polyploidy may also be found in the same nucleus (PAVAN and PERONDINI, unpublished data).

Apart from the increase in size and/or increase in number of chromosomes, the infection may induce changes in specific regions of the chromosomes. These changes are of particular interest for the study of cell metabolism.

It is of interest to be able to analyse the possible causes of the changes induced in the host cells by the infective agent, and then to correlate them with those already known to occur in the nucleus. Since the protozoa are restricted to the cytoplasm but the most obvious changes induced by the infection are those seen in the nucleus, it seems obvious that the cytoplasm must be involved in the reaction. However, there are no publications dealing with the structure of the cytoplasm of the infected cells, probably because very little can be seen by light microscopy. As a first approach to this problem we made a study, using the electron microscope, of the salivary glands of *Sciara ocellaris* larvae, both normal and infected by *Thelohania* sp. This protozoon proliferates in the cytoplasm of cells of these glands as well as of fat bodies and muscle cells.

MATERIALS AND METHODS

Salivary glands were obtained from *Sciara ocellaris* (Sciaridae, Nematocera, Diptera) larvae cultured in our laboratory in the medium previously described by LARA *et al.* (1965) for *Rynchosciara angelae* larvae. The medium was placed in agar dishes and held at room temperature.

Ultrastructural observations were performed on the median and distal parts of the salivary glands. Two series of material were prepared for these investigations. In the first, uninfected glands were dissected from uninfected larvae, infected glands were taken from infected larvae, and the ultrastructure of both were compared. The second series consisted of infected glands in which there were usually a few infected cells distributed along the gland adjacent to other cells which were apparently normal. Thus, in the second series, normal and infected cells could be compared in the same ultra-thin sections taken from the same blocks. This series of observations enabled us to exclude any doubts about the uniformity of treatment of the material prior to examination in the electron microscope. However, in both series of observations the differences between normal and infected salivary gland cell cytoplasms were the same.

After dissection, the glands were fixed with 2 to 3 ml of cold (about 2°C) solution of 1% osmium tetroxide (3 parts of Backer insect Ringer solution and 1

part of 4% osmium tetroxide solution) for 30 min, the fixative being allowed to warm up to room temperature during fixation.

Fixation was followed by a thorough rinsing with the insect Ringer solution and dehydration with graded ethanol solutions starting from 35% solution. Material was embedded in Epon or Durcupan (Araldite) using a slow rotary shaker designed for better infiltration by viscous embedding media (JURAND and IRELAND, 1965).

Sections were obtained with a Porter–Blum ultramicrotome, stained with lead citrate solution (REYNOLDS, 1963), and studied with a Siemens Elmiskop I electron microscope.

To examine quantitatively the difference in size of mitochondria in the normal and infected cells we measured the width or the diameter of 100 profiles of each group on micrographs using those of ×37,000 total magnification. The length of the profiles was not taken into account.

OBSERVATIONS

Salivary gland cells in *Sciara ocellaris* contain all the subcellular organelles typical for this tissue as described previously in *Bradysia mycorum* Frey (Sciaridae) (JACOB and JURAND, 1963), in *Smittia parthenogenetica* (Chironomidae) (JACOB and JURAND, 1965), and in *Sciara coprophila* (Sciaridae) (PHILLIPS and SWIFT, 1965). However, in the cytoplasm of normal salivary gland cells used for the present investigations, no distinct distribution of any of the subcellular organelles between the basal and apical zones of the cytoplasm was observed. The cell membrane is smooth on the basal side and is covered from the outside by a fibrous basement membrane. The apical surface is modified into what is, for these cells, a typical brush border consisting of cylindrical microvilli up to 2 μ long and 0·1 μ wide (Fig. 1).

It is noticeable that the basal side of the cell membranes of the infected cells shows a considerable pinocytic activity, whereas in the corresponding areas of cell membranes in the uninfected cells pinocytic activity is absent (see Fig. 9).

The cytoplasm of normal cells is abundantly filled with endoplasmic reticulum of two distinctly different types. In the median zone there are large condensations of rough flattened endoplasmic reticulum in the form of numerous parallel flat cysternae represented in sections by arrays of elongated profiles studded densely with ribosomes, the density being 30 to 35 ribosomal particles per 1 μ long fraction of the profile of the endoplasmic reticulum membrane (Fig. 2).

In tangential sections grazing the parallel stacks of the endoplasmic reticulum cysternae, the ribosomes, viewed from above, appear to be arranged with considerable regularity with a slight tendency to form a centre-faced hexagonal pattern of densely packed masses of ribosomal particles (Fig. 3).

The other type of endoplasmic reticulum is the vesicular type, also rough, being studded densely with ribosomes. In the micrographs it can be seen as circular or oval profiles, 0·1 to 0·15 μ in diameter, which are distributed uniformly throughout the rest of the cytoplasm (Fig. 4). There is some indication that this type of

endoplasmic reticulum is formed from the flat cysternal type by pinching off at the circumference of the flat cysternae (Fig. 2). This suggestion, however, should be regarded as speculative since it is difficult to decide which way this process is going.

Some salivary gland cells contain almost exclusively the vesicular type of endoplasmic reticulum, side by side with cells containing both types (see JACOB and JURAND, 1963). Apart from the ribosomes attached to the membranes, the cytoplasmic matrix of the normal cells contains free ribosomes in considerable quantities (Fig. 4).

In the infected cells the cysternal flattened type of endoplasmic reticulum is practically non-existent, at least in the form of stacked arrays of lamellar profiles. The only remnants of this type are found in the form of single, elongated profiles of rough endoplasmic reticulum, particularly in less infected cells (Fig. 5). There are found, however, whorls of smooth membranes and large accumulations of smooth vesicles which are not encountered in the normal cell cytoplasms. These smooth membranes presumably represent disorganized remains of the lamellar flat and vesicular types of endoplasmic reticulum (Fig. 6).

Endoplasmic reticulum seems to give rise also to the cytoplasmic vacuoles frequently found in infected cells but never in normal cells (Fig. 7).

In general, the vesicular type of endoplasmic reticulum is better preserved than the flattened cysternal type, but the ribosomes are almost completely detached from the membranes so that the vesicular profiles appear to be mostly smooth. Free ribosomes in the cytoplasmic matrix are scarce, particularly in heavily infected cells, and, therefore, the cytoplasm in general appears to be considerably more electron-transparent than that of the uninfected cells (Fig. 8).

Ultrastructural differences between adjacent uninfected and infected cells in the same salivary gland are comprehensively illustrated in Fig. 9.

In the cytoplasm of the Microsporidia free ribosomes are abundant, and endoplasmic reticulum of both vesicular and flattened types is a frequent organelle in these cells. The elongated profiles of the flattened type of endoplasmic reticulum run, as a rule, parallel to the spherical surface of the microsporidian cells. It is characteristic that the overall appearance of the ultrastructure of the parasite cell cytoplasm is found to correspond to that in many other unicellular or even metazoan organisms, whereas the adjacent host cytoplasm outside the parasite cells appears abnormal in many respects (Fig. 10).

Mitochondria in the normal cells are of the usual metazoan type. They are represented in the micrographs as elongated or round profiles with frequent dense granules in the matrix. The cristae are of lamellar type usually oriented perpendicularly or at an angle to the long axis of the mitochondrion. Parallel orientation to the long axis is in normal cells an exception rather than the rule. The diameter of the round profiles and the width of the elongated ones average 0·32 μ (Fig. 11).

In the infected cells the mitochondria are narrower and on the whole much smaller in size than in normal cells (average diameter or width, 0·14 μ). The implication about the size is indirect, however, since the length has not been

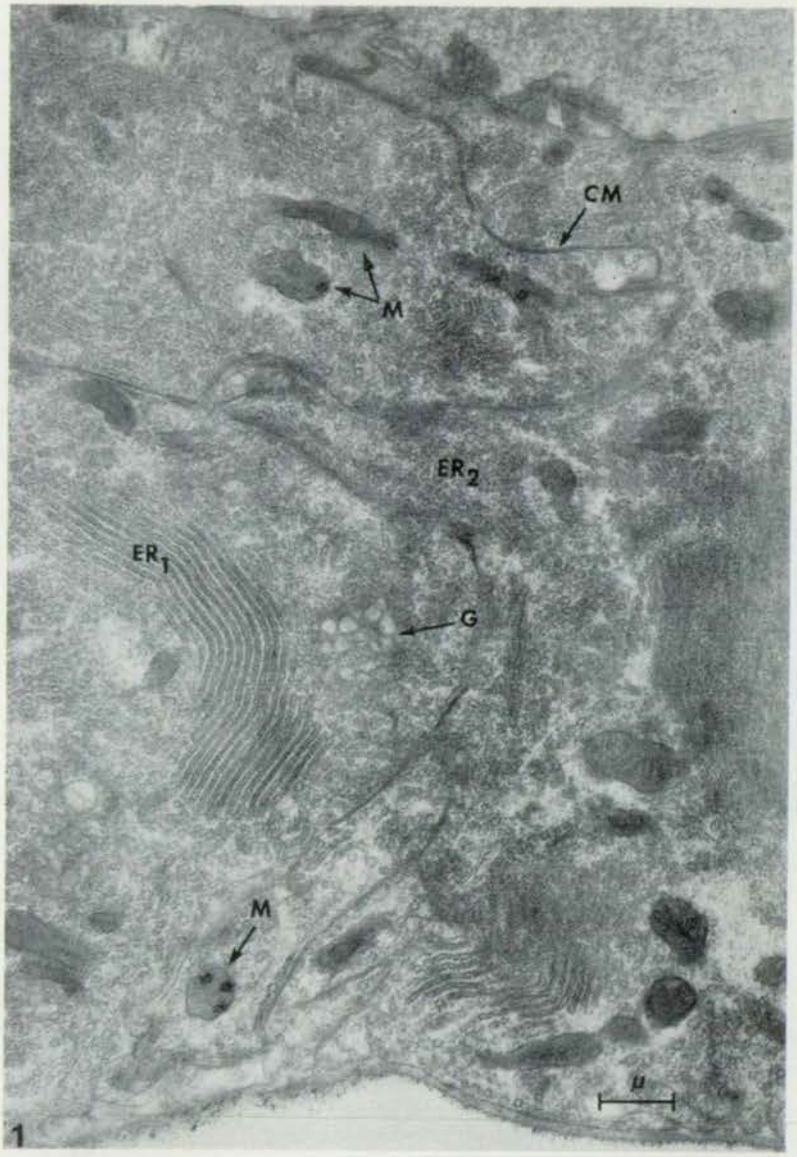

FIG. 1. General low-power view of a few adjacent cells of a normal salivary gland. The basal side is covered with a conspicuous basement membrane (bottom); the apical side is modified into a brush border (top). Note mitochondria (M), some with dense granules in the matrix, stacks of flattened cysternae of the endoplasmic reticulum (ER_1), vesicular endoplasmic reticulum (ER_2), Golgi areas (G), and cell membranes of and between the adjacent cells (CM).

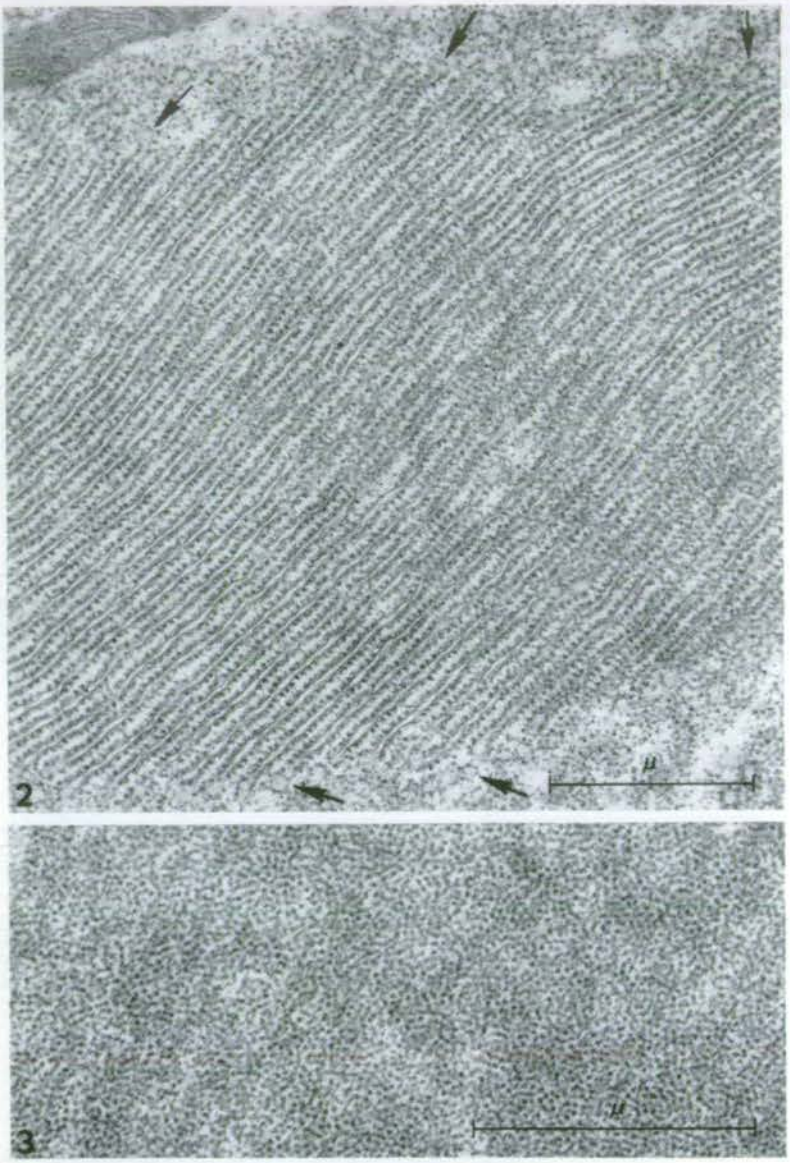

FIG. 2. Stack of parallel areas of flattened cysternae of endoplasmic reticulum densely studded with ribosomes (uninfected cells). Note formation of the vesicular endoplasmic reticulum (arrows).

FIG. 3. Tangential section through a condensation of flattened endoplasmic reticulum showing the arrangement of ribosomes (uninfected cells).

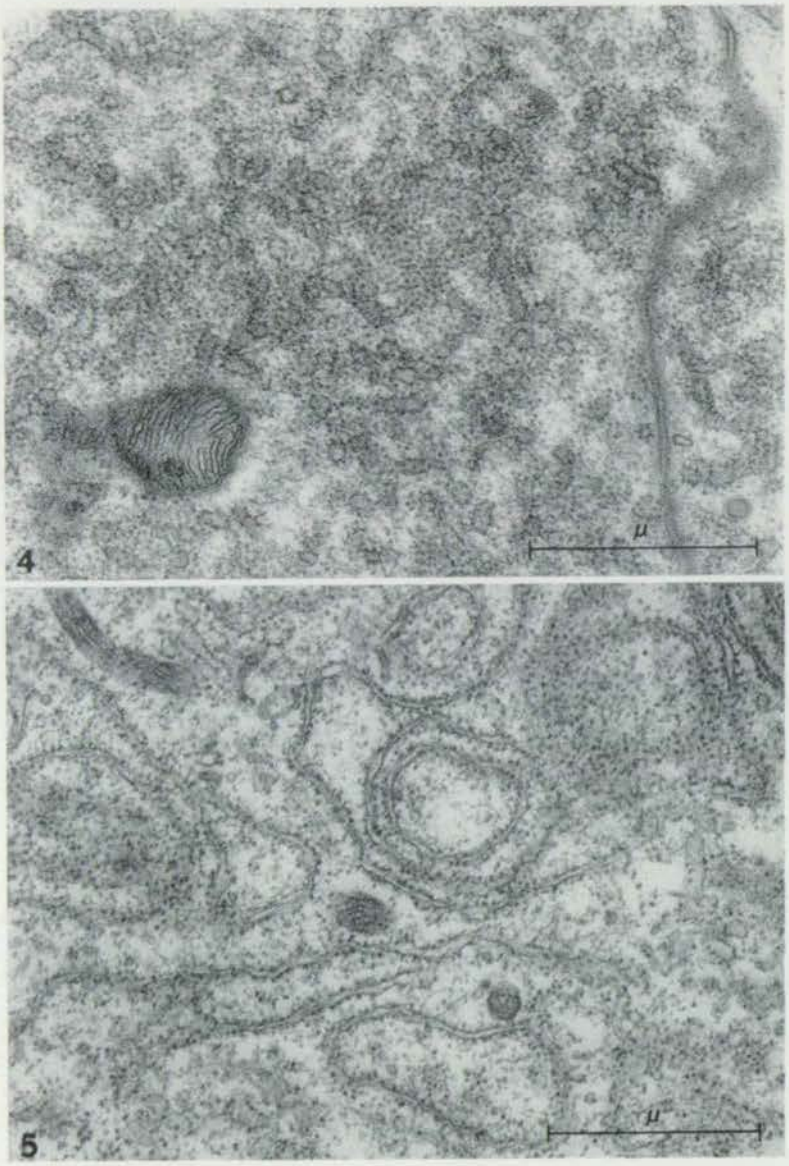

FIG. 4. Vesicular type of endoplasmic reticulum in an uninfected cell. Note free ribosomes lying in the cytoplasmic matrix.

FIG. 5. Scattered profiles of flattened endoplasmic reticulum in mildly infected cytoplasm. Note low electron density of the cytoplasmic matrix.

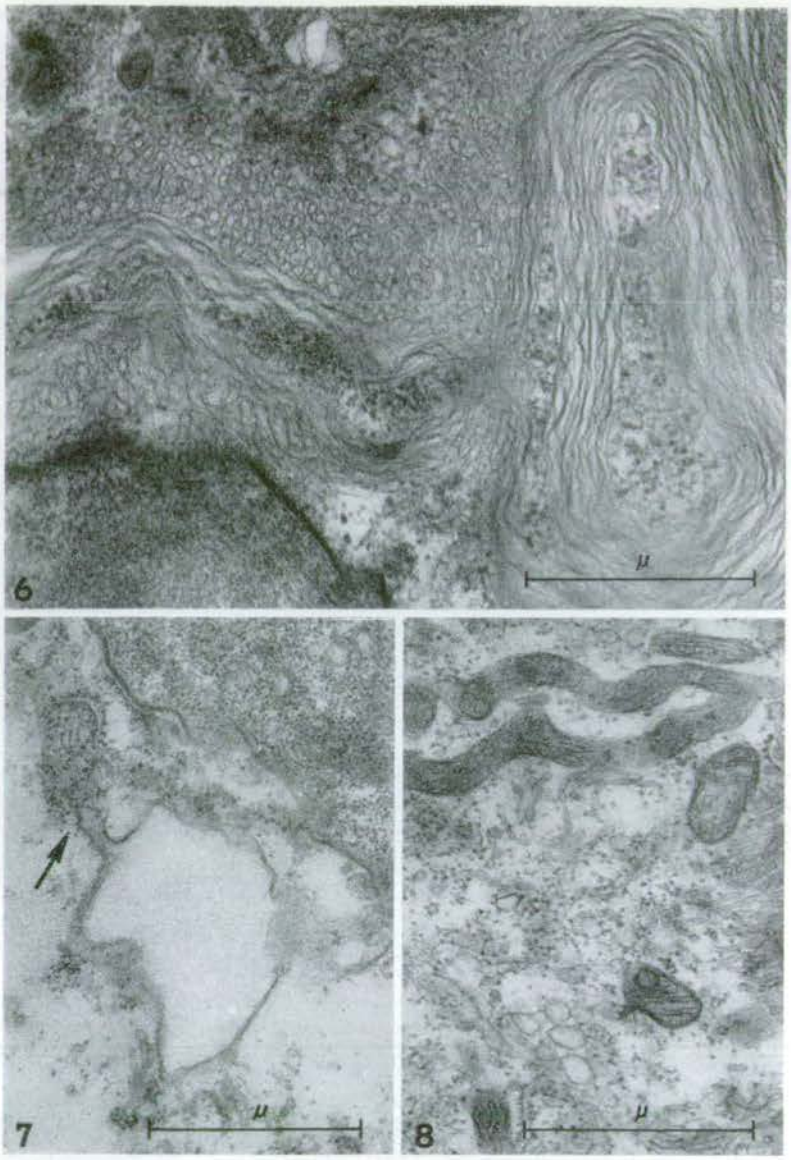

FIG. 6. Whorls of smooth membranes and vesicles in the cytoplasm of a heavily infected cell.

FIG. 7. Cytoplasmic vacuoles in an infected cell. Note connexion between vacuoles and endoplasmic reticulum profiles (arrow).

FIG. 8. Ultrastructure of the cytoplasm of an infected cell. Note smooth vesicles, flattened smooth cysternae, and scattered free ribosomes.

FIG. 9. Low-power micrograph of uninfected and infected adjacent cells of the same salivary gland. The differences pointed out in the text are clearly visible. Note that both cells are covered by a continuous basement membrane and that the infected basal cell membrane shows pinocytic activity (arrows).

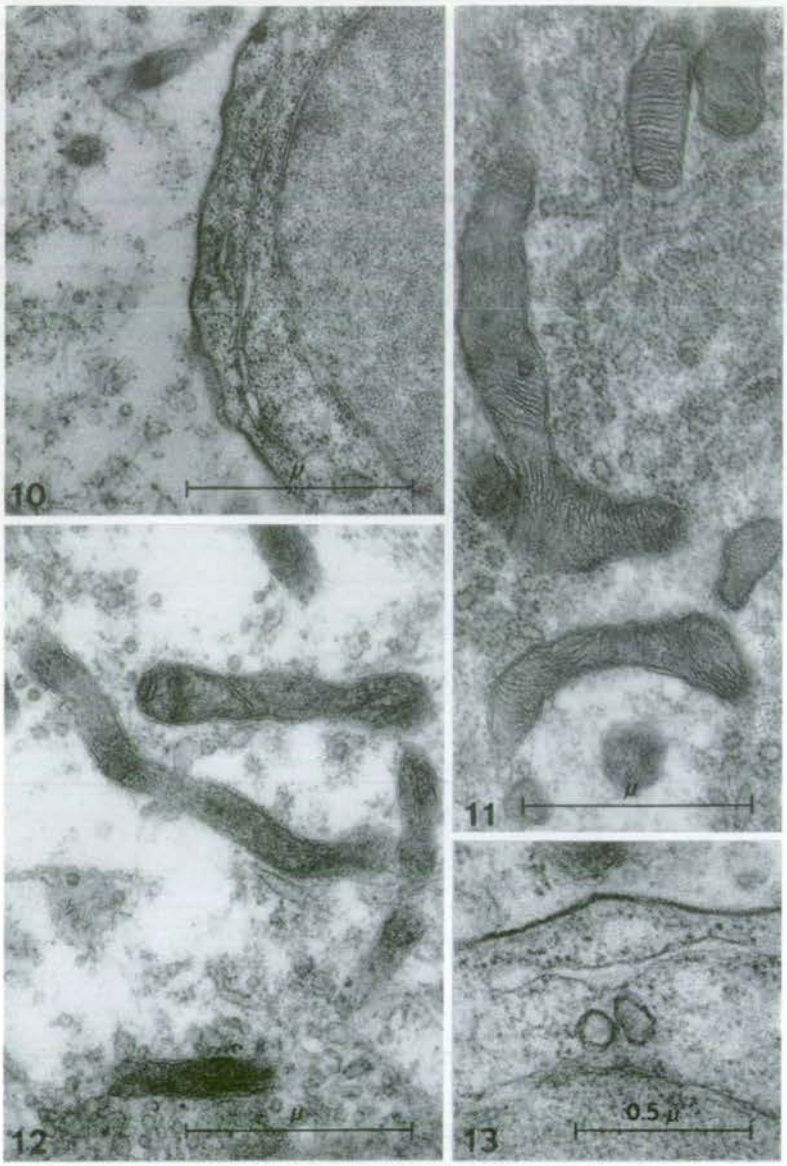

FIG. 10. A comparison between the ultrastructure of the parasite cell and that of the host cell.

FIG. 11. Typical mitochondria in normal salivary gland cells of *Sciara ocellaris*. Note dense granules in the matrix.

FIG. 12. Mitochondria in an infected salivary gland of *Sciara ocellaris*.

FIG. 13. Two vesicular bodies in the cytoplasm of a parasite cell, possibly mitochondria.

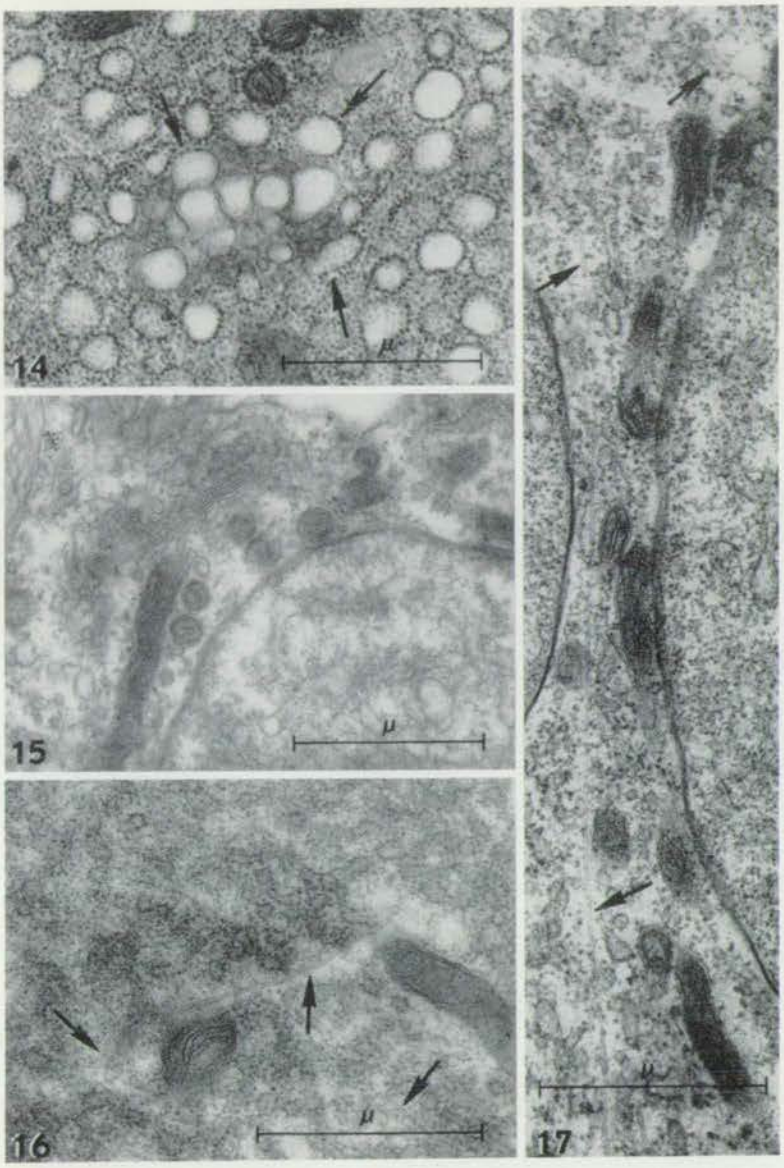

FIG. 14. Typical Golgi area consisting of larger and smaller smooth vesicles surrounded by vesicular rough endoplasmic reticulum. Arrows point out transitional profile of vesicles, partly of rough, partly of smooth vesicles.

FIG. 15. Golgi apparatus of lamellar type in the host cytoplasm next to a parasite cell.

FIG. 16. Microtubules in the normal cytoplasm (arrows).

FIG. 17. Microtubules in the cytoplasm of infected cell (arrows).

taken into account. At the same time the mitochondria are much more numerous. No dense granules are present in their matrix, and the mitochondrial cristae seem to be oriented parallel to the long axis of the organelle more often than in the normal cells (Figs. 12, 17).

Fig. 18 gives the statistical distribution of classes of the diameters of mitochondria in normal and infected cells.

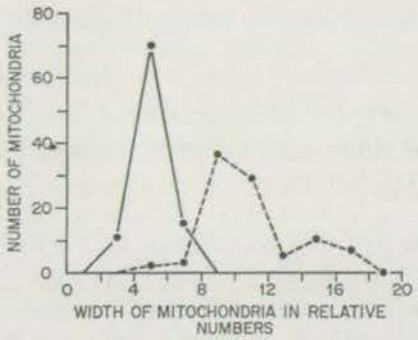

FIG. 18. Distribution graph of width classes of mitochondria in normal (- - - - -) and in infected cells (———) (width expressed in relative numbers).

We have attempted to find mitochondria in the cells of the parasite, but we can only say that there are no mitochondria of the normal protozoan type with tubular cristae in these cells. The only inclusions that we found in the cytoplasm of the parasite, and that could possibly be regarded as mitochondrial organelles, were very scarce, small, round vesicles covered with a double membrane with no obvious cristae inside (Fig. 13). The number of these inclusions is probably very small since only about one of ten investigated sections contained them, and these only a very few (one to three per section).

In normal cells, Golgi areas are evenly distributed throughout the cytoplasm. Most of them represent Golgi apparatus of the vesicular type, showing in one section an average of 20 to 30 small and large smooth vesicles easily distinguishable from the surrounding vesicular endoplasmic reticulum. The diameter of these vesicles varies between 0·1 and 0·5 μ (Fig. 14). At the periphery of these Golgi areas, however, there are sometimes found transitional profiles, partly smooth and partly rough, with ribosomal particles attached to them. This observation, which has been reported by several authors, together with the fact that Golgi areas in the present material were always surrounded by the vesicular endoplasmic reticulum, suggests that these two subcellular organelles are related. In the present material, only in a few cases was the Golgi apparatus observed in the form of the mixed type.

In heavily infected cells, Golgi areas were much less numerous and less obvious. Those which were observed were exclusively of the lamellar type usually surrounded by a number of small dense granules (Fig. 15). In the cytoplasm of the parasite cells, the Golgi apparatus was never observed as a typical subcellular entity.

In comparison with the normal host cells the infected cytoplasm contains numerous vacuoles limited by well-defined vacuolar membranes. Apart from these, as was mentioned above, the overall electron density of the cytoplasm of the infected cells is much lower, due mainly to the scarcity of endoplasmic profiles and of free ribosomes. Microtubules, however, do not appear to be affected by the presence of the parasite cells. They are seen mainly as stray tubular structures about 150 to 200 Å in diameter and up to 2 μ long scattered over the entire cytoplasm in both infected and uninfected cells in apparently similar numbers (Figs. 16 and 17).

DISCUSSION

Among the observed differences between the ultrastructure of normal and infected salivary gland cells, the most striking change is in the organization of the cytoplasmic organelles such as endoplasmic reticulum, and, topographically related with it, ribosomal particles, and changes in the width and average number of mitochondria. On the other hand, in the infected cells where the host cytoplasm is depleted of ribosomes, the microsporidial cells contain in their cytoplasm large numbers of bound and free ribosomes arranged as in other healthy organisms.

We can assume that the lower electron-opacity of the cytoplasm of infected cells is due to disarrangement of endoplasmic reticulum, depletion of ribosomal particles, and vacuolation, as is indicated in the descriptive part of this paper. It could be, however, in view of the pinocytic activity of the basal cell membranes in the infected cells, that in addition the cells become oedematous after infection and therefore the cytoplasm is less electron-dense.

Particularly interesting are the morphological changes and the increase in numbers of mitochondria due to infection. These organelles are responsible for respiratory cycles and energy-change processes. The presence of considerable numbers of intracellular parasitic Microsporidia no doubt creates abnormal conditions which induce morphological changes in mitochondria, the most evident being the change in their diameter and size. We have no data at the moment from which to determine whether this change makes mitochondria more or less efficient. It is known that mitochondria swell in the absence of phosphate acceptors. If, on the other hand, the respiratory processes are poisoned, they do not swell. The reverse phenomenon, namely shrinkage and contraction of mitochondria, occurs when they are subjected to an excess of ATP (LEHNINGER, 1964).

It is possible in the case of the microsporidian infection that the increase in the relative surface of the mitochondria makes them metabolically more efficient since the respiratory and energetic processes should be very high in the infected cells. However, the observed marked decrease in width seems to be structural and not due to simple mechanical shrinkage.

The practical non-existence of mitochondria in the parasite is not surprising, because in Sporozoa many obligate symbionts and parasites are deprived of this organelle. For example, absence of mitochondria has been demonstrated in some of the malaria parasites (PITELKA, 1963). *Plasmodium lophurae* and *Plasmodium*

berghei lack mitochondria of the usual protozoan type. In general, the more specialized the parasite the fewer mitochondria are to be expected in its cells (RUDZINSKA and TRAGER, 1957, 1959).

It is remarkable that although almost all the subcellular organelles are affected by the infection, the cytoplasmic microtubules seem to be particularly resistant. They are found in both uninfected and infected cells, often in longitudinal sections of considerable length (up to 2 μ). This fact indicates that these organelles run in straight lines rather than in convolutions, possibly because they are under certain tension due to their contractile nature (see ANDERSON *et al.*, 1966).

In nematocerous Diptera there are four distinct phases of development, in two of which (i.e. embryogenesis and pupation (metamorphosis)) large number of cell divisions take place. In the larval stages many cell types proliferate also (HINTON, 1963) but some cell types, e.g. those of salivary glands, do not divide. In the fourth phase, i.e. in the adult, cell divisions are restricted to only a very few tissues, particularly to those of the germ cell line.

A great number of cells undergo cytolysis during metamorphosis. New organs are then formed by new sets of cells derived from special organs called imaginal disks. The cells of the imaginal disks proliferate intensely in this phase of ontogeny.

Cytolysis of many cells during metamorphosis is a normal process in the development of insects, and is caused mainly by normal intracellular changes taking place during this specific phase of development. It is the cytolytic enzymes produced within the cells which lead to the cells' destruction. For instance, during the development of the salivary glands in *Chironomus*, an increase of DNAse (one of the cytolytic enzymes) was observed to occur preceding and concurrently with the decrease of DNA content of these cells (LAUFER *et al.*, 1965; LAUFER, 1965).

PAVAN and PERONDINI (unpublished) have observed that when a cell of the salivary gland is infected, the pattern of puffs which normally occurs in non-infected cells is greatly changed. Among other changes observed, the typical DNA puffs which occur at a specific stage of normal development in the salivary gland cells of *Sciara ocellaris* are clearly evident in the uninfected cells and absent in the infected ones. This shows that the presence of the micro-organism in the cytoplasm of the host cell changes the activity of genes in the polytene chromosomes and very probably changes the normal metabolism of the cell, not only quantitatively but also qualitatively.

Infection with Microsporidia has an apparently paradoxical consequence on the development of salivary gland cells. According to unpublished observations in this laboratory, although the infected cells are filled with parasite cells and the ultrastructure of their cytoplasm is greatly disorganized, they live longer than normal cells. Only some of the infected larval cells are cytolized during the pupation period. The possible explanation of this could be the following.

In the infected cells we have found that the rough endoplasmic reticulum, both lamellar and vesicular, undergoes disorganizational changes. Ribosomes decrease in number, and those that are left remain scattered as free ribosomal particles throughout the cytoplasm. In this state of abnormal organization of the cytoplasm,

protein synthesis probably becomes quite deficient in the host cells and, therefore, may influence the amount of enzymes responsible for lytic processes which will be deficient or even absent at the time of extensive cytolysis. Furthermore, it appears that the apparently disorganized cytoplasm is not so harmful to the cell itself, since some of the infected larval cells are maintained even through adult life.

It seems therefore that the association between the microsporidian parasite and the host cells, at least in some tissues of *Sciara ocellaris*, is commensal, or even endosymbiotic, rather than parasitic (see BUCHNER, 1953, for definition of endosymbiosis). Although there is extensive destruction of the endoplasmic reticulum and of other subcellular organelles in the cytoplasm of infected cells, at the same time the nucleus is very active in synthesis of DNA and RNA. Since the infected cells survive so long, it is feasible to assume that some of the cytoplasmic functions normally carried out by normal cytoplasmic constituents are now carried out by microsporidian organelles. Only future work will decide whether this hypothesis is correct.

Acknowledgements—The authors wish to express their deep gratitude to Mrs. SHIRLEY P. OGLE for her skilful work in breeding and maintaining the larvae of *Sciara ocellaris* in this laboratory and to Mrs. BARBARA R. BEATTY for help with printing the micrographs.

REFERENCES

ANDERSON W. A., WEISSMAN A., and ELLIS R. A. (1966) A comparative study of microtubules in some vertebrate and invertebrate cells. *Z. Zellforsch. mikrosk. Anat.* **71**, 1–13.

BUCHNER P. (1953) *Endosymbiose der Tiere mit pflanzlichen Mikroorganismen*. Birkhäuser, Basle.

DIAZ M. and PAVAN C. (1965) Changes in chromosomes induced by microorganism infection. *Proc. natn. Acad. Sci. U.S.A.* **54**, 1321–1327.

HINTON H. E. (1963) Metamorphosis of the epidermis and hormone mimetic substances. *Sci. Prog., Lond.* **60**, 306–322.

JACOB J. and JURAND A. (1963) Electron microscope studies on salivary gland cells of *Bradysia mycorum* Frey (Sciaridae)—III. The structure of cytoplasm. *J. Insect Physiol.* **9**, 849–857.

JACOB J. and JURAND A. (1965) Electron microscope studies on salivary gland cells—V. The cytoplasm of *Smittia parthenogenetica* (Chironomidae). *J. Insect Physiol.* **11**, 1337–1343.

JURAND A. and IRELAND M. J. (1965) A slow rotary shaker for embedding in viscous media. *Stain Technol.* **40**, 233–234.

LARA F. J. S., TAMAKI H., and PAVAN C. (1965) Laboratory culture of *Rynchosciara angelae*. *Am. Nat.* **99**, 189–191.

LAUFER H. (1965) Developmental studies of the Dipteran salivary gland.—III. Relationship between chromosomal puffing and cellular function during development. *19th Annual Symposium Fundamental Cancer Research*, pp. 237–250. Williams & Wilkins, Baltimore.

LAUFER H., RAO B., and NAKASE Y. (1965) Dipteran salivary gland metamorphosis; a self-regulating system. *Am. Zool.* **5**, 642.

LEHNINGER A. L. (1964) *The Mitochondrion. Molecular Basis of Structure and Function*. W. A. Benjamin, New York.

PAVAN C. and BASILE R. (1966a) Chromosome changes induced by infection in tissues of *Rhynchosciara angelae*. *Science, N.Y.* **151**, 1556–1558.

PAVAN C. and BASILE R. (1966b) Invertebrate pathology, cytology, and development. *Invert. Path.* **8**, 131–132.

PHILLIPS D. M. and SWIFT H. (1965) Cytoplasmic fine structure of *Sciara* salivary glands. *J. Cell Biol.* **27**, 395–409.

PITELKA D. R. (1963) *Electronmicroscopic Structure of Protozoa.* Macmillan, New York.

REYNOLDS E. S. (1963) The use of lead nitrate at high pH as an electron-opaque stain in electron microscopy. *J. Cell Biol.* **17**, 208–213.

ROBERTS P. A., KIMBALL R. F., and PAVAN C. (1966) Response of *Rynchosciara* chromosomes to microsporidian infection: Increased polyteny and generalized puffing (Abstract). *Genetics*, **54**, 357.

RUDZINSKA M. A. and TRAGER W. (1957) Intracellular phagotrophy by malaria parasites: an electron microscope study of *Plasmodium lophurae*. *J. Protozool.* **4**, 190–199.

RUDZINSKA M. A. and TRAGER W. (1959) Phagotrophy and two new structures in the malaria parasite *Plasmodium berghei*. *J. biophys. biochem. Cytol.* **6**, 103–112.

(17)

Ultrastructure of flagellated lambda symbionts in *Paramecium aurelia*

by A. Jurand and Louise B. Preer

J. gen. Microbiol. (1969), **54**, 359–364
With 3 plates
Printed in Great Britain

Ultrastructure of Flagellated Lambda Symbionts in *Paramecium aurelia*

By A. JURAND AND LOUISE B. PREER
Institute of Animal Genetics, Edinburgh, Scotland

(*Accepted for publication* 24 *July* 1968)

SUMMARY

The symbionts called 'lambda' present in the cytoplasm of killer stocks 239 (syngen 4) and 299 (syngen 8) of *Paramecium aurelia* have been investigated. Observations with the electron microscope of ultrathin sections and of negatively stained material revealed that these symbionts have peritrichous flagellation. The ultrastructures of symbionts from both stocks were identical and were those of flagellated bacteria.

INTRODUCTION

Four stocks of *Paramecium aurelia* bear cytoplasmic symbionts known as lambda: stock 239 (syngen 4), stocks, 216, 229 and 299 (syngen 8). They were described by Schneller (1957, 1961, 1962), Schneller, Sonneborn & Mueller (1959) and Sonneborn (1950, 1959, 1965). These stocks are referred to as rapid lysis killers, since sensitive paramecia are lysed within 20 min. after being exposed to them. Paramecia of syngen 3 are especially sensitive to the action of all lambda-bearing killers. Lambda particles are much larger than most of the other symbionts which have been described for *P. aurelia*. Van Wagtendonk, Clark & Godoy (1963) reported that it was possible to grow lambda particles in cell-free cultures in an axenic medium. There has been little electron microscopy of lambda reported. Sonneborn (1965) published one micrograph of this symbiont. The present paper reports investigations on lambda of *P. aurelia* stocks 239 and 299 by use of phase-contrast and electron microscopy.

METHODS

Both stocks of Paramecium were grown in lettuce medium previously inoculated with *Aerobacter aerogenes* (Sonneborn, 1950). Lambda particles outside the host cytoplasm were observed with a bright phase-contrast microscope (American Optical Co.) in animals freshly crushed between a slide and coverslip. To observe the symbionts *in situ* two methods were used. In the first, whole paramecia were observed with a dark phase-contrast microscope (Carl Zeiss), using paramecia treated with lacto-orcein according to the method of Beale & Jurand (1966). In the second, 1 μ Araldite sections were mounted on slides, stained with toluidine blue and observed with ordinary bright-field microscopy.

The ultrastructure of lambda symbionts was investigated by examination of ultrathin sections and of negatively stained isolated symbionts with the A.E.I. 6 electron microscope. For ultrathin sectioning mass cultures of each stock were fixed in one of two ways. In the first method the paramecia were concentrated by centrifugation,

and the supernatant culture medium replaced with a modified Palade (1952) fixative containing 15 mg. sucrose and 0·1 mg. calcium chloride/ml. fixative. Fixation was for 30 min. at room temperature (20°) or at 37·5°, and during this time the suspension of paramecia was gently stirred every few minutes. After fixation the paramecia were concentrated by centrifugation and dehydrated with aqueous 35, 70, 90, and 100 % ethanol, and embedded in Araldite on a slow rotary shaker (Jurand & Ireland, 1965) for 1 hr. Some preparations were made by using 1,2-epoxy-propane + Araldite before embedding in Araldite.

The second method of fixation used a 30 % (w/v) solution of osmium tetroxide in carbon tetrachloride (Afzelius, 1962). The osmium tetroxide solution was prepared just before use, and 0·3 ml. was added to a concentrated suspension of paramecia in the culture medium (0·6 to 0·8 ml.). The mixture was left for 20 min. at room temperature and the test-tube gently shaken frequently. Carbon tetrachloride and the culture medium do not mix, and fixation takes place in the culture medium into which osmium tetroxide penetrates very readily from the carbon tetrachloride layer. After fixation, 70 % (v/v) ethanol in water was slowly added and the mixture gently shaken until the two layers united. The mixture was then centrifuged, and the supernatant fluid discarded and replaced by 70 % (v/v) ethanol in water. Further dehydration and embedding was the same as in the first method. This second method of fixation is particularly suitable for preservation of various cytoplasmic symbionts in different stocks of *Paramecium aurelia*. For example, it was found to prevent shrinkage and preserve ultrastructure of refractile bodies and virus-like particles in kappa of stocks 7 and 562 (Preer & Jurand, 1968). On the other hand, the host cell organelles are usually well preserved with the modified Palade fixative (1952).

Partially purified lambda symbionts were prepared for negative staining as follows. A homogenate of 0·3 ml. of paramecia of stock 239 in 10 ml. of Dryl (1959) solution was diluted with an equal volume of 0·01 M-sodium phosphate buffer (pH 7) and passed through a cellulose column 12 mm. in diameter and 50 mm. high. The column was prepared by suspending 2 g. Whatman Ashless Filter Paper Pulp in distilled water and then washing with phosphate buffer. Examination with the bright phase-contrast microscope indicated that the turbid wash from the column was free from trichocysts and fragments of the cell body wall. The large lambda particles were separated from the lipid droplets, mitochondria and fragments of cilia in the turbid wash by a light centrifugation of 1000 *g* for 5 min. About 90 % of the particles in the pellet were lambda, with a few bacteria and mitochondria. A drop of the preparation was mixed with a drop of 5 % (w/v) phosphotungstic acid (pH 7) and examined with the electron microscope. Bacterial contaminants of two kinds were present. Their shape and small size made it possible to distinguish them readily from the numerous and much larger lambda particles.

To decrease to a minimum the number of bacteria present in the final preparation of isolated lambda particles and to aid the identification of the few bacteria which were present, a modified procedure was followed for the isolation of stock 299 lambda particles. The culture of paramecia was concentrated by centrifugation and the supernatant fluid which contained the bacteria was retained for later use as described below. The precipitate of packed paramecia was resuspended in 25 % (w/v) sterile yeast extract (Difco) at a concentration of about 0·1 ml. packed organisms in 100 ml. yeast extract solution. The paramecia were allowed to remain at room temperature

for 30 to 60 min., then filtered through cheesecloth and centrifuged. This process was repeated twice. Food vacuoles of paramecia treated in this way were seen to have no bacteria in them. These paramecia were then treated according to the procedure that was used to isolate lambda particles from stock 239. The lambda particles of stock 299 collected in the turbid wash from the cellulose column had very few contaminating bacteria among them. This preparation was examined with bright phase-contrast and electron microscopy. To establish a clear picture of the bacterial contaminants present, the original culture medium in which the paramecia had been grown, and from which they had been removed, was centrifuged at 8000 *g* for 5 min. The concentrated bacteria of the pellet were examined in bright phase-contrast and electron microscopes. This made possible the recognition of any bacteria, however few, which were in the preparations of isolated lambda particles.

RESULTS

Lambda symbionts in *Paramecium aurelia* stocks 239 and 299 were distributed throughout the host cytoplasm (Pl. 1, fig. 1 to 4). Usually there were more lambda particles present in stock 239 organisms than in stock 299 organisms grown under the same conditions. The symbionts were Gram negative bacterium-like particles, 2 to 4 μ long and about 0·5 μ wide, and were very similar in the two stocks. Lambda of crushed paramecia of stock 299 are shown as seen in the bright phase-contrast microscope in Pl. 1, fig. 5. A partially-purified preparation of lambda particles of stock 239 obtained from the cellulose column is shown in Pl. 1, fig. 6.

Examination of ultrathin sections of paramecia with the electron microscope revealed that lambda symbionts in both stocks were flagellated. The flagella were fairly evenly distributed over the entire surface of the symbiont, and the general ultrastructure of the flagella in both stocks was identical. *In situ*, the lambda particles, together with flagella, were usually enclosed within elongated vacuoles delimited from the host cytoplasm by an interface boundary. Two or three symbionts might be enclosed in a single vacuole (Pl. 1, fig. 7, 8).

The presence of numerous flagella was confirmed by examining with the electron microscope negatively stained preparations of partially purified lambda (Pl. 2, fig. 9, 10). It is difficult to give an approximate figure for the number of flagella present on one symbiont. In sectioned material the flagella were visible only as fragments, and in negatively stained preparations it was quite possible that some of the flagella may have been lost because of mechanical breakage during purification. It was estimated that there might be at least 100 flagella on the entire surface of one lambda symbiont. This estimate was made from Pl. 2, fig. 11, where there are a number of flagella sectioned transversely.

In ultra-thin sections the diameter of the flagella appeared to be about 170 Å. The ultrastructure was much less granular than in negatively stained preparations and occasionally showed transverse striations. In negatively stained preparations the measurements are uncertain because of the flattening of flagella during desiccation and because it is difficult to estimate the extent to which the negative stain penetrated the flagella. In these preparations the flagella very frequently assumed a characteristic sinusoidal form and were up to 5 μ long (Pl. 3, fig. 12). Their ultrastructure in negatively stained preparations was granular and appeared as two rows of linearly arranged

electron-dense subunits extending along the length of the flagellum symmetrically on both sides at about one quarter of its diameter (Pl. 3, fig. 13).

The lambda symbionts were enclosed in a cell wall consisting of two unit membranes. Inside the symbionts there were tightly-packed dense granules about 120 Å in diameter. The distribution of these granules, although dense, was not very uniform. There were less dense areas without granules occupied by elongated fibrillar structures about 500 Å long and 200 Å wide (Pl. 3, fig. 14).

To investigate whether flagella confer mobility on the lambda particles, paramecia were crushed between a slide and coverslip and observed with a bright phase-contrast microscope. In these conditions the lambda particles often showed a limited 'wiggling' motion, quite different from the Brownian movement. However, no clear swimming movement was observed.

DISCUSSION

Cytoplasmic symbionts in paramecia have long been regarded as bacterium-like. This idea is further supported by the present work which shows that lambda particles have several features which are characteristic of bacteria. First, the filamentous appendages of lambda resemble bacterial flagella. They are more like flagella than other similar bacterial structures such as pili (fimbriae). This conclusion is reached from a consideration of the length, diameter, surface distribution and especially the sinusoidal form of these appendages in negatively stained preparations. The length and diameter are within the ranges for these structures in bacteria (Newton & Kerridge, 1965). The more or less uniform distribution over the surface of the lambda particle is peritrichous flagellation, which is very common in bacteria (Leifson, 1960). Moreover, after drying the sinusoidal form is typical of bacterial flagella (Stocker, 1956), whereas pili are always straight (Brinton, 1965). The flagella of lambda particles are strikingly similar in shape to most of the flagella of bacteria shown in the paper of Houwink & Iterson (1950), which is a most informative work on this subject. The ultrastructure of lambda flagella is virtually identical with that of bacterial flagella, e.g. in *Proteus vulgaris* (Abram, Koffler & Vatter, 1965). Secondly, lambda particles give a negative reaction with the Gram reagents and the ultrastructure of the wall is very like that of Gram-negative bacteria such as *Escherichia coli*, Spirillum species and others (Murray, Steed & Elson, 1965; van Iterson, 1965). The two thin double-unit membranes observed in lambda are characteristic of Gram-negative bacteria. Thirdly, the ultrastructure of the intracellular content of lambda particles is similar to that of bacterial cytoplasm. The tightly packed dense granules in lambda particles resemble bacterial ribosomes, and the elongated fibrillar structures present in the less dense areas are similar to bacterial nucleoids (van Iterson, 1965; Fuhs, 1965). Altogether, filamentous appendages which resemble bacterial flagella, the ultrastructure of the cell wall which is very similar to that of Gram-negative bacteria, and the ultrastructure of the cytoplasm which is similar to the cytoplasm of bacteria, all make it evident that a lambda particle may well be regarded as a prokaryotic unicellular organism, a Gram-negative bacterium.

ADDENDUM

After this paper was sent for publication we obtained the two remaining stocks known to contain lambda particles, stocks 216 and 229 (syngen 8), and also stock 114

(syngen 2) which contains sigma particles (Sonneborn, Mueller & Schneller, 1959). These three stocks, like stocks 239 and 299, are rapid lysis killers.

The lambda particles of stock 216 and 229, and sigma of stock 114 were investigated by using the same methods as described in the main part of this paper. The lambda particles of stocks 216 and 229 appeared to be very similar to those of stocks 239 and 299. The measurements of the lambda particles, the peritrichous flagellation and the ultrastructure of the flagella in all four lambda stocks were virtually identical. Two differences were noted: in stock 229 the diameter of the flagella was the greatest of all of the lambda particles, measuring about 240 Å, whereas in stock 216 it was 200 Å, in both cases measured in sections; secondly, in stock 216, at least in the culture investigated, lambda particles were often enclosed in larger vacuoles containing several (up to 12) particles, whereas in the other stocks the symbionts usually occurred singly, or in pairs, in one vacuole. Sigma particles of stock 114 were of the same diameter as lambda particles but were 10 to 15 μ long and spirally curved. Flagella of sigma particles were very similar in ultrastructure and in their peritrichous distribution to those of lambda particles. Sigma particles were enclosed in vacuoles singly or in pairs.

In summary, all of the stocks known to kill by rapid lysis, i.e., the lambda-bearing stocks 216, 229, 239 and 299 and the sigma-bearing stock 114, contain particles which are morphologically similar. Observations with the electron microscope indicate that lambda and sigma particles are flagellated bacteria.

We wish to thank the National Science Foundation of the United States and the Phi Beta Psi Sorority for research grants to one of us (L.B.P.). We also wish to thank Professor G. H. Beale, F.R.S., and Professor J. R. Preer, Jun. for their interest and encouragement, and Dr J. F. Wilkinson of the Edinburgh School of Agriculture for discussions of relevant microbiological problems.

REFERENCES

Abram, D., Koffler, H. & Vatter, A. E. (1965). Basal structure and attachment of flagella in cells of *Proteus vulgaris*. *J. Bact.* **90**, 1337.

Afzelius, B. A. (1962). Chemical fixatives for electron microscopy. In *Interpretation of Ultrastructure*, p. 1. Ed. by R. J. C. Harris. New York and London: Academic Press.

Beale, G. H. & Jurand, A. (1966). Three different types of mate-killer (mμ) particle in *Paramecium aurelia* (syngen 1). *J. Cell Sci.* **1**, 31.

Brinton, C. C. (1965). The structure, function, synthesis and genetic control of bacterial pili and molecular model for DNA and RNA transport in Gram-negative bacteria. *Trans. N.Y. Acad. Sci.* **27**, 1003.

Dryl, S. (1959). Antigenic transformation in *Paramecium aurelia* after homologous antiserum treatment during autogamy and conjugation. *J. Protozool.* **6**, Suppl. 25.

Fuhs, G. W. (1965). Symposium on the fine structure and replication of bacteria and their parts. I. Fine structure and replication of bacterial nucleoids. *Bact. Rev.* **29**, 277.

Houwink, A. L. & van Iterson, W. (1950). Electron microscopical observations on bacterial cytology. II. A study on flagellation. *Biochim. biophys. Acta* **5**, 10.

Jurand, A. & Ireland, M. J. (1965). A slow rotary shaker for embedding in viscous media. *Stain Technol.* **40**, 233.

Leifson, E. (1960). *Atlas of Bacterial Flagellation*. New York & London: Academic Press.

Murray, R. G. E., Steed, P. & Elson, H. E. (1965). The location of the mucopeptide in sections of the cell wall of *Escherichia coli* and other Gram-negative bacteria. *Can. J. Microbiol.* **11**, 547.

NEWTON, B. A. & KERRIDGE, S. (1965). Flagellar and ciliary movement in micro-organisms. *Symp. Soc. gen. Microbiol.* **15**, 220.

PALADE, G. E. (1952). A study of fixation for electron microscopy. *J. exp. Med.* **95**, 285.

PREER, J. R. & JURAND, A. (1968). The relation between virus-like particles and R bodies of *Paramecium aurelia*. *Genet. Res.* (in the Press).

SCHNELLER, M. V. (1957). A new type of killing action in a stock of *Paramecium aurelia* from Panama. *Proc. Indiana Acad. Sci.* **67**, 302.

SCHNELLER, M. V. (1961). Genic interrelationship between two particle-bearing stocks of syngen 4, *Paramecium aurelia*. *Am. Zool.* **1**, 386.

SCHNELLER, M. V. (1962). Some notes on the rapid lysis type of killing found in *P. aurelia*. *Am. Zool.* **2**, 446.

SCHNELLER, M. V., SONNEBORN, T. M. & MUELLER, J. A. (1959). The genetic control of kappa-like particles in *Paramecium aurelia*. *Genetics*, **44**, 533.

SONNEBORN, T. M. (1950). Methods in the general biology and genetics of *Paramecium aurelia*. *J. exp. Zool.* **113**, 87.

SONNEBORN, T. M. (1959). Kappa and related particles in *Paramecium aurelia*. *Advanc. Virus Res.* **6**, 229.

SONNEBORN, T. M. (1965). The metagon: RNA and cytoplasmic inheritance. *Am. Nat.* **99**, 279.

SONNEBORN, T. M., MUELLER, J. A. & SCHNELLER, M. V. (1959). The classes of kappa particles in *Paramecium aurelia*. *Anat. Rec.* **134**, 642.

STOCKER, B. A. D. (1956). Bacterial flagella: morphology, constitution and inheritance. *Symp. Soc. gen. Microbiol.* **6**.

VAN ITERSON, W. (1965). Symposium on the structure and replication of bacteria and their parts. II. Bacterial cytoplasm. *Bact. Rev.* **29**, 299.

VAN WAGTENDONK, W. J., CLARK, J. A. D. & GODOY, G. A. (1963). The biological status of lambda and related particles in *Paramecium aurelia*. *Proc. natn. Acad. Sci. U.S.A.* **50**, 835.

EXPLANATION OF PLATES

Figs. 1 to 6 are optical micrographs. Figs. 7 to 14 are electron micrographs. Scale marks correspond to 1 μ unless otherwise indicated.

PLATE 1

Fig. 1. Section (1 μ) of *Paramecium aurelia*, stock 239, embedded in Araldite and stained with toluidine blue. × 675.

Fig. 2. Section (1 μ) of *P. aurelia*, stock 299, embedded and stained as in fig. 1. × 675.

Fig. 3. Whole mount, *P. aurelia*, stock 239, fixed with osmium tetroxide and treated with lacto-orcein. × 370.

Fig. 4. Whole mount, *P. aurelia*, stock 299, fixed and treated as fig. 3. × 370.

Fig. 5. Lambda symbionts of crushed *P. aurelia*, stock 299 (bright phase-contrast). × 2250.

Fig. 6. Partially purified symbionts of *P. aurelia*, stock 239 (bright phase-contrast). × 2250.

Fig. 7. Lambda symbionts, *P. aurelia*, stock 239. Note sections of flagella (arrow). × 15,000.

Fig. 8. Three lambda symbionts, *P. aurelia*, stock 299, enclosed in cytoplasmic vacuole. Note sections of flagella (arrow). × 15,000.

PLATE 2

Fig. 9. Negatively stained lambda symbiont, *P. aurelia*, stock 239. × 19,200.

Fig. 10. Negatively stained lambda symbiont, *P. aurelia*, stock 299. × 15,600.

Fig. 11. Oblique section of *P. aurelia*, stock 299 lambda symbiont, showing cross-sections through flagella (arrow). × 36,000.

PLATE 3

Fig. 12. Negatively stained flagella of lambda symbiont, *P. aurelia*, stock 239. × 28,000.

Fig. 13. High power electron micrograph of negatively stained flagella, *P. aurelia*, stock 239. × 160,000.

Fig. 14. Longitudinal section of lambda symbiont, *P. aurelia*, stock 239. Note the ultrastructure of the cell wall (*cw*), granular content (*g*) and less dense areas (*l*). × 28,000.

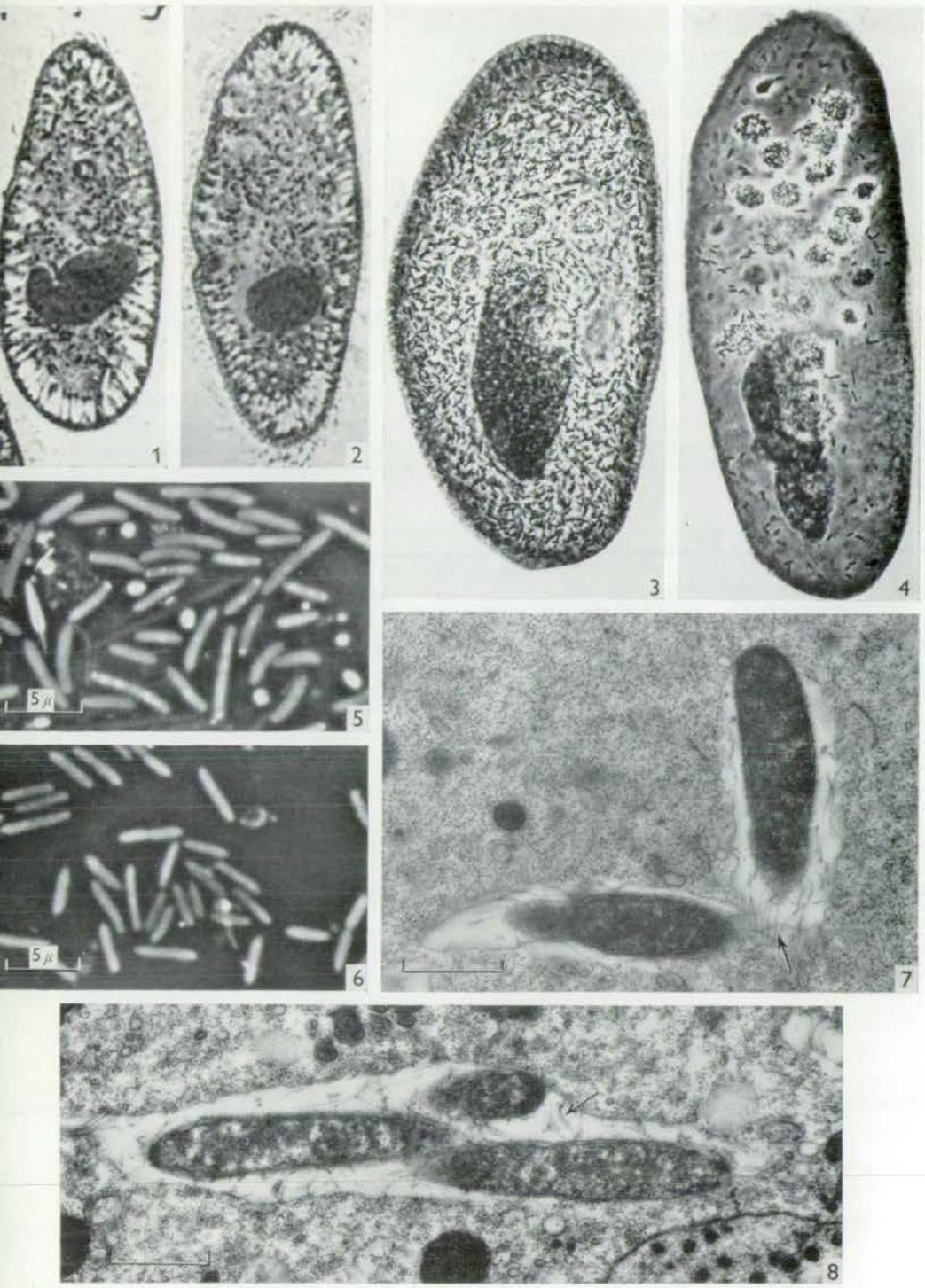
1
2
3
4
5
5 μ
6
5 μ
7
8

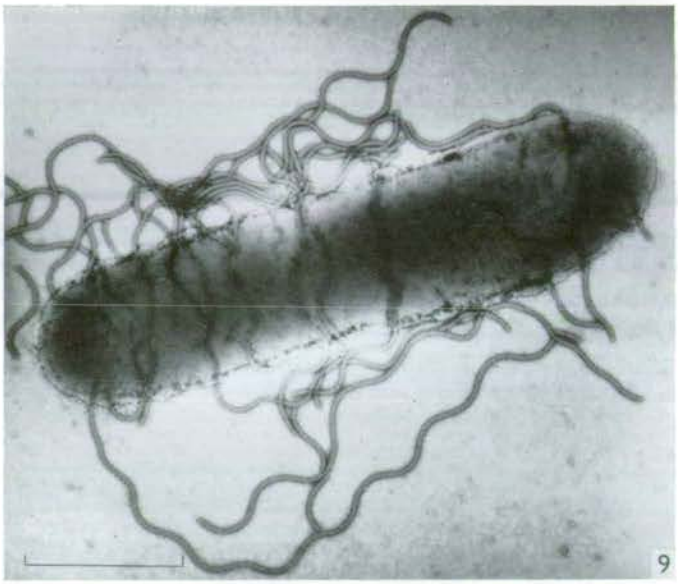
9

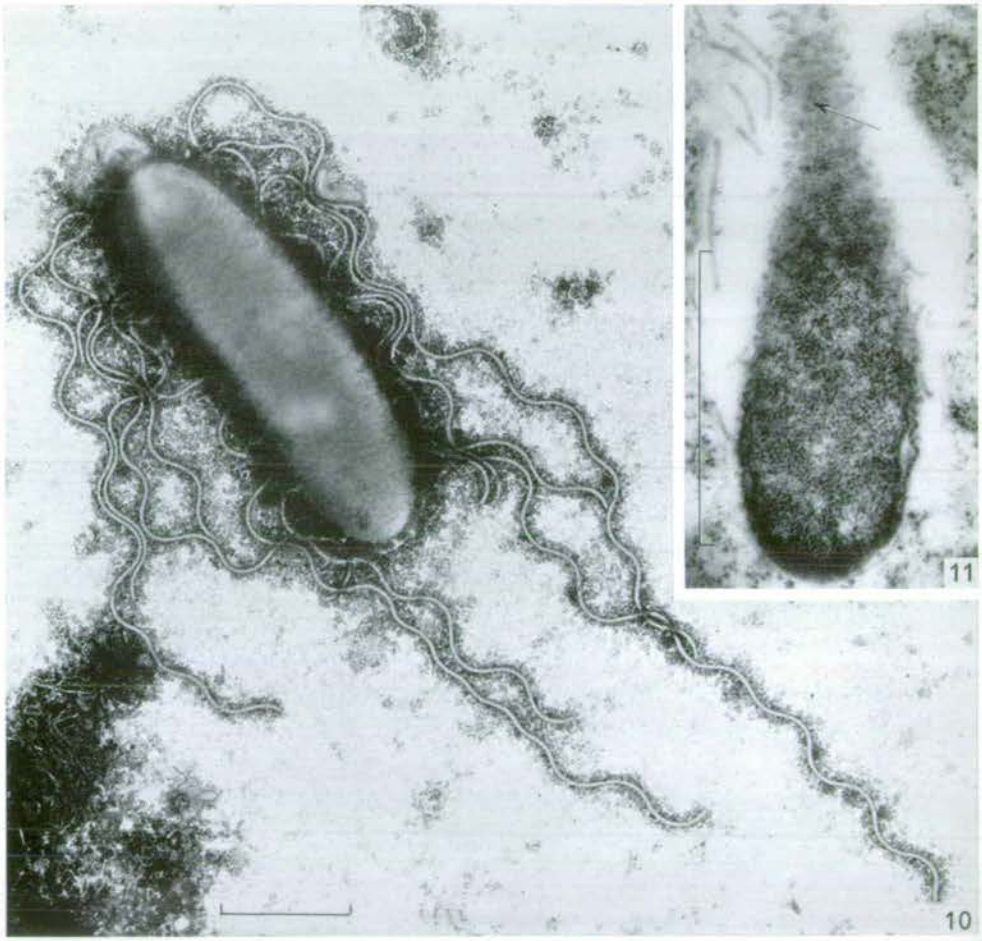
11
10

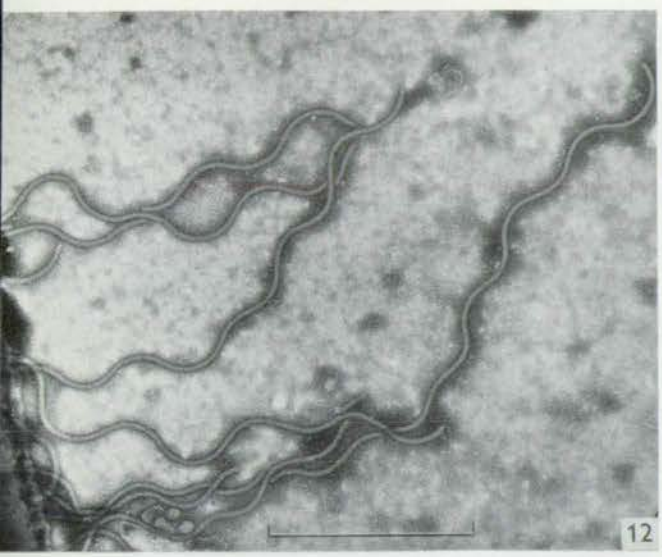
12

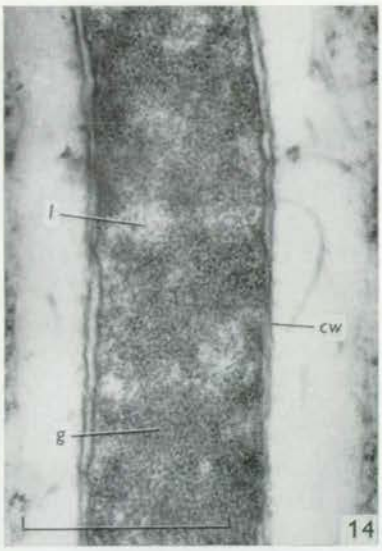
l
cw
g
14

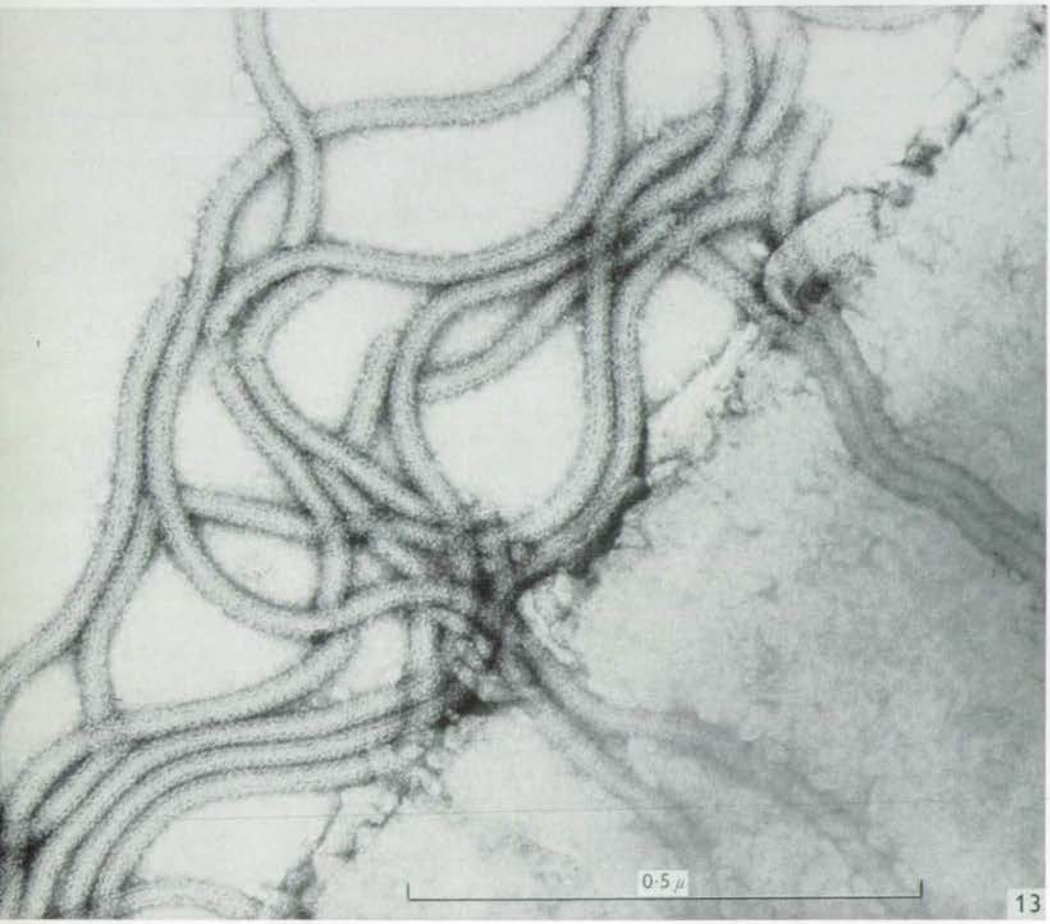
0·5 μ
13

The relation between virus-like particles and R bodies of *Paramecium aurelia*

by J.R. Preer and A. Jurand

Genet. Res., Camb. (1968), 12, pp. 331–340
With 1 plate
Printed in Great Britain

The relation between virus-like particles and R bodies of *Paramecium aurelia*

By JOHN R. PREER, JR.* AND ARTUR JURAND
Institute of Animal Genetics, West Mains Road, Edinburgh 9

(*Received* 26 *June* 1968)

1. INTRODUCTION

Kappa is a bacterium-like cytoplasmic element which is responsible for the toxic activity of certain killer strains of *Paramecium aurelia* (reviews in Sonneborn, 1959; Preer, 1968). When a killer paramecium is crushed between a coverslip and a slide and examined under the phase microscope it is found that up to 40% of the kappa particles contain a refractile structure called the R body (Preer & Stark, 1953). Kappa particles which contain an R body are called 'brights' because of their appearance in the phase microscope, and kappa particles which lack R bodies are called 'non-brights'. Some years ago it was established that non-brights are capable of giving rise to populations which contain brights, but that brights are probably non-reproductive (Preer, Siegel & Stark, 1953; Sonneborn, 1959; Smith, 1961; Mueller, 1963). R bodies have a number of remarkable features. First, each is a ribbon of protein which is normally wound in about ten turns into a roll of about 0·5 μ in diameter, but which has the capacity to unroll suddenly into a long twisted ribbon or tube-like structure some 15 μ long (Mueller, 1962; Anderson, Preer, Preer & Bray, 1964; Preer, Hufnagel & Preer, 1966). Secondly, the R body is somehow related to the toxic activity of killers, for the toxic agent itself is normally the bright; in one strain of killers, the isolated R body is toxic (Preer & Preer, 1964). Finally, if R bodies are freed from kappa particles by lysing them with suitable treatments and then inducing them to unroll by lowering the pH or treating with phosphotungstic acid, numerous virus-like particles (so-called because they look like viruses in the electron microscope) and capsomere-like elements are found sticking onto the original inner end of the unrolled tapes (Preer & Preer, 1967).

It has been suggested that the virus-like particles are the toxin and that the R body functions as a vehicle for delivering the toxin to its site of action within sensitive paramecia (Anderson *et al.* 1964; Mueller, 1965; Preer & Preer, 1967). It has also been suggested that the virus-like particles are found within non-brights in a latent form and that their induction brings about the formation both of mature virus-like particles and of the R body as well (Preer & Preer, 1967). It has been pointed out that if this last suggestion is correct, then the virus-like particles should be present in brights and absent in non-brights.

* Present address: Department of Zoology, Indiana University, Bloomington, Indiana, U.S.A.

In this paper we report a number of observations on virus-like particles and R bodies in sectioned killers. We confirm the prediction that the virus-like particles are associated primarily with the bright kappa particle. Furthermore, they are usually found in close proximity to (often within) the R bodies themselves. These findings establish a close relationship between the virus-like particles, R bodies, and toxic activity.

2. MATERIAL AND METHODS

The work was carried out with stocks 7 and 562 of syngen 2 of *P. aurelia*. Stock 7 was originally collected by T. M. Sonneborn from Pinehurst, N.C. It causes sensitives to spin on their longitudinal axes before dying. Stock 562 was collected by G. H. Beale from Milan, Italy. The original 562 contained not only kappa in its cytoplasm but also another symbiont in its macronucleus. A strain lacking the macronuclear symbiont, but containing kappa, was derived by L. B. Preer (unpublished) and used here. 562 kappa causes sensitives of syngen 1 to form large vacuoles before they die, but no spinning is induced. The paramecia were cultured in an infusion of grass (0·15 g/l., boiled, filtered and autoclaved), buffered with 1·0 g of $Na_2HPO_4.12H_20$ per l., and inoculated the day before use with *Klebsiella aerogenes*. Cultures were doubled in volume twice a week, using uninoculated infusion. Stock 7 was cultured at room temperature (about 17 °C) and stock 562 kappa was cultured at 25 °C. The cultures were filtered through cheese-cloth and centrifuged to concentrate them. Paramecia were fixed by adding 0·3 ml of 30% OsO_4 in CCl_4 to about 10^6 paramecia in 0·6 ml of their own culture medium (Afzelius, 1962; Jurand & Preer, 1968). Fixation was at room temperature for 20 min. with agitation every few minutes. The fixed paramecia were dehydrated by passing through 70%, 95% and three changes of absolute alcohol. Before embedding, absolute alcohol was replaced by 1,2-epoxypropane. Embedding was in Araldite, using a rotary mixer as described by Jurand & Ireland (1965). Thin sections were cut using glass knives in a Porter-Blum Sorvall microtome. Staining was for 20 min with a 1% potassium permanganate solution containing 2·5% uranyl acetate. Although a number of other methods of fixation and staining were tried, the above procedure gave the best results.

Kappa particles (of stock 7) were isolated by first homogenizing (in a stainless steel milk homogenizer, A. H. Thomas Co., Philadelphia) up to 4 ml of packed paramecia in 10 vol. of Dryl (1959) solution at 4 °C. A volume of 0·01 M phosphate buffer, pH 7·0, equal to the volume of Dryl solution used was then added. Twelve tablets (26 g) of filter-paper pulp (Whatman) were placed into 200 ml of distilled water and poured into a column 2·2 cm in diameter and washed with the phosphate buffer until the wash was clear. With the fluid level about a centimetre above the top of the column, the homogenate was pipetted onto the column. Additional buffer was added to the column and wash fractions were collected. The wash contained mitochondria, cilia and bacteria; kappa, trichocysts and body wall fragments were retained in the column. After the buffer wash was complete, as

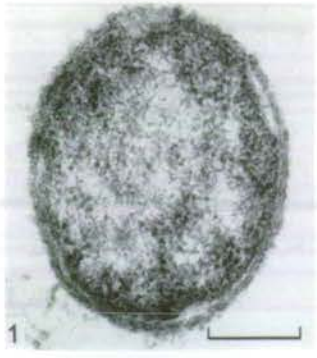
1

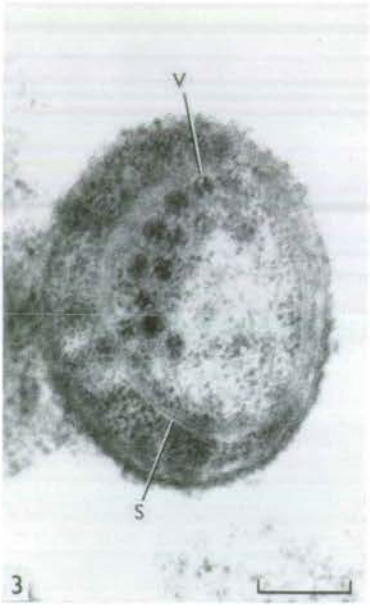
V
S
3


5

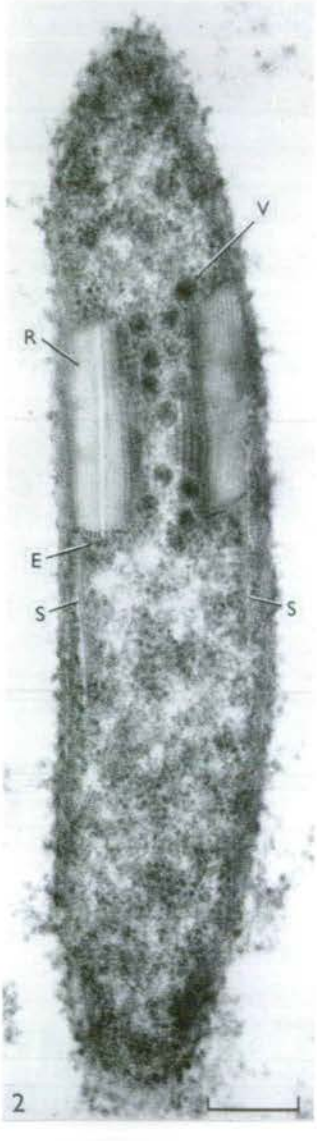
V
R
E
S
S
2

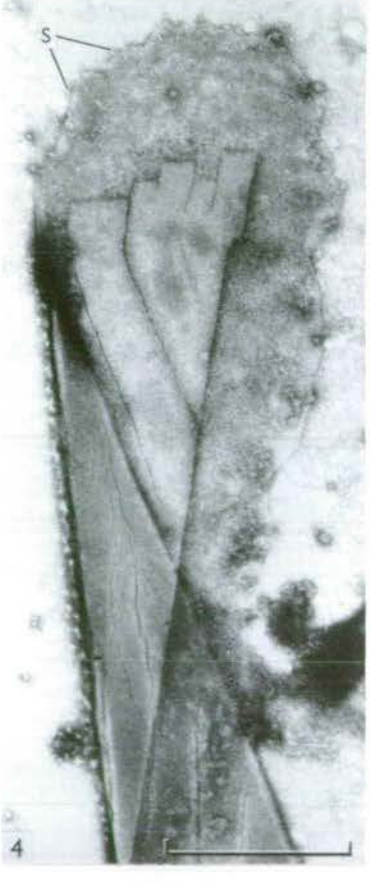
S
4


V
6


V
EV
7

judged by lack of turbidity in the fractions, the kappa particles were eluted by adding 300 ml of 0·5 M-NaCl in 0·005M-Na_2HPO_4 (pH 8·0). The turbid eluate was collected and concentrated by centrifugation. Free R bodies were obtained by lysing kappa particles with deoxycholate and paramecium extract as described earlier (Preer & Preer, 1967).

An American Optical Co. 'Bright Medium' oil-immersion phase objective was used for phase microscopy. Negative staining was carried out by adding a droplet of suspension to a grid which had been previously coated with Formvar and carbon. Another droplet of 5% phosphotungstic acid (previously adjusted to pH 7·3) was added to the grid and mixed. Excess fluid was then removed by touching a piece of filter paper to the mixed droplets. Electron microscopes were the Philips 200, AEI 6, and AEI 6B.

A number of preparations were studied in the electron microscope. For statistical purposes approximately 100 sections of kappa were chosen at random from each of three different preparations.

3. RESULTS

(i) *The presence of virus-like particles in sections*

In most of the sections lacking R bodies, no virus-like particles could be seen in either stock 7 (Pl. 1, fig. 1) or stock 562 (Pl. 1, fig. 5). In most of the sections in which R bodies could be seen, from 1 to 14 structures up to 900 Å in diameter were found both in stock 7 (Pl. 1, figs. 2 and 3) and in stock 562 (Pl. 1, fig. 6). The structures in stock 7 appeared to be identical to the virus-like particles described earlier (Preer & Preer, 1967) in negatively stained material. Negatively stained preparations of stock 562 revealed similar structures. The virus-like particles were concentrated inside the core of the R body and in the areas immediately adjacent to the core. A section with virus-like particles but without R bodies (stock 562) is shown in Pl. 1, fig. 7.

DESCRIPTION OF PLATE

All bars represent 0·2 μ. R = R body, V = virus-like particle, EV = empty virus-like particle, S = sheath, E = dark staining edges of R body.

Fig. 1. Section of kappa in stock 7 with neither virus-like particles nor R body. × 60000

Fig. 2. Longitudinal section of kappa in stock 7 showing virus-like particles, R body, and sheath. × 60000

Fig. 3. Cross-section of kappa in stock 7 through sheath, one corner of R body and virus-like particles. × 60000

Fig. 4. Outer end of an unrolled R body of stock 7 showing portions of broken sheath. Negative staining. × 120000

Fig. 5. Section of kappa in stock 562 with neither virus-like particles nor R body. × 60000

Fig. 6. Longitudinal section of kappa in stock 562 showing virus-like particles and R body. × 60000

Fig. 7. Section of kappa in stock 562 showing no R body, but virus-like particles, both filled and empty. × 60000

(ii) *The distribution of virus-like particles among brights and non-brights*

Not in every instance could individual virus-like particles in the sections be identified with certainty. Nevertheless, different observers agreed sufficiently well to justify tabulating the estimates of numbers in randomly selected sections of three preparations (Table 1). The first two preparations were both of stock 7 and were identical except that they were taken at different times. It is noted that in preparation A, 12 of 13 sections which had a portion of an R body contained virus-like particles, most containing more than one. In the same preparation only 12 of 88 sections in which an R body was absent contained virus-like particles, most of the 12 sections having only one virus-like particle. The mean number of virus-like particles per section was accordingly much higher among the sections containing an R body (5·2 in preparation A) than among the sections lacking an R body (0·2 in the same preparation). It is noted that in preparation A, although only 13 % of the sections contained R bodies, an independent determination of the fraction of brights made from crushed animals using the phase-contrast microscope gave 25 % on the same preparation. As would be expected, some sections through brights evidently fail to include the R body. These same general relations were found in the other two preparations. Thus the correlation between the presence of R bodies and virus-like particles was very high in sections.

Although the correlation between *sections* which contained part of the R body and the presence of virus-like particles was high, it was not perfect. Nevertheless, the data are entirely consistent with an absolute correlation between *whole kappa particles* containing R bodies (brights) and virus-like bodies, as will now be shown.

If all brights contain virus-like particles, an occasional section containing an R body but lacking virus-like particles would be expected, for the number of virus-like particles is low and the section thickness is only about one-seventh the diameter of the bright. Virus-like particles were observed in all but three of 26 R body-containing sections. Therefore most, and probably all, brights contain virus-like particles.

If non-brights never have virus-like particles, sections lacking an R body but containing virus-like particles would still be expected because sections through brights may fail to include the R body. The expected frequency of sections which pass through brights but fail to include the R body may be estimated from Table 1 as the difference between the percentage of whole kappas with R bodies and the percentage of sections with R bodies, or 12 % for preparation A, 5 % for B and 17 % for C. When these percentages are multiplied by the total number of sections in each preparation one obtains the expected numbers of 12 for A, 5 for B and 17 for C. The observed numbers of sections without R bodies, but with virus-like bodies, were 12 for A, 2 for B and 11 for C. These numbers agree well with the expected, especially since it is likely that sections through brights which miss the R body also sometimes fail to include virus-like bodies. The data provide no evidence that kappas without R bodies have virus-like particles. If such kappas exist they must be rare. This conclusion is substantiated by observations of around

Table 1. *The distribution of virus-like particles in random sections of kappa*

Preparation	R body in section	No. of virus-like particles in each section	No. of virus-like particles per section	Sections with virus-like particles	Totals: Sections with virus-like particles	Totals: Sections with R bodies	Totals: Whole kappa with R bodies
A. Stock 7	Present	0, 1, 2, 2, 2, 3, 4, 5, 8, 8, 9, 10, 14	68/13 = 5·2	12/13	24/101 = 24 %	13/101 = 13 %	24/97 = 25 %
	Absent	76 with 0, 1, 1, 1, 1, 1, 1, 1, 1, 2, 2, 2, 2	16/88 = 0·2	12/88			
B. Stock 7	Present	0, 0, 2, 3, 5, 5, 7, 11	33/8 = 4·1	6/8	8/95 = 8 %	8/95 = 8 %	67/500 = 13 %
	Absent	85 with 0, 1, 1	2/87 = 0·02	2/87			
C. Stock 562	Present	2, 5, 7, 8, 12	34/5 = 6·8	5/5	16/97 = 16 %	5/97 = 5 %	66/301 = 22 %
	Absent	81 with 0, 1, 2, 2, 2, 2, 2, 3, 5, 6, 11	39/92 = 0·4	11/92			

20 sections of dividing kappa particles in preparation C. Although the sections passed near the centres of the kappa particles and should have revealed R bodies had they been there, no R bodies were seen; furthermore, no definite evidence of virus-like bodies was found in any of them.

(iii) *The frequency of 'empty' virus-like particles in intact brights*

It was possible to make a rough estimate of the number of virus-like particles in the whole kappa particles from the numbers in the sections. First, the total number of virus-like particles in the 101 random sections of preparation A was taken from Table 1 as 84. Since sectioning should often cut virus-like particles into more than one part, the counts should be biased by being too high. Therefore, it is convenient to think of, and estimate, the number of *centres* of virus-like particles in the 101 sections. The diameter of a virus-like particle and the section thickness are about the same (about 800 Å), so that a single virus-like particle could be sectioned into no more than two parts; therefore, the number of centres must lie between 84 and 42. A fairly good estimate can probably be obtained if it is assumed that a virus-like particle is divided into *two* recognizable parts only if a cut passes through the middle one-half of the diameter. Two recognizable parts should therefore be produced by about one-half the cuts and one recognizable part by the other cuts. It is easily, seen, then that one-third of the recognizable sections would not have centres and 84 should be decreased by one-third to yield 56 centres. We should like to divide the number of centres, 56, by the number of volumes of brights in the sections to obtain the number of virus-like particles per bright, assuming that all the virus-like particles are present in the brights. The total volume of kappa in the 101 sections was determined by multiplying the section thickness of 800 Å by the area (estimated from photographs); a value of 7·56 μ^3 was obtained. The fraction of the 7·56 μ^3 which was derived from brights is

$$\frac{0{\cdot}37 \times 0{\cdot}25}{(0{\cdot}37 \times 0{\cdot}25) + (0{\cdot}19 \times 0{\cdot}75)} = 0{\cdot}39,$$

i.e. the average volume of brights estimated from phase microscopy at 0·37 μ^3 times the fraction of brights (found by observations on whole kappa particles of preparation A to be 24/97 or 25%) divided by the sum of the same product plus the product obtained by multiplying the average volume of a non-bright (0·19 μ^3) times the fraction of non-brights (75%). The fraction 0·39 multiplied by the total volume of sections of kappa (7·56μ^3) gave 2·95μ^3, the total volume of sections of brights. This volume divided by the volume of one bright represents 2·95/0·37 or eight brights, yielding 56/8 or seven virus-like particles per bright. A similar calculation for preparation B gave five virus-like particles per bright.

Negative staining of unrolled, isolated R bodies has revealed a small number of 'filled' virus-like particles and a larger number of 'empty' virus-like particles, along with numerous free capsomere-like structures. It has been suggested (Preer & Preer, 1967) that the filled particles consist of a thin envelope closely surrounding a protein coat made of the capsomere-like elements (and, if the structures are

viruses, an inside core of nucleic acid). The empty forms appear to consist only of the envelope. Since the virus-like particles seen in the sections stain much darker than the surrounding areas of kappa it is reasonable that they represent the filled virus-like particles. This conclusion is supported by the finding of very pale, apparently empty, virus-like particles in certain sections (Pl. 1, fig. 7). If these are the empty particles, then it is evident that they are so difficult to see in sections that they can only be observed under unusually favourable circumstances.

When 34 unrolled R bodies from a portion of the culture used for preparation B were examined in negative staining it was found that the number of filled virus-like particles per R body ranged from 0 to 9 (mean 1·0) while the number of empty virus-like particles ranged from 0 to 32 (mean 10·9). The low number of filled virus-like particles found in negative staining (mean of 1·0) compared with the number of filled particles in sections of preparation B (computed above to be about 5) might be explained by the fact that during isolation and unrolling of R bodies many virus-like particles (both full and empty) fall free of the R bodies. It may also be that some of the filled particles became empty during isolation. Nevertheless, it is unlikely that most of the numerous unfilled particles found in negative staining (10·9) were derived by the emptying of full particles, for the estimated number of filled particles in sections was only 5. These relations suggest that most of the virus-like elements are never assembled in stock 7, being present only in the form of unfilled envelopes (which are difficult to see in sections), free capsomere-like structures, and, if they are viruses, as free nucleic acid.

(iv) *The sheath and the asymmetry of the R body*

Attention should also be drawn to the sheath-like extension found on one end of the R body of stock 7 (but not stock 562) (Pl. 1, figs. 2, 3). Once observed in sections, it proved easy to find in micrographs of negatively stained material (Pl. 1, fig. 4). It is visualized as a cylindrical jacket enclosing the R body and extending outward from one end.

A hitherto unknown characteristic of the R body of stock 7 is seen in longitudinal sections and reveals an apparent asymmetry in the edges of the R body on the end from which the sheath extends. The cut ends of the ribbons stain much darker on the end adjacent to the sheath (Pl. 1, fig. 2).

4. DISCUSSION

The data show the presence of the virus-like particles in most if not all kappa particles with R bodies (brights) and their absence in most if not all kappa particles without R bodies. Since the R body has already been shown to be uniquely correlated with the toxic activity of killers, the virus-like particles also are now seen to be correlated with killing activity.

The relation between brights and the virus-like particles is in agreement with the theory that the virus-like particles are viruses which are present in non-brights in a latent form. There presumably they often become spontaneously induced,

producing viruses and resulting in the R body protein as well. Destruction of the reproductive capacity of the kappa particles in which the viruses develop must also occur, thereby explaining the fact that kappa particles containing R bodies cannot reproduce.

It is likely that many of the 'empty' virus-like particles on unrolled R bodies seen in negative staining are present in the intact kappa particles and do not arise by the emptying of filled virus-like particles during isolation of R bodies. Unfilled particles must exist in intact brights, for they can sometimes be seen in sections. Furthermore, the data suggest that the number of filled particles in sections is too low to be the source of the numerous unfilled particles seen in negative staining. If the virus-like particles are really viruses, then their developmental processes must be highly inefficient, numerous envelopes (empty virus-like particles) and capsomeres being formed but only a few ever being assembled into complete viruses. Such inefficiency may well mean degeneration and reflect a loss of the need for the viruses to retain their ability to infect, being transferred entirely by heredity. Induction may retain a selective advantage, however, in being necessary for the manifestation of the toxic activity, even though few fully mature forms are produced. In this respect the virus-like particles are suggestive of the bacteriocins (see discussion in Sonneborn, 1959) except that the latter are toxic to other bacteria rather than to cells of the same species in which the bacteria live, as in the case of the bacteria-like kappa particles and their toxin. The recent work on the toxin and inheritance in killer yeast by Woods & Bevan (1968) is also suggestive of similar elements.

The sheath which appears to enclose the R body of stock 7 is interesting from the point of view of the mechanism of the unrolling of the R body. If the sheath completely encloses the R body, as it appears to do, then it must be broken when unrolling occurs. It may be that the R body of stock 7 is always under tension, but is restrained from unrolling by the sheath. Spontaneous unrolling, which is frequently observed, would be due to spontaneous breakage of the sheath. The action of sodium dodecyl sulphate, which is known to unroll the R bodies of stock 7 (Preer & Preer, 1964), would operate by dissolving the sheath. The unrolling observed in the food vacuoles of sensitives (Preer & Preer, 1967) could be due to the action of digestive enzymes on the sheath. Unrolling of the R body of stock 7 should therefore not be reversed by removal of the conditions inducing unrolling, just as observed. The R bodies of stock 51, on the other hand, have no sheath as judged from published micrographs (Dippell, 1958; Rudenberg, 1962). It would appear that the tension conducive to unrolling in stock 51 is present only when the R bodies are at low pH, and results from a pH-dependent change in the molecular conformation of the protein of which the R body is made. As might be expected, it is reversible and independent of the agents inducing unrolling in stock 7. Nothing is known of the phenomenon of unrolling of the R bodies of stock 562 except that they do not seem to respond in the same way as the R bodies of stock 7.

The parallel between the R bodies and inclusions formed in association with cells infected with adenovirus (Morgan, Rose & Moore, 1957) has already been

pointed out (Sonneborn, 1959; Preer & Preer, 1967). Recent observations on inclusions in plant cells infected with viruses are also interesting in this regard (see, for example, Wrischer, 1968). However, the pinwheel-like structures observed in plants are markedly different in form from the R body.

SUMMARY

Virus-like particles can be seen in sections of kappa of stocks 7 and 562. The virus-like particles are specifically associated with R bodies and are rare or absent in kappa particles lacking R bodies. This observation clearly links the virus-like particles with kappa's toxic activity; it also supports the suggestion that kappa is infected with a lysogenic virus whose induction results in the production of the R body and viruses. Many 'unfilled' virus-like particles are present in whole kappa particles. Wound R bodies of stock 7 are surrounded by a sheath, whose breakage may provide the mechanism which causes the unrolling of the R body. One edge of the R body ribbon stains more intensely than the other.

This work was supported by the National Science Foundation, U.S.A., and Phi Beta Psi Sorority. The authors wish to thank Professor G. H. Beale for his interest and encouragement and for the use of his laboratory facilities. Thanks are also due to Mr E. D. Roberts for mounting the micrographs.

REFERENCES

Afzelius, B.A. (1962). Chemical fixatives for electron microscopy. In *Interpretations of Ultrastructure*, pp. 1–19. Editor: R. J. C. Harris. Academic Press: New York and London.

Anderson, T. F., Preer, J. R., Preer, L. B. & Bray, M. (1964). Studies on killing particles from *Paramecium*: the structure of refractile bodies from kappa particles. *J. Microscopie* **3**, 395–402.

Dippell, R. V. (1958). The fine structure of kappa in killer stock 51 of *Paramecium aurelia*. Preliminary observations. *J. biophys. biochem. Cytol.* **4**, 125–128.

Dryl, S. (1959). Antigenic transformation in *Paramecium aurelia* after homologous antiserum treatment during autogamy and conjugation. *J. Protozool.* **6** (suppl.), 25.

Jurand, A. & Ireland, M. J. (1965). A slow rotary shaker for embedding in viscous media. *Stain Technol.* **40**, 233–234.

Jurand, A. & Preer, L. B. (1968). Ultrastructure of flagellated lambda symbionts in *Paramecium aurelia*. *J. gen. Microbiol.* (in the Press).

Morgan, C., Rose, H. M. & Moore, D. H. (1957). An evaluation of host cell changes accompanying viral multiplication as observed in the electron microscope. *Ann. N.Y. Acad. Sci.* **68**, 302–323.

Mueller, J. A. (1962). Induced physiological and morphological changes in the B particle and R body from killer paramecia. *J. Protozool.* **9**, 26.

Mueller, J. A. (1963). Separation of kappa particles with infective activity from those with killing activity and identification of the infective particles in *Paramecium aurelia*. *Expl Cell Res.* **30**, 492–508.

Mueller, J. A. (1965). Vitally stained kappa in *Paramecium aurelia*. *J. Exptl Zool.* **160**, 369–372.

Preer, J. R. (1968. Genetics of the Protozoa. In *Research in Protozoology*, vol. 3, pp. 139–288. Ed. T. T. Chen. Oxford: Pergamon Press.

Preer, J. R., Hufnagel, L. A. & Preer, L. B. (1966). Structure and behaviour of 'R' bodies from killer paramecia. *J. Ultrastruct. Res.* **15**, 131–143.

Preer, J. R. & Preer L. B. (1967). Virus-like bodies in killer paramecia. *Proc. natn. Acad. Sci. U.S.A.* **58**, 1774–1781.

PREER, J. R., SIEGEL, R. W. & STARK, P. S. (1953). The relationship between kappa and paramecin in *Paramecium aurelia*. *Proc. natn. Acad. Sci. U.S.A.* **39**, 1228–1233.

PREER, J. R. & STARK, P. (1953). Cytological observations on the cytoplasmic factor 'kappa' in *Paramecium aurelia*. *Expl Cell Res.* **5**, 478–491.

PREER, L. B. & PREER, J. R. (1964). Killing activity from lysed kappa particles of *Paramecium*. *Genet. Res.* **5**, 230–239.

RUDENBERG, F. H. (1962). Electron microscopic observations of kappa in *Paramecium aurelia*. *Texas Reports on Biology and Medicine* **20**, 105–112.

SMITH, J. E. (1961). Purification of kappa particles of *Paramecium aurelia*, stock 51. *Am. Zool.* **1**, 390.

SONNEBORN, T. M. (1959). Kappa and related particles in *Paramecium*. *Adv. in Virus Res.* **6**, 229–356.

WOODS, D. R. & BEVAN, E. A. (1968). Studies on the nature of the killer factor produced by *Saccharomyces cerevisiae*. *J. gen. Microbiol.* **51**, 115–126.

WRISCHER, M. (1968). Cytoplasmatische Einschlüsse in virusinfizierten Bohnenblättern. *Z. Naturforsch.* **23***b*, 80–82.